# Novel Techniques for High Precision Genome Engineering

## Dissertation

zur

Erlangung der naturwissenschaftlichen Doktorwürde

(Dr. sc. nat)

vorgelegt der

Mathematisch-naturwissenschaftlichen Fakultät

der

Universität Zürich

von

**Mario Hermann**

aus

Deutschland

Promotionskomitee

Prof. Dr. med. Dr. sc. Adriano Aguzzi (Vorsitz)

Dr. Pawel Pelczar

Prof. Dr. Thorsten Buch

Zürich, 2014

# Contents

# Summary

Introducing genetic modifications into model organisms is of fundamental importance for unraveling the molecular mechanisms underlying physiological and pathological processes. Over the last decades a wide range of technologies for manipulating the mouse genome have been developed and as a result of their success the laboratory mouse is one of the most widely used animal models in biomedical research today.

One approach is pronuclear microinjection of linear recombinant DNA fragments into the fertilized oocyte. Integration of these fragments at a random position within the mouse genome allows the generation of mouse lines that overexpress proteins encoded by these transgenes.

Other genome engineering objectives such as abolishing the expression of a gene (a gene knock-out) require the targeted modification of a defined DNA sequence. This can be achieved by introducing an extrachromosomal genetic construct into mouse embryonic stem cells, which acts as a substrate for homologous recombination with the genomic locus of choice. Successfully engineered stem cell clones are subsequently used to generate chimeric founder animals for establishing a new transgenic mouse line.

Gene knock-out eliminates the expression of genes in all embryonic and adult tissues, however, the complete disruption of certain genes elicits a lethal phenotype. As an alternative, conditional gene knock-out has been introduced, which abrogates gene expression in a limited subset of tissues. Here, a functionally important segment of a gene is flanked by recognition sites for the site-specific recombinase Cre

(*loxP* sites). The expression of Cre under the control of a tissue-specific promoter is restricted to certain developmental stages and cell lineages, in which the *loxP*-flanked segment is excised resulting in gene knock-out. Furthermore, conditional transgenesis can be used to activate a traceable marker such as a fluorescent protein in precursor cells and determine the fate of their progeny cells (lineage tracing).

The general goal of this thesis was the development and validation of technologies for engineering the mouse genome with an unprecedented degree of precision and thereby overcoming major limitations of classic gene-targeting and conditional transgenesis.

Chapter 1 introduces Binary Recombinases, a class of advanced conditional transgenesis systems for controlling Cre expression by any pair of tissue-specific promoters. Two alternative Binary Recombinases, Co-Driver and Co-InCre, were established, which employ a sequential and a coincidental mechanism for dual-promoter control of Cre production, respectively. The Co-Driver cascade consists of the recombinase Dre, which activates a Dre-dependent Cre variant, Roxed-Cre, by excising a transcriptional and translational terminator from the Cre protein-coding DNA sequence. Co-InCre comprises two inactive Cre fragments, which reconstitute full-length Cre upon co-expression by the means of seamless protein trans-splicing. Co-Driver- and Co-InCre-mediated Cre activity was strictly dependent on the presence of both binary components and facilitated highly efficient processing of reporter genes in transfected cell lines and in cells of the developing mouse brain. Additionally, Co-Driver allowed for the first time to generate two clearly distinguishable patterns of Cre activation by linking two tissue-specific promoters sequentially in "forward" and "reverse" orientation.

Chapter 2 outlines experiments with the aim of harnessing the DNA double-strand break repair machinery in mouse embryos and cultured human cells for gene knock-out and targeted integration of transgenes. Custom-designed zinc finger nucleases (ZFN) and transcription activator-like effector nucleases (TALEN) were microinjected

into fertilized mouse oocytes resulting in homologous recombination between targeting constructs and the *ROSA26* locus and mutagenesis of the prion protein gene (*Prnp*) by non-homologous end joining, respectively. All engineered genetic alleles were efficiently transmitted to the offspring of founder animals. Prion protein ($PrP^C$) expression was successfully eliminated in C57BL/6 mice carrying a TALEN-induced frameshift mutation in both alleles of the *Prnp* gene. In a third approach in HEK293T cells, both copies of the human *PRNP* gene were successfully modified by using the clustered regularly interspaced short palindromic repeat (CRISPR) platform.

Binary recombinases and genome editing technologies enable the generation of sophisticated conditional transgenesis models with a defined genetic background. These models will accelerate the dissection of cell lineage relationships and will support the functional analysis of so far elusive proteins and cell types.

# Zusammenfassung

Die Veränderung genetischer Information in Modelorganismen ist von zentraler Bedeutung für das Erforschen molekularer Mechanismen, die physiologischen und pathologischen Prozessen zu Grunde liegen. Eine Vielzahl an Technologien zur genetischen Manipulation des Mausgenoms wurden über die letzen Jahrenzehnte entwickelt. Auf Grund des Erfolgs dieser Methoden ist die Labormaus heute eines der meist verwendeten Tiermodelle.

Einer dieser Technologien ist die pronukleare Mikroinjektion von linearen rekombinanten DNA Fragmenten in befruchtete Oozyten. Durch Integration dieser Fragmente an zufälligen Positionen im Mausgenom können Mauslinien generiert werden, welche Proteine mittels dieser Transgene überexprimieren.

Andere Zielsetzungen der genetischen Manipulation, wie zum Beispiel das Eliminieren der Expression eines Gens (der Gen Knock-out), setzen das gezielte Modifizieren bestimmter DNA Sequenzen voraus. Dies ist möglich durch das Einbringen eines künstlichen genetischen Konstrukts in murine embryonische Stammzellen, welches als Substrat für Homologe Rekombination mit einem ausgewählten genetischen Lokus fungiert. Erfolgreich veränderte Stammzellklone werden dann verwendet um Maus-Chimären für das Etablieren einer neuen Mauslinie zu erzeugen.

Der Gen Knock-out eliminiert die Expression eines Gens in allen embryonalen und adulten Geweben. Das vollständige Ausschalten bestimmter Gene führt jedoch zu einem letalen Phänotyp. Der konditionale Gen Knock-out stellt hier eine Alternative

dar, indem die Genexpression nur in bestimmten Geweben verhindert wird. Konditionale Gen-Varianten werden dadurch erzeugt, dass wichtige funktionale Gensegmente mit Erkennungssequenzen der Cre Rekombinase (*loxP*) flankiert werden. Mittels eines gewebe-spezifischen Promoters wird die Expression von Cre auf bestimmte Entwicklungsabschnitte und Zelllinien beschränkt, in welchen das *loxP*-flankierte Segment ausgeschnitten und ein Gen Knock-out hervorgerufen wird. Weiterhin kann konditionale Transgenese dazu eingesetzt werden, um einen Marker, wie z.B. ein fluoreszentes Protein, in Vorläuferzellen zu aktivieren und die Entwicklung ihrer Tochterzellen zu verfolgen ("lineage tracing").

Das Hauptziel dieser Doktorarbeit war die Entwicklung und Validierung von Technologien zur höchstpräzisen Manipulation des Mausgenoms, welche die wesentlichen Beschränkungen von Gene-targeting und konditionaler Transgenese überwinden.

Kapitel 1 befasst sich mit Binären Rekombinasen, eine Klasse von weiterentwickelten konditionalen Transgenesesystemen, welche die Kontrolle von Cre mit jeder Kombination zweier gewebe-spezifischer Promotoren erlaubt. Die beiden alternativen Binären Rekombinasen, Co-Driver und Co-InCre wurden etabliert, welche jeweils auf einem sequentiellen und einem simultanen Mechanismus zur Kontrolle der Cre Produktion durch zwei Promotoren beruhen. Die Co-Driver Kaskade besteht aus der Dre Rekombinase, welche eine Dre-abhängige Variante von Cre (Roxed-Cre) aktiviert, indem ein Transkriptions- und Translationsterminator aus der proteincodierenden Sequenz von Cre entfernt wird. Co-InCre ist aus zwei inaktiven Cre-Fragmenten zusammengesetzt, welche bei gleichzeitiger Expression mittels Protein-Trans-Splicings die ursprüngliche Proteinsequenz der Cre Rekombinase wiederherstellen. Co-Driver und Co-InCre Komponenten waren nur zusammen mit ihrem binären Partner aktiv und zeigten eine hohe Effizienz beim Rekombinieren von Reportergenen in transfizierten Zelllinien und in Zellen des sich entwickelten Maushirns. Zudem konnten mit Co-Driver erstmalig zwei klar unterscheidbare Cre Aktivierungsmuster generiert werden, indem zwei gewebe-spezifische Promotoren sequentiell in "vorwärts" und "rückwärts" Orientierung miteinander verbunden wurden.

Kapitel 2 umfasst Experimente mit dem Ziel, die Reparatur von DNA Doppelstrangbrüchen in Mausembryonen und humanen Zelllinien auszunützen, um Gen Knockouts und die gezielte Integration von Transgenen zu erreichen. Sequenzspezifische Zinkfinger Nukleasen (ZFN) und "transcription activator-like effector" Nukleasen (TALEN) wurden in befruchtete Mausoozyten mikroinjiziert, welche jeweils homologe Rekombination zwischen Targeting-Konstrukten und dem *ROSA26* Lokus und die Mutagenese des Prion-Protein-Gens (*Prnp*) durch nonhomologes Endjoining induzierten. Sämtliche modifizierte genetische Varianten wurden effizient an die Nachkommen von transgenen Gründertieren weitergegeben. In C57BL/6 Mäusen, welche eine TALEN-induzierte Frameshift-Mutation in beiden Allelen des *Prnp* Gens tragen, wurde die Expression des Prion-Proteins ($PrP^C$) erfolgreich eliminiert. In einem weiteren Ansatz in HEK293T Zellen konnten mittels der "clustered regularly interspaced short palindromic repeat" (CRISPR) Plattform beide Kopien des human *PRNP* Gens modifiziert werden.

Binäre Rekombinasen und Technologien für "genome editing" ermöglichen die Generierung von hochentwickelten konditionalen Transgenese Modellen mit einem definierten genetischen Hintergrund. Diese Modelle werden die Untersuchung von Entwicklungsbeziehungen verschiedener Zellstadien beschleunigen und die funktionale Analyse von bisher rätselhaften Proteinen und Zelltypen unterstützen.

# Abbreviations

| | |
|---|---|
| AAV | adeno-associated virus |
| ANOVA | analysis of variance |
| *attB/attP* | DNA recognition sites of serine recombinases such as Bxb1 |
| *attL/attR* | products of recombination between *attB* and *attP* sites |
| BAC | bacterial artificial chromosome |
| *b3* | DNA recognition site of the yeast B3 recombinase |
| CAG | CMV early enhancer element/ chicken beta-actin promoter |
| Cas9 | CRISPR-associated protein 9 |
| CAT | chloramphenicol acetyltransferase |
| CreERT2 | fusion of the Cre recombinase with a mutant estrogen receptor |
| CRISPR | clustered regularly interspaced short palindromic repeat |
| crRNA | CRISPR RNA |
| DAPI | 4,6-diamidino-2-phenylindole |
| DNA | deoxyribonucleic acid |
| DSB | double-strand break |
| EGFP | enhanced green fluorescent protein |
| ES cells | embryonic stem cells |
| *frt* | DNA recognition sites of the yeast Flp recombinase |
| GPI | glycosylphosphatidylinositol |
| HA | hemagluttinin epitope tag |
| HEK293T | human embryonic kidney cell line |
| hGFAP | human glia-fibrillary acidic protein promoter |
| HR | homologous recombination |
| *kd* | DNA recognition site of the yeast KD recombinase |

| | |
|---|---|
| *loxP* | DNA recognition site of phage P1 recombinase Cre |
| MEF | mouse embryonic fibroblasts |
| mRNA | messenger RNA |
| mTagBFP | blue fluorescent protein |
| NeuN | neuronal nucleus antigen |
| NHEJ | non-homologous end joing |
| NLS | nuclear localization signal |
| PAM | protospacer adjacent motif |
| PCR | polymerase chain reaction |
| poly(A) | polyadenylation signal |
| *PRNP* | human prion protein gene |
| *Prnp* | mouse prion protein gene |
| $PrP^C$ | cellular prion protein |
| RNA | ribonucleic acid |
| *ROSA26* | the *gt(ROSA26)Sor* locus on mouse chromosome 6 |
| *rox* | DNA recognition site of the phage D6 Dre recombinase |
| RVD | repeat variable diresidues |
| S.D. | standard deviation |
| sgRNA | single-chain guide RNA |
| *Sirpa* | mouse gene encoding signal regulatory protein $\alpha$ |
| SNP | single nucleotide polymorphism |
| SSR | site-specific recombinase |
| SV40 | simian virus 40 |
| SVZ | subventricular zone |
| TALEN | transcription activator-like effector nucleases |
| Thy1.2 | thymocyte differentiation antigen 1.2 |
| tracrRNA | trans-activing CRISPR RNA |
| VZ | ventricular zone |
| WPRE | woodchuck hepatitis virus post-transcriptional regulatory element |
| ZFN | zinc finger nuclease |

# 1. Binary Recombinases for High Resolution Conditional Mutagenesis

This chapter includes unpublished material as well as sections that were adapted or reproduced from the following publication.

Nucleic Acids Research | April 2014 | Volume 42 | Issue 6 | 3894-3907 | doi: 10.1093/nar/gkt1361

**Binary recombinase systems for high resolution conditional mutagenesis**

Mario Hermann[1,2], Patrick Stillhard[1], Hendrik Wildner[3], Davide Seruggia[4,5], Viktor Kapp[1], Héctor Sánchez-Iranzo[6], Nadia Mercader[6], Lluís Montoliu[4,5], Hanns Ulrich Zeilhofer[3,7] and Pawel Pelczar[1,*]

[1]Institute of Laboratory Animal Science, University of Zurich, Zurich, Switzerland
[2]Institute of Neuropathology, University Hospital of Zurich, Zurich, Switzerland
[3]Institute of Pharmacology and Toxicology, University of Zurich, Zurich, Switzerland
[4]National Centre for Biotechnology (CNB-CSIC), Madrid, Spain
[5]CIBERER-ISCIII, Madrid, Spain
[6]Program of Cardiovascular Development, Department of Cardiovascular Development and Repair, Centro Nacional de Investigaciones Cardiovasculares Carlos III, Madrid, Spain
[7]Institute of Pharmaceutical Sciences, Swiss Federal Institute of Technology (ETH) Zurich, Zurich, Switzerland

*To whom correspondence should be addressed. Email: pawel.pelczar@ltk.uzh.ch

Individual contributions of authors are summarized in “Contributions to Published Work” on page 135.

# 1.1. Introduction

## 1.1.1. Mechanisms of site-specific recombination

Site-specific recombination is a process that involves one or two DNA substrates and a recombinase protein that recognizes specific sites present within these substrates and catalyzes breakage and rejoining of DNA without a requirement for DNA synthesis or energy-rich nucleotide cofactors (Grindley et al., 2006). In their simplest form, site-specific recombinase (SSR) recognition sites are 20-30 bp of double-stranded DNA containing a pair of recognition sequences in inverted orientation flanking the site of breakage and joining (the crossover site) in the center. These sites are typically occupied by either a recombinase dimer or two recombinase monomers.

Based on the intial orientation of the recognition sites, site-specific recombination can result in integration, excision, or inversion of DNA segments (Grindley et al., 2006). Integration requires recombination between two circular or a linear and a circular DNA molecule each of which is carrying a single recognition site. Recognition sites that are located on the same DNA molecule in a head-to-tail orientation facilitate excision of the flanked region, whereas inversion results from sites in a head-to-head orientation.

Nearly all SSRs belong to one of two families, tyrosine recombinases and serine recombinases. The recombination mechanism of tyrosine family SSRs such as the phage P1 Cre and the yeast Flp recombinase in combination with their native recognition sites typically favors excision over insertion reactions, while inversions of DNA are generally reversible as long as the SSR is present. Serine family SSRs such as ΦC31 (*Streptomyces* phage) and Bxb1 (mycobacteriophage) on the other hand are capable of carrying out unidirectional excisions and inversions. This is possible due to the processing of their *attB/attP* recognition sites to *attL/attR* sites, which are no longer a substrate for recombination (Grindley et al., 2006).

### 1.1.2. Classic conditional transgenesis

Conditional mutagenesis in mice typically employs the Cre recombinase, which is expressed in a spatially and temporally restricted manner (Nagy, 2000). Distinct Cre expression profiles result from the transcriptional control exercised by regulatory elements of well characterized promoters that are used to drive expression of conventional transgenes or of large fragments of genomic DNA that are routinely used to generate bacterial artificial chromosome (BAC) transgenics (Gong et al., 2003). Alternatively, the fidelity of expression can be assured by directly inserting the Cre protein-coding sequence into a native gene locus using gene-targeting. Cre driver mouse lines generated with any of these strategies can be crossed to a wide variety of mice carrying Cre-responsive alleles. Depending on the responder allele, the Cre driver can mediate either gene ablation through the removal of *loxP*-flanked (floxed) coding sequences or gene activation caused by the removal of floxed STOP-cassettes (Nagy, 2000). Although elegant, conditional mutagenesis approaches are sometimes limited, as the regulatory elements of a single gene not always suffice for directing Cre to distinct subsets of cells in complex organs such as the brain or the immune system. One way of enhancing the specificity of conditional somatic mutagenesis has been the development of the CreERT2 system, which allows temporal regulation of recombination through timed administration of tamoxifen (Feil et al., 1997). While this approach has allowed labeling and tracking of cells with increased temporal precision, it is still limited to cell populations that can be targeted by a single-promoter strategy.

### 1.1.3. Binary recombinase systems

To date two strategies have been developed to enable dual-promoter transcriptional control of SSRs, which can be broadly summarized as binary SSRs. The Cre reconstitution approach is based on splitting Cre into inactive polypeptide chains, expressing these fragments from two individual tissue-specific promoters and allowing the

assembly of active Cre in cells where the transcriptional profiles of both promoters intersect. Several Cre reconstitution strategies have been described. Namely, the spontaneous reassembly of Cre fragments by $\alpha$-complementation (Casanova et al., 2003), fusing Cre fragments to protein dimerization domains in order to enhance Cre reassembly (Hirrlinger et al., 2009b,a; Jullien et al., 2003, 2007), or covalent reconstitution of Cre with the help of split-intein-mediated protein trans-splicing (Wang et al., 2012). All Cre reconstitution strategies strictly depend on promoters that allow simultaneous expression of the inactive Cre fragments.

However, another intersectional dual-promoter strategy that combines two orthogonally active SSRs, Cre and Flp, allows promoters with non-overlapping temporal profiles to be used for restricting reporter expression. The Cre/Flp strategy employs reporter constructs that carry *loxP*- and *frt*-flanked STOP-cassettes in various configurations (Dymecki et al., 2010) to selectively label cell sub-populations. Although elegant, this approach is generally not applicable to generate conditional knockout mice since conditional alleles usually only contain *loxP* sites that facilitate removal of exon sequences (Nagy, 2000). Additionally, *frt* sites are now frequently found in conditional alleles as a result of their assembly by recombineering (Madisen et al., 2010; Skarnes et al., 2011), thus severely limiting the application of Flp-mediated conditional transgenesis in the mouse and restricting its use to lineage tracing studies using Cre/Flp-responsive reporter alleles. The phage D6 recombinase Dre (Sauer and McDermott, 2004) faithfully processes its cognate recognition sites known as *rox* sites and does not cross-react with *loxP* sites in transgenic mice (Anastassiadis et al., 2009). Thus, Dre represents a potential alternative to Flp for achieving dual-recombinase conditional transgenesis, however Cre/Dre-responsive reporter genes have not been reported so far.

## 1.2. Outline

In this chapter I describe the construction and functional validation of novel dual-promoter-driven conditional transgenesis systems. By combining the transcriptional profiles of two distinct promoters the expression of the site-specific recombinase (SSR) Cre can be targeted to subsets of cells for which single promoter strategies are not established. Throughout this chapter, I will refer to all two-component conditional transgenesis systems both introduced in this study as well as the ones described in earlier publications as *Binary SSRs*. Furthermore Binary SSRs will be classified according to their mechanism of Cre activation (Figure 1.1). Sequential binary SSRs comprise a primary SSR, a Co-Driver, which can process the protein-coding DNA sequence and thus initiate expression of an otherwise inactive secondary SSR (the driver). Coincidental Binary SSRs such as Co-InCre on the other hand rely on splitting Cre (or any other SSR) into inactive fragments that are expressed using two individual promoters and on generating functional Cre by a protein reconstitution mechanism.

The choice of a suitable promoter pair, which drives Binary SSR components is critical to achieve Cre expression in the cellular sub-population of interest. The targeting strategy for certain cell types may require the pairing of two promoters, which are active during different developmental stages and do not show any temporal overlap of their transcriptional profiles. Coincidental Binary SSRs rely on simultaneous expression of both components for efficient Cre activation and thus exclude the use of promoter pairs with non-overlapping transcriptional profiles. The sequential Binary SSR approach on the other hand allows for the first time to exploit the transcriptional domains of any given pair of promoters (with the exception of a scenario where driver expression precedes and does not overlap with Co-Driver expression, Figure 1.1B).

I report in this chapter the construction of the first sequential Binary SSR, Co-Driver, which is based on Dre and Roxed-Cre, a Dre-dependent Cre variant. Co-Driver efficiently recombined reporter genes when constitutively expressed in cell lines and

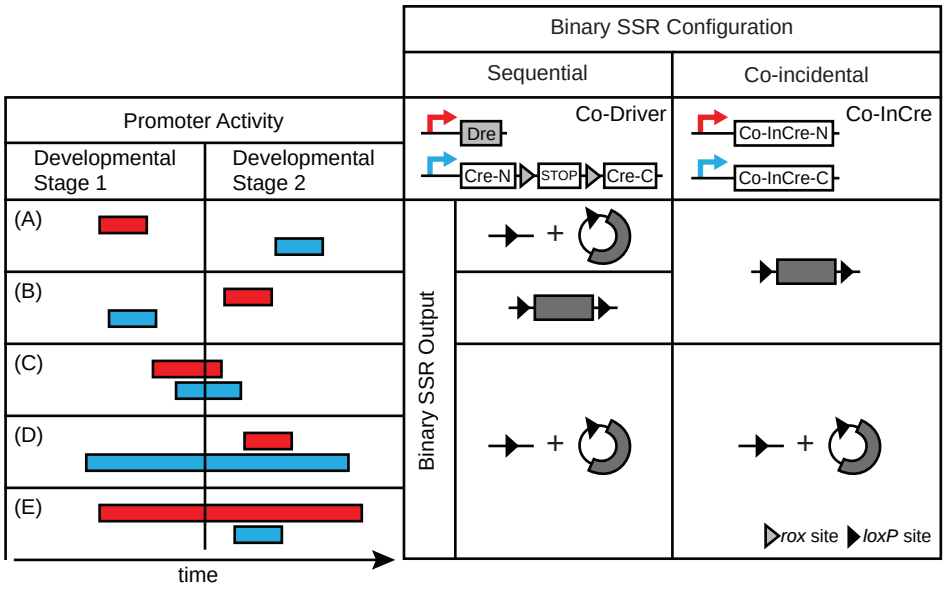


**Figure 1.1.: Sequential and coincidental Binary SSRs.** Binary SSRs can be controlled using two distinct promoters with non-overlapping (A, B) or overlapping (C-E) temporal expression profiles. Sequential Binary SSRs such as Co-Driver can produce a final output e.g. the excision of an arbitrary *loxP*-flanked sequence (grey box) in all overlapping scenarios as well as in non-overlapping scenario (A). coincidental Binary SSRs such as Co-InCre rely on protein reconstitution and thus on simultaneous expression of both N- and C-terminal Cre-fragments to produce a final output (C-E).

the developing mouse neocortex. When Dre and Roxed-Cre were expressed from two promoters with non-identical transcriptional profiles Co-Driver integrated both tissue-specific and temporal layers of control. Co-InCre, a newly developed coincidental Binary SSR incorporating highly active split-inteins showed a significant improvement of recombination efficiency over previously published systems.

# 1.3. Results

## 1.3.1. Dre as the optimal Co-Driver recombinase

The basic concept of the Co-Driver cascade requires the use of a highly active SSR that will operate orthogonally with Cre. I considered SSRs to be promising Co-Driver candidates if they fulfilled two essential conditions. First, the specificity of the SSRs for their cognate recognition sites (and the absence of cross reactivity with other SSR recognition sites) should have been determined previously and preferentially also validated in a mammalian system. Second, the Co-Driver candidate and its recognition sites should not be routinely utilized for cloning or recombineering of transgenic constructs. Selecting SSRs by these criteria should minimize the risk of unintended recombination events when Co-Driver is combined with currently available transgenic alleles. Following these considerations I selected four Co-Driver candidates including the phage recombinases Dre (Anastassiadis et al., 2009; Sauer and McDermott, 2004) and Bxb1 (Ghosh et al., 2005, 2003; Mediavilla et al., 2000) as well as the yeast recombinases B3 and KD (Nern et al., 2011). I excluded the extensively characterized SSRs Flp and $\Phi$C31 since a large number of established mouse lines carry conditional mutagenesis cassettes, which already contain *frt* and $\Phi$C31 *attB/attP* recognition sites (Madisen et al., 2010; Skarnes et al., 2011).

To date, no comparative assessment of recombination efficiency of these SSRs has been performed in a standardized mammalian system. Therefore, I systematically compared their recombination efficiencies relative to the highly active Cre recombinase. First, I designed standardized SSR overexpression constructs by fusing all the codon-optimized SSR protein-coding sequences to an N-terminal SV40-NLS and a HA-tag and placing them under control of a constitutively active CAG promoter (Figure 1.2A). B3, KD, and Dre are members of the tyrosine SSR family whereas Bxb1 is the only representative of the serine family of recombinases.

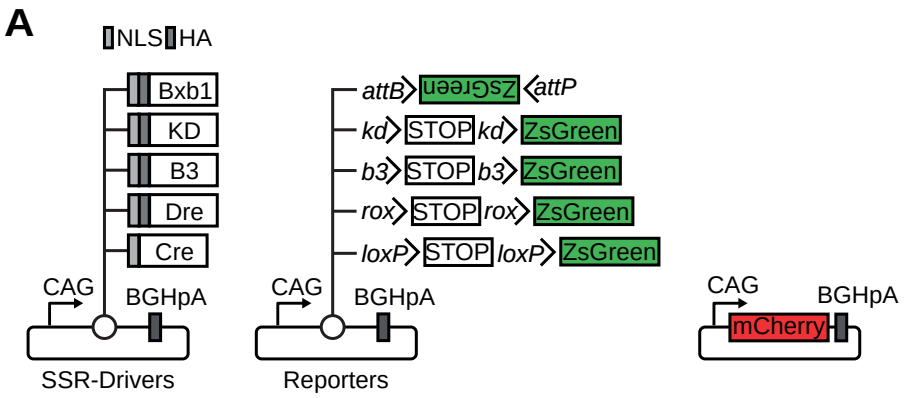
A
NLS
HA
Bxb1
KD
B3
Dre
Cre
CAG
BGHpA
SSR-Drivers
attB
ZsGreen
attP
kd
STOP
ZsGreen
b3
rox
loxP
Reporters
mCherry

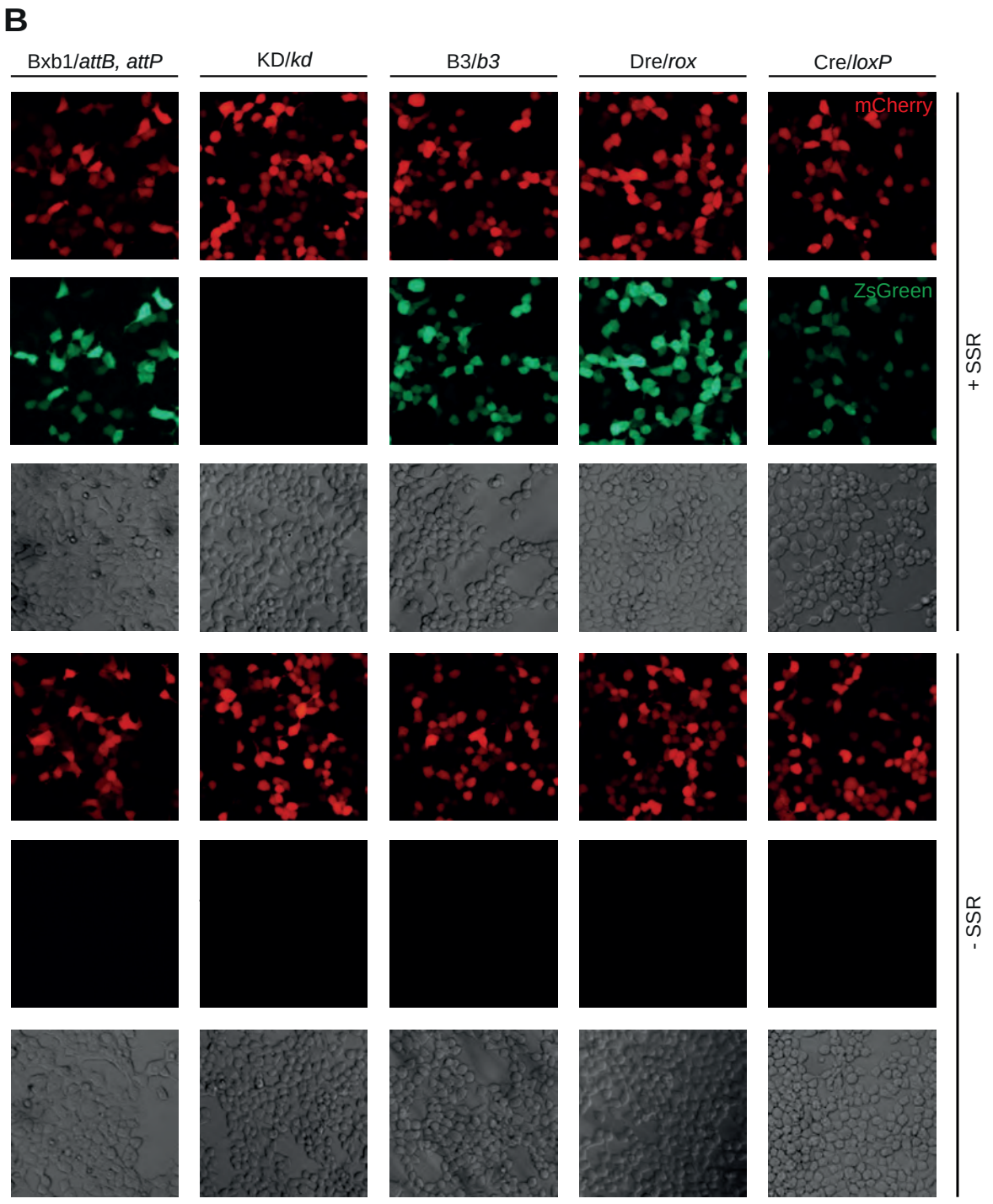
B
Bxb1/attB, attP
KD/kd
B3/b3
Dre/rox
Cre/loxP
mCherry
ZsGreen
+ SSR
- SSR

**Figure 1.2.: Evaluation of Co-Driver candidate recombinases.** (A) Diagrams of standardized SSR-driver and respective reporter plasmids that are co-transfected with a constitutively expressing mCherry plasmid into HEK293T cells. Transfected cells are mCherry$^+$, and SSR activity is detected for Bxb1 using an inverted ZsGreen reporter or a STOP-cassette-based ZsGreen reporter for KD, B3 and Dre. Arrowheads indicate the orientation of individual SSR recognition sites.(B) HEK293T were transfected with a constitutive mCherry plasmid, a SSR-specific ZsGreen-fluorescent reporter constructs and either adding (+ SSR, top panel) or omitting (- SSR, bottom panel) a constitutive SSR expressing plasmid. Transfected SSRs and cognate reporters, Bxb1/*attB, attP*, KD/*kd*, B3/*b3*, Dre/*rox*, and Cre/*loxP* are indicated on top. Fluorescent microscopy images for mCherry and ZsGreen fluorescence as well as Nomarski light microscopic images of transfected HEK293T cells are shown.

As my intent was to exploit the DNA inversion mechanism of Bxb1 to construct a Bxb1/Cre SSR cascade, I assessed the efficiency of Bxb1 in the context of a fluorescent reporter construct carrying a reverse-complementary ZsGreen protein-coding sequence flanked by Bxb1 recognition sites (Figure 1.2A). Conversely, the DNA excision activity of the three tyrosine recombinases was assessed using reporter constructs carrying ZsGreen preceded by a STOP-cassette (Madisen et al., 2010) flanked by the cognate recognition sites of the respective SSR. In order to ascertain SSR activity, HEK293T cells were transfected with a constitutively expressing mCherry plasmid, SSR drivers, and their respective reporters and individual transfections were initially assessed by fluorescence microscopy (Figure 1.2A). In the absence of SSRs none of the reporter constructs produced any visible ZsGreen signal in transfected mCherry$^+$ cells, while co-transfection of the respective SSR resulted in strong ZsGreen expression for all Co-Driver candidates with the exception of KD (Figure 1.2B).

Having established the basic functionality of all Co-Driver candidate ZsGreen-reporter pairs (except KD) I compared recombination efficiencies of the candidate SSRs by

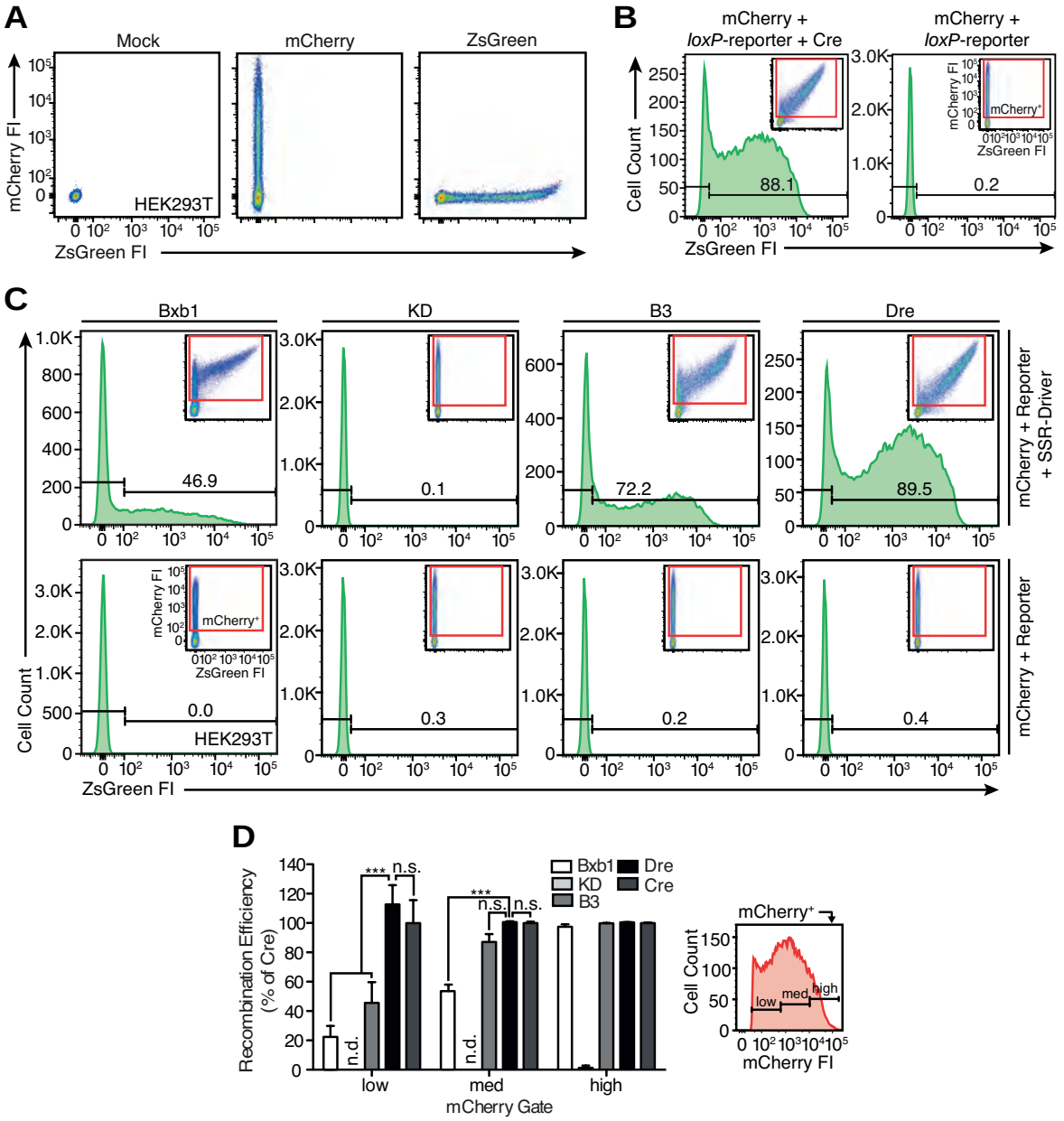


**Figure 1.3.: Recombination efficiency of Co-Driver candidates.** HEK293T were analyzed by flow cytometry 24h after transfection with (A) a mCherry or ZsGreen single color control plasmid, (B) with Cre and a *loxP*-reporter, or (C) Co-Driver candidates. Numbers within histograms represent the percentage of transfected cells showing recombination activity. Insets, scatter plots showing living cells and gating for mCherry$^+$ cells (red rectangle). FI, relative fluorescence intensities in arbitrary units. (D) Quantification of recombination efficiency. Bars represent the percentage of cells showing recombination activity in subsets of mCherry$^+$ cells (gating within the mCherry$^+$ gate is shown right to bar graph). Average data of three independent experiments with standard deviation and normalized to 100% Cre average recombination efficiency are shown. n.d., not detectable. Statistics: two-way ANOVA with Bonferroni post hoc test; n.s., not significant; *P<0.05; **P<0.01; ***P<0.001.

employing flow cytometric measurement of single-cell mCherry and ZsGreen fluorescence intensities (Figure 1.3). In transfected HEK293T cells that constitutively expressed either mCherry or ZsGreen, no crosstalk between mCherry and ZsGreen fluorescence was detected (Figure 1.3A). Next I performed co-transfections of a constitutively active mCherry plasmid with either a *loxP*-ZsGreen reporter alone or in combination with Cre (Figure 1.3B). All transfected cells were detected by mCherry fluorescence (24 h post-transfection) while recombination activity of the SSR was indicated by ZsGreen fluorescence in cells of the mCherry-positive population. In the absence of Cre less than 0.5% of mCherry$^+$ cells showed ZsGreen fluorescence confirming the tight control of ZsGreen expression by the *loxP*-flanked STOP cassette. When Cre was added to the transfections over 85% of transfected cells showed recombination activity.

For the evaluation of Co-Driver candidates, Cre was used as a reference for recombination efficiency and the performance of other SSRs is expressed as percentage of Cre efficiency. This definition of recombination efficiency is used for all flow cytometric analyses throughout this chapter. All Co-Driver candidate reporter constructs showed a tight control of ZsGreen expression similar to the Cre-reporter (Figure 1.3C). When Co-Driver candidates were co-transfected with their respective reporters Dre showed the highest recombination efficiency with a percentage of ZsGreen-positive cells as high as Cre, while B3 and Bxb1 were less efficient (Figure 1.3C). KD activity was undetectable confirming the initial microscopic analysis.

In order to obtain a detailed profile of Co-Driver candidate performances I determine recombination efficiencies in subsets of cells with overall low, medium, and high expression levels. I defined three equally sized gates within the mCherry$^+$ gate covering the full range of mCherry fluorescence intensities for all SSR transfections (Figure 1.3D). Again, Dre recombination levels were comparable to Cre in all subpopulations including mCherry$^{low}$ cells, while B3 reached only about 50% of Cre activity in this population. Bxb1-mediated inversion of the ZsGreen reporter was only 20% as efficient than Cre-mediated STOP-cassette excision in mCherry$^{low}$ cells.

These results prompted me to consider Dre as the optimal Co-Driver of all SSRs tested for constructing a sequential binary recombinase system.

### 1.3.2. A Dre-responsive Cre driver design

Having selected Dre as the Co-Driver SSR, I evaluated several *rox*-flanked STOP-cassette designs with the aim to tightly control Cre expression in the absence of Dre. I adapted two STOP-cassette configurations that were shown previously to completely block transgene expression and at the same time facilitated efficient transgene reactivation upon the removal of the STOP-cassette by Cre recombination. The 3× poly(A) STOP cassette incorporates STOP codons in all three reading frames followed by three consecutive SV40 poly(A) sequences and is part of the Ai6 and Ai14 conditional reporter alleles (Madisen et al., 2010). The CAT-poly(A) STOP cassette is composed of the chloramphenicol acetyltransferase (CAT) gene and a poly(A) signal and has been shown to tightly control multi-copy transgenes (Araki et al., 1995). Both *rox*-flanked STOP-cassettes were cloned upstream of Cre (Figure 1.4A) and each of these constructs together with constitutive mCherry plasmid, Cre-inducible ZsGreen reporter and either adding or omitting a constitutive Dre expression construct was transfected into HEK293T (Figure 1.4B). I observed substantial levels of *loxP* recombination events in the absence of Dre regardless of which *rox*-flanked STOP cassette was present upstream of Cre (Figure 1.4B and Figure 1.5).

I hypothesized that the transcriptional termination by the upstream STOP cassettes is incomplete thus allowing sufficient translation of Cre for *loxP* recombination to occur. Therefore, I devised a strategy that would interrupt Cre expression at both the transcriptional and translational level. In the Roxed-Cre construct (Figure 1.4A), the Cre open reading frame is interrupted by the 3× poly(A) STOP cassette between amino acids 59 and 60. Thus Roxed-Cre generates an inactive N-terminal Cre fragment (Jullien et al., 2003, 2007; Hirrlinger et al., 2009b; Wang et al., 2012) in the

absence of Dre recombination (and in the case of transcriptional read-through the also inactive C-terminal Cre fragment). Once the *rox*-flanked STOP cassette is removed a Cre variant with an 11 amino acid insertion resulting from translation of the remaining *rox*-site is expressed. In the absence of Dre, Roxed-Cre reduced unintended *loxP* recombination below detectable levels in all mCherry$^+$ cells, while appearing to be equally efficient as Cre when Dre was added to Roxed-Cre transfections (Figure 1.5).

In transgenic mice, Cre is typically employed to recombine hemizygous reporter genes or homozygous *loxP*-flanked conditional alleles. It has been shown that while

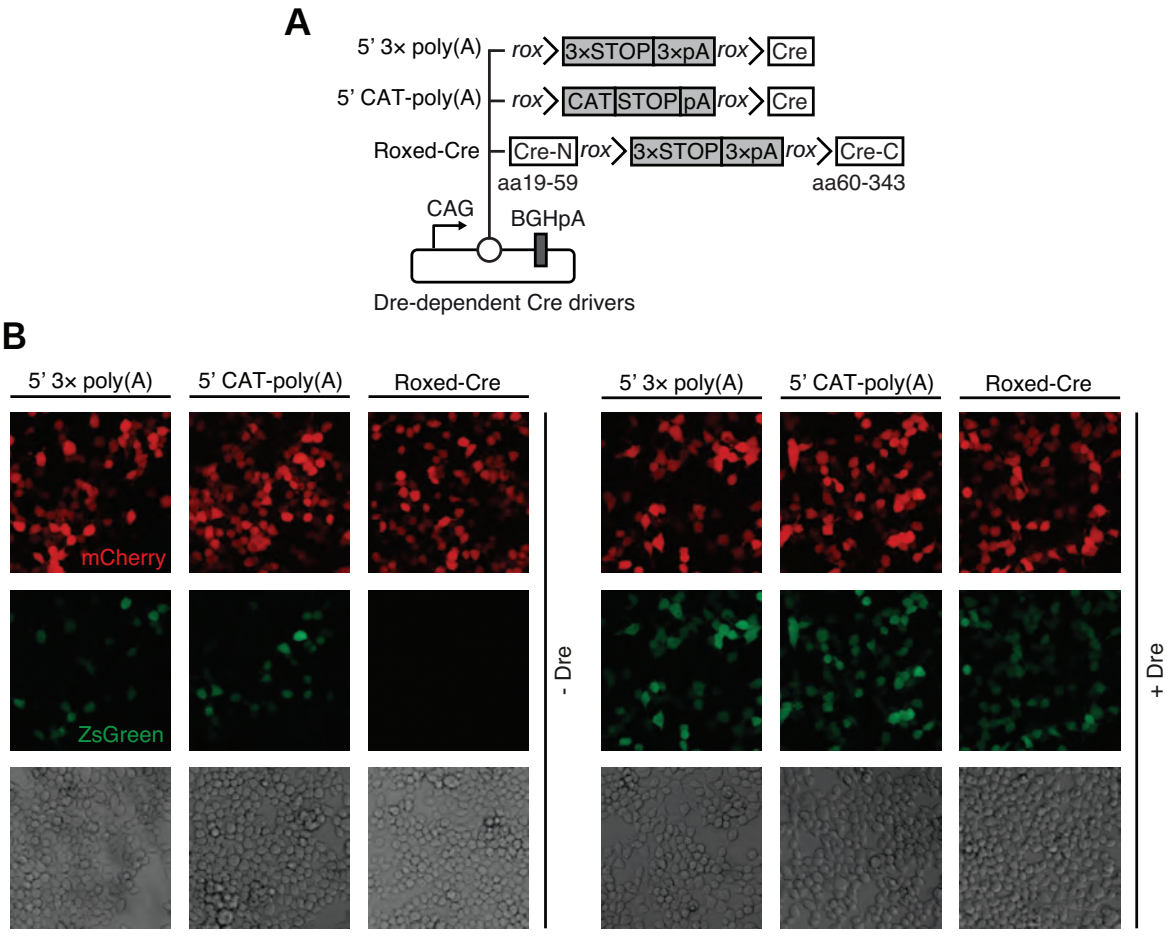


**Figure 1.4.: Dre-dependent activation of Cre.** (A) Diagram depicting Dre-dependent Cre driver candidates 5' 3× poly(A), 5' CAT-poly(A), and Roxed-Cre. (B) Fluorescence microscopic analysis 24h after transfection of HEK293T with Cre driver candidates alone (top panel, - Dre) or in combination with Dre (bottom panel, + Dre).

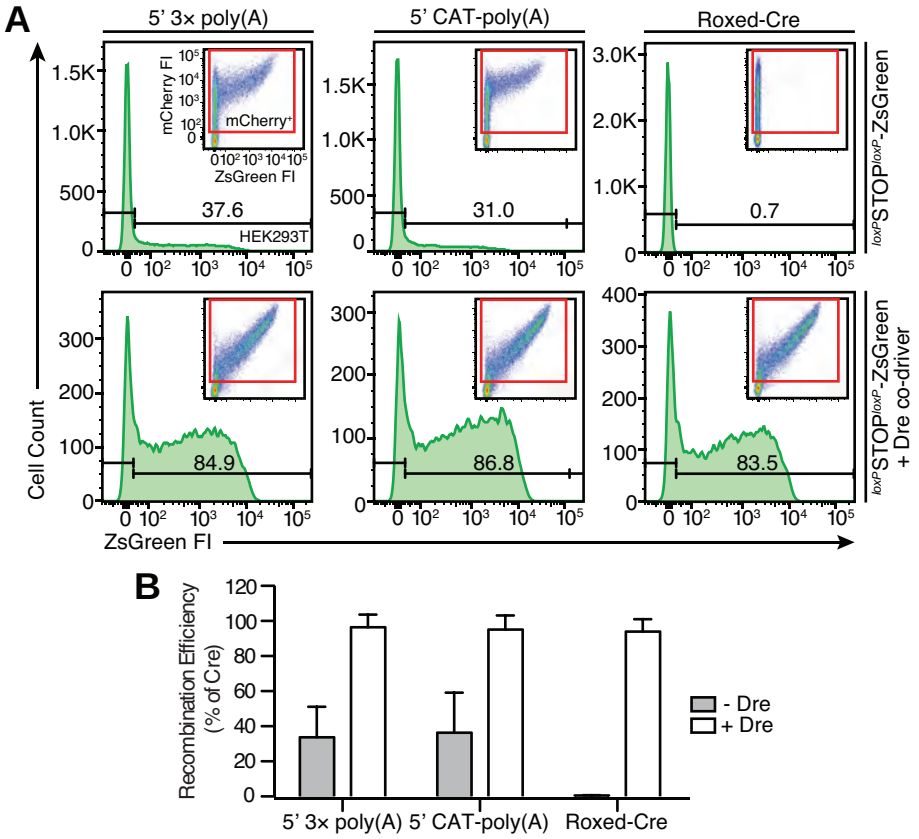


**Figure 1.5.: Quantitative assessment of Dre-dependent Cre driver candidates.** (A) Representative flow plots 24h after transfection of HEK293T cells with a *loxP*-flanked ZsGreen reporter, Cre-Driver candidates and either omitting (top row) or adding (bottom row) Dre. (B) Quantification of recombination activity of Cre driver candidates with or without Dre Co-Driver. Bars represent the percentage of transfected cells showing recombination activity. Average data of three independent experiments are shown with standard deviation and normalized to 100% Cre average recombination efficiency.

Cre maintains high activity on both plasmid-based and chromatin targets other recombinase systems such as FLP/*frt* are significantly less efficient in processing the latter (Andreas et al., 2002). In order to assess Co-Driver performance in an experimental environment that closely resembles in vivo conditions I established a mouse embryonic fibroblast (MEF) cell line that carries a single-copy Cre-inducible ZsGreen reporter (MEF-Ai6 derived from hemizygous Ai6 mice (Madisen et al., 2010), Figure 1.6A). MEF-Ai6 displayed green fluorescence with uniform intensity 72 hours after Co-Driver transfection (Figure 1.6B) as expected for a *ROSA26*-targeted reporter

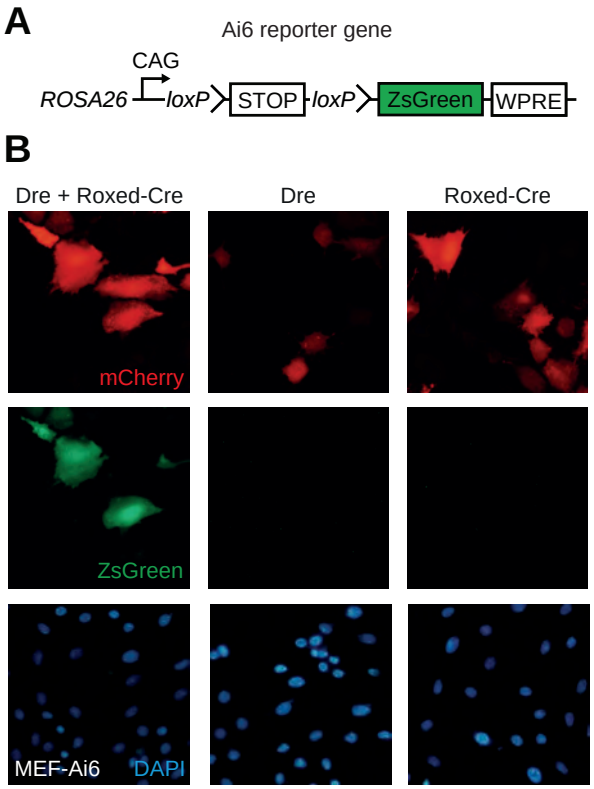


**Figure 1.6.: MEF-Ai6 - a cell line harboring a single-copy Cre-responsive fluorescent reporter.** (A) MEFs derived from hemizygous Ai6 reporter mice (MEF-Ai6) express ZsGreen from the single copy Ai6 transgene upon STOP-cassette excision by Cre (WPRE, woodchuck hepatitis virus post-transcriptional regulatory element). (B) Fluorescence microscopy analysis of MEF-Ai6 72h after transfection with either both or single Co-Driver components, Dre and Roxed-Cre. Nuclei of individual transfected cells were identified using DAPI staining.

(Soriano, 1999). As expected from the observations with a plasmid-based Cre reporter in HEK293T, transfections of MEF-Ai6 with single Co-Driver components did not result in detectable ZsGreen fluorescence.

When MEF-Ai6 transfected with Cre were analyzed by flow cytometry ZsGreen-positive cells showed a homogeneous fluorescent intensity consistent with the microscopic observations (Figure 1.7A). Flow cytometric analysis of MEF-Ai6 72h post-transfection confirmed that only combined but not individual Co-Driver modules, Dre and Roxed-Cre, induce ZsGreen expression (Figure 1.7B). The correct processing of the Ai6 allele was also clearly evidenced by PCR analysis (Figure 1.7C).

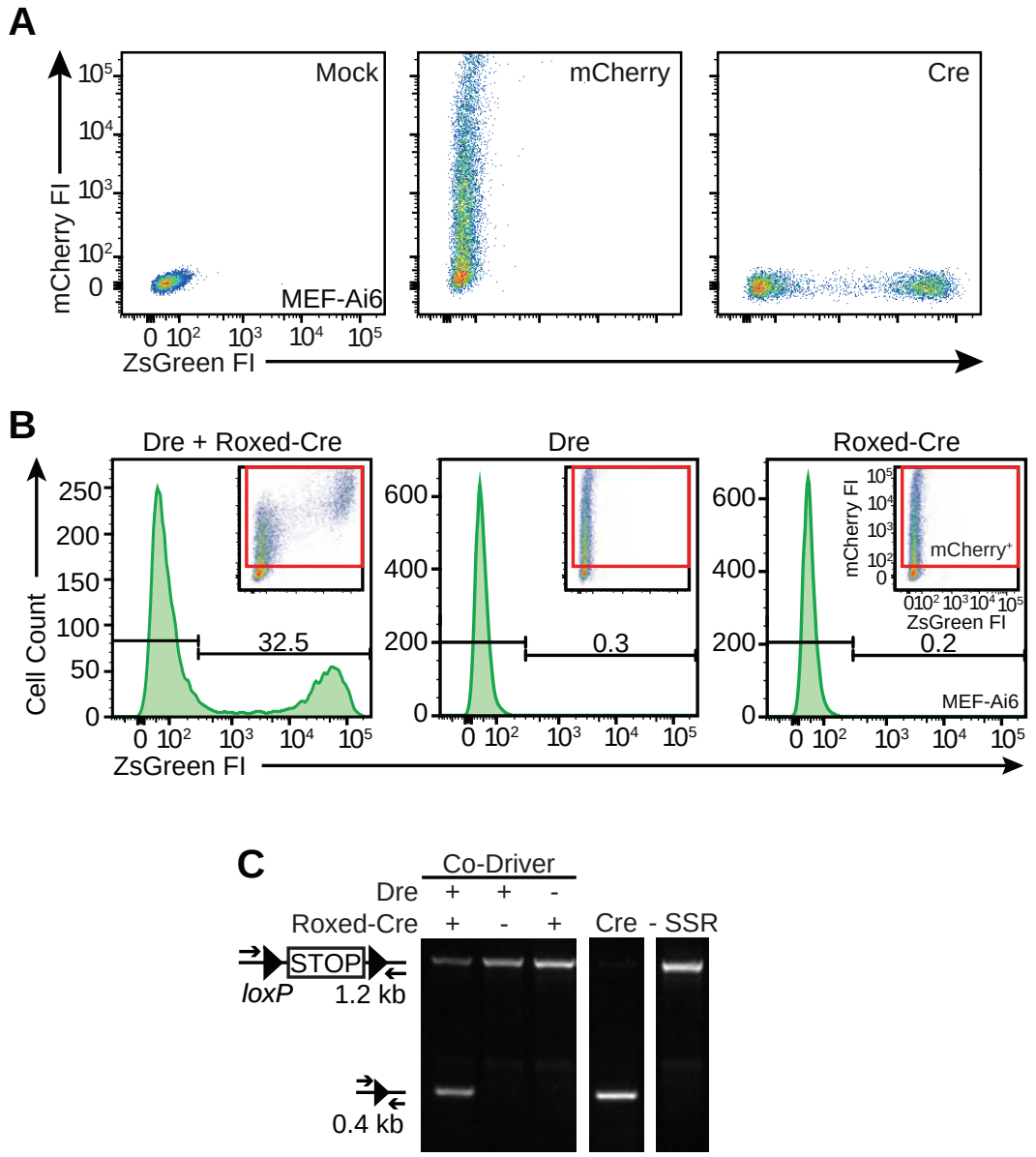


**Figure 1.7.: Quantitative analysis of Co-Driver activity in the MEF-Ai6 reporter cell line.** (A) mCherry and ZsGreen (induced by transfection of Cre) single color controls for flow cytometric analysis of transfected MEF-Ai6. Recombination activity of paired or single Co-Driver components, Dre and Roxed-Cre, in MEF-Ai6 72 h after transfection was assessed by (B) flow cytometric quantification of ZsGreen-positive cells (percentage shown in flow plots) and (C) by PCR analysis of the Ai6 reporter gene for Cre-induced excision of the STOP-cassette. Primer binding sites are located outside of the *loxP*-flanked STOP-cassette. Excision of the STOP-cassette is detected by the presence of a 0.4 kb PCR fragment, while a larger-sized PCR fragment of 1.2 kb is generated from the unmodified Ai6 gene.

### 1.3.3. Co-InCre - seamless Cre reconstitution

Besides my attempts to identify the optimal sequential binary SSR configuration I was also interested in constructing a coincidental binary SSR with high recombination efficiency. All previously published coincidental Binary SSRs (Jullien et al., 2007; Hirrlinger et al., 2009b; Wang et al., 2012) as well as the sequential Co-Driver system generate Cre-variants with insertions of non-native amino acid sequences in-between Cre amino acids 59 and 60. Although this has not been studied in detail for most Binary SSRs, these insertions together with low efficiency of Cre reconstitution potentially have a negative effect on the activity of the respective Cre variants. Therefore an alternative reconstitution domain providing fast kinetics as well as seamless reassembly of native Cre would be highly desirable.

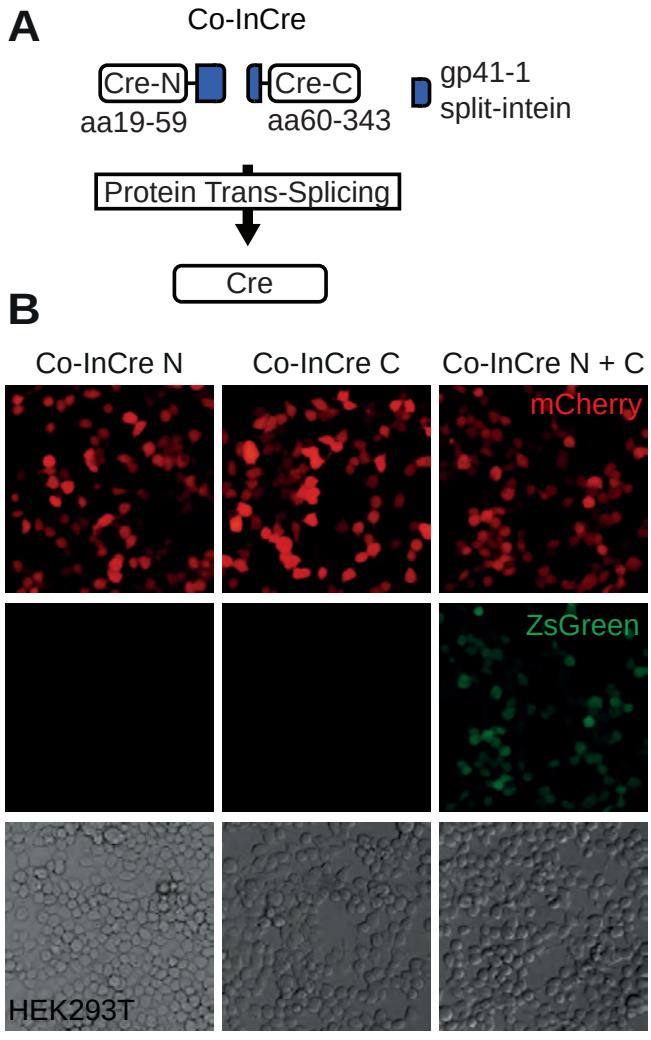


**Figure 1.8: Co-InCre - a coincidental Binary SSR based on split-inteins.** (A) Diagram depicting the configuration of the N-terminal and C-terminal Co-InCre fragments, which facilitate Cre reconstitution by seamless protein-trans-splicing. (B) Fluorescence microscopy images of HEK293T 24 h after transfection with a constitutively active mCherry plasmid, a Cre-inducible ZsGreen reporter and either combined or individual Co-InCre components.

Here, I capitalized on the recently described gp41-1 split-intein (Carvajal-Vallejos et al., 2012; Dassa et al., 2009) to construct Co-InCre (Figure 1.8A). Co-InCre reconstitutes Cre by protein-trans-splicing akin to the previously described split-intein-split-Cre (Wang et al., 2012). gp41-1 exhibits the highest trans-splicing activity at 37℃ of all split-inteins described to date and does not require any native extein sequences to catalyze this reaction (Carvajal-Vallejos et al., 2012). Initial fluorescence microscopy analysis of transfected HEK293T cells showed Cre activity only when both Co-InCre N- and C-terminal fragments were present. Single components did not elicit any detectable recombination-induced ZsGreen reporter expression (Figure 1.8B). These observations could be confirmed by flow cytometry (Figure 1.9).

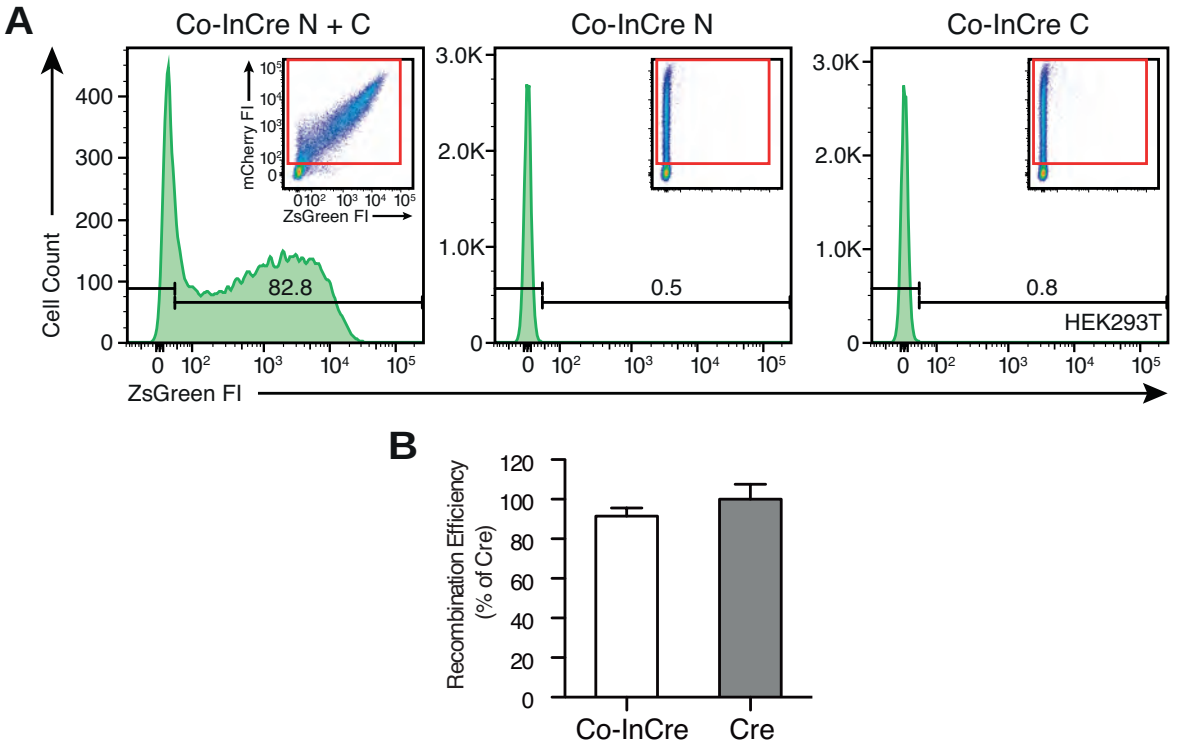


**Figure 1.9.: Flow cytometric analysis of Co-InCre recombination activity.** (A) Flow cytometric analysis 24 h after transfection of HEK293T with a constitutively active mCherry plasmid, a Cre-inducible ZsGreen reporter and either combined or single Co-InCre components. (B) Quantification of Co-InCre recombination efficiency in HEK293T. Average data of three independent experiments are shown with standard deviation and normalized to 100% Cre average recombination efficiency.

Co-transfection of Co-InCre components resulted in a high percentage of recombination-positive cells with over 80% of the efficiency of Cre, while single Co-InCre N or Co-InCre C transfections showed less than 1% of ZsGreen-positive cells. High activity as well as low background recombination levels of single Co-InCre modules was also observed in transfected MEF-Ai6 cells (Figure 1.10) that were analyzed by microscopy, flow cytometry, and a PCR indicating the excision of the Ai6 STOP cassette.

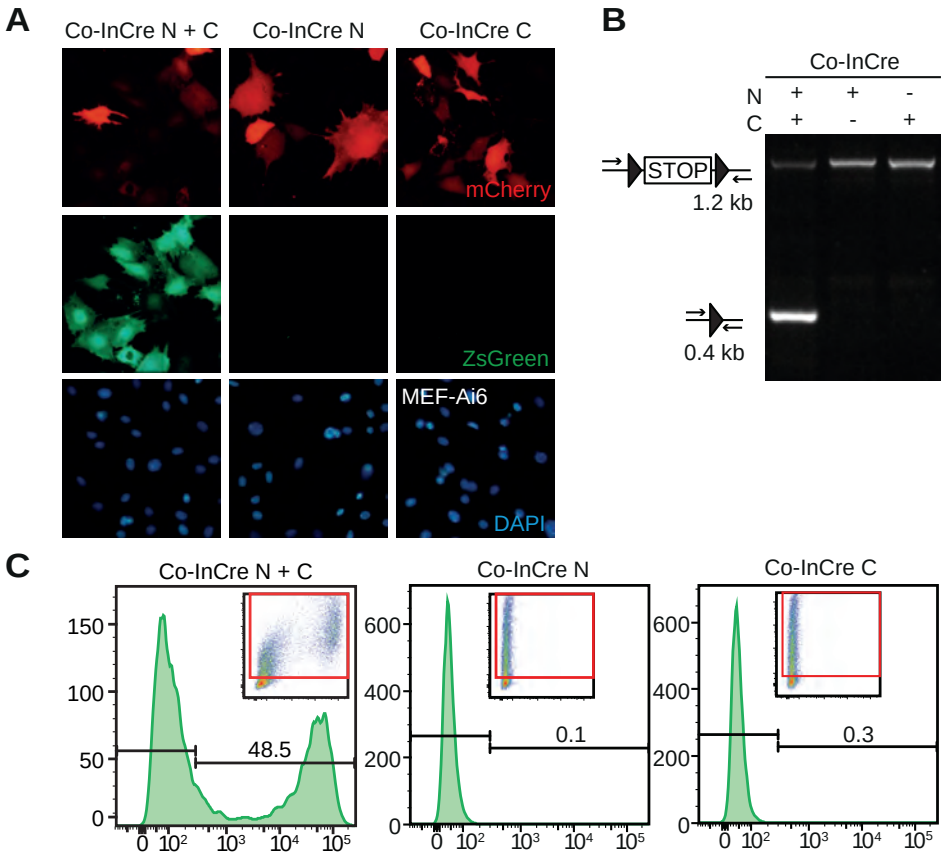


**Figure 1.10.: Co-InCre-mediated recombination of the single-copy Ai6 reporter gene.** MEF-Ai6 were analyzed 72h after transfection with either both or single Co-InCre modules. (A) Fluorescence microscopy images, nuclei of individual transfected cells were identified using DAPI staining. (B) PCR analysis of the Ai6 reporter gene. Primer binding sites are located outside of the *loxP*-flanked STOP-cassette. Excision of the STOP-cassette is detected by the presence of a 0.4 kb PCR fragment, while a larger-sized PCR fragment of 1.2 kb is generated from the unmodified Ai6 gene. (C) Flow cytometric analysis showing the percentage of recombination-positive MEF-Ai6 cells.

### 1.3.4. Co-Driver & Co-InCre are highly efficient binary SSRs

Having established that both Co-Driver and Co-InCre are obligate binary SSRs I went on to evaluate their performance in relation to Cre and other binary SSR systems. I first asked how efficiently the Cre variant translated from Dre-processed Roxed-Cre (CreRox60-70), the final output of the Co-Driver cascade, would process the Ai6 reporter gene. In transfected MEF-Ai6, CreRox60-70 (expressed from a construct mimicking complete processing of Roxed-Cre plasmids by Dre) showed a 30-40% lower recombination activity than native Cre (Figure 1.11). Since the Co-Driver strategy (Figure 1.12A) seems to achieve tight control of Cre expression at the expense of reduced Cre activity I considered an alternative SSR cascade that would yield native Cre upon primary SSR activity and thus potentially higher binary recombination efficiency.

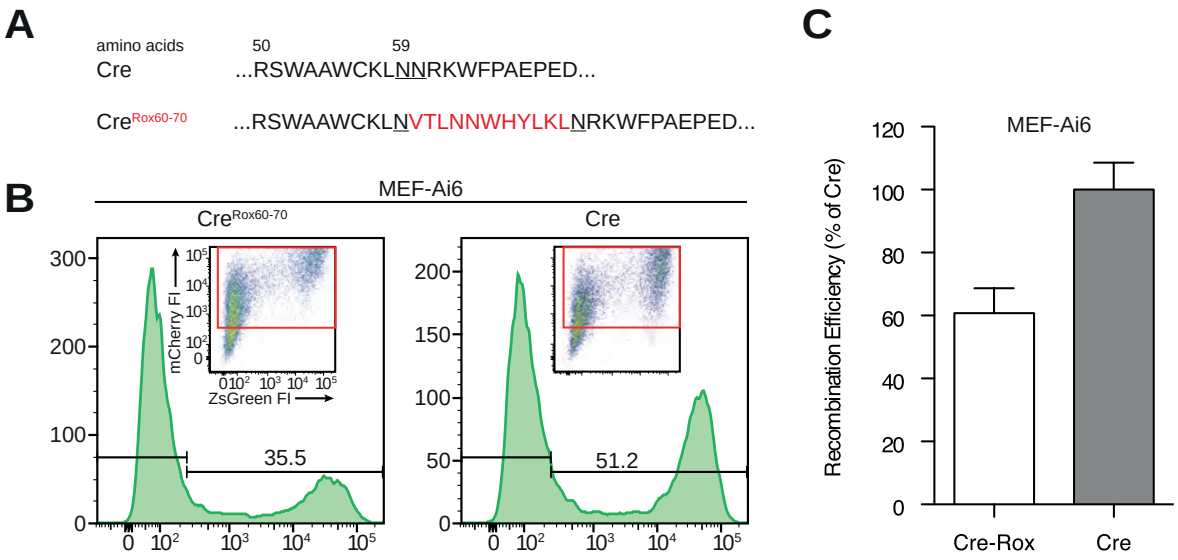


**Figure 1.11.: Effect of translated *rox*-site in the Co-Driver component Roxed-Cre.** (A) Amino acid changes introduced in CreRox$^{60\text{-}70}$ (the resulting Cre variant expressed from Dre-processed Roxed-Cre). (B) Flow cytometric analysis of CreRox$^{60\text{-}70}$ SSR activity in MEF-Ai6 cells. (C) Quantification of CreRox$^{60\text{-}70}$ recombination efficiency. Average data of three independent experiments are shown with standard deviation and normalized to 100% Cre average recombination efficiency.

Here, I capitalized on the unidirectional inversion mechanism of the serine recombinase Bxb1 (Figure 1.12A). I designed a Bxb1-responsive Cre expression construct based on the reverse complementary (rc) Cre DNA sequence flanked by Bxb1 *attB* and *attP* recognition sites in head-to-head orientation. Once rcCre is placed downstream of a promoter Cre recombinase can only be expressed upon Bxb1-mediated inversion of the Cre protein-coding sequence into the correct transcriptional orientation.

After having constructed Co-Driver, Bxb1-rcCre, and Co-InCre I also cloned the previously published coincidental Binary SSRs Split-Cre (Hirrlinger et al., 2009b, based on Cre complementation) and split-intein-split-Cre (Wang et al., 2012, based on protein-trans-splicing) into my standard expression vector (Figure 1.12B). Thus similar expression levels for all binary components should be achieved allowing the unbiased comparison of the recombination efficiencies of all systems. All Binary SSRs and native Cre were transfected into MEF-Ai6 and recombination efficiency was assessed using flow cytometry (Figure 1.12C). Similar to the comparison of Co-Driver SSR candidates, I analyzed subsets of mCherry$^{+}$ MEF-Ai6 with low, medium, and high mCherry fluorescent intensities (Figure 1.12D).

Not surprisingly, none of the binary SSRs reached the recombination efficiency of Cre in mCherry$^{low}$ or mCherry$^{med}$ cell populations, however there were significant differences in performance between the individual systems (Figure 1.12D). In mCherry$^{low}$ cells, Co-Driver and Bxb1-rcCre showed about 20% of Cre efficiency, which was similar to split-intein-split-Cre and slightly above Split-Cre. Remarkably, Co-InCre was more than twice as active as any other binary SSR reaching more than 50% of Cre efficiency. Co-InCre also showed the highest performance in mCherry$^{med}$ cells with about 80% of Cre efficiency. Here, Co-Driver activity was superior to Split-Cre, while being slightly lower than Bxb1-rcCre and split-intein-split-Cre. Thus, a considerable gain in efficiency at low expression levels could be achieved by the seamless protein trans-splicing of Co-InCre.

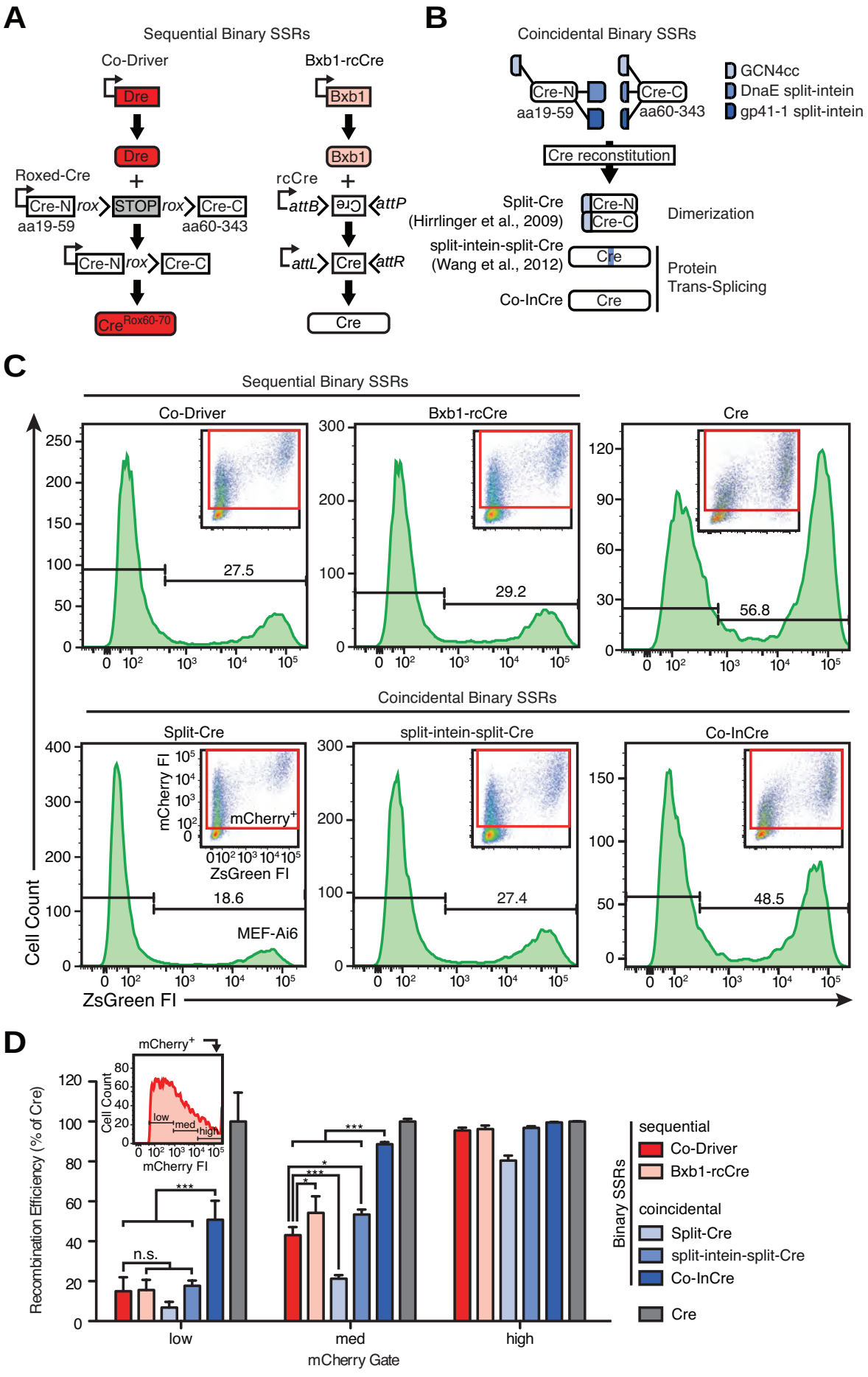
A
Sequential Binary SSRs
Co-Driver
Dre
Dre
Roxed-Cre
Cre-N
rox
STOP
rox
Cre-C
aa19-59
aa60-343
Cre-N
rox
Cre-C
Cre Rox60-70
Bxb1-rcCre
Bxb1
Bxb1
rcCre
attB
attP
attL
Cre
attR
Cre
B
Coincidental Binary SSRs
Cre-N
aa19-59
Cre-C
aa60-343
GCN4cc
DnaE split-intein
gp41-1 split-intein
Cre reconstitution
Split-Cre
(Hirrlinger et al., 2009)
Cre-N
Cre-C
Dimerization
split-intein-split-Cre
(Wang et al., 2012)
Cre
Co-InCre
Cre
Protein
Trans-Splicing
C
Sequential Binary SSRs
Co-Driver
Bxb1-rcCre
Cre
27.5
29.2
56.8
Coincidental Binary SSRs
Split-Cre
split-intein-split-Cre
Co-InCre
mCherry FI
mCherry+
ZsGreen FI
18.6
27.4
48.5
MEF-Ai6
Cell Count
ZsGreen FI
D
mCherry+
Cell Count
low
med
high
mCherry FI
Recombination Efficiency (% of Cre)
n.s.
***
*
low
med
high
mCherry Gate
Binary SSRs
sequential
Co-Driver
Bxb1-rcCre
coincidental
Split-Cre
split-intein-split-Cre
Co-InCre
Cre

**Figure 1.12.: Recombination efficiency of Co-Driver and Co-InCre.** (A) Diagrams depicting the sequential Binary SSR cascades of Co-Driver and Bxb1-rcCre. Rectangles with arrows represent expression constructs, rounded rectangles represent proteins. (B) Illustrations of coincidental Binary SSRs. Cre reconstitution domains are shown in different shades of blue for each system and references for earlier published systems are indicated. (C) MEF-Ai6 were transfected with a plasmid for constitutive mCherry expression and either two plasmids for the expression of both binary SSR modules or a single Cre plasmid. Representative flow plots 72 h post-transfection show the percentage of transfected cells with recombination activity. Insets show gating for transfected cells. (E) Recombination efficiency, defined as ratio of mCherry$^+$ cells showing ZsGreen-expression, was determined in subsets of mCherry$^+$ cells with low, medium (med), or high mCherry FI (gating within the mCherry$^+$ gate is shown in the graph). Binary SSRs with sequential or coincidental mode of action are color-coded in shades of red, or blue, respectively. Average data of three independent experiments are shown with standard deviation and normalized to 100% Cre recombination efficiency. Statistics: two-way ANOVA with Bonferroni post-hoc test; n.s., not significant; *$p < 0.05$; **$p < 0.01$; ***$p < 0.001$.

Bxb1-rcCre on the other hand only permitted an increased SSR activity relative to Co-Driver in cells with higher expression levels. In cells with the highest levels of mCherry fluorescent intensity basically all cells expressed ZsGreen as a result of Binary SSR activity with the exception of Split-Cre indicating that Cre activation mechanisms based on by protein-trans-splicing or excision of an internal STOP cassette are generally superior to Cre complementation.

### 1.3.5. Binary SSR activity in the developing mouse neocortex

The utility of SSRs for *in vivo* conditional transgenesis depends on their functionality within rapidly changing cellular environments during organogenesis or differentiation processes on-going during adulthood. In the developing mouse neocortex, heterogeneous populations of progenitor cells residing in the ventricular (VZ) and the subventricular zone (SVZ) start to produce neurons around embryonic day (E)10.5. Corticogenesis proceeds in an “inside-out” fashion, i.e. neocortical layer VI is established first, followed by layers V, IV and lastly layers II/III (Greig et al., 2013). After neurogenesis is completed around E16.5, progenitors start to generate astrocytes and oligodendrocytes (Greig et al., 2013; Kriegstein and Alvarez-Buylla, 2009).

Between E12.5 and E16.5, VZ progenitor cells can be transiently transfected using *in utero* electroporation of mouse embryos (Saito and Nakatsuji, 2001; Tabata and Nakajima, 2001). Here, progenitors receive a limited number of plasmid copies, which, upon cell division, are inherited by daughter cells. While gene expression from introduced plasmid DNA is remarkably stable in postmitotic cells, it is rapidly lost in dividing progenitors, probably due to the successive loss of the extrachromosomal plasmids with each cell division. As a result neural cells differentiating shortly after electroporation will show the highest level of transgene expression while those born later only show low levels or no expression at all. Neurons born before the time point of electroporation will not receive any plasmid DNA and as a consequence will

not express the transgene. Depending on the embryonic stage at which electroporation is performed the progeny of the transfected progenitors will populate specific cortical layers and express one or multiple introduced transgenes in the adult brain (Saito and Nakatsuji, 2001; Tabata and Nakajima, 2001; Langevin et al., 2007).

To evaluate the full recombination potential of the novel binary SSRs *in vivo*, CAG-driven Co-Driver or Co-InCre plasmids were electroporated together with a CAG-driven EGFP plasmid into the embryonic (E14.5) brains of Ai14 tdTomato reporter mice (Madisen et al., 2010) (Figure 1.13A). All *in utero* electroporations were performed by Hendrik Wildner at the Institute of Neuropharmacology, University of Zurich. I identified electroporation-positive brain areas in postnatal mice (P9-P10, Figure 1.13B) and imaged coronal brain sections for $EGFP^+$ and $tdTomato^+$ cells using confocal microscopy (Figure 1.13C-F). Confirming my previous observations in transfected MEF-Ai6 cells, single binary SSR modules (Figure 1.13C, E) did not trigger any detectable tdTomato expression over a time period of more than two weeks following electroporation. Brains of mice electroporated with binary Co-Driver or Co-InCre showed extensive tdTomato-fluorescence in the transfected hemispheres with the vast majority of positive cells being found in upper cortical layers (Figure 1.13C, E). High magnification images revealed that $tdTomato^+$ cells substantially outnumbered those that were $EGFP^+$ (Figure 1.13D) indicating that cells, which had received a number of plasmid copies below the threshold for EGFP detection, were nevertheless able to produce amounts of Cre that were sufficient for the processing of the Ai14 reporter gene. In all mice analyzed, gross morphology of the cortex appeared normal. Fluorescently labeled neurons projected locally to neurons of deeper cortical layers as well as through the corpus callosum (Figure 1.13D) towards distal regions in the contralateral hemisphere. Thus, Co-Driver and Co-InCre activity was well tolerated by neuronal populations and their precursor cells in the developing mouse brain.

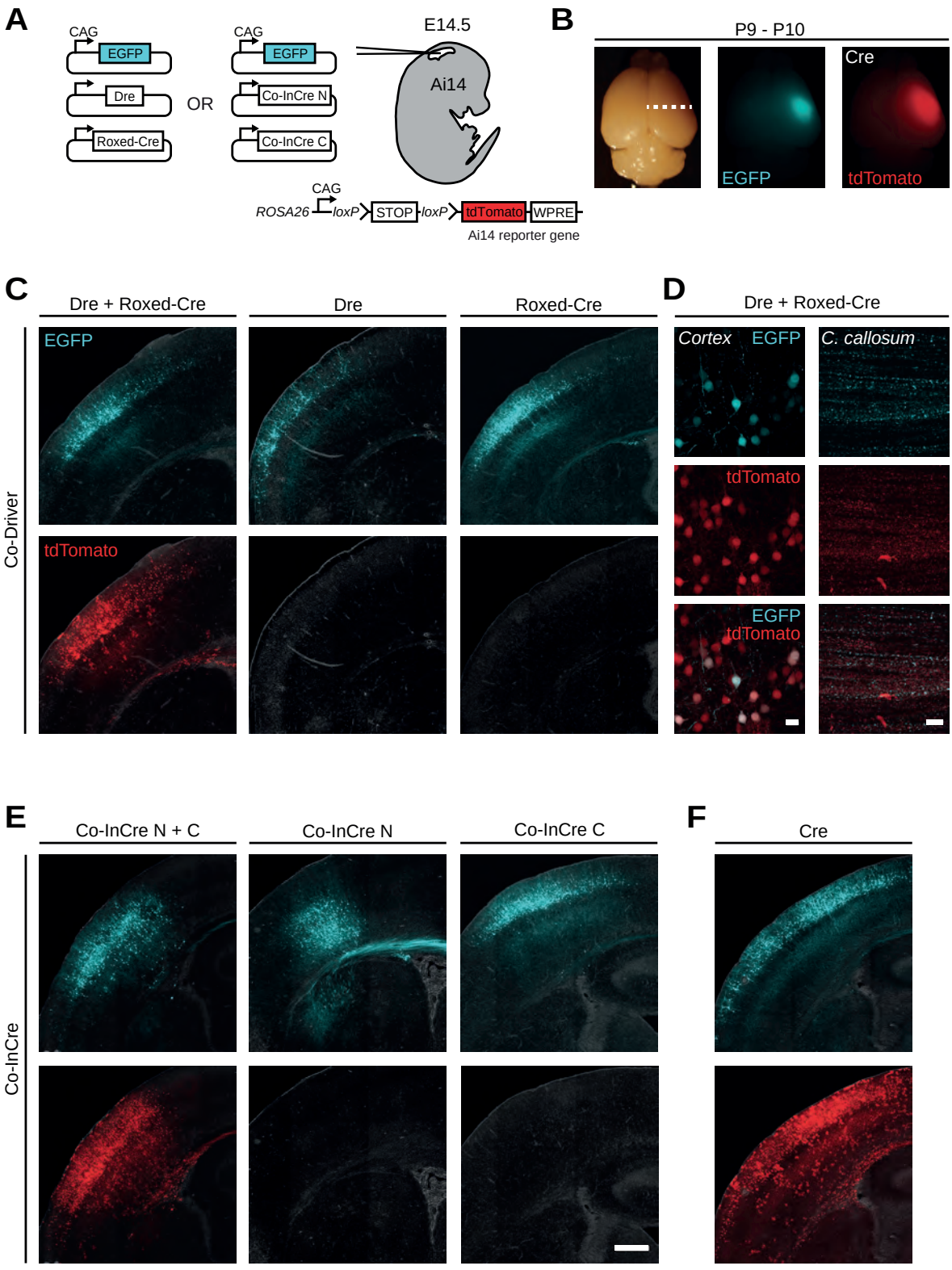
A
CAG
EGFP
Dre
Roxed-Cre
OR
CAG
EGFP
Co-InCre N
Co-InCre C
E14.5
Ai14
CAG
ROSA26
loxP
STOP
loxP
tdTomato
WPRE
Ai14 reporter gene
B
P9 - P10
Cre
EGFP
tdTomato
C
Dre + Roxed-Cre
Dre
Roxed-Cre
Co-Driver
EGFP
tdTomato
D
Dre + Roxed-Cre
Cortex
EGFP
C. callosum
tdTomato
EGFP
tdTomato
E
Co-InCre N + C
Co-InCre N
Co-InCre C
Co-InCre
F
Cre

**Figure 1.13.: Co-Driver and Co-InCre trigger efficient recombination in the developing mouse brain.** (A) Diagrams depicting plasmid combinations introduced into the embryonic brain of Ai14 reporter by *in utero* electroporation (Ai14 reporter gene is shown below mouse embryo, WPRE, woodchuck hepatitis virus post-transcriptional regulatory element). (B) Coronal sections of fluorescence-positive brain areas (white dashed line) were prepared from postnatal day 9-10 (P9-P10) mice. (C-F) Maximum intensity projections (MIP) of electroporation-positive brain areas. (C) Electroporations of combined and single Co-Driver components, Dre and Roxed-Cre. Fluorescent signals are merged with phase-contrast images of brain sections. (D) High magnification MIP of recombination-positive areas in the cortex and in the corpus (c.) callosum. (E) Electroporation of combined and individual Co-InCre modules. (F) Control electroporation using full-length Cre recombinase. Scale bar for panels (C), (E), and (F), 500 µm. Scale bars for panel (D), 20 µm.

### 1.3.6. Sequential expression of Co-Driver modules in the mouse neocortex

In a final series of experiments, I asked whether I could manipulate the output of Co-Driver, i.e. the timing and cell-type specificity of Cre recombination, by producing Dre and Roxed-Cre from distinct tissue-specific expression constructs. To address this question, I cloned Dre and Roxed-Cre into a human glia-fibrillary acidic protein (hGFAP)-promoter (Zhuo et al., 1997) cassette and the Thy1.2 expression cassette (Caroni, 1997) to generate hGFAP-Dre, hGFAP-Roxed-Cre, Thy1.2-Dre, and Thy1.2-Roxed-Cre constructs (Figure 1.14). I also attempted to track the activity of the Dre-driving promoter in the adult brain to gain insights into the individual contribution of the hGFAP and Thy1.2 expression profiles to the final Co-Driver output. Therefore, I fused Dre to the porcine teschovirus-1 (P)2A sequence (Szymczak et al., 2004) and the blue fluorescent protein, mTagBFP (Subach et al., 2008). This strategy should allow blue-fluorescent labeling of cells, which express Dre at the time point of analysis in parallel with assessing Co-Driver-mediated processing of the Ai14 reporter gene.

hGFAP-Cre transgenic mice express Cre in radial glia, the principal VZ precursor cells, between E13-E17 and in the adult brain in astrocytes but not in neurons or oligodendrocytes (Malatesta et al., 2003). Since radial glia give rise to neurons, astrocytes, and oligodendrocytes, activation of a Cre-dependent reporter allele in

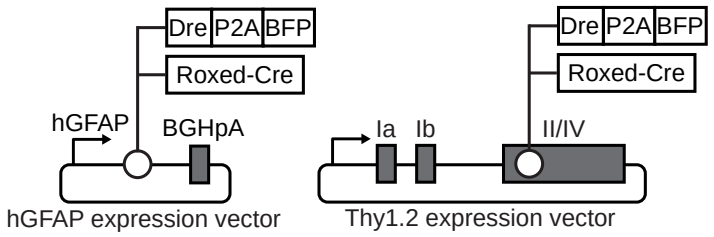


**Figure 1.14.: Construction of human (h)GFAP and Thy1.2 Co-Driver expression vectors.** Promoter sequences are indicated by arrows, other sequences by grey boxes, and exons are denoted by roman numerals.

radial glia results in labeling of all three cell lineages in the adult brain. In the postnatal mouse neocortex, Thy1.2-driven fluorescent proteins can be detected in neurons throughout cortical layers II-VI (Feng et al., 2000) and two lines of Thy1.2-brainbow mice showed expression in astrocytes (Livet et al., 2007). For a large number of transgenic lines, Thy1.2-driven transgenes have been reported to reach detectable expression levels in the postnatal brain (Caroni, 1997; Feng et al., 2000; Kelley et al., 1994). However, several lines of Thy1.2-Cre mice already showed reporter gene activation during embryonic development (Campsall et al., 2002).

In a first step, I assessed the expression profiles of single Thy1.2- and hGFAP-driven Roxed-Cre plasmids by combining each of them with the continuously expressing CAG-Dre construct (Figure 1.15). In the postnatal brains of Ai14 mice that were electroporated at E14.5 with CAG-Dre, Thy1.2-Roxed-Cre and CAG-EGFP, recombination was restricted to $NeuN^+$ cortical neurons, which typically also exhibited EGFP fluorescence (Figure 1.15B). Combining CAG-Dre with hGFAP-Roxed-Cre resulted in a more extensive pattern of recombination within and beyond the area of $EGFP^+$ cells. Here, I observed tdTomato-labeling of $NeuN^+$ neurons and $NeuN^-$ cells morphologically resembling astrocytes in the cortex and $tdTomato^+$ $NeuN^-$ cells in proximity of the corpus callosum (Figure 1.15C).

In a final series of experiments the Co-Driver pairs, hGFAP-Dre with Thy1.2-Roxed-Cre (hGFAP $\Rightarrow$ Thy1.2) and Thy1.2-Dre with hGFAP-Roxed-Cre (Thy1.2 $\Rightarrow$ hGFAP), were introduced into the embryonic mouse brain. Confocal imaging of postnatal coronal brain sections consistently showed reporter gene activation by both Co-Driver pairs. However, there was a remarkable difference in the lineage identity and radial positions of $tdTomato^+$ cells relative to $EGFP^+$ cells for hGFAP $\Rightarrow$ Thy1.2 and Thy1.2 $\Rightarrow$ hGFAP electroporations, respectively (Figure 1.16). In hGFAP $\Rightarrow$ Thy1.2-electroporated brains the vast majority of $tdTomato^+$ cells stained positive for NeuN (Figure 1.17) and large numbers of these neurons either showed EGFP fluorescence themselves or occupied similar radial positions relative to their $EGFP^+$ neighbors (Figure 1.16B).

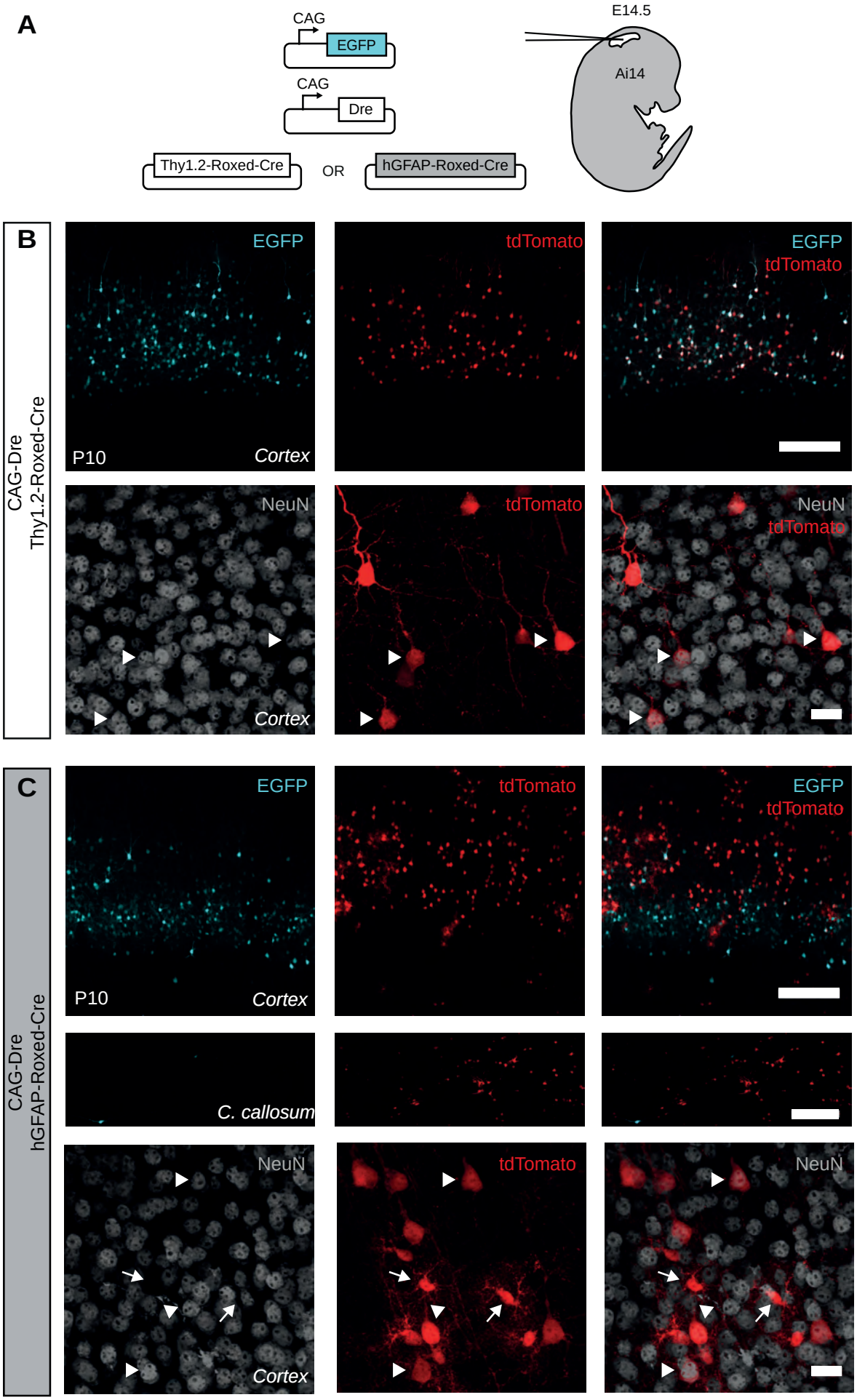
A
CAG
EGFP
CAG
Dre
Thy1.2-Roxed-Cre
OR
hGFAP-Roxed-Cre
E14.5
Ai14
B
CAG-Dre
Thy1.2-Roxed-Cre
EGFP
tdTomato
EGFP
tdTomato
P10
Cortex
NeuN
tdTomato
NeuN
tdTomato
Cortex
C
CAG-Dre
hGFAP-Roxed-Cre
EGFP
tdTomato
EGFP
tdTomato
P10
Cortex
C. callosum
NeuN
tdTomato
NeuN
Cortex

**Figure 1.15.: Cell type specificity of human GFAP and Thy1.2 constructs.** (A) Embryos carrying the Ai14 reporter gene were electroporated with constitutively expressing EGFP and Dre plasmids in combination with (B) Thy1.2-Roxed-Cre or (C) hGFAP-Roxed-Cre. Representative low magnification single-plane confocal images of fluorescence-positive areas within the cortex and additionally for (B) in proximity to the corpus (c.) callosum of postnatal day (P)10 mice are shown (top rows within each panel). High magnification maximum intensity projections (MIP) (bottom rows within each panel) show tdTomato-positive cells and staining for neuronal nuclei (NeuN) within the cortex. Arrow heads denote tdTomato- fluorescent cells with positive NeuN-staining. Arrows denote tdTomato-positive cells that are negative for NeuN. Scale bar low magnification, 200 μm; high magnification, 20 μm.

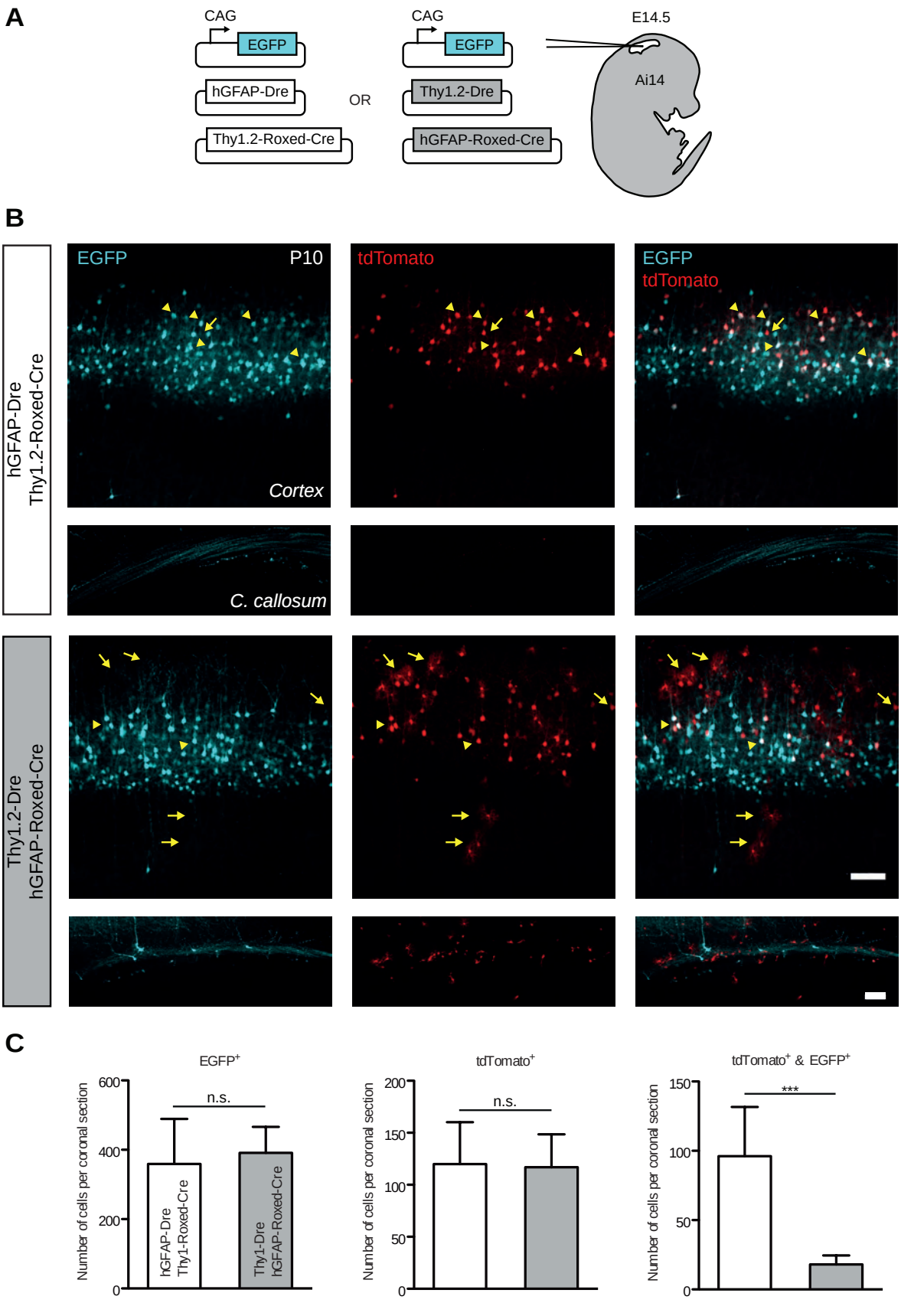
A
CAG
EGFP
hGFAP-Dre
Thy1.2-Roxed-Cre
OR
CAG
EGFP
Thy1.2-Dre
hGFAP-Roxed-Cre
E14.5
Ai14
B
hGFAP-Dre
Thy1.2-Roxed-Cre
EGFP
P10
Cortex
tdTomato
EGFP
tdTomato
C. callosum
Thy1.2-Dre
hGFAP-Roxed-Cre
C
EGFP+
n.s.
Number of cells per coronal section
600
400
200
0
hGFAP-Dre
Thy1-Roxed-Cre
Thy1-Dre
hGFAP-Roxed-Cre
tdTomato+
n.s.
200
150
100
50
0
tdTomato+ & EGFP+
***
150
100
50
0

**Figure 1.16.: Sequential expression of Co-Driver components in the developing mouse neocortex.** (A) E14.5 embryos carrying a single-copy Cre-inducible tdTomato reporter gene (Ai14) were electroporated with a constitutively expressing EGFP plasmid and either hGFAP-Dre with Thy1.2-Roxed-Cre (white rectangles) or Thy1.2-Dre with hGFAP- Roxed-Cre (gray rectangles). (B) Representative single-plane confocal images of fluorescence-positive areas within the cortex and MIP of areas in proximity to the corpus (c.) callosum of post-natal day (P)10 mice are shown (top panel, hGFAP-Dre with Thy1.2-Roxed-Cre electroporations; bottom panel, Thy1.2-Dre with hGFAP-Roxed-Cre electroporations). Arrow heads denote cells within the cortex that show both EGFP and tdTomato fluorescence, arrows denote cells with single tdTomato fluorescence. Scale bars, 100mm. (C) Quantification of EGFP-positive cells (left), tdTomato-positive cells (middle) and tdTomato/EGFP double-positive cells (right) in coronal brain sections. Average data of three animals and three coronal sections per animal with standard deviation are shown. Statistics: unpaired Student's t-test; ***P < 0.001.

Thy1.2 ⇒ hGFAP on the other hand targeted tdTomato expression predominantly to EGFP$^{-}$ cells with tdTomato$^{+}$ NeuN$^{+}$ neurons occupying positions closer to the pial surface and tdTomato$^{+}$ NeuN$^{-}$ non-neuronal cells residing also in lower cortical layers and in the white matter proximal to EGFP$^{+}$ fibers of callosal projection neurons (Figure 1.16B, Figure 1.17).

While both hGFAP- and Thy1.2-constructs seemed to reliably produce sufficient amounts of Dre I was unable to detect BFP fluorescence in postnatal brains indicating that at the time of analysis the respective activity of neither promoter was sufficient to generate detectable amounts of BFP. In order to substantiate the qualitative assessment of Cre recombination patterns, I quantified the numbers of EGFP$^{+}$

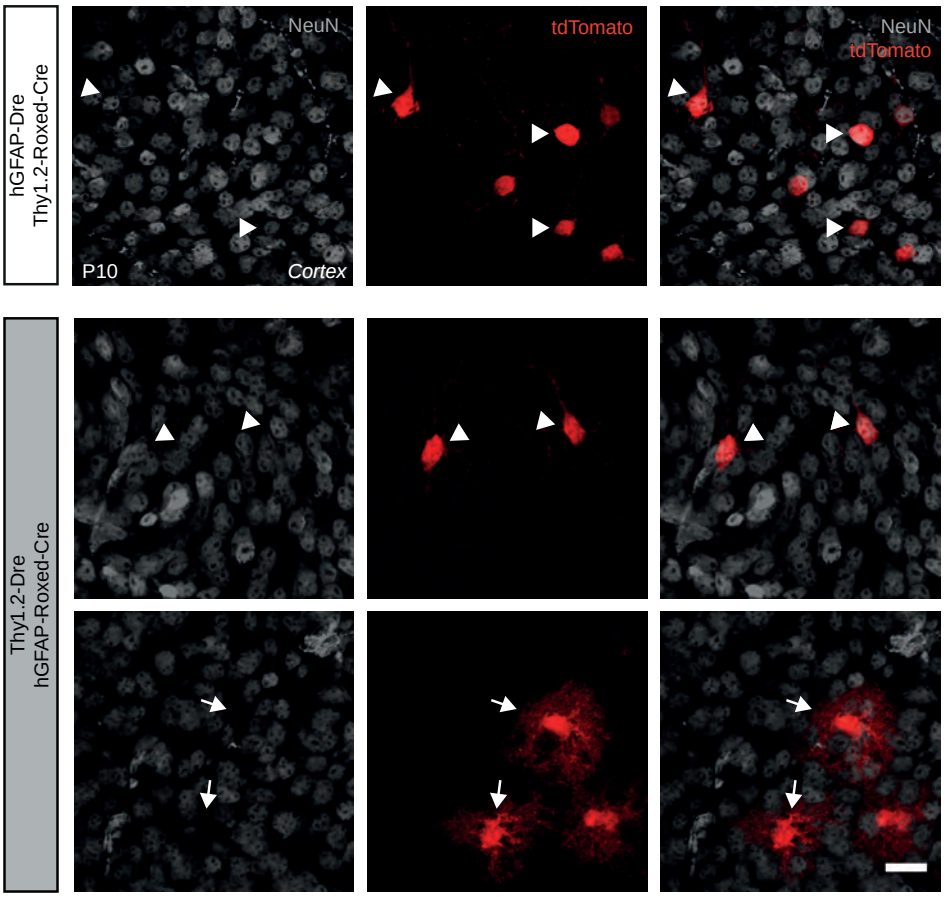


**Figure 1.17.: Neuronal marker expression in cells labeled by sequential Co-Driver activation.** Representative high magnification MIP of electroporation-positive areas are shown. Arrow heads denote tdTomato-fluorescent cells with positive NeuN-staining. Arrows denote tdTomato-positive cells that are negative for NeuN. Scale bar, 20 μm.

cells, tdTomato$^+$ cells, and EGFP$^+$ tdTomato$^+$ cells in electroporation-positive coronal brain sections that were randomly selected along the rostral-caudal brain axis (3 brains for each Co-Driver pair with 3 sections per brain, Figure 1.16C). Cell counts per coronal section were similar for EGFP$^+$ cells (hGFAP $\Rightarrow$ Thy1.2, 359 ± 130 and Thy1.2 $\Rightarrow$ hGFAP, 391 ± 75) and tdTomato$^+$ (120 ± 40 and 117 ± 32), while there was a significantly higher number of cells showing cytoplasmic co-localization of EGFP and tdTomato in hGFAP $\Rightarrow$ Thy1.2 brain sections (96 ± 36 and 18 ± 7). Considering that expression of detectable levels of EGFP is restricted to cells born shortly after in utero electroporation was performed (Langevin et al., 2007) these observations suggest that the Thy1.2 $\Rightarrow$ hGFAP Co-Driver pair targeted reporter gene activation mainly to cells that were born later relative to the tdTomato$^+$ cells observed as a result of hGFAP $\Rightarrow$ Thy1.2 Co-Driver activity.

# 1.4. Discussion

## 1.4.1. Implementation of sequential lineage tracing

The principal aim of this work was to design and validate binary SSR systems that can integrate the transcriptional profiles of a wide range of promoters and thus hold the potential to significantly increase the resolution of genetic lineage tracing. Co-Driver demonstrates for the first time the implementation of the sequential lineage tracing concept by using a cascade of two orthogonally active SSRs, which we termed sequential binary SSR. This concept relies on exploiting the temporal activity profiles of two individual promoters to create a genetic record in a distinct sub-population of a cell lineage.

The generation of a high fidelity binary SSR system requires the design of two modules that can only produce the desired output in combination but not individually. I challenged the individual Co-Driver modules Dre and Roxed-Cre in several biological systems such as transfected cell lines with plasmid-based or chromosomal Cre-dependent fluorescent reporters and in the developing brains of Cre reporter mice without detecting any spurious recombination events caused by either Dre or Roxed-Cre. Thus Co-Driver is essentially an obligate binary SSR, with production of functional Dre solely depending on the expression profile of the Dre-driving promoter, while active Cre is only produced when two conditions are fulfilled, 1) the Roxed-Cre gene has been processed by Dre and 2) the Roxed-Cre-driving promoter is transcriptionally active.

Tissue-specific promoters and expression cassettes harbor regulatory elements that exercise control over the cell-type specificity as well as the timing of gene expression. I could show that Co-Driver integrates both tissue-specific and temporal layers of control when Dre and Roxed-Cre are expressed from two promoters with non-identical transcriptional profiles. This directional mechanism of integrating transcriptional activities of two individual promoters was evident in the developing mouse

neocortex. Here, the combination of hGFAP and Thy1.2 expression constructs targeted activation of a Cre reporter gene to distinct cell populations depending on which expression construct harbored Dre or Roxed-Cre, respectively. While hGFAP-dependent Thy1.2-Roxed-Cre expression restricted reporter gene expression to neurons that were born shortly after these constructs were introduced into precursors by in utero electroporation, Thy1.2-dependent hGFAP-Roxed-Cre expression resulted in reporter gene activation in later-born neurons as well as cells of the glial lineages.

### 1.4.2. Novel binary SSRs & the established toolkit for mouse transgenesis

In terms of versatility, Co-Driver combines the advantages of two classes of previously published binary SSR systems. Co-Driver relies exclusively on Cre-dependent alleles to generate a binary output akin to Cre reconstitution systems (Hirrlinger et al., 2009b; Wang et al., 2012) thus making it compatible with a plethora of available Cre reporter lines (Madisen et al., 2010; Soriano, 1999; Livet et al., 2007; Schepers et al., 2012), diphtheria toxin-based responder mice for conditional cell ablation (Buch et al., 2005; Wu et al., 2006), and mice that harbor conditional knockout alleles (Skarnes et al., 2011). However, unlike these complementation systems that function best when similar amounts of the two inactive Cre precursor polypeptides are expressed, the Co-Driver cascade of two highly active SSRs should better tolerate a mismatch of transcriptional levels between the two driving promoters in a manner similar to Cre/Flp systems (Dymecki et al., 2010). Conversely, the Cre/Flp approach facilitates intersectional labeling of cells but relies on purpose-designed dual-stop-cassette reporters and thus cannot be combined with currently available Cre-responsive alleles.

In addition to Co-Driver, I have developed and characterized two additional obligate binary SSR systems. First, a binary SSR cascade could also be constructed using the alternative SSR pair Bxb1/Cre, which generates native Cre recombinase

upon Bxb1-mediated inversion of a reverse-complementary Cre expression cassette. Thus we provide evidence that construction of sequential binary SSRs is a generally applicable concept for potentially any combination of SSRs, which exhibit high individual recombination efficiencies and do not cross-react with each other's recognition sites. Linking SSRs in series could for example be used to connect several SSR-based genetic logic circuits (Bonnet et al., 2013; Siuti et al., 2013) to obtain higher order logic devices for synthetic biology applications in bacteria and mammalian cells.

Second, I have constructed Co-InCre, a coincidental binary SSR system employing highly active split-inteins to reconstitute a native Cre polypeptide from N- and C- terminal precursors upon their simultaneous expression. Co-InCre showed unprecedented activity particularly in low-expressing transfected cells with a 2.5-fold increase in recombination efficiency of a genomic target relative to other binary SSRs tested. The improvement in recombination efficiency of Co-InCre over the recently published DnaE-based split-intein-split-Cre (Wang et al., 2012) most likely results from the combined effects of higher expression levels facilitated by mammalian codon-optimized Cre (Shimshek et al., 2002) in combination with seamless and faster protein-splicing activity of the gp41-1 split-intein (Carvajal-Vallejos et al., 2012). In combination with simultaneously active promoters, Co-InCre most likely provides faster kinetics by reconstituting Cre on a protein level than sequential binary SSRs, which rely on two individual recombinases and thus on two subsequent cycles of transcription and translation.

### 1.4.3. Considerations for generating binary SSR-transgenic animals

Since its discovery, Cre recombinase has been unrivaled in creating tissue-specific driver lines and most complications observed in Cre-mediated conditional transgenesis seem to be related to the choice of promoters and design of expression cassettes

rather than intrinsic Cre SSR activity (Schmidt-Supprian and Rajewsky, 2007). My aim was to generate binary SSRs with the highest possible activity and therefore we focused on optimizing recombination efficiency in standardized model systems that allowed direct comparison with Cre. This strategy should result in dual-promoter-driven conditional transgenic animals that match the advantageous characteristics of many Cre driver lines. However, just as in the case of Cre, not every promoter combination will result in informative recombination patterns. Conversely, for certain populations of cells a strategy incorporating binary SSRs expressed from two strong yet intersectional promoters might be superior to Cre being controlled by a single promoter that is specific but low in transcriptional output.

The need for identifying cell sub-populations with an increased resolution is highlighted by the continuous improvements of histological methods (Gerner et al., 2012) and flow cytometry (Bendall et al., 2011) with the goal to increase the number of markers that can be analyzed simultaneously. I expect that high-resolution lineage tracing will complement these efforts with its unique capacity to create genetic records of developmental transitions. This will facilitate the inference of relationships between precursor and differentiated cells or cells that undergo transdifferentiation processes, which is difficult to conclude from immunodetection methods capturing only the current state of expressed markers. For certain biological questions temporal control of binary SSR function might be required. Ligand-dependent variants of all Co-Driver and Co-InCre components can be created with suitable solutions reported in the form of CreERT2 (Feil et al., 1997), DrePBD* (Anastassiadis et al., 2009), Split-CreERT2 (Hirrlinger et al., 2009a), and more recently trimethoprim-controlled destabilized Cre (Sando et al., 2013). Performing binary SSR-based lineage tracing requires the generation of mice that, including the Cre-responsive gene, harbor at least three transgenes. Recent advances in genome editing technologies (see also Chapter 2 of this thesis) such as combinations of ZFN (Cui et al., 2011; Hermann et al., 2012; Meyer et al., 2010) or TALEN (Wang et al., 2013a) with

plasmid-based targeting constructs promise the rapid generation of animals with targeted integration of Co-Driver or Co-InCre components into genomic loci providing suitable expression profiles. Potentially, a binary SSR founder animal can be produced in one step by CRISPR/Cas9-mediated multiplexed genome editing in the mouse embryo (Yang et al., 2013).

# 1.5. Methods

## Gene synthesis and template plasmids

Codon-optimized SSRs Bxb1, B3 and KD (Genscript) and gp41-1 and DnaE split-inteins (IDT) were gene-synthesized. DreO was a generous gift from C. Monetti. For the construction of Co-InCre expression plasmids codon-optimized Cre (iCre, Shimshek et al., 2002) was split into a N-terminal (aa 19-59) and a C-terminal (aa 60-343) fragment. Amino acid sequences for gp41-1N and gp41-1C split-intein fragments (Dassa et al., 2009) were back-translated using Emboss Backtranseq (http://www.ebi.ac.uk/Tools/st/emboss_backtranseq/) with mouse codon usage and fused to N- and C-terminal iCre fragments respectively.

The Roxed-Cre expression plasmid was constructed by introducing a *rox*-flanked STOP cassette (based on the STOP cassette of the Ai6 targeting construct, Madisen et al., 2010, Addgene plasmid 22798) in between iCre codons 177 (aa 59) and 180 (aa 60). A single nucleotide (G) was introduced 5' of the rox-site to create an in-frame insertion of 33 bp into the iCre open reading frame upon Dre recombination.

## Golden Gate cloning

All constructs for constitutive mammalian expression were assembled using Golden Gate cloning (Engler et al., 2008) of PCR products into a pCAG-T7 destination vector. The standard pCAG-T7 destination vector is based on the plasmid pCAG-RabZFN-L (a generous gift by R. Kühn, Meyer et al., 2012). The RabZFN-L CDS was excised using BglII and SacI. A BglII-Esp3I-LacZ-Esp3I-SacI fragment was generated using PCR with primer overhangs from pTAL4 (Cermak et al., 2011), digested with BglII and SacI and ligated with the linearized pCAG-T7 backbone generating the pCAG-T7 destination vector.

Esp3I digestion of the pCAG-T7 destination vector excises the LacZ cassette and generates a 3' GTGG overhang downstream of the CAG/T7 promoter and a 5' GTCA

overhang upstream of the polyadenylation signal. Single or multiple inserts for golden gate cloning into pCAG-T7 destination were generated by PCR using primers, which add Esp3I recognition sites and appropriate overhangs to the 5' and 3' ends of the PCR products. Primers were designed in a way that Esp3I digestion of PCR products always generates a 5' CACC overhang on the first insert and 3' CAGT overhang on the last insert, which each are compatible with the overhangs in the pCAG-T7 destination vector. Additional 4 bp overhangs required for the ligation of multiple inserts to each other are designed in a way that the 3' overhang of the first insert is compatible with the 5' overhang of the second insert and so on. Additionally, 4 bp overhangs for linking inserts 1 with 2 and 2 with 3 and so on were selected by the following design rules to avoid incorrect assembly of multiple fragments. All overhangs (including the overhangs compatible with the destination vector) should differ from each other in at least two subsequent bases and overhangs should be non-palindromic. PCR fragments for golden gate assembly were amplified using the proofreading polymerase Herculase (Agilent) and purified using either the QIAquick PCR Purification Kit or the QIAquick Gel Extraction Kit (both Qiagen).

Golden gate reactions were set up with (1) 75 ng or 150 ng of pCAG-T7 destination vector, (2) insert(s) in a 2:1 molar ratio to the destination plasmid, (3) 1x T4 ligase buffer (NEB), (4) T4 ligase (400 U, NEB), (5) Esp3I (10 U, Thermo Scientific). Golden Gate reactions were incubated in a thermocycler with the following program, (37℃/5 min, 16℃/10 min) 10-50 cycles, 50℃/5 min, 80℃/5 min.

## Standard cloning

hGFAP and Thy1.2 expression constructs were assembled using standard cloning techniques. hGFAP expression constructs are based on hGFAP-fLuc (Cho et al., 2009, Addgene plasmid 40589). The luciferase polyadenylation signal (pA) cassette was excised from hGFAP-fLuc using the restriction enzymes HindIII and BamHI. A

HindIII-EcoRI-Dre-P2A-BFP-pA-BglII insert was created by PCR with primer overhangs from the template pCAG-T7-Dre-P2A-BFP, digested with HindIII and BglII, and cloned into the HindIII/BamHI linearized hGFAP backbone to create hGFAP-Dre-P2A-BFP. Subsequently Dre-P2A-BFP-PA was excised using EcoRI and SalI and a EcoRI-Roxed-Cre-SalI fragment was inserted to create hGFAP-Roxed-Cre. Thy1.2 expression constructs are based on Thy1 promoter construct (Feng et al., 2000, Addgene plasmid 20736). The Thy1 promoter construct was linearized using XhoI and XhoI-flanked Dre-P2A-BFP or a SalI-flanked Roxed-Cre fragment was inserted to create Thy1.2-Dre-P2A-BFP and Thy1.2-Roxed-Cre, respectively.

All plasmids that were submitted for public distribution to Addgene are shown in Table A.1 in the Appendix.

## Transformation of *E. coli* and plasmid purification

Ligation reactions were desalted using drop dialysis with membrane filters (25 mm, pore size 0.025 µm, Millipore) on dd$H_2O$. Electrocompetent *E. coli* (Top10 Electrocomp, Life Technologies) were transformed using a MicroPulser electroporation apparatus (Biorad) and electroporation cuvettes (1 mm, Cell Projects). Bacteria were plated on Luria-Bertani (LB) agar (Sigma) plates with the appropriate antibiotic (Ampicillin, 100 µg/ml; Kanamycin, 50 µg/ml; Spectinomycin, 50 µg/ml; Tetracycline 10 µg/ml) and if blue-white selection was required additionally with 40 µg/ml Xgal (5-bromo-4-chloro-3-indolyl-beta-D-galactopyranoside, Sigma). Plasmids were purified from 2-5 ml bacterial culture (in LB, Sigma) using the QIAprep Spin Miniprep Kit and from 50-100 ml culture using the Plasmid Midi Kit (both Qiagen).

## Animals

Ai6 and Ai14 mice (Madisen et al., 2010) were purchased from Jackson Laboratories, USA and CD1 mice were purchased from Charles River, Germany. All animals were

maintained in temperature- and light-controlled rooms (12 light/12 dark, light on from 6:00 a.m.) with food and water ad libidum. All experiments including laboratory animals were approved by the Cantonal Veterinary Office of Zurich. The protocol of animal handling and treatment was in accordance with Swiss Federal and Cantonal regulations as well as the internal guidelines of the University of Zurich.

## Cell-lines and Transfection

MEF-Ai6 were derived from hemizygous Ai6 reporter mice (Madisen et al., 2010) and immortalized using standard methods (Xu, 2005). HEK293T and MEF-Ai6 were cultured in Opti-MEM and DMEM, respective, each with the addition of 10% fetal bovine serum (FBS), 1% Glutamax, and Penicillin/Streptomycin (all Gibco). HEK293T and MEF-Ai6 were transfected in a 6 well format using X-tremeGene 9 (Roche) in a 4:1 transfection reagent/DNA ratio. Individual combinations of pCAG-T7 plasmids encoding recombinases reporters were adjusted to a total DNA amount of 1 µg using pUC57 as an inert carrier plasmid. The specific amounts of plasmids transfected into HEK293T were 50 ng for mCherry, 100 ng each for all plasmids encoding SSRs, Dre-dependent Cre variants, or coincidental SSR components, and 250 ng for all ZsGreen-based SSR reporter plasmids and for single color ZsGreen and mCherry control transfections. Transfections of MEF-Ai6 included 50 ng each for all types of plasmids.

For quantifications, transfections of each distinct combination of plasmids were repeated three times with each replicate experiment including independent DNA preparations for each plasmid, independent transfection reagent/medium preparations and independently seeded cell populations.

For MEF-Ai6, Cre-mediated excision of the Ai6 stop cassette was detected using genotyping PCR with the primers Ai6-F, TTT TCC TAC AGC TCC TGG GC; Ai6-R, GGC ATT AAA GCA GCG TAT CC.

## Flow Cytometry

HEK293T and MEF-Ai6 cells were trypsinized and collected in PBS with 10% fetal bovine serum (FBS) 24h and 72h after transfection, respectively. Cells were analyzed on a BD LSRII Fortessa. ZsGreen fluorescent protein was excited using a 488 nm laser and detected using a 525/50 filter. mCherry fluorescent protein was excited using a 561 nm laser and detected using a 610/20 filter. Single color controls are shown in Supplementary Figure 8. For HEK293T, a minimum of 20.000 and for MEF-Ai6, a minimum of 5.000 mCherry-positive events were recorded. Data analysis was performed using FlowJo software and flow plots were processed using Adobe Illustrator.

## *in utero* Electroporation

Uteri of timed-pregnant mothers (CD1, 14.5 days after mating with Ai14-homozygous males) anaesthetized with isoflurane in an oxygen carrier (Merial Animal Health) were exposed through a 2 cm incision in the ventral peritoneum. Embryos were lifted through the incision and placed on humidified gauze pads. DNA (0.5 µg of each recombinase plasmid and 1 µg of EGFP plasmid) was injected through the uterine wall into the telencephalic vesicle using pulled borosilicate needles and a Femtojet microinjector (Eppendorf). Electric pulses were applied using 5 mm platinum tweezers electrodes (CUY650P5, Nepagene) and an ECM-830 BTX square wave electroporator (BTX, Gentronic, Inc.). Uterine horns were then placed back into the abdominal cavity and the abdomen wall and skin were sutured using surgical needle and thread.

## Histology, Immunohistochemistry, and Fluorescence Imaging

In utero electroporated Ai14-hemizygous mice were sacrificed at P9-10 and perfused with ice-cold 4% PFA in PBS. Brains were harvested and post-fixed in 4%

PFA in PBS for at least 4h on ice. Whole-mount brains were visually inspected using an Olympus SZX12 stereo microscope equipped with epi-fluorescence illumination and brains with similar-sized areas of EGFP fluorescence were selected for further analyses. 50-60 µm-thick coronal brain sections were prepared using a VT 1000S vibratome (Leica), mounted (Dako Fluorescence Mounting Medium) and imaged using a Fluoview FV10i confocal microscope (Olympus).

Immunostainings were performed by permeabilizing and blocking free floating brain sections in PBS with 1% bovine serum albumin (BSA, Sigma) and 0.5% Triton X-100 (Sigma) at 4℃ over night. Primary and secondary antibodies were diluted in PBS with 0.5% BSA and 0.25% Triton X-100 and brain slices were incubated with primary antibody at 4℃ for 48h and with secondary antibody for 24h. Slices were washed with PBS with 0.5% BSA and 0.25% Triton X-100 in-between incubations and with PBS prior to mounting. A mouse monoclonal anti-NeuN antibody (1 µg/ml, clone A60, Millipore) and a goat anti-mouse Alexa Fluor 647 secondary antibody (Life Technologies) were used for immunostainings.

Images were processed using ImageJ or Imaris (Bitplane Scientific Software) and panels were arranged using Adobe Illustrator.

## Quantifications and Statistical Analysis

Recombination efficiency was determined as the percentage of mCherry-positive cells showing ZsGreen fluorescence. Cre recombination efficiency served as a standard and all replicates were divided by mean Cre recombination efficiency thus transforming data to percentage of Cre recombination efficiency. Standard deviation (S.D.) was calculated for transformed replicates and is shown as error bars in bar graphs. Two-way ANOVA with Bonferroni post-hoc test was used to compare multiple means. The number of $EGFP^+$ cells and $tdTomato^+$ cells per coronal brain sections was determined in a single confocal plane and for each fluorescent channel

individually using the automatic spot detection function with default parameters (estimated xy diameter = 12.4 µm) implemented in Imaris (Bitplane Scientific Software). The spot detection threshold was manually set using the “quality filter” and detected spots were manually curated to eliminate spots marking false-positive detected cell bodies and add spots for false-negative undetected cell bodies. Based on the proximity of individual spots marking EGFP$^+$ and tdTomato$^+$ cells, respectively, EGFP$^+$ tdTomato$^+$ cells were annotated manually and EGFP/tdTomato co-localization was validated in an overlay image of the green and red fluorescence channels (the workflow is outline in the Appendix, Figure A.1). Average numbers of cells were calculated for three mice per group and three coronal sections per mouse. Student’s t-test (two-tailed) was used to compare two means. For all statistical analyses, a p-value of less than 0.05 was considered significant.

# 2. Generation of Isogenic Models for Prion Research by Genome Editing

This chapter includes unpublished material as well as sections that were adapted or reproduced from the following publications.

PLOS ONE | September 2012 | Volume 7 | Issue 9 | e41796 | doi: 10.1371/journal.pone.0041796
**Evaluation of OPEN Zinc Finger Nucleases for Direct Gene Targeting of the *ROSA26* locus in Mouse Embryos**

Mario Hermann[1,5], Morgan L. Maeder[2], Kyle Rector[3], Joseph Ruiz[3], Burkhard Becher[4], Kurt Bürki[1], Cyd Khayter[2], Adriano Aguzzi[5], J. Keith Joung[2,6], Thorsten Buch[5,7,8,*], Pawel Pelczar[1,9,*]

[1]Institute of Laboratory Animal Science, University of Zurich, Zurich, Switzerland
[2]Molecular Pathology Unit, Center for Cancer Research, and Center for Computational and Integrative Biology, Massachusetts General Hospital, Charlestown, MA 02129 USA
[3]Transposagen Biopharmaceuticals, Inc., Lexington, USA
[4]Institute for Experimental Immunology, Department of Pathology, University of Zurich, Zurich, Switzerland
[5]Institute of Neuropathology, University of Zurich, Zurich, Switzerland
[6]Department of Pathology, Harvard Medical School, Boston, MA 02115 USA
[7]Institute for Medical Microbiology, Immunology, and Hygiene, Technische Universität München, Munich, Germany
[8]Email: Thorsten.Buch@mikrobio.med.tum.de
[9]Email: pawel.pelczar@ltk.uzh.ch
* these authors contributed equally to this work

Journal of Visualized Experiments | April 2014 | Issue 86 | doi: 10.3791/50930
**Mouse Genome Engineering using Designer Nucleases**

Mario Hermann[1], Tomas Cermak[2], Daniel F. Voytas[2], Pawel Pelczar[1]

[1]Institute of Laboratory Animal Science, University of Zurich
[2] Department of Genetics, Cell Biology & Development and Center for Genome Engineering University of Minnesota

Correspondence to: Pawel Pelczar at pawel.pelczar@ltk.uzh.ch

Individual contributions of authors are summarized in “Contributions to Published Work” on page 135.

# 2.1. Introduction

## 2.1.1. The cellular prion protein & its physiological functions

The cellular prion protein, $PrP^C$, is a highly conserved and ubiquitously expressed glycosylphosphatidylinositol (GPI)-anchored extracellular protein (Aguzzi et al., 2008). The protein-coding sequence of mouse $PrP^C$ (254 amino acids) is incorporated into a single exon of the *Prnp* gene located on chromosome 2. Nascent $PrP^C$ contains an N-terminal secretory signaling peptide (aa 1-22) and a C-terminal membrane anchor region (aa 232-254), which are both cleaved off during export and GPI-anchoring of $PrP^C$ to the cell surface. Mature $PrP^C$ consists in principle of two structurally distinct domains, the N-terminal flexible tail (aa 23-123) and the C-terminal globular domain (aa 124-231) (Riek et al., 1996; Hornemann et al., 1997). Within the flexible tail two charged clusters ($CC_1$ and $CC_2$) flank five octapeptide repeats (ORs) and are followed by the hydrophobic core (HR). The globular domain is comprised of three $\alpha$-helices and two $\beta$-strands. In prion diseases, also known as transmissible spongiform encephalopathies, $PrP^C$ is converted into $PrP^{Sc}$, a misfolded conformer, which forms extracellular aggregates (Aguzzi et al., 2008).

In the mouse, *Prnp* mRNA expression was detected as early as embryonic day 8.5 (Miele et al., 2003) and abundance of both *Prnp* mRNA and protein increases postnatally throughout most regions of the brain (Linden et al., 2008). In adult animals, $PrP^C$ is detected in a multitude of cells in neural and non-neural tissues (Linden et al., 2008) indicating important functions of $PrP^C$ across different organ systems. Despite extensive efforts revealing the physiological role of $PrP^C$ has proven difficult. Several *Prnp*$^{-/-}$ mouse lines created independently by classic gene-targeting (see below) have been subjected to phenotypic analysis however many functions attributed to $PrP^C$ based on these experiments are not well understood on a mechanistic level and have often been disputed in subsequent studies (Steele et al., 2007; Striebel et al., 2013). The most striking phenotype of *Prnp*$^{-/-}$ mice is their resistance

to prion disease showing that the cellular prion protein is absolutely required for disease progression (Büeler et al., 1993). One of the best documented physiological roles of $PrP^C$ has been demonstrated in the peripheral nervous system. Here, $PrP^C$ expressed on neurons plays a role in long-term maintenance of the myelin sheath as aged *Prnp*$^{-/-}$ mice and mice with conditional neuronal ablation of *Prnp* suffer from a chronic demyelinating polyneuropathy (Bremer et al., 2010).

### 2.1.2. Gene-targeting & the implications for mouse genetics

Over the past 20 years, gene-targeting based on homologous recombination in mouse embryonic stem (ES) cells has been the core technology for introducing a wide variety of modifications into the mouse genome (Capecchi, 2005). In ES cells, homologous recombination between a target locus and a targeting vector carrying the investigator-defined gene modification occurs at a low frequency. Thus ES cell clones carrying the desired modification are enriched by a positive-negative regimen (Capecchi, 2005). Successfully targeted clones are then injected into a mouse blastocyst and these manipulated embryos are transferred to a pseudo-pregnant foster mother. Offspring are chimeric mice, which have a tissue composition that is partially derived from the engineered ES cells. Germline-competent chimeric founders can then be used to established a mouse line carrying the desired gene modification in all cells.

Gene-targeting has proven successful with the generation of several 1000 mouse lines harboring targeted gene modifications. However, using these mice as genetic models is often accompanied by several challenges due to the technical limitations in manipulating ES cells. Most notably, the derivation of highly germline-competent ES cells has for a long time been restricted to non-standard mouse strains such as 129 and has only recently been successfully adapted for the widely used C57BL/6 strain (Poueymirou et al., 2007). As a result chimeric founders were typically extensively backcrossed to C57BL/6 mice with the goal to generate congenic mice that

carry the intended genetic modification but are otherwise genetically highly similar or identical with wild-type C57BL/6 mice. In many cases such as congenic *Prnp*$^{-/-}$ mice long stretches of ES cell-derived genomic DNA flank the modified locus and can harbor several 100 polymorphic genes. Some single nucleotide polymorphisms (SNPs), which co-segregate with the *Prnp*$^{-/-}$ allele might affect the expression levels or the function of flanking gene products. These unintended genetic alterations could confound functions attributed to $PrP^C$ based on the phenotype of *Prnp*$^{-/-}$ mice. Nuvolone et al., 2013 have recently shown that the hyperphagocytic phenotype observed in *Prnp*$^{-/-}$ mice is not related to the ablation of $PrP^C$ but the presence of a 129-derived variant of the *Sirpa* (signal regulatory protein $\alpha$) gene. Similarly, additional polymorphic flanking genes could be responsible for other disputed *Prnp*$^{-/-}$ phenotypes such as susceptibility to experimentally induced seizures (Striebel et al., 2013). Thus a *Prnp*$^{-/-}$ mouse with a pure C57BL/6 genetic background would be highly desirable for avoiding genetic confounders in the search for the physiological functions of $PrP^C$.

### 2.1.3. Genome Editing Technologies

**Nucleases with protein-based DNA recognition domains.** Zinc fingers and transcription activator-like effectors are currently the most widely used modular DNA-binding protein domains for the construction of designer nucleases. Zinc finger nucleases (ZFN) incorporate $Cys_2His_2$ zinc finger modules, which are derived from naturally occurring eukaryotic transcription factors. Each zinc finger consists of about 30 amino acids forming one $\alpha$-helix and two $\beta$-strands (Berg, 1988; Pavletich and Pabo, 1991). Individual zinc fingers typically contact 3 bp in the major groove of DNA and functional synthetic zinc finger arrays incorporate three to six modules recognizing 9-18 bp DNA sequences (Liu et al., 1997). Several openly accessible as well as proprietary libraries of natural and artificial zinc finger modules recognizing the majority of the 64 possible nucleotide triplets have been established (Carroll, 2014; Urnov et al., 2010). Zinc finger arrays with custom specificities can be produced by modular assembly of one-finger (Carroll et al., 2006; Wright et al., 2006)

or two-finger modules (Moore et al., 2001; Doyon et al., 2008) with predefined binding characteristics or by selection-based methods such as the Oligomerized Pool Engineering (OPEN) protocol (Maeder et al., 2009).

The DNA-binding domains of transcription activator-like effector nucleases (TALEN) are derived from transcriptional activators that plant-pathogenic bacteria of the genus *Xanthomonas* introduce into host cells to facilitate infection (Bogdanove and Voytas, 2011). TALE specificity is mainly determined by a series of repeat domains 33-35 amino acids in length, which contain so called repeat variable diresidues (RVD) in positions 12 and 13. Residue 13 of each RVD contacts a single DNA base pair with standard RVDs HD recognizing C:G, NG recognizing T:A, NN recognizing G:C and NI recognizing A:T (Boch et al., 2009; Moscou and Bogdanove, 2009). TALE recognition sites are commonly 15-21 bp in length with an additional preferred T in position 0, which is recognized by a cryptic module in the TALE N-terminus (the last base pair of a target site is recognized by a partial repeat, referred to as half-repeat). The repetitive nature of TALE domains presents a technical challenge for assembling custom arrays but several molecular cloning techniques have been introduced that allow rapid construction of custom TALENs (Cermak et al., 2011; Reyon et al., 2012; Briggs et al., 2012; Schmid-Burgk et al., 2013).

Both ZFN and TALEN function as pairs with scission of a DNA double strand performed by the dimerizing *Fok*I cleavage domain (Li et al., 1992), which is fused to the C-terminus of each ZFN and TALEN monomer (Kim et al., 1996; Christian et al., 2010). An important parameter for productive FokI dimerization is the size of the spacer between nuclease monomer binding sites. For ZFN a spacer of 5 or 6 bp is required, while the the truncated TALEN architecture introduced by Miller et al., 2011 tolerates 12-20 bp with an optimum at 14-16 bp. FokI domains have been engineered to function as heterodimers (Miller et al., 2007) with the aim to substantially reduce dimerization of identical nuclease monomers, which could cause cleavage at undesired off-target sites. Further directed evolution of FokI performed by Guo et al.,

2010 and Doyon et al., 2011 has led to an improved activity of these heterodimeric domains.

**Programmable RNA-guided nucleases.** Another addition to the collection of designer nucleases originates from an adaptive immune system frequently found in bacteria and archaea (Sorek et al., 2013). These organisms when invaded by phages or plasmids are capable of capturing fragments of foreign DNA with a size of approximately 20 bp and integrate these sequences known as protospacers into their own genome to form a clustered regularly inerspaced short palindromic repeat (CRISPR). In the case of Type II CRISPR systems, these CRISPR loci are transcribed into CRISPR RNA (crRNA) containing a single protospacer and part of a repeat and a second trans-activing crRNA (tracrRNA), which is partially complementary to the repeat. Association of both crRNA and tracrRNA with the CRISPR-associated protein (Cas)9 results in the formation of an active DNA endonuclease. The Cas9-crRNA/tracrRNA complex recognizes and cleaves a 23-bp DNA sequence, which is composed of the guide sequence, i.e. the protospacer, in the crRNA and a 5'-NG/AG consensus sequence, which is recognized by Cas9 itself and was termed protospacer adjacent motif (PAM) (Kim and Kim, 2014).

The RNA-guided mechanism of Cas9 DNA cleavage allows investigators to target novel DNA sequences without the need to re-engineer proteins as it is the case for genome editing with ZFN or TALEN. Several groups have constructed hybrids of crRNA/tracrRNA (Hsu et al., 2013; Jinek et al., 2013), which are now generally referred to as single-chain guide RNAs (sgRNA) and are transcribed using plasmids containing an RNA polymerase III promoter.

**Gene disruption and targeted integration.** The basic principle of genome editing is the introduction of a DNA double-strand break (DSB) at a defined target site by using one of the designer nuclease platforms. DSBs are repaired by cells using two alternative mechanisms (Symington and Gautier, 2011), homologous recombination (HR) with an intact sister chromatid or homologous chromosome or non-homologous

end joining (NHEJ). While HR typically results in faithful repair of a DSB, NHEJ is error-prone causing small insertions and deletions in repaired genomic sequences.

Mutagenic NHEJ-repair triggered by designer nucleases within protein-coding sequences can introduce a frameshift mutation, which disrupts the function of a gene (Carroll, 2014). Some frameshift mutations will additionally result in the introduction of a premature stop codon leading to production of mRNA, which is degraded by nonsense-mediated decay (Huang and Wilkinson, 2012). Genome editing approaches aiming at gene disruption by NHEJ have so far been successful in virtually all organisms and cell-types that are amenable to the introduction of foreign nucleic acids (Carroll, 2014).

When designer nucleases are combined with extrachromosomal repair templates, which are often referred to as donor constructs, the introduction of a DSB can be exploited for the targeted insertion of exogenous DNA sequences by HR (Moehle et al., 2007). To serve as an HR substrate donor constructs must have sufficient homology with the target locus. Double-stranded donors typically include homology arms with a length in the range of 800 to 4000 bp (Meyer et al., 2010; Cui et al., 2011; Perez-Pinera et al., 2012). Single-stranded oligonucleotide donors with as little as 40 bp total homology have also been successfully used (Chen et al., 2011). However, partial integration is frequently reported for this type of donor (Chen et al., 2011; Wefers et al., 2013), which typically is not the case when long double-stranded targeting constructs are used. In general, NHEJ-mediated repair has been observed with higher frequencies than targeted integration by HR independent of the type of designer nuclease or donor configuration (Meyer et al., 2010, 2012; Yang et al., 2013; Perez-Pinera et al., 2012; Bedell et al., 2012).

Genomic loci that have received special interest for nuclease-assisted targeted integration of large (> 2 kb) transgenes are the so called safe harbors, which allow stable ubiquitous expression in the vast majority of cell types and during most developmental stages. The most frequently used safe harbor target sites are located within intron 1 of the mouse *gt(ROSA26)Sor* (or *ROSA26*) on chromosome 6 (Zambrowicz et al.,

1997) and a locus between exon 1 and intron 1 of the human *PPP1R12C* gene, which is an integration site of the human adeno-associated virus (AAV) (Samulski et al., 1991). Both sites have been accessible to classic gene-targeting and *ROSA26* has become the standard locus for the integration of reporter genes in transgenic mice (Soriano, 1999; Madisen et al., 2010).

## 2.2. Outline

In this chapter I present the development and adaptation of designer nucleases for editing the mouse and human prion protein gene as well as the mouse *ROSA26* locus. The experiments outlined here aimed at identifying designer nuclease architectures providing high DNA cleavage efficiency.

Two distinct ZFN pairs allowed the targeted integration of large reporter genes into the *ROSA26* locus directly in mouse embryos. The first *Prnp* knock-out mouse with a pure C57BL/6 genetic background was generated by microinjecting embryos with *Prnp*-specific TALEN pair. A CRISPR/Cas9-based approach allowed bi-allelic modification of the human *PRNP* gene in HEK293T cells.

Isogenic C57BL/6 *Prnp* knock-out mice and *PRNP* knock-out HEK293T cells are valuable model systems for dissecting the physiological function of $PrP^C$. Importantly these two systems avoid genetic confounders present in other knock-out mice generated by gene-targeting in mouse ES-cells. ZFN-based *ROSA26* targeting significantly accelerates the generation of mice harboring conditional alleles for tissue-specific expression of reporters and orther transgenes. Since this approach is not limited to mice with a particular genetic background *ROSA26* targeting can also be performed directly in C57BL/6 *Prnp* knock-out animals.

# 2.3. Results

## 2.3.1. ZFN-mediated targeted integration into the *ROSA26* locus

The mouse *ROSA26* locus is a “safe harbor” frequently used for site-specific insertion of transgenes by HR. Previous studies have demonstrated the feasibility of gene targeting in the *ROSA26* locus by use of commercially available ZFNs (Meyer et al., 2010). In a complementary approach I investigated whether OPEN ZFNs (provided by J. Keith Joung and Morgan Maeder, Massachusetts General Hospital) also allow modification of the *ROSA26* locus. Due to design constraints of the OPEN system it was, however, not possible to target a ZFN pair directly to the XbaI site in the *ROSA26* locus that is frequently used to insert transgenes. Instead, two ZFN pairs that could mediate DNA cuts in proximity of this XbaI site were used. These ZFN pairs, 90/91 and 204/205, target the *ROSA26* sequence 75 and 403 bp upstream of the XbaI site, respectively (Figure 2.1A).

Initial experiments aiming at the selection of the most active OPEN design and optimization of microinjection conditions were conducted by Pawel Pelczar and Thorsten Buch. All microinjections shown in this chapter were performed by Pawel Pelczar. ZFN architectures incorporated either homodimeric or first generation heterodimeric FokI domains that were reported to reduce ZFN-induced off-target mutagenesis (Miller et al., 2007). All ZFN pairs were *in vitro* transcribed and polyadenylated to generate mRNA for cytoplasmic microinjections of zygotes.

Cytoplasmic microinjection of mRNAs encoding the OPEN 90/91 heterodimeric pair did not result in any discernible ZFN activity either in the form of imprecise NHEJ or through HR upon co-injecting the pRosa26.8 donor construct (Meyer et al., 2010) that targets the XbaI site 75 bp downstream of the 90/91 cleavage site (Table 2.1). Also cytoplasmic microinjection of mRNAs encoding the OPEN 204/205 homodimeric ZFN pair at a concentration of 10 ng/µl did not result in genome modification through NHEJ. Co-injection of the same mRNAs with a newly constructed targeting

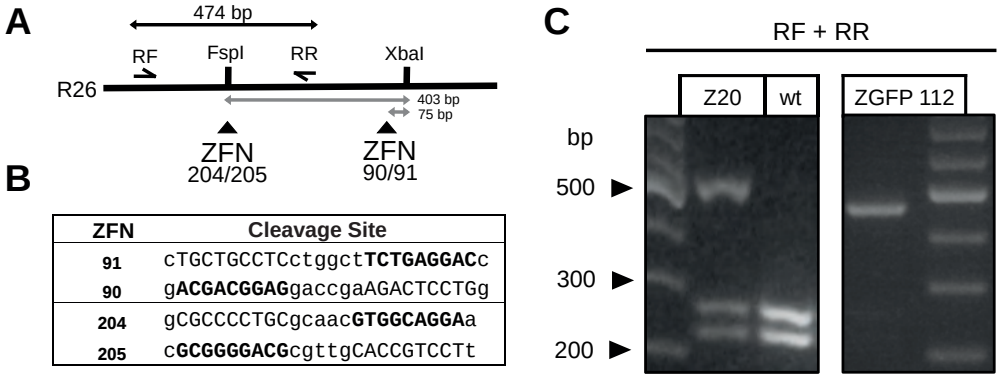


**B**

| ZFN | Cleavage Site |
|---|---|
| 91 | cTGCTGCCTCctggct**TCTGAGGAC**c |
| 90 | g**ACGACGGAG**gaccgaAGACTCCTGg |
| 204 | gCGCCCCTGCgcaac**GTGGCAGGA**a |
| 205 | c**GCGGGGACG**cgttgCACCGTCCTt |

**D**

| Pup/Fetus | Sequence | Ins/Del |
|---|---|---|
| | TCTGGCCGCG**CGCCCCTGC**GCAAC**GTGGCAGGA**AGCGCGCGCTG (ZFN 204 / ZFN 205) | wt |
| Z20 | TCTGGCCGCGCGCCCCCCT:::::GTGGCAGGAAGCGCGCGCTG | Δ8 +3 |
| Z23 | TCTGGCCGCGCGCCCCTGCGCGACGTGGCAGGAAGCGCGCGCTG | Δ1 +1 |
| ZGFP35 | TCTGGCCGCGCGCCCCTGC:::::::::AGGAAGCGCGCGCTG | Δ10 |
| ZGFP70 | TCTGGCCGCGCGCCCCCCT:::::GTGGCAGGAAGCGCGCGCTG | Δ8 +3 |
| ZGFP76 | TCTGGCCGCGCGCCCCTG:::::::GCAGGAAGCGCGCGCTG | Δ9 |
| ZGFP90 | TCT:::::::::::::::::::::::GGAAGCGCGCGCTG | Δ27 |
| ZGFP103 | TCTGGCCGCGCGCCCCTGC:::::::::AGGAAGCGCGCGCTG | Δ10 |
| ZGFP112* | TC:::::::::::::::::::::TGGCAGGAAGCGCGCGCTG | Δ23 |
| ZTOM6 | TCTGGCCGCGCGCCCCTGCGCCAACGTGGCAGGAAGCGCGCGCTG | +1 |
| ZTOM25 | :::::::::::::::::::::::::::::::::::::::::: | Δ66 |
| ZTOM37 | TCTGGCCGCGCGCCCCTGCG:AACGTGGCAGGAAGCGCGCGCTG | Δ1 |
| ZTOM55 | TCTGGCCGCGCGCCCCTGCG:::CGTGGCAGGAAGCGCGCGCTG | Δ3 |

*biallelic modification with identical Δ23 deletion

**Figure 2.1.: OPEN ZFN-induced NHEJ repair within the *ROSA26* locus.** (A) Schematic of ZFN 90/91 and 204/205 target sites within *ROSA26* intron 1. RF and RR (black arrows), *ROSA26* forward and reverse primers generating a 474 bp PCR fragment used for NHEJ analysis by FspI digestion as exemplified in (C). (B) DNA-binding sites (bold font) of individual ZFN proteins. (C) Most error-prone NHEJ repair events eliminate the FspI recognition sequence (underlined in C) resulting in an indigestible band at 474 bp. In the majority of founders such as Z20 both modified and wt alleles were detected, however only mutated alleles were present in founder ZGFP112. (C) Cloning and sequencing of undigested PCR products reveals mutations close to the ZFN204/205 cleavage site. Founder ZGFP112 carried an identical Δ23 deletion in both ROSA26 alleles. ZFN 204/205 recognition sites are highlighted in bold font and the spacer region in grey color.

vector gtR26_EGFP containing an EGFP expression cassette and equipped with 1.4 kb and 1.8 kb long homology arms flanking the ZFN recognition site (Figure 2.2) appeared, however, to be toxic. This toxicity also persisted upon co-injecting reduced concentrations (2 ng/µl) of 204/205 homodimeric mRNAs. Most importantly, none of the experiments performed with the homodimeric pairs 90/91 and 204/205 led to any discernible activity in mouse zygotes.

Since mice showing mutagenesis of ROSA26 could not be recovered from zygotes injected with homodimeric 90/91 and 204/205 ZFN I proceeded with generating mRNAs encoding the heterodimeric OPEN ZFN 204/205 pair. Cytoplasmic injections of heterodimeric OPEN 204/205 ZFN mRNAs were well tolerated by the embryos and led to efficient disruption of the ZFN 204/205 target sequence in a total of 12 founder animals. Modifications of the *ROSA26* target sequence was initially detected by FspI digestion of a PCR product (Figure 2.1C) and confirmed through Sanger sequencing (Figure 2.1D). Founders carrying NHEJ-mediated disruptions were consistently obtained across several injection sessions (Table 2.1). One of the injection series yielded a founder in which both *ROSA26* alleles had been mutated. These alleles, which could be discriminated by a C/T SNP 33 bp upstream of the ZFN cleavage site, contained identical 23 bp deletions (Figure 2.1C,D).

In order to investigate the potential of the 204/205 ZFN pair to recruit the HR repair machinery to the ZFN cleavage site, we co-injected the ZFN mRNAs with a linear DNA fragment of the targeting vector gtR26_EGFP. We identified 16 green-fluorescent founder animals and could confirm that one of them carried the EGFP cassette from the targeting vector correctly integrated into the ZFN target site. The fidelity of integration of the targeting vector by HR was confirmed by Southern blot analysis (Figure 2.2B) as well as by junction PCR and sequencing (Figure 2.2C, Figure 2.3). The integrated EGFP transgene was transmitted through the germ line to the next generation and remained active in F1 offspring (Figure 2.2C, D).

In further experiments the full-length super-coiled gtR26_EGFP targeting vector was co-injected, since vectors with super-coiled topology served as efficient donors in

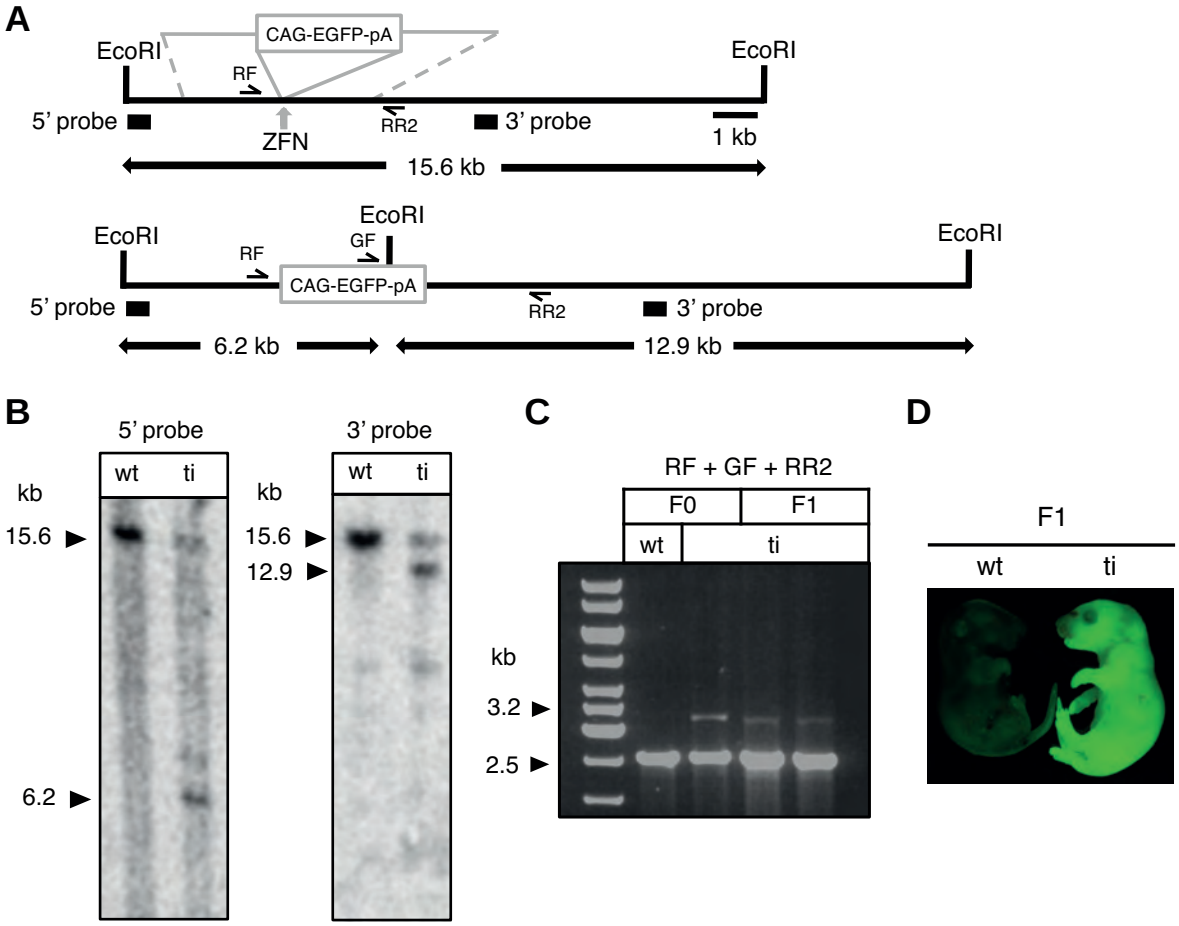


**Figure 2.2.: OPEN ZFN promote *ROSA26* targeting by homologous recombination.** (A) HR targeting strategy for the insertion of the targeting vector gtR26_EGFP carrying EGFP driven by a CAG promoter into the *ROSA26* locus. (B) Southern blot analyses of EcoRI digested genomic DNA from a GFP-fluorescent animal showing site-specific integration into the ROSA26 locus. Both 5' and 3' probes detect only one expected fragment in the DNA of wild-type (wt) animal. Additional fragments detected in the DNA of targeted animal (ti) are consistent with the integration of the CAG-EGFP cassette into one of the *ROSA26* alleles. (C) Germ line transmission of the ROSA26-CAG-EGFP allele was confirmed by junction PCR in two F1 mice (ti allele, 3.2 kb, wt allele, 2.5 kB), one of which is depicted in (D).

**Figure 2.3.:** Integration of gtR26_EGFP by HR into the *ROSA26* locus. The junction PCR product shown in Figure 2.2C was cloned, partially sequenced and an alignment of the sequencing results with the expected architecture of *ROSA26* after gtR26_EGFP targeted integration was generated.


EGFP
Primer GF
RabBGlobin pA
gtR26-204205 3' homology arm
Primer RR2
R26-CAG-EGFP
(1)
(2)
(1)
vector
Primer GF
RabBGlobin pA
(2)
gtR26-204205 3' homology arm
Primer RR2
vector

previous studies (Meyer et al., 2010; Cui et al., 2011). I observed a decrease in random integration events compared to a linearized donor but failed, however, to detected HR in this setup (Table 2.1). To test whether integration at the ZFN 204/205 cleavage site would allow transgene expression under the transcriptional control of the *ROSA26* promoter, co-injections of ZFN with the linear targeting construct gtR26_tdT carrying a splice-acceptor tdTomato cassette were performed. Despite identifying 12 pups that expressed tdTomato and several others carrying independent NHEJ events, I could not identify any animals with homologous integration of the gtR26_tdT vector. This result shows that in the presence of active ZFN gtR26_tdT failed to serve as a donor construct for HR despite including homology arms that were identical to gtR26_EGFP. The 12 tdTomato expressing mice are most likely the result of random transgene integration and a partially active *ROSA26* promoter that was included in the left homology arm of the gtR26_tdT construct.

Considering the outcome of all microinjection experiments, the percentage of founder animals carrying genomic modifications resulting from OPEN ZFN activity seemed to be significantly lower in comparison to other reports in which proprietary ZFN technology was employed (Carbery et al., 2010; Meyer et al., 2010; Cui et al., 2011). These studies also indicated a positive correlation between the frequency of ZFN-induced NHEJ and HR events in mouse zygotes. Thus, an alternative highly active (and freely accessible) designer nuclease targeting the *ROSA26* locus would be highly desirable in order to establish reliable targeted integration in mouse zygotes.

Gersbach and colleagues showed that highly efficient targeted integration can be achieved in transfected mouse Neuro2A cells by *ROSA26* ZFN that were constructed by modular assembly (Perez-Pinera et al., 2012). This ZFN pair, designated R4/L6, targets the standard integration site within intron 1 of *ROSA26* by utilizing DNA-binding domains of four and six individual zinc finger modules, respectively. This pair also incorporates second generation heterodimeric FokI domains with improved cleavage activity (Doyon et al., 2011; Guo et al., 2010). I adapted the R4/L6 ZFN pair for microinjection of mouse embryos by cloning them into my standard pCAG-T7

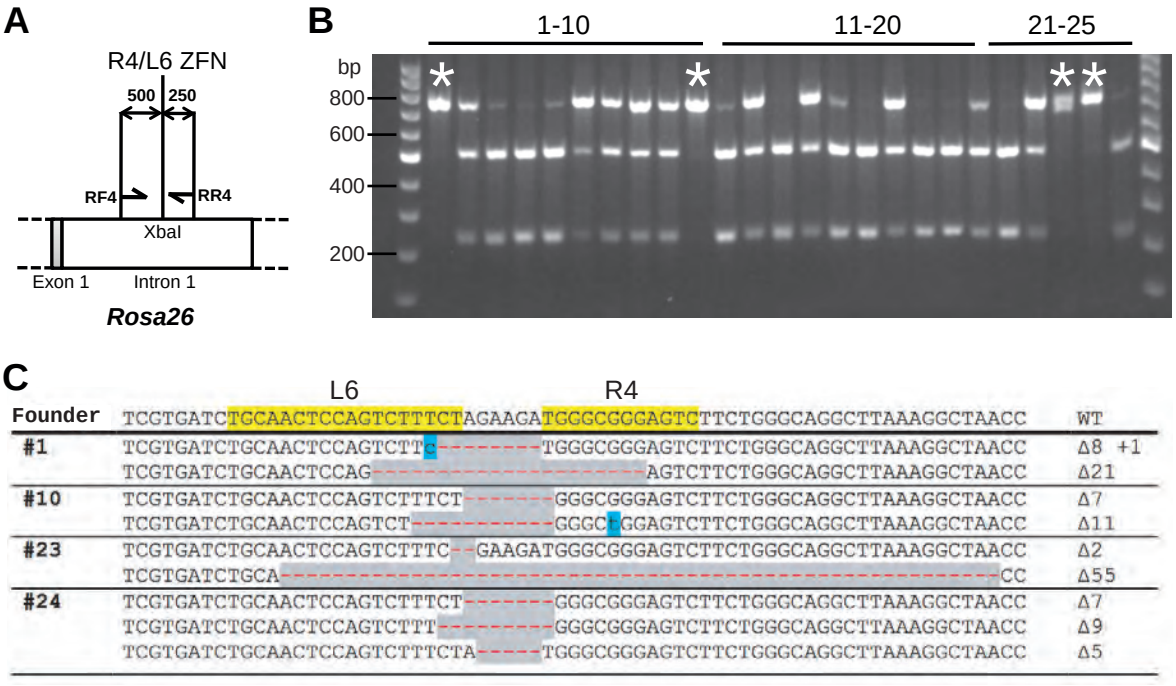


**Figure 2.4.: Highly efficient induction of NHEJ repair by the *ROSA26* ZFN pair R4/L6.** (A) Diagram depicting the ZFN R4/L6 target site within the *ROSA26* locus and the location of primer binding sites (F, R) utilized for detecting NHEJ events by XbaI digestion of PCR products shown in (B). The presence of a full-length PCR product after XbaI digestion indicates ZFN-induced mutagenesis. Stars denote founders with biallelic modifications of the *ROSA26* locus as indicated by the complete absence of a XbaI digestion product and confirmed by Sanger sequencing in (C).

vector and *in vitro* synthesis of ZFN mRNAs. PCR analysis of founder animals born after R4/L6 ZFN microinjection revealed a remarkably high rate of NHEJ-induced mutagenesis. 20 out of 25 founders exhibited a partial (16 animals) or complete (4 animals) loss of an XbaI site as result of ZFN R4/L6-induced NHEJ repair (Figure 2.4). Sequencing of PCR products that were fully resistant to XbaI digestion confirmed the absence of both wild-type *ROSA26* alleles in animals, #1, #10, #23 and #24. Animal #24 harbored at least three distinct *ROSA26* mutations indicating that ZFN were active beyond the one-cell embryonic stage leading to a mosaic genotype in this animal.

Having identified the highly active ZFN pair R4/L6 I attempted to target a large conditional transgene to the *ROSA26* locus. Therefore, the CAG promoter, a *loxP*-flanked

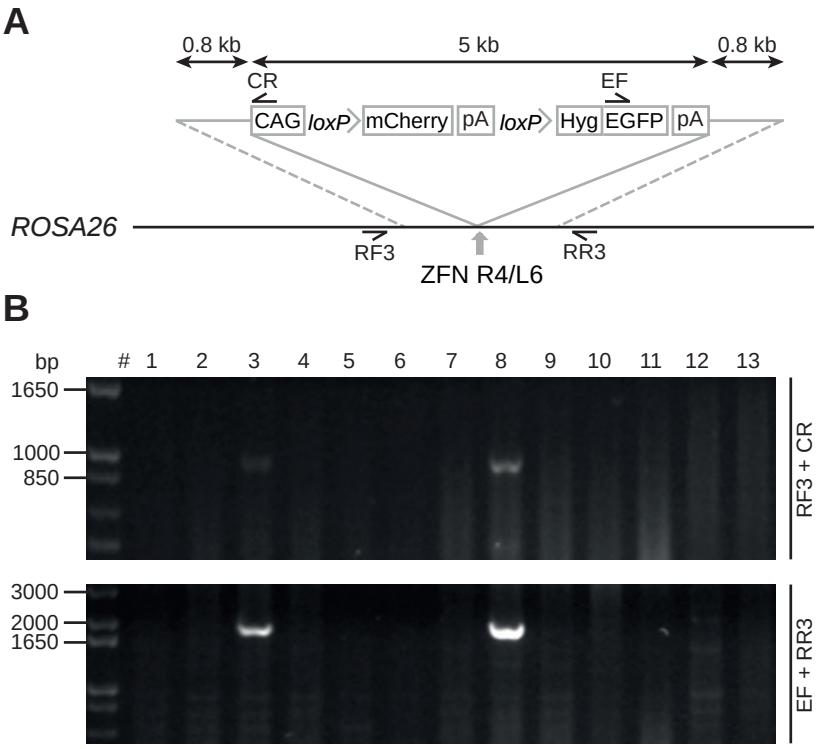


**Figure 2.5.: Targeted integration of a conditional Hygromycin-EGFP transgene into *ROSA26*.** (A) Targeting strategy based on ZFN R4/L6 and the donor construct dR26_HygEGFP. Components of the targeting constructs, sizes of the insert and the ROSA26 homology arms, and location of junction PCR primers used in (B) are shown. pA, polyadenylation site; Hyg, Hygromycin. (B) Junction PCRs for indentifying founders with targeted integration of the donor. Positive founders were identified by the presence of a PCR product of 1 kb with primers RF + CR and a 1.8 kb PCR product with primers EF + RR.

STOP cassette containing mCherry and a polyadenylation signal, and a Hygromycin-EGFP cassette followed by a polyadenylation signal were inserted into the *ROSA26* targeting vector pzDonor-R26 (Perez-Pinera et al., 2012) thus generating the donor construct R26_HygEGFP (Figure 2.5A). Co-injection of mouse zygotes with ZFN R4/L6 and R26_HygEGFP resulted in the birth of 43 potential founder animals (16 of the strain C57Bl6, and 27 BDF1), out of which 13 exhibited mCherry fluorescence indicating an integration event of the R26_HygEGFP donor. Junction PCR analyses of the *ROSA26* locus of these 13 animals revealed that 2 animals (one each of the strains C57BL/6 and BDF1) were positive for targeted integration of R26_HygEGFP (Figure 2.5B, Table 2.1).

**Table 2.1.:** Summary of *ROSA26*-targeted genome editing in mouse zygotes.

| ***ROSA26*** ZFN | ZFN mRNA conc. ng/µl | Donor | Donor conc. ng/µl | Zygotes injected | Zygotes transferred | Pups (p) fetuses (f) | NHEJ positive (% of F0) | TI positive (% of F0) | RI positive |
|---|---|---|---|---|---|---|---|---|---|
| OPEN 90/91 (het1) | 10+10 | pRosa26.8 | 5 | 594 | 345 | 30p | 0 | 0 | ND |
| OPEN 204/205 (hom) | 10+10 | - | - | 123 | 36 | 8p | 0 | - | - |
| OPEN 204/205 (hom) | 10+10 | gtR26_EGFP | 4 | 705 | 382 | 4p | 0 | 0 | ND |
| OPEN 204/205 (hom) | 2+2 | gtR26_EGFP | 1 | 1243 | 711 | 51p | 0 | 0 | ND |
| OPEN 204/205 (het1) | 10+10 | - | - | 358 | 192 | 27p | 2 (7.4) | - | - |
| OPEN 204/205 (het1) | 10+10 | gtR26_EGFP | 5 | 585 | 256 | 51p | 2 (3.9) | 1 (2.0) | 15 |
| OPEN 204/205 (het1) | 10+10 | gtR26_EGFP[a] | 10 | 275 | 195 | 46f | 4 (8.7) | 0 | 2 |
| OPEN 204/205 (het1) | 10+10 | gtR26_tdT | 5 | 640 | 287 | 87f | 4 (4.6) | 0 | 12 |
| MA R4/L6 (het2) | 2.5+2.5 | - | - | 170 | 96 | 25p | 20 (80) | - | - |
| MA R4/L6 (het2) | 2.5+2.5 | dR26_HygEGFP | 3 | 162[b] | 102 | 16p | ND | 1 (6.3) | 5 |
| MA R4/L6 (het2) | 2.5+2.5 | dR26_HygEGFP | 3 | 170 | 130 | 27p | ND | 1 (3.7) | 6 |

OPEN or Modular Assembly (MA) ZFN incorporating homodimeric (hom), first (het1), or second generation heterodimeric (het2) FokI domains; (a) donor in circular confirmation injected, otherwise linearized donors were used; (b) C57BL/6 zygotes were injected, otherwise BDF1; NHEJ, non-homologous end-joining; TI, targeted integration; RI, random integration; F0, founder animals; ND, not determined

### 2.3.2. TALEN-mediated knock-out of *Prnp* in C57BL/6 mice

Targeting the *ROSA26* locus with ZFN provided an experimental paradigm for optimizing the parameters of genome editing in mouse zygotes as well as for establishing screening methods for identifying founder animals with suitable genomic modifications. However, for editing genomic loci other than *ROSA26* it seemed to be difficult to identify suitable target sites for ZFN based on the publicly available OPEN and modular assembly zinc finger libraries.

Earlier studies using genome editing approaches with the aim of disrupting the expression of a protein typically relied on introducing a DNA double-strand within the genes protein coding sequence in close proximity to the start codon. Error-prone NHEJ-repair of this double-strand break often introduces a frameshift and in some cases a premature stop codon in the protein coding sequence of the gene of interest (Geurts et al., 2009; Carbery et al., 2010). Depending on the nature of the introduced mutation and the exon/intron architecture of a specific gene, translation of the mRNA produced from a NHEJ-modified allele yields a non-functional or truncated version of the native protein and mRNAs carrying premature stop codons can be degraded by the non-sense-mediated mRNA decay pathway (Huang and Wilkinson, 2012).

The gene encoding the mouse prion protein, *Prnp*, consists of three exons with exon 3 containing the complete open reading frame coding for $PrP^C$. Thus, in order to completely abolish $PrP^C$ expression, the introduction of a premature stop codon close to the start of the open reading frame in exon 3 would be highly desirable. To achieve this goal I employed a new class of designer nucleases known as TALEN (Christian et al., 2010; Miller et al., 2011). TALEN consist of conserved N-terminal and C-terminal domains (a FokI DNA cleavage domain is fused to the C-terminus), which flank the main region providing DNA-binding specificity. Specific DNA sequences are bound by an array of repeat-variable di-residues (RVDs), with a single

RVD recognizing an individual base of the DNA strand (Boch et al., 2009; Moscou and Bogdanove, 2009).

For the design and construction of a TALEN pair that would specifically recognize a DNA sequence in the *Prnp* open reading frame I adapted a TALEN assembly strategy reported by Cermak et al. 2011 (Figure 2.6). This method is based on two Golden Gate cloning steps (Engler et al., 2008) and allows the assembly of a user-defined RVD array into a TALEN expression vector, which harbors the TALE N-terminus and the C-terminus fused to the FokI domain. Since the original TALEN assembly kit only included TALEN destination vectors for the expression in yeast and plants, I developed a bi-functional TALEN expression vector, which allows production of TALEN in transfected mammalian cells from the strong CAG promoter and *in vitro* synthesis of TALEN mRNA from the T7 promoter (Figure 2.6B). To ensure optimal dimerization and high cleavage activity of the FokI domains, CAG-T7 TALEN expression constructs included truncated N- and C-terminal TALE domain reported earlier by Miller et al., 2011 fused to second generation heterodimeric FokI domains (Doyon et al., 2011; Guo et al., 2010).

The TALEN architecture introduced by Miller et al., 2011 provided the highest cleavage activity when the spacer region between the two TALEN monomers (where the FokI domains dimerize) is 14-16 bp in length. Considering this parameter together with the other TALEN design constraints (Bogdanove and Voytas, 2011) I could identify a TALEN binding site approximately 40 bp downstream of the *Prnp* start codon with the left TALEN recognizing 16 bp, the right TALEN recognizing 17 bp, and a spacer region of 16 bp (Figure 2.7A). I assembled this TALEN pair and produced TALEN mRNAs using *in vitro* transcription.

TALEN mRNAs were microinjected into C57BL/6 fertilized oocytes at the concentrations of 10 ng/µl and 100 ng/µl each in order to empirically determine the optimal conditions for embryo survival and efficiency of on-target genome editing. A total of 94 pups were born, which were analyzed for NHEJ-mediated mutagenesis using PCR and T7 endonuclease digestion (Figure 2.7B, C). Microinjections of TALEN

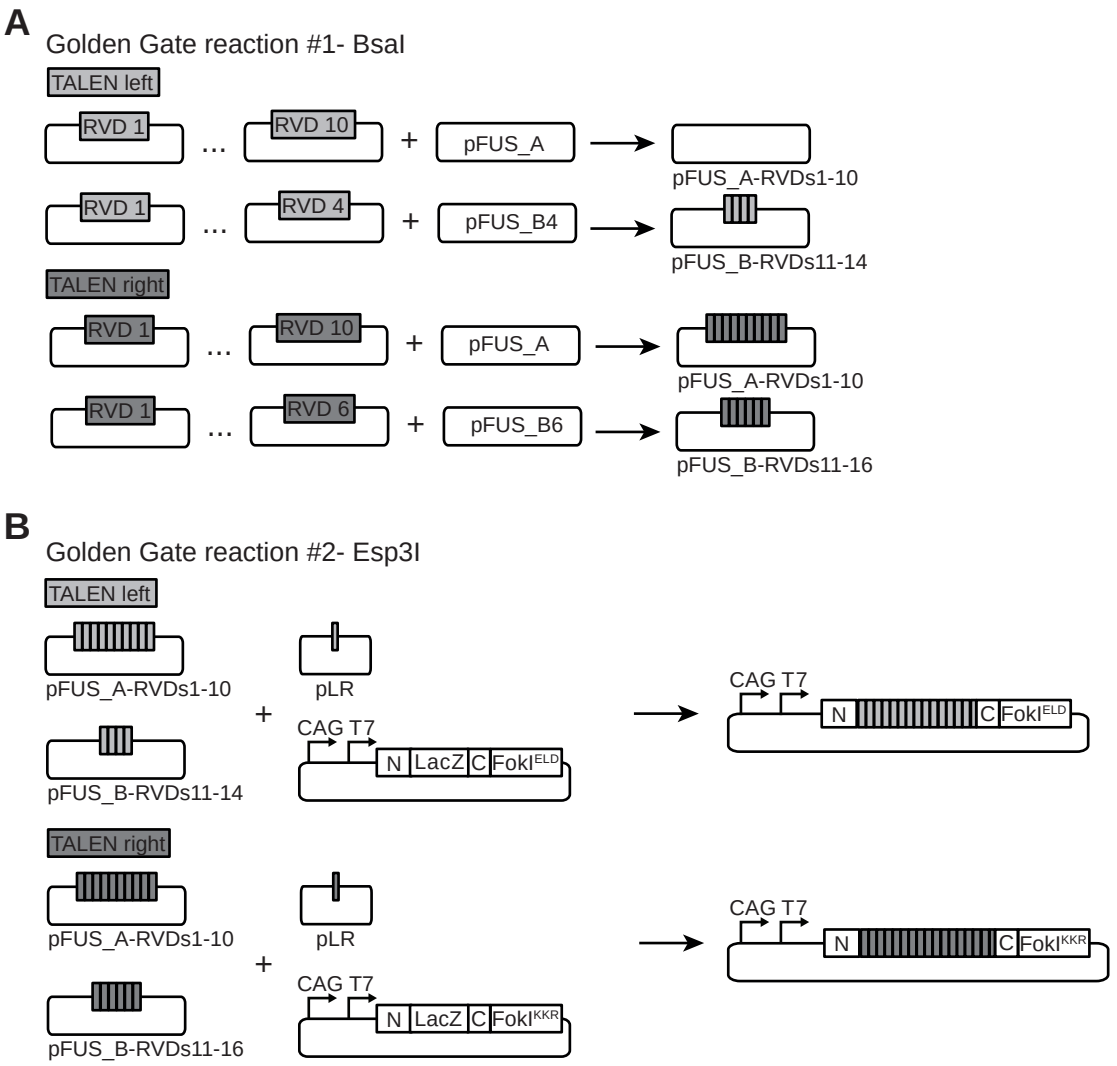


**Figure 2.6.: Golden Gate TALEN assembly strategy.** (A) Up to 10 repeat-variable di-residues (RVDs) are preassembled into pFUS vectors using Golden Gate cloning with the Type II restriction enzyme BsaI. (B) Full-length TALEN are generated by inserting RVD-arrays within pFUS vectors and the last half-repeat (within pLR) into the CAG-T7 TALEN expression vectors with heterodimeric FokI domains ($FokI^{ELD}$, $FokI^{KKR}$) using Golden Gate cloning with the Type II restriction enzyme Esp3I. The assembly strategy was adapted from Cermak et al., 2011 and the TALEN destination constructs were specifically developed for mammalian expression and *in vitro* synthesis of TALEN mRNA.

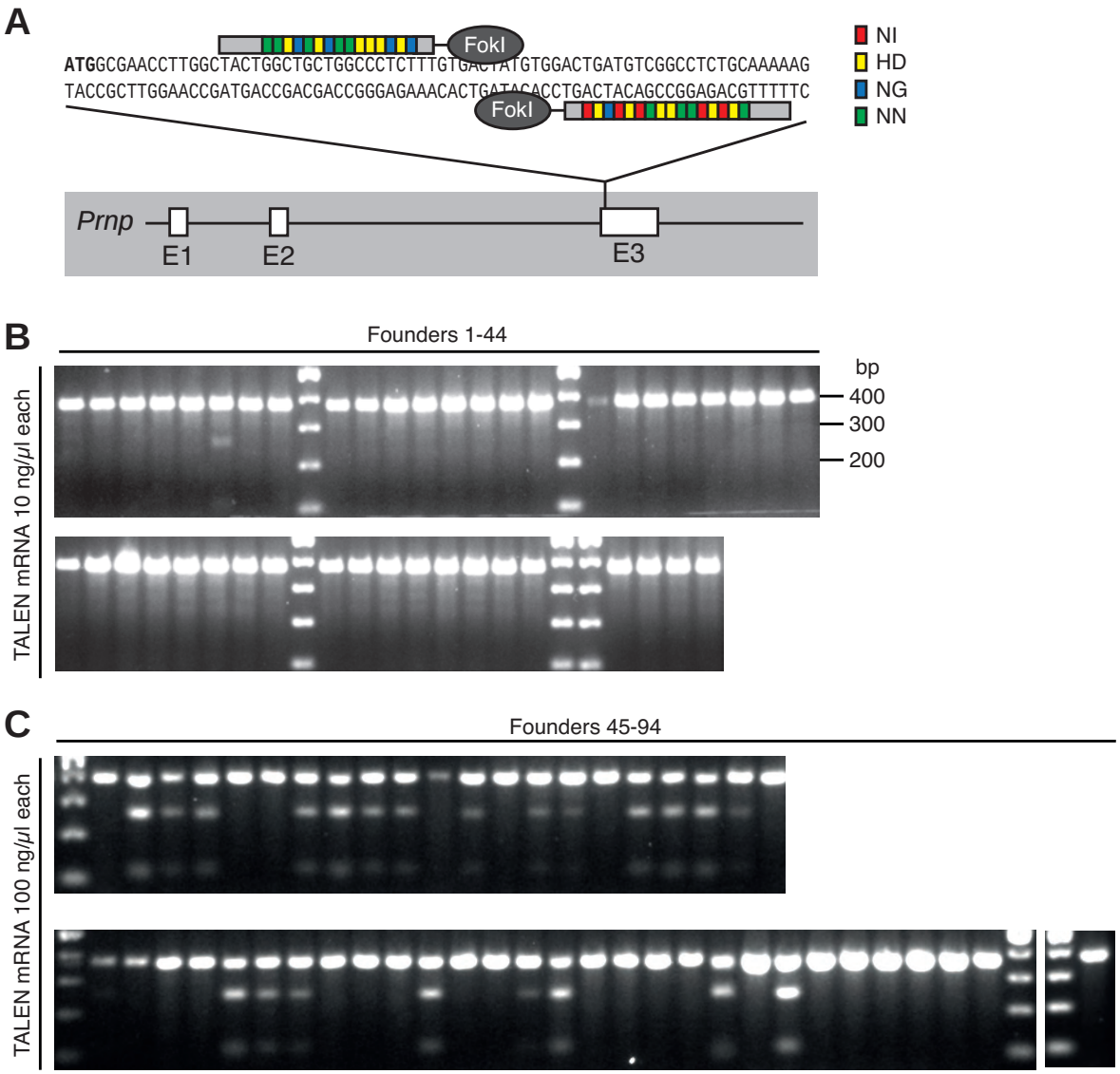


D

| TALEN pair | TALEN mRNA conc. ng/µl | Zygotes injected | Zygotes transferred | Pups | NHEJ positive (% of F0) |
|---|---|---|---|---|---|
| Prnp | 10+10 | 239 | 149 | 44 | 1 (2.3) |
| Prnp | 100+100 | 142 | 110 | 50 | 23 (46.0) |

**Figure 2.7.: Identification of founders with TALEN-mediated mutagenesis of *Prnp.*** (A) Schematic of the TALEN binding site within the *Prnp* protein-coding sequence. RVDs binding individual bases are color-coded (legend on the right). Analysis of genomic DNA obtained from founders after microinjection of zygotes with (B) 10 ng/µl TALEN mRNAs and (C) 100 ng/µl TALEN mRNAs for TALEN-induced error-prone NHEJ repair. A PCR was performed with primers flanking the *Prnp* TALEN target site with subsequent T7 endonuclease digestion of PCR products. NHEJ positive animals can be identified by the presence of T7 endonuclease digestion products.

**A**

| Founder | Sequence | Ins/Del |
|---|---|---|
| wt | **ATG**GCGAACCTTGGCTAC**TGGCTGCTGGCCCTCT**TTGTGACTATGTGGAC**TGATGTCGGCCTCTGCA**AAAAGCGGC | |
| TP6 | ATGGCGAACCTTGGCTACTGGCTGCTGGCCCTCTTTGTG--------GACTGATGTCGGCCTCTGCAAAAAGCGGC | Δ8 |
| TP46 | ATGGCGAACCTTGGCTACTGGCTGCTGGCCCTCTTT---------TGGACTGATGTCGGCCTCTGCAAAAAGCGGC | Δ9 |
| TP47 | ATGGCGAACCTTGGCTACTGGCTGCTGGCCCTCTTTGTGACT-AGTGGACTGATGTCGGCCTCTGCAAAAAGCGGC | Δ1 |
| TP48 | ATGGCGAACCTTGGCTACTGGCTGCTGGCCCTCTTTGTGACT---------GATGTCGGCCTCTGCAAAAAGCGGC | Δ9 |
| TP51 | ATGGCGAACCTTGGCTACTGGCTGCTGGCCCTCTTTGTGACT--GTGGACTGATGTCGGCCTCTGCAAAAAGCGGC | Δ2 |
| TP52 | ATGGCGAACCTTGGCTACTGGCTGCTGGCCCTCTTTGTG--------GACTGATGTCGGCCTCTGCAAAAAGCGGC | Δ8 |
| TP53 | ATGGCGAACCTTGGCTACTGGCTGCTGGCCCTCTTTGTGACT--GTGGACTGATGTCGGCCTCTGCAAAAAGCGGC | Δ2 |
| TP54 | ATGGCGAACCTTGGCTACTGGCTGCTGGCCCTCTTTGTG----TGTGGACTGATGTCGGCCTCTGCAAAAAGCGGC | Δ4 |
| TP56 | ATGGCGAACCTTGGCTACTGGCTGCTGGCCCTCTTTGTGACT---------GATGTCGGCCTCTGCAAAAAGCGGC | Δ9 |
| TP61 | ATGGCGAACCTTGGCTACTGGCTGCTGGCCCTCTTTGTGAC---GTGGACTGATGTCGGCCTCTGCAAAAAGCGGC | Δ3 |
| TP62 | ATGGCGAACCTTGGCTACTGGCTGCTGGCCCTCTTTGTG--------GACTGATGTCGGCCTCTGCAAAAAGCGGC | Δ8 |
| TP63 | ATGGCGAACCTTGGCTACTGGCTGCTGGCCCTCTTTGTG--------GACTGATGTCGGCCTCTGCAAAAAGCGGC | Δ8 |
| TP70 | ATGGCGAACCTTGGCTACTGGCTGCTGGCCCTCTTTGTG--------GACTGATGTCGGCCTCTGCAAAAAGCGGC | Δ8 |
| TP76 | ATGGCGAACCTTGGCTACTGGCTGCTGGCCCTCTTTGTGACT--GTGGACTGATGTCGGCCTCTGCAAAAAGCGGC | Δ2 |
| TP79 | ATGGCGAACCTTGGCTACTGGCTGCTGGCCCTCTTTGTGAC---GTGGACTGATGTCGGCCTCTGCAAAAAGCGGC | Δ3 |
| TP80 | ATGGCGAACCTTGGCTACTGGCTGCTGGCCCTCTTTGTGAC---GTGGACTGATGTCGGCCTCTGCAAAAAGCGGC | Δ3 |
| TP85 | ATGGCGAACCTTGGCTACTGGCTGCTG----------------GTGGACTGATGTCGGCCTCTGCAAAAAGCGGC | Δ17 |
| TP87 | ATGGCGAACCTTGGCTACTGGCTGCTGGCCCTCTTTGTGA---TGTGGACTGATGTCGGCCTCTGCAAAAAGCGGC | Δ3 |

**B**

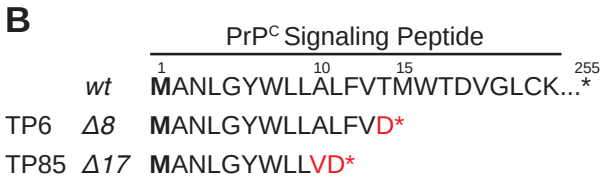


**Figure 2.8.: Sequence analysis of TALEN-induced mutations in *Prnp*.** (A) Founders with mutated *Prnp* alleles. The *Prnp* start codon (bold) and TALEN binding sites (bold, yellow) are highlighted in the wt *Prnp* sequence. (B) Founders TP6 and TP85 carry the *Prnp* alleles Δ8 and Δ17, respectively, which introduce a premature stop codon (*) in proximity to the *Prnp* start codon.

mRNAs at 10 ng/µl each resulted in 1 out of 44 newborns showing a T7 digestion pattern indicative of mutagenesis at the TALEN target site. When TALEN mRNAs were injected at 100 ng/µl a significantly higher number of pups (23 out of 50) were NHEJ-positive (Figure 2.7D).

Subsequently, I determined the exact seqence of *Prnp* mutations present in NHEJ-positive mice by cloning of PCR products and Sanger sequencing. Modified *Prnp* alleles exhibited deletions with a size range of 1 to 17 bp within the TALEN spacer region (Figure 2.8A). Interestingly, a deletion of 8 bp (Δ8) occurred with an increased frequency in multiple NHEJ-positive mice (5 out 18 mutated alleles) and seemed to

be the result of microhomology-mediated end joining repair (McVey and Lee, 2008) based on a TGTG motif within the TALEN target site. This *Prnp* $\triangle$8 mutation as well as the *Prnp* $\triangle$17 mutation introduced a premature stop codon in close proximity to the *Prnp* start codon and thus seemed to be promising candidates for disrupting the expression of $PrP^C$ (Figure 2.8B). Additionally, both deletions eliminated an additional in-frame ATG coding for methionine[15], which could potentially serve as an alternative start codon and the translation of $PrP^C$ with an N-terminally truncated signaling peptide. Thus, founders TP6 ($\triangle$8) and TP85 ($\triangle$17) were bred to C57BL/6 with the goal to generate homozygous *Prnp* $\triangle$8 and $\triangle$17 mice in the F2 generation.

The code determining the nucleotide specificity of TALEN RVDs has been established both by experimental (Boch et al., 2009) and bioinformatic (Moscou and Bogdanove, 2009) means. However the overall DNA binding specificity of TALEN proteins remains poorly characterized and TALENs might introduce DNA double-strand breaks at unintended off-target sites. These off-target mutations, if passed on undetected to the offspring of *Prnp* $\triangle$8 and $\triangle$17 founders, might elicit phenotypes erroneously attributed to the ablation of *Prnp.* Therefore I screened a limited number of off-target sites for NHEJ-mediated mutagenesis. I first used the TAL Effector-Nucleotide Targeter tools (Doyle et al., 2012) to predict the most likely off-target sites for both TALEN monomers within the mouse genome based on sequence similarity to the *Prnp* TALEN target site. I selected 12 off-target sites at which both TALEN monomers would bind with a spacer length allowing productive FokI dimerization (Figure 2.9A). Four of these sites seemed to be located within repetitive regions of the mouse genome preventing the design of suitable primers for PCR-based analysis of off-target TALEN cleavage. The remaining 8 off-target sites were probed for TALEN-induced mutagenesis using T7 endonuclease digestion of PCR products (Figure 2.9B). None of the investigated genomic loci, both in the *Prnp* $\triangle$8 and the $\triangle$17 founder, showed a T7 digestion pattern that would indicate NHEJ-mediated mutagenesis at the predicted off-target sites.

**A**

| | Chromo-some | Score TALEN left | Score TALEN right | Spacer length |
|---|---|---|---|---|
| ***Prnp*** | **2** | **6.19** | **6.07** | **16** |
| **OT1** | 19 | 13.9 | 9.45 | 18 |
| **OT2** | X | 6.87 | 16.56 | 14 |
| **OT3** | X | 13.69 | 9.77 | 22 |
| **OT4** | 5 | 15.29 | 8.23 | 19 |
| OT5 | 2 | 12.53 | 11.21 | 12 |
| **OT6** | 5 | 12.9 | 10.89 | 16 |
| **OT7** | 8 | 10.41 | 13.45 | 23 |
| OT8 | 1 | 10.47 | 13.44 | 12 |
| OT9 | 3 | 12.3 | 11.68 | 16 |
| OT10 | 19 | 9.37 | 14.64 | 18 |
| **OT11** | 11 | 12.41 | 11.72 | 18 |
| **OT12** | 6 | 17.56 | 6.59 | 18 |

**B**

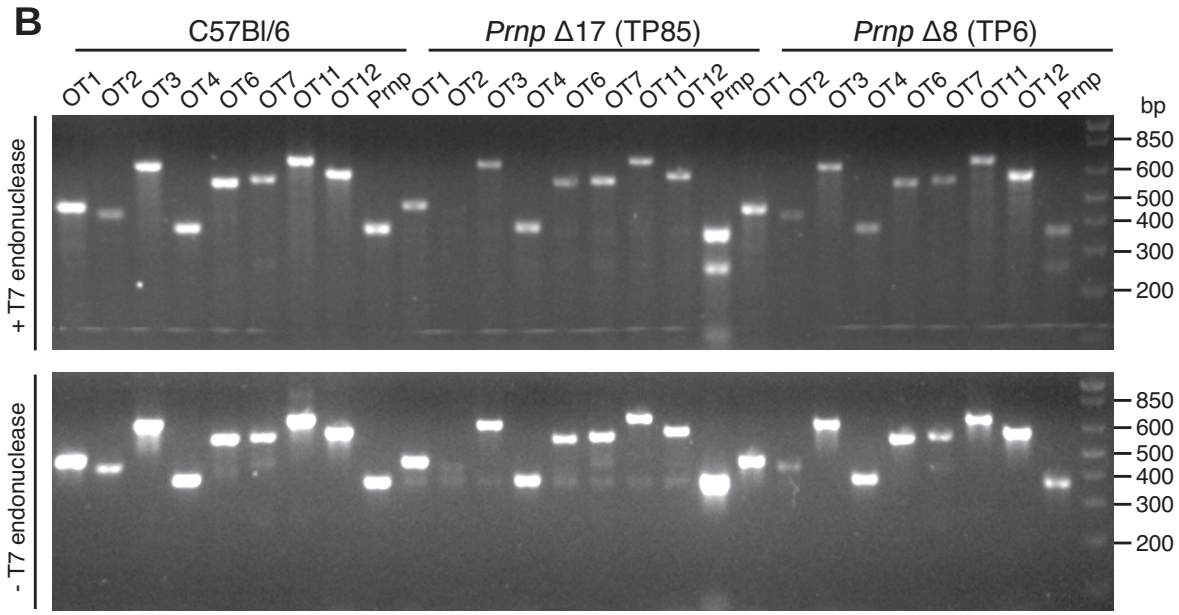


**Figure 2.9.: Analysis for off-target cleavage of *Prnp*-TALEN.** (A) Predicted off-target sites (OT) based on binding specificities of individual RVDs within the in Prnp-*TALEN.* Lower scores indicate a higher probability of binding for a TALEN monomer. OTs in bold font could be analyzed by PCR, suitable primers could not be designed for other OTs. (B) T7 endonuclease digestion of PCR products generated from OTs indicated above gels and *Prnp* as a digestion positive control (lower gel undigested PCR products). Analysis was performed for founders carrying *Prnp* Δ8 and Δ17 alleles, respectively and C57BL/6 mice.

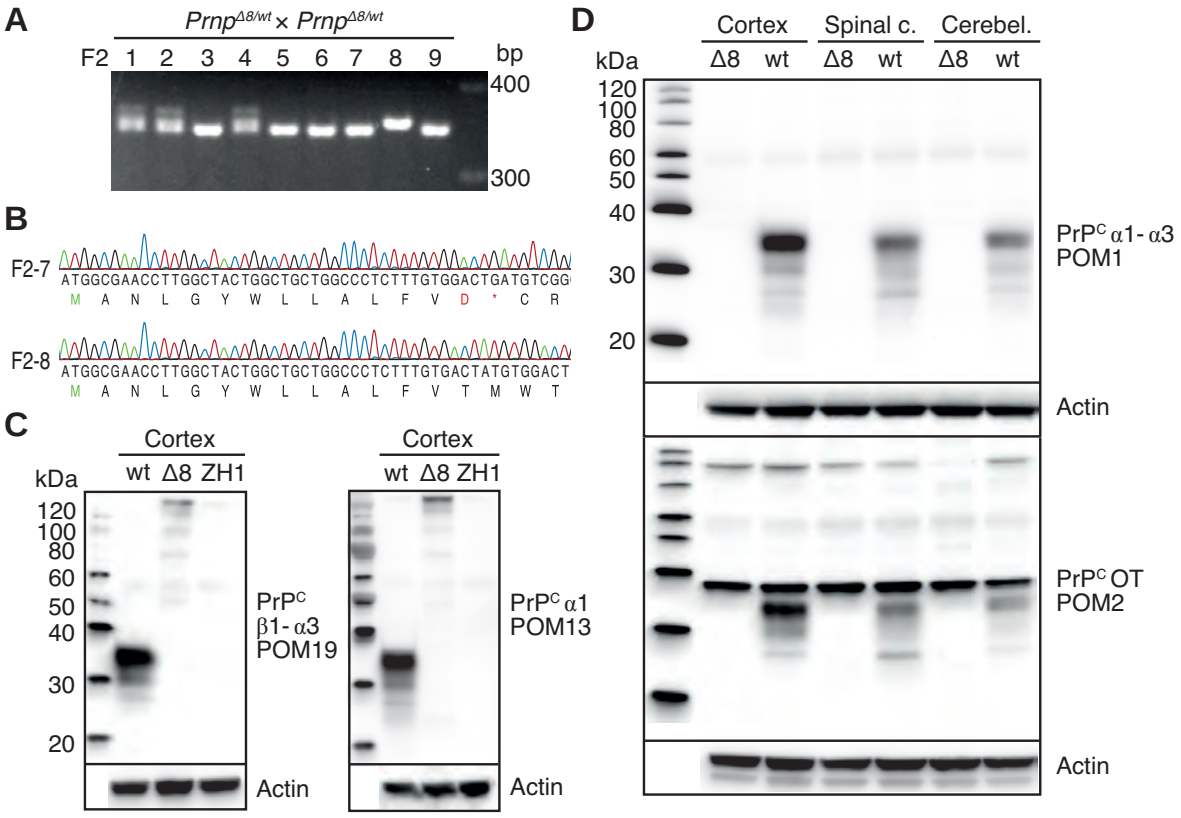


**Figure 2.10.: Ablation of PrP$^C$ expression in *Prnp*$^{\Delta 8/\Delta 8}$ mice.** (A) Hemizygous *Prnp*$^{\Delta 8/wt}$ were bred and the offspring (F2 generation) was genotyped. *Prnp*$^{\Delta 8/\Delta 8}$mice can be identified by a single PCR product smaller in size compared to the PCR product amplified from *Prnp*$^{wt/wt}$ genomic DNA. Multiple bands are detected for *Prnp*$^{\Delta 8/wt}$ mice. (B) Genotypes were confirmed by direct sequencing of PCR products. Exemplary sequencing results for mice F2-8 (*Prnp*$^{wt/wt}$) and F2-9 (*Prnp*$^{\Delta 8/wt}$) are shown. (C) Western blot analysis of PrP$^C$ expression in the cortex of a *Prnp*$^{\Delta 8/\Delta 8}$ animal (Δ8) using antibodies POM19 and POM13 with epitopes in the c-terminal globular domain of PrP$^C$. C57BL/6 (wt) and Zurich I *Prnp*$^{O/O}$ (ZH1) serve as controls. (D) Analysis of PrP$^C$ expression in cortex, spinal cord, and cerebellum using antibodies POM1 (globular domain) and POM2 (N-terminal octarepeat region, OT).

At the time of writing, homozygous *Prnp* $\Delta$17 mice were not yet available and thus only the characterization of homozygous *Prnp* $\Delta$8 is reported. Once germ line transmission of the $\Delta$8 allele was confirmed, $Prnp^{\Delta 8/wt}$ were bred and the offspring were genotyped (Figure 2.10A, B). Using PCR, gel electrophoresis, and sequencing, I could identify 5/9 mice with a $Prnp^{\Delta 8/\Delta 8}$ genotype. Genomic DNA of one of these $Prnp^{\Delta 8/\Delta 8}$ animals was subjected to whole-genome SNP scanning (provided by Taconic) to confirm it's C57BL/6J genetic background. The interrogation of 1459 SNPs distributed across the 19 autosomes and the X chromosome showed that based on these markers the $Prnp^{\Delta 8/\Delta 8}$ mouse was genetically indistinguishable from a wt C57BL/6J animal (Appendix, Table A.2).

$PrP^C$ expression levels in the central nervous system of a $Prnp^{\Delta 8/\Delta 8}$ animal were determined using western blot (Figure 2.10C, D). Protein extracts from the cortex, the cerebellum, and the spinal cord were probed using a panel of antibodies (POM19, POM13, POM1, and POM2), which bind to distinct epitopes in the N-terminal flexible tale and the C-terminal globular domain of $PrP^C$. $PrP^C$ could not be detected in any of the $Prnp^{\Delta 8/\Delta 8}$ tissues providing strong evidence that the premature stop codon present in the $\Delta$8 allele is sufficient to completely suppress the translation of $PrP^C$ and is not permissive for the production of truncated $PrP^C$.

*Prnp* knock-out mice generated by classic gene-targeting in mouse ES-cells such as Zurich I carry a transgenic cassette integrated into *Prnp* locus. These exogenous DNA sequences can be used for genotyping by designing primers that are specific for the Zurich I but not the wt *Prnp* allele. However, since the *Prnp* $\Delta$8 allele only differs from the wt allele by the loss of 8 base pairs, I evaluated alternative genotyping strategies based on the size difference of PCR products (Figure 2.11). Here, I took advantage of high-resolution capillary electrophoresis. First, I assessed the precision of size calling for single PCR products generated from $Prnp^{\Delta 8/\Delta 8}$ and $Prnp^{wt/wt}$ genomic DNA. I compared two PCRs with primers flanking the *Prnp* TALEN target site that produce PCR bands from wt *Prnp* with a length of 86 bp and 356 bp, respectively (Figure 2.11A). Both PCRs allowed discriminating $Prnp^{\Delta 8/\Delta 8}$ and $Prnp^{wt/wt}$ mice

based on the detected sizes of the PCR products, however size calling was more precise for the 86 bp PCR compared to the 356 bp PCR. Hemizygous *Prnp*$^{\Delta 8/wt}$ mice could be easily discriminated from the homozygous genotypes by the presence of multiple PCR bands present in both PCRs.

Next, I attempted to genotype newborn mice and again compared the two PCR approaches. These mice were the offspring of three different breeding schemes,

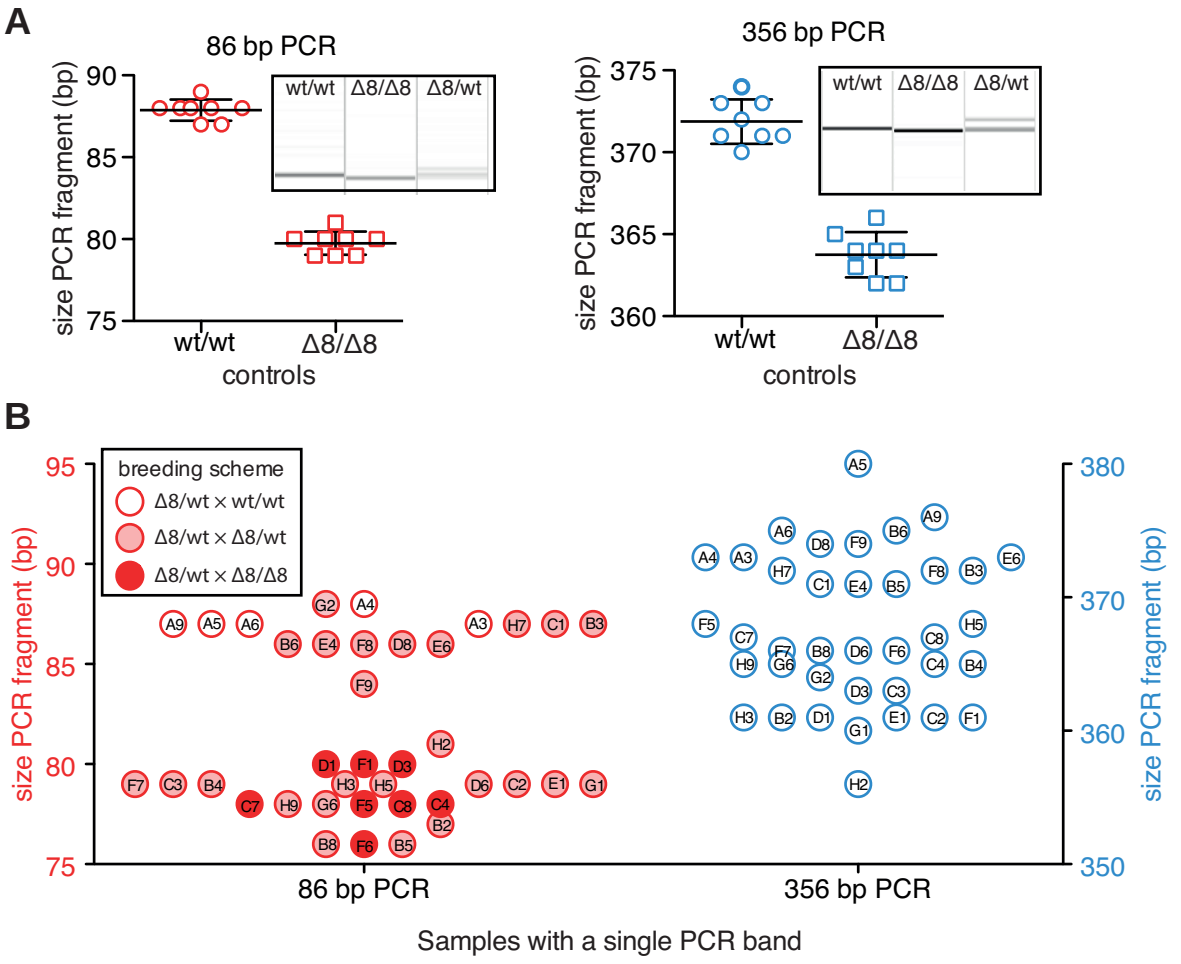


**Figure 2.11.:** High-resolution genotyping of *Prnp* Δ8 mice. (A) Evaluation of the resolution of Qiaxcel capillary electrophoresis using two PCRs that generate products with the expected sizes of 86 bp and 356 bp for wt *Prnp*, respectively. Genomic DNA of *Prnp*$^{wt/wt}$, *Prnp*$^{\Delta 8/\Delta 8}$, and *Prnp*$^{\Delta 8/wt}$ mice previously genoptyped by gel electrophoresis was used (8 PCR reactions/genotype, insets show Qiaxcel virtual gel images). bp, base pairs. (B) Sizes of PCR products for mice with unknown genotype. Individual animals with single-product PCRs are shown and color-coded according to the genotypes of their parents.

*Prnp*$^{\Delta 8/wt}$ × *Prnp*$^{wt/wt}$, *Prnp*$^{\Delta 8/wt}$ × *Prnp*$^{\Delta 8/wt}$, or *Prnp*$^{\Delta 8/wt}$ × *Prnp*$^{\Delta 8/\Delta 8}$ (Figure 2.11B). The sizes of single PCR bands formed two clearly distinguishable clusters around 85 bp and 80 bp for the shorter PCR fragments, while the sizes of the longer PCR products were difficult to discriminate due to low resolution (Figure 2.11B). Importantly, all mice originating from *Prnp*$^{\Delta 8/wt}$ × *Prnp*$^{wt/wt}$ breedings were correctly genotyped either as *Prnp*$^{wt/wt}$ (85 bp cluster) or as *Prnp*$^{\Delta 8/wt}$, while the offspring of the *Prnp*$^{\Delta 8/wt}$ × *Prnp*$^{\Delta 8/\Delta 8}$ breeding was either *Prnp*$^{\Delta 8/wt}$ or *Prnp*$^{\Delta 8/\Delta 8}$ (80 bp cluster). Thus genotyping of *Prnp* $\Delta$8 mice can be performed reliably using PCR combined with capillary electrophoresis.

### 2.3.3. CRISPR-mediated knock-out of *PRNP* in HEK293T cells

Having succeeded to generate a C57BL/6 *Prnp*$^{-/-}$ mouse using TALEN-mediated genome editing, I attempted to genetically ablate *PRNP* in the widely used human embryonic kidney cell line HEK293T. While in mice gene knock-out can be achieved by modifying one allele in microinjected embryos and subsequent breeding to homozygosity, all copies of a gene need to be mutated in a single HEK293T cell in order to establish a clonal *PRNP* knock-out cell line.

Genome editing based on CRISPR/Cas9 has been shown to be highly efficient in modifying a number of human genes in cell lines (Cho et al., 2013; Jinek et al., 2013; Mali et al., 2013; Cong et al., 2013) making this technology the ideal choice for genetic ablation of *PRNP* in HEK293T cells. Additionally, the simple construction of CRISPR guide RNA expression plasmids offers a significant advantage over TALEN and ZFN when simultaneous editing of multiple genomic targets is required.

Since the complete *PRNP* protein-coding sequence is located within a single exon, I devised two alternative strategies for *PRNP* knock-out (Figure 2.12). First, a CRISPR guide RNA target site (PRNP1) in close proximity to the *PRNP* start codon was identified (Figure 2.12A). Cas9-mediated cleavage and NHEJ-repair at this site can be exploited for the introduction of a premature stop codon analogous to the TALEN-based knock-out strategy in mouse embryos. An alternative strategy was based on simultaneously cleaving two target sites, which would allow the complete excision of the *PRNP* protein-coding sequence. For this purpose a second guide RNA (PRNP2) targeting the *PRNP* stop codon was designed, which can be combined with PRNP1 targeting the start codon (Figure 2.12A).

Guide RNAs PRNP1 and PRNP2 were cloned into expression constructs that facilitate gRNA expression *in vivo* using the RNA polymerase III–dependent U6 promoter (Addgene plasmid 43860, J.K. Joung lab, unpublished). HEK293T cells were then transfected with a Cas9 plasmid and either single or combined *PRNP*-targeting guide RNA constructs (Figure 2.12B). Both single PRNP1 and PRNP2 guide RNA

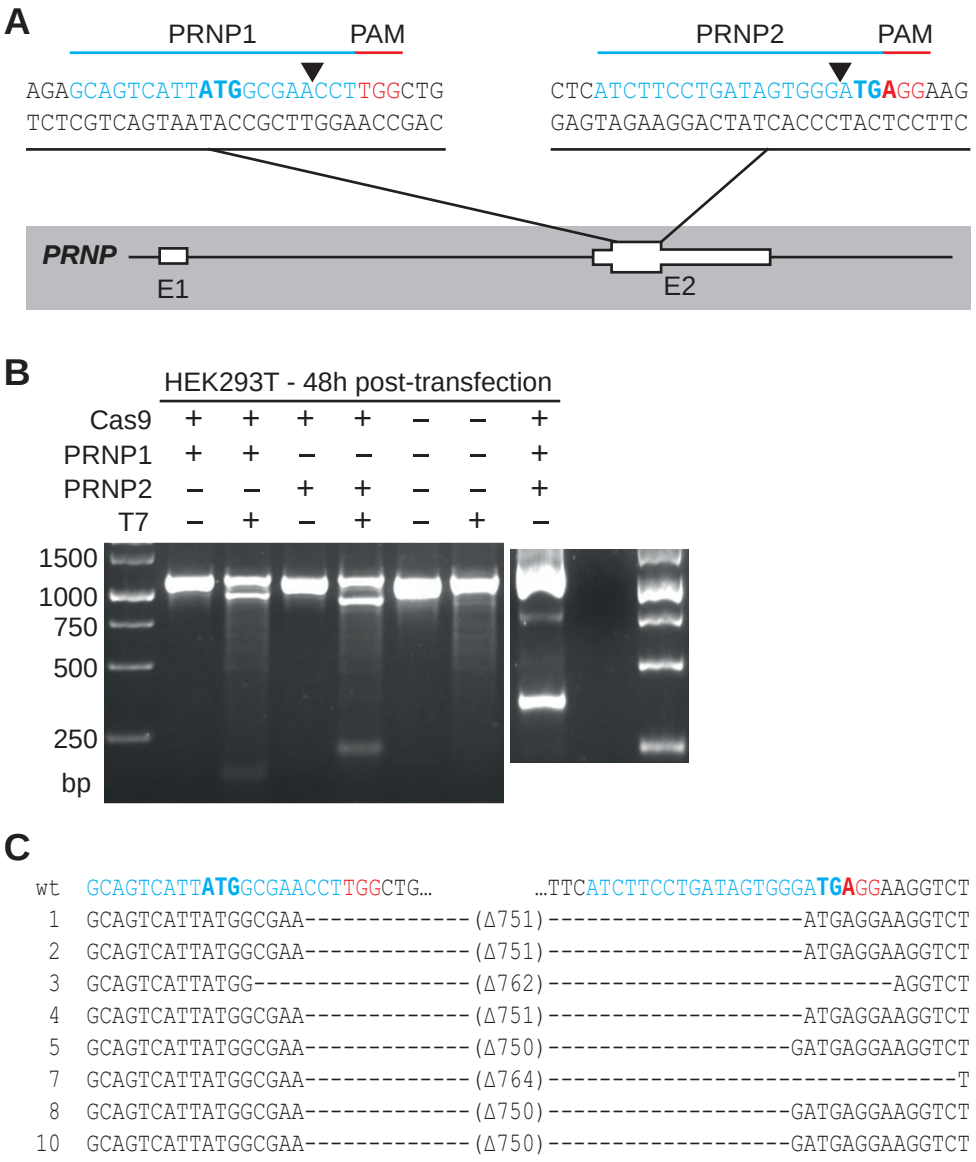


**Figure 2.12.: Strategies for genetic ablation of *PRNP* in HEK293T.** (A) The CRISPR guide RNAs PRNP1 and PRNP2 target sequences in proximity to the start and the stop codon (bold font, gRNA binding site in blue) of the *PRNP* protein-coding sequence, respectively. PAM, protospacer-adjacent motif (highlighted red on sequence). (B) Genomic DNA was extracted from HEK293T 48h after transfection with indicated plasmids and was analyzed by PCR and T7 endonuclease assay for NHEJ repair. In case of co-transfection of Cas9 with PRNP1 and PRNP2 a PCR product with an approximate size of 350 bp indicates excision of the DNA sequence flanked by both guide RNAs. (C) Cloning and sequencing of PCR products confirms the presence of large deletions within the *PRNP* open reading frame.

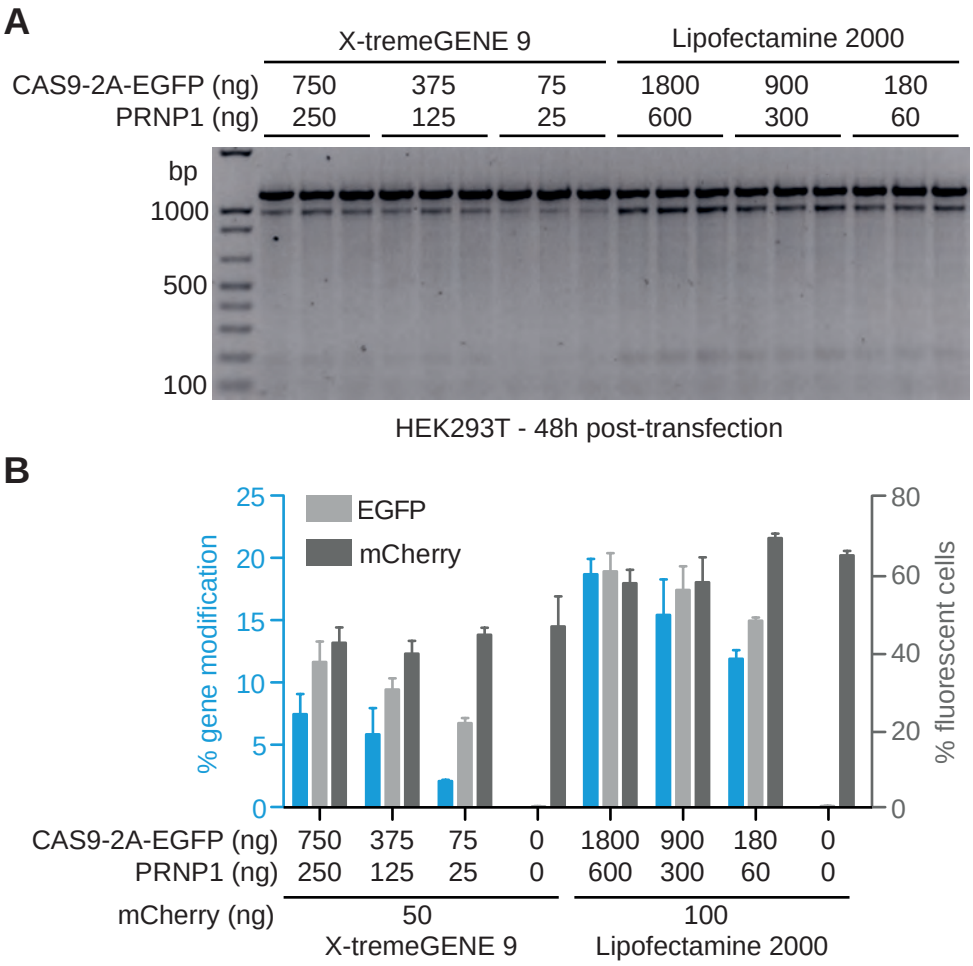


**Figure 2.13.: Optimization of CRISPR-mediated editing of *PRNP*.** (A) Titration of plasmids encoding Cas9-2A-EGFP and guide RNA PRNP1 and comparison of X-tremeGENE 9 and Lipofectamine 2000 transfection reagents. NHEJ repair within *PRNP* is detected using PCR and T7 endonuclease digestion. (B) Quantification of the intensity of T7 endonuclease-digested PCR products to determine gene modification efficiency (blue bars). The percentage of Cas9-expressing cells was monitored by flow cytometric measurement of EGFP fluorescent intensity in single cells (light grey bars). The percentage of viable transfected cells was assessed using a co-transfected constitutively expressing mCherry plasmid (dark grey bars).

transfections resulted in efficient mutagenesis at their respective target sites as revealed by PCR and T7 endonuclease digestion. When PRNP1 and PRNP2 were combined, the same PCR with primers located outside of the *PRNP* protein coding sequence showed an additional product 750 bp shorter in length the expected full-length 1100 bp PCR product. Cloning and sequencing of this shorter PCR product confirmed the presence of several distinct *PRNP* variants with an almost complete lack of the protein-coding sequence.

Thus both the single- and the dual-guide RNA strategy showed potential for achieving *PRNP* knock-out in HEK293T cells. However, since introduction of an early stop codon was sufficient to ablate expression of the mouse prion protein and the presumably lower risk of off-target Cas9 cleavage, I focused on the single PRNP1 guide RNA strategy for generating HEK293T clones with suitable biallelic mutations. Next I optimized Cas9/guide RNA transfection conditions to achieve high modification rates of *PRNP* along with optimal survival of transfected cells. I compared the transfection reagents X-tremeGENE 9 (Roche) and Lipofectamine 2000 (Life Technologies) each with three different dosages of Cas9 and guide RNA plasmids (Figure 2.13).

Here, a Cas9-2A-EGFP plasmid was used to achieve stochiometric co-expression of Cas9 and EGFP. Thus, EGFP fluorescent intensity served as a surrogate measurement for Cas9 expression levels in individual cells. Additionally, I co-transfected a constant amount of a constitutively expressing mCherry plasmid for identifying all transfected cells independent of their Cas9/EGFP expression levels and assessed the percentage of $mCherry^+$ and $EGFP^+$ cells using flow cytometry. As expected, both transfection methods showed a clear positive correlation between amount of DNA transfected and the percentage of $EGFP^+$ cells as well the rate of *PRNP* modification, which was measured by PCR and T7 endonuclease digestion (Figure 2.13B). The highest gene modification rate of approximately 20% was observed when Lipofectamine 2000 combined with the highest recommended DNA amount was employed. Importantly, these high amounts of Cas9 and PRNP1 guide RNA

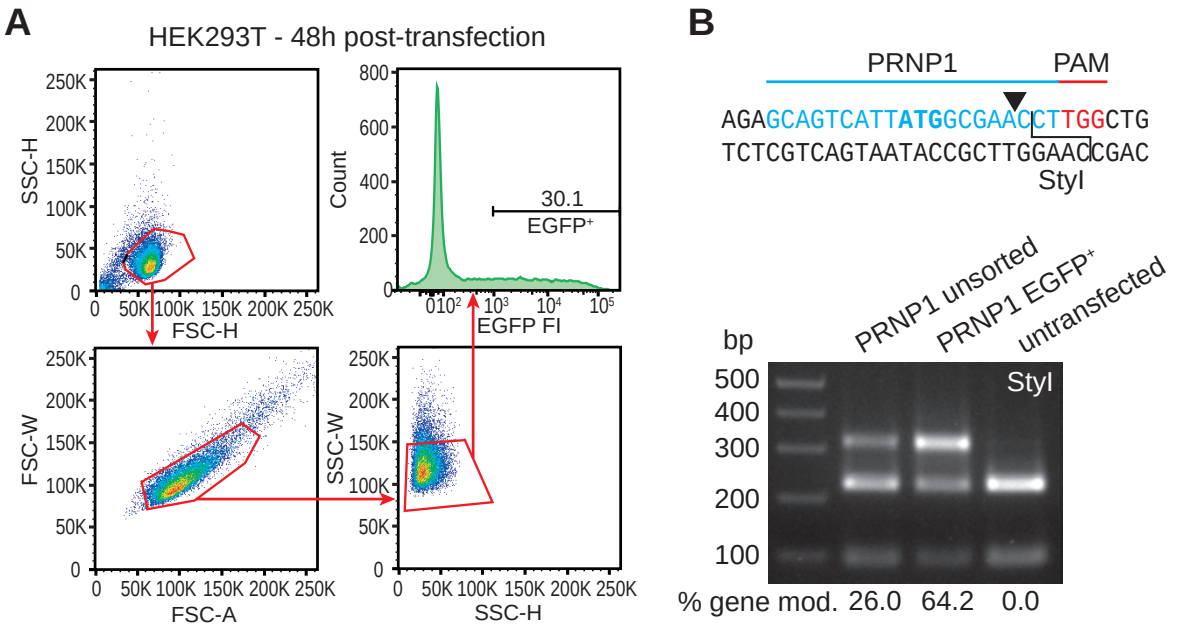


**Figure 2.14.: Single cell sorting of HEK293T transfected with Cas9 and PRNP1 guide RNA.** (A) Sorting strategy for viable EGFP$^+$ HEK293T 48h after transfection. (B) *PRNP* gene modification efficiency was assessed using PCR and digestion of PCR products with the restriction enzyme StyI (location of restriction site relative to PRNP1 binding site shown on top). The intensity of the undigested band (310 bp) indicates the frequency of NHEJ repair within *PRNP*.

had no effect on the percentage of mCherry$^+$ , i. e. viable transfected, cells as compared to mCherry-only transfections. Thus Cas9/PRNP1-mediated DNA-cleavage within *PRNP* allows high gene modification rates without eliciting detectable levels of cytotoxicity in transfected HEK293T cells.

Having established the optimal transfection conditions for Cas9-mediated editing of *PRNP*, I transfected HEK293T with Cas9-2A-EGFP and PRNP1 and performed single cell FACS in collaboration with Hitoshi Takizawa (Division of Hematology, USZ) 48h after transfection (Figure 2.14). Since optimization experiments had shown that EGFP fluorescent intensity correlates with Cas9 expression levels and thus with *PRNP* modification efficiency I reasoned that sorting viable EGFP$^+$ HEK293T would enrich cells with NHEJ-modified *PRNP* alleles and thus increase the probability of identifying individual clones carrying biallelic *PRNP* mutations. Single EGFP$^+$ cells

were sorted into 96 well plates and $10^5$ EGFP$^+$ cells were sorted into DNA lysis buffer for analysis of *PRNP* modification efficiency. For this purpose and the subsequent screening of individual HEK293T clones, I identified the restriction enzyme StyI, which recognizes and cleaves a DNA sequence, which partially overlaps with the Cas9/PRNP1 cleavage site and the PAM consensus sequence (Figure 2.14B). As expected, StyI digestion of a *PRNP*-specific PCR product showed that sorting of

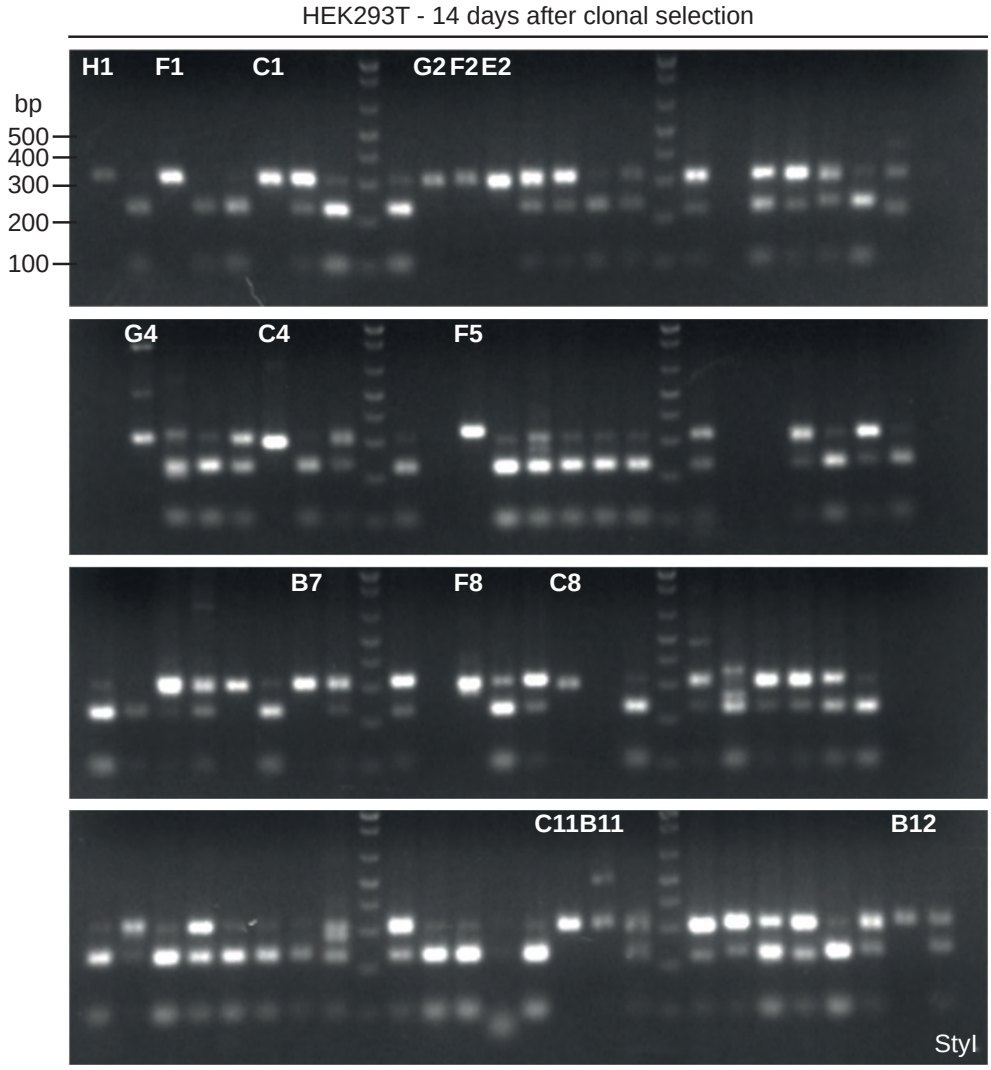


**Figure 2.15.: Identification of HEK293T with biallelic modification of *PRNP*.** Analysis of 96 HEK293T *PRNP* knock-out candidates by PCR and StyI restriction digest 14 days after clonal selection of single cells transfected with Cas9 and PRNP1 guide RNA. 15 clones show PCR products completely resistant to StyI digestion indicating biallelic modification of *PRNP.*

**A**

| HEK293T clones | PRNP1 target sequence | |
|---|---|---|
| | GCAGTCATT**ATG**GCGAACCTTGGCTGCTGGATGCTGGT | wt |
| B7 | GCAGTCATT**ATG**GCGAAC-TTGGCTGCTGGATGCTGGT | Δ1 |
| | GCAGTCATT**ATG**GCGAA----------GGATGCTGGT | Δ11 |
| C1 | GCAGTCATT**ATG**GC----------TGCTGGATGCTGGT | Δ10 |
| | GCAGTCATT**ATG**GCGAA-----GCTGCTGGATGCTGGT | Δ5 |
| C4 | GCAGTCATT**ATG**GCGAA----------TGCTGGT | Δ14 |
| | GCAGTC----------GGCTGCTGGATGCTGGT | Δ15 |
| E2 | GCAGTCATT**ATG**GC----------TGCTGGATGCTGGT | Δ10 |
| | GCAGTCATT----------TGGATGCTGGT | Δ18 |
| F2 | GCAGTCATT**ATG**GCGAA-----GCTGCTGGATGCTGGT | Δ5 |
| | GCAGTCATT**ATG**GC----------TGCTGGATGCTGGT | Δ10 |
| F5 | GCAGTCATT**ATG**GCATTAAATGCCATAATTTAATGCCAGTTG | Δ5 +25 |
| | GCAGTCATT**ATG**GCATTAAATGCCATTATTTAATGCCAGTTG | Δ5 +25 |
| H1 | GCAGTCATT**ATG**GCGAATCCAGCATTATGGCTGCTGGATGCT | Δ3 +10 |

**B**

| | | PrP$^{C}$ Signaling Peptide (10 / 20 / 254) |
|---|---|---|
| | wt | **M**ANLGCWMLVLFVATWSDLGLC...* |
| B7 | Δ1 | **M**ANLAAGCWFSLWPHGVTWAS...* 97 |
| | Δ11 | **MA**KDAGSLCGHME* 14 |
| C1/F2 | Δ5 | **MA**KLLDAGSLCGHME* 16 |
| | Δ10 | **MA**AGCWFSLWPHGVTWASAR...* 44 |
| F5 | Δ5 +25 | **MA**LNAII* 8 |
| | Δ5 +25 | **MA**LNAII* 8 |
| H1 | Δ3 +10 | **M**ANPALWLLDAGSLCGHME* 20 |

**Figure 2.16.: HEK293T *PRNP* knock-out candidates.** (A) Deletions (red on grey background) and insertions (blue background) detected HEK293T cells with biallelic modifications of *PRNP* (start codon in bold font). (B) Clones carrying mutations that introduce frameshifts and premature stop codons in both *PRNP* alleles. Mutated amino acids in red, stop codon,*, numbers indicate distance from initial methionine.

EGFP$^{+}$ Cas9/PRNP1 transfected cells resulted in a 2.5-fold increase of *PRNP* modification rate within this pooled cell population as compared to unsorted transfected cells.

Following single cell sorting, individual clones were expanded for 14 days and screened for biallelic mutagenesis of *PRNP* by PCR and StyI digestion (Figure 2.15). Of the 96 expanded clones analyzed, 15 exhibited PCR products completely resistant to StyI digestion indicating the absence of wt *PRNP* in these cell populations. The majority of cell populations showed a partial StyI digestion pattern, which is consistent

with either the modification of a single *PRNP* allele in a clonal population of cells or an oligoclonal mixture of cells with several possible combinations of modified and unmodified *PRNP* alleles.

In order to select HEK293T *PRNP* knock-out candidates I determined the precise mutations in 7 out of 15 biallelicly modified clones by cloning of PCR products and Sanger sequencing (Figure 2.16). Sequencing confirmed the absence of wt *PRNP* for all clones analyzed. With the exception of clone H1, where only one *PRNP* mutation could be identified, all Cas9/PRNP1-modified HEK293T carried two distinct *PRNP* alleles with short deletions or insertions in proximity to the *PRNP* start codon (Figure 2.16A). Sequence analysis revealed the presence of premature stop codons in both modified *PRNP* protein coding sequences of clones B7, C1, F2, F5, H1 (Figure 2.16B). Premature stop codons could be detected as early as 6 amino acids downstream of the initial methionine (clone F5, both $\triangle$5 +25 alleles), however some mutations such as $\triangle$1 present in clone B7 result in a frameshift that allows translation of relatively long polypeptides (96 amino acids in the case of $\triangle$1) before termination. By coincidence clones C1 and F2 carried the same combination of a $\triangle$5 and a $\triangle$10 *PRNP*.

At the time of writing analysis of $PrP^C$ expression in clones F2, F5, and H1 was ongoing (clone B7 was excluded from the analysis due to a growth defect and atypical cell morphology) in order to confirm *PRNP* knockout for these three candidates.

# 2.4. Discussion

## 2.4.1. Potential & limitations of genome editing

The results presented in this thesis clearly show that all three genome editing technologies, ZFN, TALEN, and CRISPR, can achieve high levels of gene modification in the mouse zygote as well as in standard cell lines such as HEK293T. The currently available genome editing technologies provide sufficiently high rates of NHEJ-mediated repair to ablate genes in any organism that can be manipulated by the introduction of foreign nucleic acids. For the mouse and the human genome libraries of TALEN and CRISPR guide RNAs targeting several 1000 protein-coding genes have been synthesized (Kim et al., 2013; Koike-Yusa et al., 2013; Shalem et al., 2014; Wang et al., 2014). These developments establish high-throughput gene-knockout as a valuable alternative to whole-genome siRNA screens, where protein production is typically reduced but not completely eliminated (Mohr et al., 2010). Additionally, the relatively simple construction of a large number of CRISPR guide-RNAs makes this technology the ideal choice for multiplexed genome editing, i.e. the simultaneous editing of multiple loci in the same cell or embryo (Wang et al., 2013b; Niu et al., 2014).

I have also shown that targeted integration can be achieved in mouse zygotes that were micro-injected with designer nucleases and an HR donor construct. This approach has several advantages over gene-targeting in mouse ES cells such as a shorter time-frame and a better cost efficiency for generating germline-competent founders as well as the freedom of introducing gene modification in any strain of mice. Genome editing in mouse embryos excels at introducing precise changes, such as SNPs, into genes of interest since introducing a selectable marker is not required for identifying correctly targeted alleles (Chen et al., 2011; Wefers et al., 2013).

The results presented here demonstrate the feasibility of integrating large transgenes into defined genomic loci directly in mouse zygotes but also illustrate the need for improving the efficiency of this approach. Not surprisingly, designer nucleases achieving higher cleavage efficiencies also warrant more robust HR-mediated integration of a donor, which became apparent when I compared OPEN and MA ZFNs targeting *ROSA26*. These experiments also suggest that a variety of donors with different configurations, in particular the length of homology arms, can serve as HR repair templates. Ultimately, the frequency of targeted integration events is limited by the endogenous double-strand break repair machinery of mammalian cells, which initiates NHEJ rather than HR by default. Could the repair pathway choice be skewed towards HR by inhibiting components of the NHEJ pathway? Experiments in *Drosophila* (Beumer et al., 2008) and *C. elegans* (Morton et al., 2006) have shown that knocking-out ligase IV, a key component of the NHEJ pathway, significantly improved the HR/NHEJ ratio, however in mice the loss of ligase IV is embryonically lethal (Frank et al., 1998). RNAi screens have identified several additional members of the NHEJ pathway as potential targets for increasing HR repair frequency (Słabicki et al., 2010; Certo et al., 2011). These observations raise the possibility of transient NHEJ-inhibition in mouse embryos. This could be achieved by co-injecting siRNA against one or a combination of these targets together with designer nucleases and targeting constructs or by bath application of small-molecule inhibitors while embryos are in culture.

None of the three genome editing systems offers perfect recognition of a DNA target sequence and cleavage at unintended off-targets has to be taken into consideration. Potential off-target sites can be identified by sequence similarity to the main target site with online resources available for ZFN (Cradick et al., 2011), TALEN (Doyle et al., 2012), and CRISPR (Hsu et al., 2013). With an increasing number of designer nucleases being subjected to high-throughput analysis of binding specificity (Pattanayak et al., 2011, 2013; Guilinger et al., 2014) a continuing improvement of these computational tools can be expected.

If off-target cleavage occurs in a founder animal unintended mutations can be eliminated by successively back-crossing fertile founders and their offspring to wild-type mice (as long as off-target sites are not genetically linked to the modified gene of interest). The absence of off-target cleavage at a limited number of interrogated sites in the genome of C57BL/6 *Prnp*$^{-/-}$ confirms the general view that heterodimeric TALENs are highly specific for their target (Carroll, 2014). A recent study by Guilinger et al., 2014 suggests that TALEN specificity can be further increased by mutating positively charged amino acids in the TALE N- and C-terminus.

For CRISPR/CAS9 two strategies have been suggest to reduce off-target cleavage. First, a CAS9 nickase has been introduced, which can only trigger a double-strand break in combination with two guide RNAs that bind on opposite DNA strands in close proximity to each other (Ran et al., 2013). Second, it has been suggested that truncated guide-RNAs (18 bp instead of the canonical 20 bp) show an improved ratio of on-target over off-target cleavage (Fu et al., 2014).

### 2.4.2. Re-evaluating the functions of PrP$^{C}$ in health and disease

*Prnp*$^{-/-}$ mouse lines have been crucial models for investigating putative physiological functions of PrP$^{C}$. However, several studies have produced contradictory findings with regard to whether the ablation or PrP$^{C}$ is underlying the phenotypic changes in these mice (Steele et al., 2007). Recent studies have highlighted the influence of polymorphic genes flanking the *Prnp*$^{-/-}$ alleles on phenotypes such as increased phagocytosis (Nuvolone et al., 2013) and seizure sensitivity (Striebel et al., 2013). Most likely there are more cases in which a function attributed to PrP$^{C}$ is actually performed by a protein encoded by one of the *Prnp* flanking genes. Experimental strategies such as comparing phenotypes in several strains of *Prnp*$^{-/-}$ mice with distinct genetic backgrounds and rescue experiments including *Prnp*$^{-/-}$ mice intercrossed with a PrP$^{C}$ -overexpresing line such as tga20 (Fischer et al., 1996) allow to some extend to control for genetic confounders (Bremer et al., 2010; Striebel et al.,

2013). However, wild-type and *Prnp*$^{-/-}$ mice with in principal identical genetic backgrounds such as the C57BL/6 *Prnp*$^{-/-}$ presented in this thesis are advantageous for studying more subtle phenotypes.

Comparing phenotypes in C57BL/6 wild-type and *Prnp*$^{-/-}$ mice can potentially help to clarify disputed roles of $PrP^C$ in diverse physiological processes such as synaptic transmission (Collinge et al., 1994; Lledo et al., 1996) or autophagy (Oh et al., 2008; Korom et al., 2013) and pathological conditions such as toxicity of A$\beta$ aggregates (Laurén et al., 2009; Calella et al., 2010) or neuroinflammation (Tsutsui et al., 2008, Kana et al., unpublished).

Membrane-bound $PrP^C$ is indispensable for prion replication (Büeler et al., 1993). However it is currently unknown whether proteins other than $PrP^C$ might modulate the rate of prion replication. Once the knockout of human $PrP^C$ in HEK293T cells is confirmed mouse $PrP^C$ could be introduced into these cells. HEK293T cells expressing mouse but not human $PrP^C$ could serve as a safe model system (avoiding human prions) for performing an unbiased human transcriptome siRNA knockdown screen to unravel potential modulators of prion replication. In case a “druggable” modulator is identified these findings could path the way to therapeutically slowing the progression of human prion diseases.

## 2.5. Methods

### ZFN construction

Zinc finger proteins binding target sites 75 and 403 bp upstream of the XbaI site within the ROSA26 intron 1 were selected using the previously described OPEN method (Maeder et al., 2008). Selected zinc fingers were cloned as XbaI-BamHI fragment into either the expression vectors pST1374 or pMLM290/pMLM292 that express homo- or heterodimeric ZFNs, respectively (Miller et al., 2007). In both ZFN expression vectors, the CMV promoter was replaced by a CMV early enhancer element/chicken beta-actin promoter (CAG) promoter (Okabe et al., 1997). ROSA26 ZFN R4 and L6 (Perez-Pinera et al., 2012) were inserted into the standard pCAG-T7 expression vector using Golden Gate cloning.

### TALEN construction

The TALEN expression vector pCAG-T7-TALEN(Sangamo)-Destination was derived from the yeast TALEN expression vector pTAL4 (Cermak et al., 2011). Two PCR fragments were generated from pTAL4. The first fragment included a truncated TALEN N-terminus (153 aa), followed by a Esp3I-flanked LacZ cassette flanked and truncated TALEN C-terminus (63 aa). TALEN truncations correspond to the TALEN architecture described by Sangamo Biosciences (Miller et al., 2011). A 5' BglII site and a 3' BamHI site were added to the fragment by primer overhangs. The second PCR fragment included the wt FokI domain flanked by a 5' BamHI site and 3' SacI site. The plasmid pCAG-RabZFN-L (a generous gift by R. Kühn, Meyer et al., 2012) was linearized using BglII (3' of T7 promoter) and SacI (5' of polyadenylation signal) and the pCAG-T7 backbone was gel-purified. Both BglII-TALE-LacZ-BamHI and BamHI-FokI-SacI fragments were ligated in a single reaction with the pCAG-T7 backbone to generate pCAG-T7-TALEN(Sangamo)-Destination. TALEN expression vectors with second generation heterodimeric FokI domains (Doyon et al., 2011; Guo et al., 2010)

were generated by excising the wt FokI domain from pCAG-T7-TALEN(Sangamo)-Destination using BamHI and SacI and inserting BamHI/SacI-flanked FokI-ELD and FokI-KKR fragments that were generated by PCR from the plasmids pCMV-RosaR4 KKR and pCMV-RosaL6 ELD (Addgene plasmids 37198, 37198, Perez-Pinera et al., 2012). TALEN expression plasmids described in this thesis are available on Addgene (Table A.1 in the Appendix).

The *Prnp* TALEN target site was identified using the TAL Effector Nucleotide Targeter 2.0 (https://tale-nt.cac.cornell.edu/, Doyle et al., 2012). A *Prnp*-specific TALEN pair was assembled using the Golden Gate TALEN and TAL Effector Kit (Cermak et al., 2011) and the here described heterodimeric pCAG-T7-TALEN(Sangamo)-Destination vectors.

## Cas9 and guide RNA construction

The codon-optimized Cas9 protein coding DNA sequence was created by gene synthesis (Genscript). The expression plasmid pCAG-T7-Cas9-P2A-EGFP for simultaneous production of Cas9 and EGFP was generated using Golden Gate cloning of two PCR products. The first PCR construct included Cas9 with a C-terminal fusion of a partial P2A sequence, the second product consisted of the remaining P2A sequence fused to the N-terminus of EGFP.

U6-promoter driven specific guide RNA plasmids were constructed using the vector MLM3636 (Addgene plasmid 43860, J.K. Joung lab, unpublished). Target sequences for guide RNAs 20 bp in length were identified using the http://crispr.mit.edu/ design tool. For construction of the MLM3636-based guide RNA plasmids PRNP1 and PRNP2, following single-stranded oligos were synthesized (Microsynth), PRNP1-top, ACA CCG CAG TCA TTA TGG CGA ACC TG, PRNP1-bottom, AAA ACA GGT TCG CCA TAA TGA CTG CG, PRNP2-top, ACA CCA TCT TCC TGA TAG TGG GAT GG, PRNP2-bottom, AAA ACC ATC CCA CTA TCA GGA AGA TG. To generate double-stranded oligos with a 5' ACAC and a 3' AAAA overhang, 1 nmol each of top

and bottom oligo were mixed with NEB buffer 2 (final volume 100 µl) and incubated in a water bath under slow cooling from 95℃ to room temperature. Double-stranded oligos were ligated into MLM3636 using Golden Gate cloning.

## *In vitro* mRNA synthesis

Template plasmids for mRNA synthesis were linearized and purified (QIAquick PCR Purification Kit, Qiagen). pCAG-T7-based TALEN and ZFN plasmids were linearized using SacI and OPEN ZFN plasmids were linearized using PmeI.

*In vitro* mRNA transcription, capping and polyadenylation, was performed using the mMESSAGE mMACHINE T7 Ultra Kit. Prior to injection the mRNAs were purified using the NucAway Spin Columns (Ambion). mRNA quality was verified by denaturing gel electrophoresis and concentration was quantified using spectrophotometry.

## Construction of *ROSA26* targeting vectors

Targeting vector GTR26204/205 includes a 1.4 kB 5' ROSA26 homology arm and a 1.8 kB 3' ROSA26 homology arm flanking a central SwaI restriction site. An expression cassette consisting of a 1.6 kB CAG promoter/enhancer followed by the 720 bp EGFP coding region and the 531 bp rabbit beta-globin polyadenylation site was inserted by blunt cloning into the SwaI site to generate targeting vector GTR26204/205-CAG-EGFP. To generate targeting vector GTR26204/205-SA-tdTom a cassette including the 104 bp Ad2 splice-acceptor followed by a 590 bp triple-STOP-pCMV-IRES fragment, the 1.4 kB tdTomato coding region and the 256 bp TK polyadenylation signal was PCR-amplified from pXLBluescriptII PTS tdTomato (gift of J. Ruiz and K. Rector) using primers AGG GCG CAG TAG TCC AGG GTT TCC and GGC TAT GGC AGG GCT TGC CGC C with Pfu polymerase and cloned into the SwaI site of the gtR26-204/205 targeting vector. To generate a linear fragment all GTR26204/205 -based targeting vectors were PacI digestion prior to microinjection.

Targeting vector dR26_HygEGFP is based on pDonor MCS Rosa26 (Addgene plasmid 37200, Perez-Pinera et al., 2012). pDonor MCS Rosa26 was linearized using XbaI, a CAG-T7-Esp3I-LacZ-Esp3I-pA fragment was excised from pCAG-T7-Destination using SpeI and ligated into to pDonor MCS Rosa26 to generated dR26-Destination. A *loxP*-mCherry-pA-*loxP*-HygromcinEGFP-pA cassette was introduced into dR26-Destination to generate dR26_HygEGFP.

## Animals

Females and males of BDF1 (B57BL/6 x DBA/2), C57BL/6, and CD1 mice were purchased from a commercial breeder (Charles River, Germany). All animals were maintained in temperature- and light-controlled rooms (12 light/12 dark, light on from 6:00 a.m.) with food and water ad libidum. All experiments including laboratory animals were approved by the Cantonal Veterinary Office of Zurich. The protocol of animal handling and treatment was in accordance with Swiss Federal and Cantonal regulations as well as the internal guidelines of the University of Zurich.

## Embryo Collection, Culture and Manipulation

B6D2F1 or C57BL/6 female mice underwent ovulation induction by intra peritoneal (i.p.) injection of 5 IU pregnant mare's serum gonadotrophin (PMSG; Folligon – InterVet, Switzerland), followed by i.p. injection of 5 IU human chorionic gonadotropin (hCG; Pregnyl – Essex Chemie, Switzerland) 48 h later. For the recovery of zygotes, the B6D2F1 and C57BL/6 females were mated with the males of the same strain immediately after the administration of hCG. All zygotes were collected from oviducts 24 h after the hCG injection and were then freed from any remaining cumulus cells by a 1-2 min treatment of 0.1% hyaluronidase (Sigma) dissolved in M2 medium. Mouse embryos were cultured in M16 (Sigma) medium at 37℃ and 5% CO2. For micromanipulation the embryos were transferred into M2 medium (Sigma).

## Cytoplasmic and pronuclear microinjections

All microinjections were performed using a microinjection system comprised of an inverted microscope equipped with Nomarski optics (Nikon, Japan), set of micromanipulators (Narashige, Japan) and a FemtoJet microinjection unit (Eppendorf, Germany). ZFN mRNAs were injected into the cytoplasm whereas the DNA expression constructs and DNA targeting fragments were injected into the male pronuclei; in experiments where mRNA and DNA were co-injected the RNA DNA mixture was first injected into the male pronucleus and subsequently into the cytoplasm upon the withdrawal of the microinjection capillary. Specific concentrations of injected mRNAs and DNA constructs are compiled in Table 1.

## Embryo Transfer

Embryos that survived the microinjection were transferred on the same day into the oviducts of 8-16 weeks old pseudopregnant CD-1 females (0.5 days post coitus) that have been mated with sterile TgV males (Haueter et al., 2010) on the day before embryo transfer. Pregnant females were allowed to deliver and raise their pups or were sacrificed at 14-16 days post embryo transfer so that the developing fetuses could be removed for analysis.

## Transfection and single cell sorting of HEK293T

HEK293T were transfected in 6-well format with 1.8 µg of pCAG-T7-Cas9-P2A-EGFP and 0.6 µg of PRNP1 guide RNA. Cells were trypsinized 48h after transfection, washed with PBS and respuspended in PBS with 10% FBS. Sorting of single $EGFP^+$ HEK293T into individual wells containing culture medium (96 well format) was performed using a BD FACSAria III with a 100 µm diameter nozzle. EGFP fluorescence was excited using a 488 nm laser and detected using a 530/30 filter.

## *ROSA26* NHEJ and targeted integration detection assays

Genomic DNA was extracted from mouse biopsies or fetal tissue using a buffer containing 10 mM Tris-HCl pH 9, 50 mM KCl, 0.45% Nonidet p40, 0.45% Tween 20 and Proteinase K. Extracts were subjected to Phenol/Chloroform/Isoamyl alcohol purification, precipitated with Isopropanol, and dissolved in EB buffer (Qiagen). For detecting NHEJ repair at the ROSA26 locus, primers RF (GCC GCC CAC CCT CCC CTT CCT C) and RR (CGC CTA CT CCA CTG CAG CTC CC) were used to amplify a 474 bp fragment covering the ZFN204/205 target site and primers RF4 (AAG TTG AGT CCA TCC GCC GGC) and RR4 (AAA TAC TCC GAG GCG GAT CAC AAG C) were used to amplify a 748 bp fragment covering the ZFN R4/L6 target site. 25 µl of each PCR product were digested with FspI (ZFN204/205) or XbaI (ZFN R4/L6) and subsequently resolved on a 2% agarose gel. Samples including undigested PCR fragments were cloned into pGEM-T easy (Promega) for Sanger sequencing.

Targeted integration of donor vectors was assessed by junction PCR and Southern blotting. In case of ZFN204/205 –mediated ROSA26 targeting primers GF (GCC GGG ATC ACT CTC GGC ATG) and RR2 (CAC CAC TGG CTG GCT AAA CTC TGG) amplified the 3' junction that is specific for the integration of GTR26-204/205-CAG-EGFP. For targeted integration of dR26_HygEGFP into the ZFN R4/L6 site, primers RF3 (CTG ATT GGC TTC TTT TCC TCC CGC C) with CR (GAA CAT ACG TCA TTA TTG ACG TCA ATG GGC) for the 5' junction and RR3 (ATT GGG GGA GGA GAC ATC CAC CTG GAA ACC) with EF (CCT ACG GCG TGC AGT GCT TCA GC) for the 3' junction were used.

For Southern Blot analysis of ZFN204/205 targeting experiments 10 µg of genomic DNA were digested overnight at 37℃ with EcoRI, resolved on a 0.7% agarose gel, and transferred to nylon membranes. Membranes were heat-fixated at 65℃ for 1 h and incubated with prehybdrization solution over night at 65℃. The Rosa 26 5' probe, a 695 bp EcoRI/PacI fragment, was generated from the "Orkin" plasmid. The ROSA26 3' probe, a 615 bp, EcoRI fragment, was generated from plasmid

pCRII-Rosa 3'. Hybridization probes were heat denatured, labeled with P32 marked dCTP (Perkin Elmer) using the Ladderman Labelling Kit (Takara). The labeled probe was purified with illustra MicroSpin S-200 HR columns (GE Healthcare) and heat-denatured probe in hybridization buffer was added to the membranes for overnight rotation at 65℃. Membranes were washed three times (5 min) using 2x SSC. The membranes were exposed for at room temperature 1-3 days and imaged using a Storm 840 phospho-imager (Molecular Dynamics). Digital images of Southern Blots were processed with ImageJ.

## *Prnp* TALEN on- and off-target NHEJ analysis

TALEN-induced mutagenesis of *Prnp* was analyzed using primers PrnpF (AGA TGT CAA GGA CCT TCA GCC) and PrnpR (TAT GGG TAC CCC CTC CTT GG). For initial screening of founders for NHEJ activity, PCR products (356 bp) were subjected to heteroduplex formation using the following conditions in a thermocycler, 95℃ 2 min, 95℃ to 85℃ (-2℃/s), 85℃ to 25℃ (-0.1℃/s) and digested by T7 endonuclease (NEB) for 20 min at 37℃. Digestion products were resolved on a 2% agarose gel. For Sanger sequencing PCR products were cloned into pGEM-T easy (Promega).

*Prnp* $\triangle$8 and $\triangle$17 were genotyped using primers PrnpF/R or primers generating a shorter (86 bp) PCR fragment, PrnpF2 (ATC ATG GCG AAC CTT GGC T) and PrnpR2 (GGC TTT GGC CGC TTT TTG C) and PCRs were resolved on a 3% agarose gel or by Qiaxcel capillary electrophoresis (Qiagen).

Potential off-target sites for the *Prnp* TALEN pair were identified using TAL Effector Nucleotide Targeter 2.0 (https://tale-nt.cac.cornell.edu/, Doyle et al., 2012). Sites with a high predicted probably of binding of the left and the right TALEN with a spacer length that would allow efficient FokI dimerization were prioritized. Off-target sites were screened using T7 endonuclease digestion of PCR products generated with the following primers,

OT1 | GGAGACTAAGTGGGTGATGTTGT | AGGTGATGATTCACTGTGAGCTT

OT2 | CTAAGACCCTTGGGTCCATAAGC | GACATAGAAGGCCAATCTGACCA

OT3 | TCAAATCCAACTACCAGGGTCTG | GTGGGGTATCACAGTATCCTTCC

OT4 | CTGTCCTGGTTTGTTTAAGTGGC | AAGATCTTCTCAGCAGGCTTTCA

OT6 | AACTGTGGTCAAAGATGGAAGGA | CCCGTGCATAGGGATCAGAATTA

OT7 | CAATGCTTTTAGAGGAATGGCCC | CTGACACCTGTATCTTTGACCCA

OT11 | GAAGATGTGCACAAGGAAAGGAC | GAGACCACAGCCAATTAGACACT

OT12 | TGACACTGTTTTGCTAGGTCTGA | ATGTGAATGTGGGTATTCTGCCT.

### *PRNP* CRISPR NHEJ analysis

CRISPR-mediated editing of *PRNP* was analyzed by PCR using the primers PRNP-F (TGC TTCA GAG AAG TAC AGG GTG) and PRNP-R (ATG AAC TCA ATC AAA GGG GGC T) for transfections of guide RNAs PRNP1 or PRNP2 (or the combination of both) or by primers PRNP-F2 (TGG AGC AGG AGA AAG AGT TGT GT) and PRNP-R2 (CAG TGT TCC ATC CTC CAG GCT TC) specific for the PRNP1 target site. NHEJ-induced mutagenesis was analyzed using T7 endonuclease digestion for PRNP1 and PRNP2 target sites or by StyI digestion for the PRNP1 target site. Densities of digested and undigested PCR bands resolved on 1.5% or 2% agarose gels were integrated using ImageJ. Gene modification efficiency was derived from integrated band densities for T7 endonuclease digested products as described by Guschin et al., 2010 using the following equation , $\%\,gene\,modifcation = 100 \times (1 - \sqrt{1 - \frac{\sum cleaved\,bands}{\sum all\,bands}})$. For StyI digested PCR products, gene modification efficiency was calculated by $\%\,gene\,modification = 100 \times \frac{uncleaved\,band}{\sum all\,bands}$.

## Protein Analysis

Homogenates of mouse cortex, cerebellum and spinal cord were prepared in PBS, 0.05% sodium deoxycholate, and 0.05% Nonidet P-40. Protein concentration was

determined using the bicinchoninic acid assay (BCA, Pierce). Samples were prepared in loading buffer (NuPAGE, Life Technologies) and boiled at 95℃ for 10 min. Proteins (17 µg per lane) were separated on a 12% Bis-Tris polyacrylamide gel (NuPAGE, Life Technologies) and blotted onto a nitrocellulose membrane (Whatman). Membranes were blocked with PBS with 0.1% Tween 20 and 5% Top block (LuBio Science). Primary antibodies were diluted in PBS with 0.1% Tween 20 and 1% Top block. Mouse monoclonal antibodies were anti-$PrP^C$ antibodies (produced in-house) POM1 (280 ng/ml), POM2, POM13, and POM19 (all 400 ng/ml) and anti-actin antibody clone C4 (Millipore, 125 ng/ml). Membranes were incubated with primary antibodies at 4℃ over night and subsequently washed with BS with 0.1% Tween 20 and 1% Top block. Membranes were incubated with a HRP-conjugated goat anti-mouse secondary antibody (Life Technologies, 1:17000) at room temperature for one hour. Blots were developed using Luminata Crescendo reagent (Millipore) and were exposed using a Stella detector (Raytest).

# References


Aguzzi A, Sigurdson C, Heikenwaelder M (2008) Molecular mechanisms of prion pathogenesis. *Annu Rev Pathol* 3:11–40.

Anastassiadis K, Fu J, Patsch C, Hu S, Weidlich S, Duerschke K, Buchholz F, Edenhofer F, Stewart AF (2009) Dre recombinase, like cre, is a highly efficient site-specific recombinase in e. coli, mammalian cells and mice. *Dis Model Mech* 2:508–515.

Andreas S, Schwenk F, Küter-Luks B, Faust N, Kühn R (2002) Enhanced efficiency through nuclear localization signal fusion on phage phic31-integrase: activity comparison with cre and flpe recombinase in mammalian cells. *Nucleic Acids Res* 30:2299–2306.

Araki K, Araki M, Miyazaki J, Vassalli P (1995) Site-specific recombination of a transgene in fertilized eggs by transient expression of cre recombinase. *Proc Natl Acad Sci U S A* 92:160–164.

Bedell VM, Wang Y, Campbell JM, Poshusta TL, Starker CG, Krug n RG, Tan W, Penheiter SG, Ma AC, Leung AYH, Fahrenkrug SC, Carlson DF, Voytas DF, Clark KJ, Essner JJ, Ekker SC (2012) In vivo genome editing using a high-efficiency talen system. *Nature* 491:114–8.

Bendall SC, Simonds EF, Qiu P, Amir EaD, Krutzik PO, Finck R, Bruggner RV, Melamed R, Trejo A, Ornatsky OI, Balderas RS, Plevritis SK, Sachs K, Pe'er D, Tanner SD, Nolan GP (2011) Single-cell mass cytometry of differential immune and drug responses across a human hematopoietic continuum. *Science* 332:687–96.

Berg JM (1988) Proposed structure for the zinc-binding domains from transcription factor iiia and related proteins. *Proc Natl Acad Sci U S A* 85:99–102.

Beumer KJ, Trautman JK, Bozas A, Liu JL, Rutter J, Gall JG, Carroll D (2008) Efficient gene targeting in drosophila by direct embryo injection with zinc-finger nucleases. *Proc Natl Acad Sci U S A* 105:19821–6.

Boch J, Scholze H, Schornack S, Landgraf A, Hahn S, Kay S, Lahaye T, Nickstadt A, Bonas U (2009) Breaking the code of dna binding specificity of tal-type iii effectors. *Science* 326:1509–12.

Bogdanove AJ, Voytas DF (2011) Tal effectors: customizable proteins for dna targeting. *Science* 333:1843–1846.

Bonnet J, Yin P, Ortiz ME, Subsoontorn P, Endy D (2013) Amplifying genetic logic gates. *Science* 340:599–603.

Bremer J, Baumann F, Tiberi C, Wessig C, Fischer H, Schwarz P, Steele AD, Toyka KV, Nave KA, Weis J, Aguzzi A (2010) Axonal prion protein is required for peripheral myelin maintenance. *Nat Neurosci* 13:310–8.

Briggs AW, Rios X, Chari R, Yang L, Zhang F, Mali P, Church GM (2012) Iterative capped assembly: rapid and scalable synthesis of repeat-module dna such as tal effectors from individual monomers. *Nucleic Acids Res* 40:e117.

Buch T, Heppner FL, Tertilt C, Heinen TJ, Kremer M, Wunderlich FT, Jung S, Waisman A (2005) A cre-inducible diphtheria toxin receptor mediates cell lineage ablation after toxin administration. *Nat Methods* 2:419–426.

Büeler H, Aguzzi A, Sailer A, Greiner RA, Autenried P, Aguet M, Weissmann C (1993) Mice devoid of prp are resistant to scrapie. *Cell* 73:1339–47.

Calella AM, Farinelli M, Nuvolone M, Mirante O, Moos R, Falsig J, Mansuy IM, Aguzzi A (2010) Prion protein and abeta-related synaptic toxicity impairment. *EMBO Mol Med* 2:306–14.

Campsall KD, Mazerolle CJ, De Repentingy Y, Kothary R, Wallace VA (2002) Characterization of transgene expression and cre recombinase activity in a panel of thy-1 promoter-cre transgenic mice. *Dev Dyn* 224:135–143.

Capecchi MR (2005) Gene targeting in mice: functional analysis of the mammalian genome for the twenty-first century. *Nat Rev Genet* 6:507–512.

Carbery ID, Ji D, Harrington A, Brown V, Weinstein EJ, Liaw L, Cui X (2010) Targeted genome modification in mice using zinc-finger nucleases. *Genetics* 186:451–459.

Caroni P (1997) Overexpression of growth-associated proteins in the neurons of adult transgenic mice. *J Neurosci Methods* 71:3–9.

Carroll D, Morton JJ, Beumer KJ, Segal DJ (2006) Design, construction and in vitro testing of zinc finger nucleases. *Nat Protoc* 1:1329–1341.

Carroll D (2014) Genome engineering with targetable nucleases. *Annu Rev Biochem* .

Carvajal-Vallejos P, Pallissé R, Mootz HD, Schmidt SR (2012) Unprecedented rates and efficiencies revealed for new natural split inteins from metagenomic sources. *J Biol Chem* 287:28686–28696.

Casanova E, Lemberger T, Fehsenfeld S, Mantamadiotis T, Schütz G (2003) Alpha complementation in the cre recombinase enzyme. *Genesis* 37:25–29.

Cermak T, Doyle EL, Christian M, Wang L, Zhang Y, Schmidt C, Baller JA, Somia NV, Bogdanove AJ, Voytas DF (2011) Efficient design and assembly of custom talen and other tal effector-based constructs for dna targeting. *Nucleic Acids Res* 39.

Certo MT, Ryu BY, Annis JE, Garibov M, Jarjour J, Rawlings DJ, Scharenberg AM (2011) Tracking genome engineering outcome at individual dna breakpoints. *Nat Methods* 8:671–676.

Chen F, Pruett-Miller SM, Huang Y, Gjoka M, Duda K, Taunton J, Collingwood TN, Frodin M, Davis GD (2011) High-frequency genome editing using ssdna oligonucleotides with zinc-finger nucleases. *Nat Methods* 8:753–5.

Cho SW, Kim S, Kim JM, Kim JS (2013) Targeted genome engineering in human cells with the cas9 rna-guided endonuclease. *Nat Biotechnol* 31:230–2.

Cho W, Hagemann TL, Johnson DA, Johnson JA, Messing A (2009) Dual transgenic reporter mice as a tool for monitoring expression of glial fibrillary acidic protein. *J Neurochem* 110:343–351.

Christian M, Cermak T, Doyle EL, Schmidt C, Zhang F, Hummel A, Bogdanove AJ, Voytas DF (2010) Targeting dna double-strand breaks with tal effector nucleases. *Genetics* 186:757–61.

Collinge J, Whittington MA, Sidle KC, Smith CJ, Palmer MS, Clarke AR, Jefferys JG (1994) Prion protein is necessary for normal synaptic function. *Nature* 370:295–7.

Cong L, Ran FA, Cox D, Lin S, Barretto R, Habib N, Hsu PD, Wu X, Jiang W, Marraffini LA, Zhang F (2013) Multiplex genome engineering using crispr/cas systems. *Science* 339:819–23.

Cradick TJ, Ambrosini G, Iseli C, Bucher P, McCaffrey AP (2011) Zfn-site searches genomes for zinc finger nuclease target sites and off-target sites. *BMC Bioinformatics* 12:152.

Cui X, Ji D, Fisher DA, Wu Y, Briner DM, Weinstein EJ (2011) Targeted integration in rat and mouse embryos with zinc-finger nucleases. *Nat Biotechnol* 29:64–67.

Dassa B, London N, Stoddard BL, Schueler-Furman O, Pietrokovski S (2009) Fractured genes: a novel genomic arrangement involving new split inteins and a new homing endonuclease family. *Nucleic Acids Res* 37:2560–2573.

Doyle EL, Booher NJ, Standage DS, Voytas DF, Brendel VP, Vandyk JK, Bogdanove AJ (2012) Tal effector-nucleotide targeter (tale-nt) 2.0: tools for tal effector design and target prediction. *Nucleic Acids Res* 40:W117–22.

Doyon Y, McCammon JM, Miller JC, Faraji F, Ngo C, Katibah GE, Amora R, Hocking TD, Zhang L, Rebar EJ, Gregory PD, Urnov FD, Amacher SL (2008) Heritable targeted gene disruption in zebrafish using designed zinc-finger nucleases. *Nat Biotechnol* 26:702–708.

Doyon Y, Vo TD, Mendel MC, Greenberg SG, Wang J, Xia DF, Miller JC, Urnov FD, Gregory PD, Holmes MC (2011) Enhancing zinc-finger-nuclease activity with improved obligate heterodimeric architectures. *Nat Methods* 8:74–9.

Dymecki SM, Ray RS, Kim JC (2010) Mapping cell fate and function using recombinase-based intersectional strategies. *Methods Enzymol* 477:183–213.

Engler C, Kandzia R, Marillonnet S (2008) A one pot, one step, precision cloning method with high throughput capability. *PLoS One* 3.

Feil R, Wagner J, Metzger D, Chambon P (1997) Regulation of cre recombinase activity by mutated estrogen receptor ligand-binding domains. *Biochem Biophys Res Commun* 237:752–757.

Feng G, Mellor RH, Bernstein M, Keller-Peck C, Nguyen QT, Wallace M, Nerbonne JM, Lichtman JW, Sanes JR (2000) Imaging neuronal subsets in transgenic mice expressing multiple spectral variants of gfp. *Neuron* 28:41–51.

Fischer M, Rülicke T, Raeber A, Sailer A, Moser M, Oesch B, Brandner S, Aguzzi A, Weissmann C (1996) Prion protein (prp) with amino-proximal deletions restoring susceptibility of prp knockout mice to scrapie. *EMBO J* 15:1255–64.

Frank KM, Sekiguchi JM, Seidl KJ, Swat W, Rathbun GA, Cheng HL, Davidson L, Kangaloo L, Alt FW (1998) Late embryonic lethality and impaired v(d)j recombination in mice lacking dna ligase iv. *Nature* 396:173–7.

Fu Y, Sander JD, Reyon D, Cascio VM, Joung JK (2014) Improving crispr-cas nuclease specificity using truncated guide rnas. *Nat Biotechnol* .

Gerner MY, Kastenmuller W, Ifrim I, Kabat J, Germain RN (2012) Histo-cytometry: a method for highly multiplex quantitative tissue imaging analysis applied to dendritic cell subset microanatomy in lymph nodes. *Immunity* 37:364–376.

Geurts AM, Cost GJ, Freyvert Y, Zeitler B, Miller JC, Choi VM, Jenkins SS, Wood A, Cui X, Meng X, Vincent A, Lam S, Michalkiewicz M, Schilling R, Foeckler J, Kalloway S, Weiler H, Ménoret S, Anegon I, Davis GD, Zhang L, Rebar EJ, Gregory

PD, Urnov FD, Jacob HJ, Buelow R (2009) Knockout rats via embryo microinjection of zinc-finger nucleases. *Science* 325:433–433.

Ghosh P, Kim AI, Hatfull GF (2003) The orientation of mycobacteriophage bxb1 integration is solely dependent on the central dinucleotide of attp and attb. *Mol Cell* 12:1101–1111.

Ghosh P, Pannunzio NR, Hatfull GF (2005) Synapsis in phage bxb1 integration: selection mechanism for the correct pair of recombination sites. *J Mol Biol* 349:331–348.

Gong S, Zheng C, Doughty ML, Losos K, Didkovsky N, Schambra UB, Nowak NJ, Joyner A, Leblanc G, Hatten ME, Heintz N (2003) A gene expression atlas of the central nervous system based on bacterial artificial chromosomes. *Nature* 425:917–925.

Greig LC, Woodworth MB, Galazo MJ, Padmanabhan H, Macklis JD (2013) Molecular logic of neocortical projection neuron specification, development and diversity. *Nat Rev Neurosci* 14:755–769.

Grindley ND, Whiteson KL, Rice PA (2006) Mechanisms of site-specific recombination. *Annu Rev Biochem* 75:567–605.

Guilinger JP, Pattanayak V, Reyon D, Tsai SQ, Sander JD, Joung JK, Liu DR (2014) Broad specificity profiling of talens results in engineered nucleases with improved dna-cleavage specificity. *Nat Methods* 11:429–35.

Guo J, Gaj T, Barbas r CF (2010) Directed evolution of an enhanced and highly efficient foki cleavage domain for zinc finger nucleases. *J Mol Biol* 400:96–107.

Guschin DY, Waite AJ, Katibah GE, Miller JC, Holmes MC, Rebar EJ (2010) A rapid and general assay for monitoring endogenous gene modification. *Methods Mol Biol* 649:247–56.

Haueter S, Kawasumi M, Asner I, Brykczynska U, Cinelli P, Moisyadi S, Bürki K, Peters AH, Pelczar P (2010) Genetic vasectomy-overexpression of prm1-egfp

fusion protein in elongating spermatids causes dominant male sterility in mice. *Genesis* 48:151–160.

Hermann M, Maeder ML, Rector K, Ruiz J, Becher B, Bürki K, Khayter C, Aguzzi A, Joung JK, Buch T, Pelczar P (2012) Evaluation of open zinc finger nucleases for direct gene targeting of the rosa26 locus in mouse embryos. *PLoS One* 7.

Hirrlinger J, Requardt RP, Winkler U, Wilhelm F, Schulze C, Hirrlinger PG (2009a) Split-creert2: temporal control of dna recombination mediated by split-cre protein fragment complementation. *PLoS One* 4.

Hirrlinger J, Scheller A, Hirrlinger PG, Kellert B, Tang W, Wehr MC, Goebbels S, Reichenbach A, Sprengel R, Rossner MJ, Kirchhoff F (2009b) Split-cre complementation indicates coincident activity of different genes in vivo. *PLoS One* 4.

Hornemann S, Korth C, Oesch B, Riek R, Wider G, Wüthrich K, Glockshuber R (1997) Recombinant full-length murine prion protein, mprp(23-231): purification and spectroscopic characterization. *FEBS Lett* 413:277–81.

Hsu PD, Scott DA, Weinstein JA, Ran FA, Konermann S, Agarwala V, Li Y, Fine EJ, Wu X, Shalem O, Cradick TJ, Marraffini LA, Bao G, Zhang F (2013) Dna targeting specificity of rna-guided cas9 nucleases. *Nat Biotechnol* 31:827–32.

Huang L, Wilkinson MF (2012) Regulation of nonsense-mediated mrna decay. *Wiley Interdisciplinary Reviews: RNA* 3:807–828.

Jinek M, East A, Cheng A, Lin S, Ma E, Doudna J (2013) Rna-programmed genome editing in human cells. *Elife* 2:e00471.

Jullien N, Goddard I, Selmi-Ruby S, Fina JL, Cremer H, Herman JP (2007) Conditional transgenesis using dimerizable cre (dicre). *PLoS One* 2.

Jullien N, Sampieri F, Enjalbert A, Herman JP (2003) Regulation of cre recombinase by ligand-induced complementation of inactive fragments. *Nucleic Acids Res* 31.

Kelley KA, Friedrich VL, Sonshine A, Hu Y, Lax J, Li J, Drinkwater D, Dressler H, Herrup K (1994) Expression of thy-1/lacz fusion genes in the cns of transgenic mice. *Brain Res Mol Brain Res* 24:261–274.

Kim H, Kim JS (2014) A guide to genome engineering with programmable nucleases. *Nat Rev Genet* .

Kim YG, Cha J, Chandrasegaran S (1996) Hybrid restriction enzymes: zinc finger fusions to fok i cleavage domain. *Proc Natl Acad Sci U S A* 93:1156–1160.

Kim Y, Kweon J, Kim A, Chon JK, Yoo JY, Kim HJ, Kim S, Lee C, Jeong E, Chung E, Kim D, Lee MS, Go EM, Song HJ, Kim H, Cho N, Bang D, Kim S, Kim JS (2013) A library of tal effector nucleases spanning the human genome. *Nat Biotechnol* 31:251–8.

Koike-Yusa H, Li Y, Tan EP, Velasco-Herrera MDC, Yusa K (2013) Genome-wide recessive genetic screening in mammalian cells with a lentiviral crispr-guide rna library. *Nat Biotechnol* .

Korom M, Wylie KM, Wang H, Davis KL, Sangabathula MS, Delassus GS, Morrison LA (2013) A proautophagic antiviral role for the cellular prion protein identified by infection with a herpes simplex virus 1 icp34.5 mutant. *J Virol* 87:5882–94.

Kriegstein A, Alvarez-Buylla A (2009) The glial nature of embryonic and adult neural stem cells. *Annu Rev Neurosci* 32:149–184.

Langevin LM, Mattar P, Scardigli R, Roussigné M, Logan C, Blader P, Schuurmans C (2007) Validating in utero electroporation for the rapid analysis of gene regulatory elements in the murine telencephalon. *Dev Dyn* 236:1273–1286.

Laurén J, Gimbel DA, Nygaard HB, Gilbert JW, Strittmatter SM (2009) Cellular prion protein mediates impairment of synaptic plasticity by amyloid-beta oligomers. *Nature* 457:1128–32.

Li L, Wu LP, Chandrasegaran S (1992) Functional domains in fok i restriction endonuclease. *Proc Natl Acad Sci U S A* 89:4275–9.

Linden R, Martins VR, Prado MAM, Cammarota M, Izquierdo I, Brentani RR (2008) Physiology of the prion protein. *Physiol Rev* 88:673–728.

Liu Q, Segal DJ, Ghiara JB, Barbas r CF (1997) Design of polydactyl zinc-finger proteins for unique addressing within complex genomes. *Proc Natl Acad Sci U S A* 94:5525–30.

Livet J, Weissman TA, Kang H, Draft RW, Lu J, Bennis RA, Sanes JR, Lichtman JW (2007) Transgenic strategies for combinatorial expression of fluorescent proteins in the nervous system. *Nature* 450:56–62.

Lledo PM, Tremblay P, DeArmond SJ, Prusiner SB, Nicoll RA (1996) Mice deficient for prion protein exhibit normal neuronal excitability and synaptic transmission in the hippocampus. *Proc Natl Acad Sci U S A* 93:2403–7.

Madisen L, Zwingman TA, Sunkin SM, Oh SW, Zariwala HA, Gu H, Ng LL, Palmiter RD, Hawrylycz MJ, Jones AR, Lein ES, Zeng H (2010) A robust and high-throughput cre reporting and characterization system for the whole mouse brain. *Nat Neurosci* 13:133–140.

Maeder ML, Thibodeau-Beganny S, Osiak A, Wright DA, Anthony RM, Eichtinger M, Jiang T, Foley JE, Winfrey RJ, Townsend JA, Unger-Wallace E, Sander JD, Müller-Lerch F, Fu F, Pearlberg J, Göbel C, Dassie JP, Pruett-Miller SM, Porteus MH, Sgroi DC, Iafrate AJ, Dobbs D, McCray PB, Cathomen T, Voytas DF, Joung JK (2008) Rapid "open-source" engineering of customized zinc-finger nucleases for highly efficient gene modification. *Mol Cell* 31:294–301.

Maeder ML, Thibodeau-Beganny S, Sander JD, Voytas DF, Joung JK (2009) Oligomerized pool engineering (open): an 'open-source' protocol for making customized zinc-finger arrays. *Nat Protoc* 4:1471–1501.

Malatesta P, Hack MA, Hartfuss E, Kettenmann H, Klinkert W, Kirchhoff F, Götz M (2003) Neuronal or glial progeny: regional differences in radial glia fate. *Neuron* 37:751–764.

Mali P, Yang L, Esvelt KM, Aach J, Guell M, DiCarlo JE, Norville JE, Church GM (2013) Rna-guided human genome engineering via cas9. *Science* 339:823–6.

McVey M, Lee SE (2008) Mmej repair of double-strand breaks (director's cut): deleted sequences and alternative endings. *Trends Genet* 24:529–38.

Mediavilla J, Jain S, Kriakov J, Ford ME, Duda RL, Jacobs WR, Hendrix RW, Hatfull GF (2000) Genome organization and characterization of mycobacteriophage bxb1. *Mol Microbiol* 38:955–970.

Meyer M, de Angelis MH, Wurst W, Kühn R (2010) Gene targeting by homologous recombination in mouse zygotes mediated by zinc-finger nucleases. *Proc Natl Acad Sci U S A* 107:15022–15026.

Meyer M, Ortiz O, Hrabé de Angelis M, Wurst W, Kühn R (2012) Modeling disease mutations by gene targeting in one-cell mouse embryos. *Proc Natl Acad Sci U S A* 109:9354–9.

Miele G, Alejo Blanco AR, Baybutt H, Horvat S, Manson J, Clinton M (2003) Embryonic activation and developmental expression of the murine prion protein gene. *Gene Expr* 11:1–12.

Miller JC, Holmes MC, Wang J, Guschin DY, Lee YL, Rupniewski I, Beausejour CM, Waite AJ, Wang NS, Kim KA, Gregory PD, Pabo CO, Rebar EJ (2007) An improved zinc-finger nuclease architecture for highly specific genome editing. *Nat Biotechnol* 25:778–785.

Miller JC, Tan S, Qiao G, Barlow KA, Wang J, Xia DF, Meng X, Paschon DE, Leung E, Hinkley SJ, Dulay GP, Hua KL, Ankoudinova I, Cost GJ, Urnov FD, Zhang HS, Holmes MC, Zhang L, Gregory PD, Rebar EJ (2011) A tale nuclease architecture for efficient genome editing. *Nat Biotechnol* 29:143–148.

Moehle EA, Moehle EA, Rock JM, Rock JM, Lee YL, Lee YL, Jouvenot Y, Jouvenot Y, DeKelver RC, Dekelver RC, Gregory PD, Gregory PD, Urnov FD, Urnov FD, Holmes MC, Holmes MC (2007) Targeted gene addition into a specified location in the human genome using designed zinc finger nucleases. *Proc Natl Acad Sci U S A* 104:3055–60.

Mohr S, Bakal C, Perrimon N (2010) Genomic screening with rnai: results and challenges. *Annu Rev Biochem* 79:37–64.

Moore M, Klug A, Choo Y (2001) Improved dna binding specificity from polyzinc finger peptides by using strings of two-finger units. *Proc Natl Acad Sci U S A* 98:1437–1441.

Morton J, Davis MW, Jorgensen EM, Carroll D (2006) Induction and repair of zinc-finger nuclease-targeted double-strand breaks in caenorhabditis elegans somatic cells. *Proc Natl Acad Sci U S A* 103:16370–5.

Moscou MJ, Bogdanove AJ (2009) A simple cipher governs dna recognition by tal effectors. *Science* 326:1501.

Nagy A (2000) Cre recombinase: the universal reagent for genome tailoring. *Genesis* 26:99–109.

Nern A, Pfeiffer BD, Svoboda K, Rubin GM (2011) Multiple new site-specific recombinases for use in manipulating animal genomes. *Proc Natl Acad Sci U S A* 108:14198–14203.

Niu Y, Shen B, Cui Y, Chen Y, Wang J, Wang L, Kang Y, Zhao X, Si W, Li W, Xiang AP, Zhou J, Guo X, Bi Y, Si C, Hu B, Dong G, Wang H, Zhou Z, Li T, Tan T, Pu X, Wang F, Ji S, Zhou Q, Huang X, Ji W, Sha J (2014) Generation of gene-modified cynomolgus monkey via cas9/rna-mediated gene targeting in one-cell embryos. *Cell* 156:836–43.

Nuvolone M, Kana V, Hutter G, Sakata D, Mortin-Toth SM, Russo G, Danska JS, Aguzzi A (2013) Sirp$\alpha$ polymorphisms, but not the prion protein, control phagocytosis of apoptotic cells. *J Exp Med* 210:2539–52.

Oh JM, Shin HY, Park SJ, Kim BH, Choi JK, Choi EK, Carp RI, Kim YS (2008) The involvement of cellular prion protein in the autophagy pathway in neuronal cells. *Mol Cell Neurosci* 39:238–47.

Okabe M, Ikawa M, Kominami K, Nakanishi T, Nishimune Y (1997) 'green mice' as a source of ubiquitous green cells. *FEBS Lett* 407:313–319.

Pattanayak V, Lin S, Guilinger JP, Ma E, Doudna JA, Liu DR (2013) High-throughput profiling of off-target dna cleavage reveals rna-programmed cas9 nuclease specificity. *Nat Biotechnol* 31:839–43.

Pattanayak V, Ramirez CL, Joung JK, Liu DR (2011) Revealing off-target cleavage specificities of zinc-finger nucleases by in vitro selection. *Nat Methods* 8:765–70.

Pavletich NP, Pabo CO (1991) Zinc finger-dna recognition: crystal structure of a zif268-dna complex at 2.1 a. *Science* 252:809–17.

Perez-Pinera P, Ousterout DG, Brown MT, Gersbach CA (2012) Gene targeting to the rosa26 locus directed by engineered zinc finger nucleases. *Nucleic Acids Res* 40:3741–3752.

Poueymirou WT, Auerbach W, Frendewey D, Hickey JF, Escaravage JM, Esau L, Doré AT, Stevens S, Adams NC, Dominguez MG, Gale NW, Yancopoulos GD, DeChiara TM, Valenzuela DM (2007) F0 generation mice fully derived from gene-targeted embryonic stem cells allowing immediate phenotypic analyses. *Nat Biotechnol* 25:91–9.

Ran FA, Hsu PD, Lin CY, Gootenberg JS, Konermann S, Trevino AE, Scott DA, Inoue A, Matoba S, Zhang Y, Zhang F (2013) Double nicking by rna-guided crispr cas9 for enhanced genome editing specificity. *Cell* 154:1380–9.

Reyon D, Tsai SQ, Khayter C, Foden JA, Sander JD, Joung JK (2012) Flash assembly of talens for high-throughput genome editing. *Nat Biotechnol* 30:460–5.

Riek R, Hornemann S, Wider G, Billeter M, Glockshuber R, Wüthrich K (1996) Nmr structure of the mouse prion protein domain prp(121-231). *Nature* 382:180–2.

Saito T, Nakatsuji N (2001) Efficient gene transfer into the embryonic mouse brain using in vivo electroporation. *Dev Biol* 240:237–246.

Samulski RJ, Zhu X, Xiao X, Brook JD, Housman DE, Epstein N, Hunter LA (1991) Targeted integration of adeno-associated virus (aav) into human chromosome 19. *EMBO J* 10:3941–50.

Sando R, Baumgaertel K, Pieraut S, Torabi-Rander N, Wandless TJ, Mayford M, Maximov A (2013) Inducible control of gene expression with destabilized cre. *Nat Methods* 10:1085–1088.

Sauer B, McDermott J (2004) Dna recombination with a heterospecific cre homolog identified from comparison of the pac-c1 regions of p1-related phages. *Nucleic Acids Res* 32:6086–6095.

Schepers AG, Snippert HJ, Stange DE, van den Born M, van Es JH, van de Wetering M, Clevers H (2012) Lineage tracing reveals lgr5+ stem cell activity in mouse intestinal adenomas. *Science* 337:730–735.

Schmid-Burgk JL, Schmidt T, Kaiser V, Höning K, Hornung V (2013) A ligation-independent cloning technique for high-throughput assembly of transcription activator–like effector genes. *Nat Biotechnol* 31:76–81.

Schmidt-Supprian M, Rajewsky K (2007) Vagaries of conditional gene targeting. *Nat Immunol* 8:665–668.

Shalem O, Sanjana NE, Hartenian E, Shi X, Scott DA, Mikkelsen TS, Heckl D, Ebert BL, Root DE, Doench JG, Zhang F (2014) Genome-scale crispr-cas9 knockout screening in human cells. *Science* 343:84–7.

Shimshek DR, Kim J, Hübner MR, Spergel DJ, Buchholz F, Casanova E, Stewart AF, Seeburg PH, Sprengel R (2002) Codon-improved cre recombinase (icre) expression in the mouse. *Genesis* 32:19–26.

Siuti P, Yazbek J, Lu TK (2013) Synthetic circuits integrating logic and memory in living cells. *Nat Biotechnol* 31:448–452.

Skarnes WC, Rosen B, West AP, Koutsourakis M, Bushell W, Iyer V, Mujica AO, Thomas M, Harrow J, Cox T, Jackson D, Severin J, Biggs P, Fu J, Nefedov M, de Jong PJ, Stewart AF, Bradley A (2011) A conditional knockout resource for the genome-wide study of mouse gene function. *Nature* 474:337–342.

Słabicki M, Theis M, Krastev DB, Samsonov S, Mundwiller E, Junqueira M, Paszkowski-Rogacz M, Teyra J, Heninger AK, Poser I, Prieur F, Truchetto J, Confavreux C, Marelli C, Durr A, Camdessanche JP, Brice A, Shevchenko A, Pisabarro MT, Stevanin G, Buchholz F (2010) A genome-scale dna repair rnai screen identifies spg48 as a novel gene associated with hereditary spastic paraplegia. *PLoS Biol* 8:e1000408.

Sorek R, Lawrence CM, Wiedenheft B (2013) Crispr-mediated adaptive immune systems in bacteria and archaea. *Annu Rev Biochem* 82:237–66.

Soriano P (1999) Generalized lacz expression with the rosa26 cre reporter strain. *Nat Genet* 21:70–71.

Steele AD, Lindquist S, Aguzzi A (2007) The prion protein knockout mouse: a phenotype under challenge. *Prion* 1:83–93.

Striebel JF, Race B, Chesebro B (2013) Prion protein and susceptibility to kainate-induced seizures: genetic pitfalls in the use of prp knockout mice. *Prion* 7:280–5.

Subach OM, Gundorov IS, Yoshimura M, Subach FV, Zhang J, Grüenwald D, Souslova EA, Chudakov DM, Verkhusha VV (2008) Conversion of red fluorescent protein into a bright blue probe. *Chem Biol* 15:1116–1124.

Symington LS, Gautier J (2011) Double-strand break end resection and repair pathway choice. *Annu Rev Genet* 45:247–71.

Szymczak AL, Workman CJ, Wang Y, Vignali KM, Dilioglou S, Vanin EF, Vignali DA (2004) Correction of multi-gene deficiency in vivo using a single 'self-cleaving' 2a peptide-based retroviral vector. *Nat Biotechnol* 22:589–594.

Tabata H, Nakajima K (2001) Efficient in utero gene transfer system to the developing mouse brain using electroporation: visualization of neuronal migration in the developing cortex. *Neuroscience* 103:865–872.

Tsutsui S, Hahn JN, Johnson TA, Ali Z, Jirik FR (2008) Absence of the cellular prion protein exacerbates and prolongs neuroinflammation in experimental autoimmune encephalomyelitis. *Am J Pathol* 173:1029–41.

Urnov FD, Rebar EJ, Holmes MC, Zhang HS, Gregory PD (2010) Genome editing with engineered zinc finger nucleases. *Nat Rev Genet* 11:636–646.

Wang H, Hu YC, Markoulaki S, Welstead GG, Cheng AW, Shivalila CS, Pyntikova T, Dadon DB, Voytas DF, Bogdanove AJ, Page DC, Jaenisch R (2013a) Talen-mediated editing of the mouse y chromosome. *Nat Biotechnol* 31:530–532.

Wang H, Yang H, Shivalila CS, Dawlaty MM, Cheng AW, Zhang F, Jaenisch R (2013b) One-step generation of mice carrying mutations in multiple genes by crispr/cas-mediated genome engineering. *Cell* 153:910–8.

Wang P, Chen T, Sakurai K, Han BX, He Z, Feng G, Wang F (2012) Intersectional cre driver lines generated using split-intein mediated split-cre reconstitution. *Sci Rep* 2:497–497.

Wang T, Wei JJ, Sabatini DM, Lander ES (2014) Genetic screens in human cells using the crispr-cas9 system. *Science* 343:80–4.

Wefers B, Meyer M, Ortiz O, Hrabé de Angelis M, Hansen J, Wurst W, Kühn R (2013) Direct production of mouse disease models by embryo microinjection of talens and oligodeoxynucleotides. *Proc Natl Acad Sci U S A* 110:3782–7.

Wright DA, Thibodeau-Beganny S, Sander JD, Winfrey RJ, Hirsh AS, Eichtinger M, Fu F, Porteus MH, Dobbs D, Voytas DF, Joung JK (2006) Standardized reagents and protocols for engineering zinc finger nucleases by modular assembly. *Nat Protoc* 1:1637–1652.

Wu S, Wu Y, Capecchi MR (2006) Motoneurons and oligodendrocytes are sequentially generated from neural stem cells but do not appear to share common lineage-restricted progenitors in vivo. *Development* 133:581–590.

Xu J (2005) Preparation, culture, and immortalization of mouse embryonic fibroblasts In Ausubel FM, Brent R, Kingston RE, Moore DD, Seidman J, Smith JA, Struhl K, editors, *Current Protocols in Molecular Biology*. John Wiley & Sons, Inc., Hoboken, NJ, USA.

Yang H, Wang H, Shivalila CS, Cheng AW, Shi L, Jaenisch R (2013) One-step generation of mice carrying reporter and conditional alleles by crispr/cas-mediated genome engineering. *Cell* 154:1370–1379.

Zambrowicz BP, Imamoto A, Fiering S, Herzenberg LA, Kerr WG, Soriano P (1997) Disruption of overlapping transcripts in the rosa beta geo 26 gene trap strain leads to widespread expression of beta-galactosidase in mouse embryos and hematopoietic cells. *Proc Natl Acad Sci U S A* 94:3789–94.

Zhuo L, Sun B, Zhang CL, Fine A, Chiu SY, Messing A (1997) Live astrocytes visualized by green fluorescent protein in transgenic mice. *Dev Biol* 187:36–42.

# List of Figures

# List of Tables

# Acknowledgements

I am particularly grateful to Dr. Pawel Pelczar and Prof. Adriano Aguzzi for giving me the unique opportunity to work on these interesting projects at the interface of neurobiology and genetic engineering, for providing continuous inspiration, guidance, and support, and for all the important challenges beyond project work such as presenting at seminars and conferences and supervising students.

I would like to thank Prof. Thorsten Buch for his insights and support as a member of my thesis committee and for his help in initiating important collaborations for our projects.

I would also like to thank my collaborators on the binary SSR and genome editing projects:

Patrick Stillhard for his great help in getting the binary SSR project off the ground during his master thesis, for many interesting discussions and all the good times inside and outside of the lab.

Dr. Hendrik Wildner for his crucial contributions in performing binary SSR *in vivo* experiments. I would also like to thank him and Prof. Hanns Ulrich Zeilhofer for very helpful discussions during drafting and revising the respective manuscript.

Dr. Mario Nuvolone for sharing his expertise on mouse genetics, many helpful discussions, and his and Yvonne Fuhrers help on characterizing *Prnp* knock-out mice.

Viktor Kapp, Davide Seruggia, and Carmine Cerrato for conducting experiments for both projects during their time in the lab.

Dr. Morgan Maeder, Prof. J. Keith Joung, Dr. Tomas Cermak, Prof. Daniel Voytas, Dr. Pablo Perez-Pinera, and Prof. Charles Gersbach for sharing genome editing reagents with us and their insightful discussions on experimental approaches and during the drafting of manuscripts.

Furthermore I would like to thank:

Monika Tarnowska, Ewa Skoczylas, Cornelia Albrecht, and Livia Takacs for excellent technical support and animal caretaking.

Dr. Sabine Spath, Florian Mair, Vinko Tosevski, and Dr. Hitoshi Takizawa for their support with performing Southern blot and flow cytometry/FACS experiments.

All the current and former members of the Institute of Neuropathology for creating a stimulating and collaborative research environment and the enjoyable times in Zurich.

The Swiss National Science Foundation and the ZNZ International PhD Program in Neuroscience for generous project and travel funding.

I dedicate this thesis to my parents who have never stopped believing in me and for their support and encouragement especially during the difficult times.

I want to express my deepest gratitude to my wife, Carolina Cunha, for her unconditional love, for filling every day of my life with joy, and for her never-ending patience and understanding throughout the past years.

# Contributions to Published Work

Throughout this thesis I have opted to use the first-person narrative in order to unequivocally identify those experiments which I have performed personally. The work contributed by co-workers and external collaborators is clearly stated within the respective results sections. I would also like to highlight the individual contributions of my co-authors and I to the published findings presented in this thesis:

Nucleic Acids Research | April 2014 | Volume 42 | Issue 6 | 3894-3907 | doi: 10.1093/nar/gkt1361

**Binary recombinase systems for high resolution conditional mutagenesis**

P. Pelczar, M. Hermann, and H. Wildner conceived and designed experiments. M. Hermann, P. Stillhard, H. Wildner, D. Seruggia, and V. Kapp performed experiments. P. Pelczar and M. Hermann analyzed the data and wrote the manuscript. H. Sánchez-Iranzo, N. Mercader, L. Montoliu, and H. U. Zeilhofer eagents, materials, and analysis tools. P. Pelczar, H. U. Zeilhofer, and L. Montoliu supervised the experiments.

PLOS ONE | September 2012 | Volume 7 | Issue 9 | e41796 | doi: 10.1371/journal.pone.0041796

**Evaluation of OPEN Zinc Finger Nucleases for Direct Gene Targeting of the *ROSA26* locus in Mouse Embryos**

T. Buch, P. Pelczar. and J. K. Joung conceived and designed experiments. M. Hermann, T. Buch, P. Pelczar, M. L. Maeder, K. Rector, and C. Khayter performed experiments. M. Hermann, T. Buch, and P. Pelczar analyzed the data. A. Aguzzi, B. Becher, K. Bürki, K. Rector, and J. Ruiz contributed reagents, materials, and analysis tools. T. Buch, P. Pelczar and M. Hermann wrote the paper. T. Buch, P. Pelczar, A. Aguzzi, B. Becher, Kurt Bürki, and J. K. Joung supervised the experiments.

Journal of Visualized Experiments | April 2014 | Issue 86 | doi: 10.3791/50930

**Mouse Genome Engineering using Designer Nucleases**

P. Pelczar and M. Hermann performed experiments and wrote the experimental protocol and film script. T. Cermak and D. F. Voytas provided eagents, materials, and analysis tools.

# A. Appendix

**Table A.1.:** Plasmids that were generated in this thesis and are publicly available on www.addgene.org.

| Plasmid | Addgene ID |
|---|---|
| pCAG-T7-TALEN(Sangamo)-Destination | 37184 |
| pCAG-T7-TALEN(Sangamo)-FokI-KKR-Destination | 40131 |
| pCAG-T7-TALEN(Sangamo)-FokI-ELD-Destination | 40132 |
| pCAG-Golden-Gate-Esp3I-Destination | 51278 |
| pCAG-NLS-HA-Dre | 51272 |
| pCAG-NLS-HA-B3 | 51270 |
| pCAG-NLS-HA-Bxb1 | 51271 |
| pCAG-roxSTOProx-ZsGreen | 51273 |
| pCAG-b3STOPb3-ZsGreen | 51266 |
| pCAG-attBr-ZsGreen-attP | 51265 |
| pCAG-loxPSTOPloxP-ZsGreen | 51269 |
| pCAG-Roxed-Cre | 51273 |
| pCAG-attBr-Cre-rc-attP | 51264 |
| Thy1.2-NLS_HA_Dre-P2A-BFP | 51275 |
| Thy1.2-Roxed-Cre | 51276 |
| hGFAP-NLS-HA-Dre-P2A-BFP | 51277 |
| hGFAP-Roxed-Cre | 51263 |
| pCAG-Co-InCreN | 51267 |
| pCAG-Co-InCreC | 51268 |

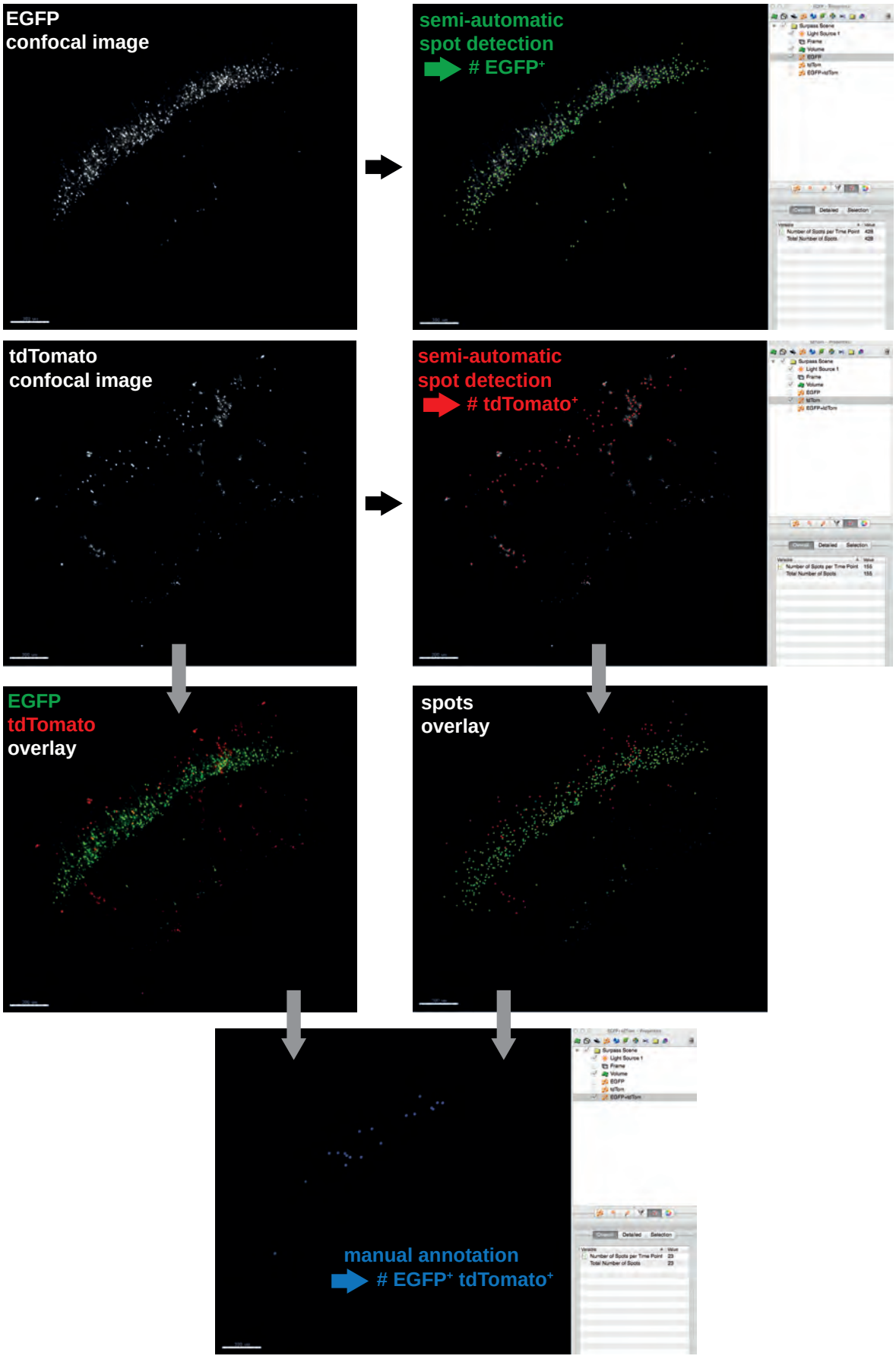


**Figure A.1.:** Imaris workflow for counting fluorescent cells following *in utero* electroporation of Co-Driver.

**Table A.2.:** SNP analysis of *PRNP*$^{\Delta 8/\Delta 8}$ mouse.

| Index | Name | Chr | Position | SNPs that differentiate between C57BL/6NTac and C57BL/6J | 129S6/SvEvTac_Ref2.GType | BALB/cAnNTac_Ref1.GType | C3H/HeNTac-1_Ref.GType | C57BL/6J | Line Zurich_del8_7_1300013530__Unk__SNP test__1333-4a_2013/08/26_BSC.GType | Line Zurich_del8_8_1300013530__Unk__SNP test__1333-4a_2013/08/26_BSC.GType | Line Zurich_del8_7_1300013530__Unk__SNP test__1333-4a_2013/08/26_BSC.GType | Line Zurich_del8_8_1300013530__Unk__SNP test__1333-4a_2013/08/26_BSC.GType |
|---|---|---|---|---|---|---|---|---|---|---|---|---|
| 1 | rs3683945 | 1 | 3201415 | | AA | AA | BB | AA | AA | AA | 1 | 1 |
| 2 | rs6269442 | 1 | 3495168 | | BB | AA | BB | AA | AA | AA | 1 | 1 |
| 3 | rs13475701 | 1 | 4538744 | | AA | BB | BB | AA | AA | AA | 1 | 1 |
| 4 | rs13475706 | 1 | 5917284 | | AA | BB | AA | AA | AA | AA | 1 | 1 |
| 5 | rs3684358 | 1 | 8111551 | | AA | AA | BB | BB | BB | BB | 1 | 1 |
| 6 | rs3716083 | 1 | 9092463 | | AA | BB | AA | BB | BB | BB | 1 | 1 |
| 7 | rs3722996 | 1 | 11348581 | | AA | AA | BB | AA | AA | AA | 1 | 1 |
| 8 | rs13475729 | 1 | 12981709 | | AA | AA | AA | BB | BB | BB | 1 | 1 |
| 9 | rs3671256 | 1 | 16443156 | | BB | BB | BB | AA | AA | AA | 1 | 1 |
| 10 | rs13475745 | 1 | 17512198 | | AA | BB | BB | BB | BB | BB | 1 | 1 |
| 11 | rs13475750 | 1 | 19680103 | | BB | BB | BB | AA | AA | AA | 1 | 1 |
| 12 | rs6404446 | 1 | 20994482 | | AA | AA | AA | BB | BB | BB | 1 | 1 |
| 13 | mCV23695025 | 1 | 22386585 | | BB | AA | BB | AA | AA | AA | 1 | 1 |
| 14 | rs6173215 | 1 | 22977896 | | AA | BB | BB | AA | AA | AA | 1 | 1 |
| 15 | mCV24784983 | 1 | 25471405 | | AA | BB | BB | AA | AA | AA | 1 | 1 |
| 16 | rs6166266 | 1 | 26136349 | | AA | AA | BB | AA | AA | AA | 1 | 1 |
| 17 | rs3677683 | 1 | 27510356 | | BB | BB | BB | AA | AA | AA | 1 | 1 |
| 18 | rs3695988 | 1 | 29990732 | | BB | AA | BB | AA | AA | AA | 1 | 1 |
| 19 | rs4137502 | 1 | 31102378 | | BB | BB | AA | BB | BB | BB | 1 | 1 |
| 20 | rs3707642 | 1 | 32799125 | | AA | AA | AA | BB | BB | BB | 1 | 1 |
| 21 | rs3681732 | 1 | 34414162 | | BB | AA | BB | AA | AA | AA | 1 | 1 |
| 22 | rs3683997 | 1 | 36198091 | | BB | BB | AA | BB | BB | BB | 1 | 1 |
| 23 | rs4222295 | 1 | 39320203 | | BB | AA | AA | BB | BB | BB | 1 | 1 |
| 24 | gnf01.036.770 | 1 | 40297949 | | AA | BB | AA | BB | BB | BB | 1 | 1 |
| 25 | rs13475827 | 1 | 41262551 | | AA | BB | BB | BB | BB | BB | 1 | 1 |
| 26 | rs13475834 | 1 | 42789902 | | BB | AA | BB | AA | AA | AA | 1 | 1 |
| 27 | CEL-1_44668113 | 1 | 44668113 | | AA | AA | BB | AA | AA | AA | 1 | 1 |
| 28 | rs13475847 | 1 | 46277649 | | BB | AA | BB | AA | AA | AA | 1 | 1 |
| 29 | rs13475851 | 1 | 47845326 | | AA | BB | BB | AA | AA | AA | 1 | 1 |
| 30 | CEL-1_49993068 | 1 | 49993068 | | AA | BB | AA | BB | BB | BB | 1 | 1 |
| 31 | rs3724092 | 1 | 50613798 | | AA | BB | AA | BB | BB | BB | 1 | 1 |
| 32 | rs13475866 | 1 | 51771264 | | BB | AA | AA | BB | BB | BB | 1 | 1 |
| 33 | rs6183203 | 1 | 53853346 | | BB | AA | BB | BB | BB | BB | 1 | 1 |
| 34 | rs6386920 | 1 | 54482766 | | AA | BB | AA | AA | AA | AA | 1 | 1 |
| 35 | rs3723035 | 1 | 55942220 | | BB | AA | BB | BB | BB | BB | 1 | 1 |
| 36 | rs13475881 | 1 | 58775689 | | BB | AA | AA | AA | AA | AA | 1 | 1 |
| 37 | rs6353774 | 1 | 60126995 | | BB | AA | BB | BB | BB | BB | 1 | 1 |
| 38 | rs3716105 | 1 | 61943426 | | AA | BB | AA | AA | AA | AA | 1 | 1 |
| 39 | rs6322485 | 1 | 63649681 | | AA | BB | AA | BB | BB | BB | 1 | 1 |
| 40 | rs6395308 | 1 | 65272783 | | BB | BB | BB | BB | BB | BB | 1 | 1 |
| 41 | rs13475902 | 1 | 66810982 | | BB | AA | AA | AA | AA | AA | 1 | 1 |
| 42 | rs6288543 | 1 | 68917890 | | AA | AA | AA | BB | BB | BB | 1 | 1 |
| 43 | rs6312657 | 1 | 69408967 | | BB | AA | BB | AA | AA | AA | 1 | 1 |
| 44 | rs6191076 | 1 | 72377589 | | AA | AA | BB | AA | AA | AA | 1 | 1 |
| 45 | rs13475919 | 1 | 73407862 | | BB | BB | AA | BB | BB | BB | 1 | 1 |
| 46 | rs3713616 | 1 | 74900046 | | BB | AA | BB | AA | AA | AA | 1 | 1 |
| 47 | rs13475931 | 1 | 76832354 | | BB | AA | AA | AA | AA | AA | 1 | 1 |
| 48 | gnf01.075.385 | 1 | 78359030 | | AA | AA | AA | BB | BB | BB | 1 | 1 |
| 49 | rs13475939 | 1 | 79202787 | | AA | AA | AA | BB | BB | BB | 1 | 1 |
| 50 | mCV23431007 | 1 | 80839073 | | BB | BB | BB | BB | BB | BB | 1 | 1 |
| 51 | rs13475946 | 1 | 81235702 | | AA | BB | BB | BB | BB | BB | 1 | 1 |
| 52 | gnf01.079.218 | 1 | 82668689 | | BB | AA | BB | AA | AA | AA | 1 | 1 |
| 53 | rs3723062 | 1 | 85865441 | | AA | BB | AA | BB | BB | BB | 1 | 1 |
| 54 | UT_1_89.100476 | 1 | 87104170 | | BB | AA | BB | AA | AA | AA | 1 | 1 |
| 55 | rs6195073 | 1 | 88494443 | | BB | AA | AA | AA | AA | AA | 1 | 1 |
| 56 | rs13475980 | 1 | 91575836 | | AA | AA | BB | BB | BB | BB | 1 | 1 |
| 57 | rs6268443 | 1 | 93319361 | | BB | BB | BB | AA | AA | AA | 1 | 1 |
| 58 | rs6157345 | 1 | 95497940 | | BB | AA | AA | AA | AA | AA | 1 | 1 |
| 59 | rs3726669 | 1 | 96875139 | | AA | BB | BB | BB | BB | BB | 1 | 1 |
| 60 | rs13476003 | 1 | 97677389 | | BB | AA | AA | AA | AA | AA | 1 | 1 |
| 61 | rs13476012 | 1 | 99797518 | | BB | AA | AA | AA | AA | AA | 1 | 1 |
| 62 | rs6368370 | 1 | 101749052 | | AA | BB | BB | BB | BB | BB | 1 | 1 |
| 63 | CEL-1_103251925 | 1 | 103251925 | | BB | AA | AA | BB | BB | BB | 1 | 1 |
| 64 | CEL-1_105423103 | 1 | 105423103 | | BB | AA | AA | BB | BB | BB | 1 | 1 |
| 65 | rs13476036 | 1 | 106831730 | | BB | AA | AA | AA | AA | AA | 1 | 1 |
| 66 | rs3685919 | 1 | 109634975 | | AA | AA | AA | BB | BB | BB | 1 | 1 |
| 67 | rs13476050 | 1 | 110616212 | | BB | BB | BB | AA | AA | AA | 1 | 1 |
| 68 | rs3726043 | 1 | 111780707 | | BB | BB | BB | AA | AA | AA | 1 | 1 |
| 69 | rs13476061 | 1 | 113899609 | | BB | BB | AA | AA | AA | AA | 1 | 1 |
| 70 | mCV24201027 | 1 | 115751113 | | BB | BB | AA | BB | BB | BB | 1 | 1 |
| 71 | rs3674655 | 1 | 117379659 | | AA | AA | AA | BB | BB | BB | 1 | 1 |
| 72 | rs3695581 | 1 | 118500635 | | BB | BB | AA | BB | BB | BB | 1 | 1 |
| 73 | rs3678634 | 1 | 120380872 | | AA | BB | AA | BB | BB | BB | 1 | 1 |
| 74 | rs3717360 | 1 | 122796548 | | BB | BB | BB | AA | AA | AA | 1 | 1 |
| 75 | rs3694822 | 1 | 123642529 | | AA | AA | AA | BB | BB | BB | 1 | 1 |
| 76 | rs4137908 | 1 | 125475941 | | AA | AA | BB | BB | BB | BB | 1 | 1 |

**Taconic Key**

| Symbol | Definition |
|---|---|
| AA | Homozygous for Allele1 |
| AB | Heterozygous 1/2 |
| BB | Homozygous for Allele2 |
| | |
| 1 | Homozygous for C57BL/6J SNP |
| 0.5 | Heterozygous for C57BL/6J SNP and non-C57BL/6J SNP |
| 0 | Homozygous for non-C57BL/6J SNP |
| NC=no call | |
| Highlighted region indicates the region 25 MBp on either side of the known chromosomal modification | |

| | | | | | | | | | | | |
|---|---|---|---|---|---|---|---|---|---|---|---|
| 77 | rs6228473 | 1 | 126460218 | AA | AA | AA | BB | BB | BB | 1 | 1 |
| 78 | rs13476104 | 1 | 128094625 | AA | AA | BB | BB | BB | BB | 1 | 1 |
| 79 | rs3699561 | 1 | 130962369 | AA | AA | BB | BB | BB | BB | 1 | 1 |
| 80 | rs3724826 | 1 | 131376437 | BB | BB | AA | AA | AA | AA | 1 | 1 |
| 81 | rs13476119 | 1 | 134099450 | AA | AA | BB | AA | AA | AA | 1 | 1 |
| 82 | rs8250053 | 1 | 135044501 | BB | AA | BB | AA | AA | AA | 1 | 1 |
| 83 | rs6279930 | 1 | 137268795 | BB | AA | AA | AA | AA | AA | 1 | 1 |
| 84 | gnf01.137.841 | 1 | 138089211 | AA | AA | BB | AA | AA | AA | 1 | 1 |
| 85 | rs13476141 | 1 | 140472264 | BB | AA | BB | AA | AA | AA | 1 | 1 |
| 86 | rs6382880 | 1 | 142470600 | BB | AA | BB | AA | AA | AA | 1 | 1 |
| 87 | rs13476152 | 1 | 144012938 | BB | AA | BB | AA | AA | AA | 1 | 1 |
| 88 | rs3672697 | 1 | 145088382 | BB | BB | AA | BB | BB | BB | 1 | 1 |
| 89 | rs13476163 | 1 | 146776886 | BB | AA | AA | AA | AA | AA | 1 | 1 |
| 90 | rs6411476 | 1 | 148913234 | AA | BB | BB | BB | BB | BB | 1 | 1 |
| 91 | rs6393307 | 1 | 150967309 | BB | BB | BB | BB | BB | BB | 1 | 1 |
| 92 | CEL-1_152747565 | 1 | 152747565 | AA | BB | BB | BB | BB | BB | 1 | 1 |
| 93 | rs13476187 | 1 | 154187910 | BB | BB | BB | BB | BB | BB | 1 | 1 |
| 94 | UT_1_113.684537 | 1 | 156044150 | AA | BB | BB | AA | AA | AA | 1 | 1 |
| 95 | rs3719034 | 1 | 157158100 | BB | AA | BB | BB | BB | BB | 1 | 1 |
| 96 | rs6387609 | 1 | 157898706 | AA | BB | AA | AA | AA | AA | 1 | 1 |
| 97 | rs3693161 | 1 | 160294867 | BB | AA | BB | BB | BB | BB | 1 | 1 |
| 98 | rs13476208 | 1 | 162037129 | AA | BB | BB | AA | AA | AA | 1 | 1 |
| 99 | UT_1_167.58185 | 1 | 164012960 | BB | BB | BB | BB | BB | BB | 1 | 1 |
| 100 | rs13476219 | 1 | 166263327 | BB | BB | BB | BB | BB | BB | 1 | 1 |
| 101 | rs6399765 | 1 | 167289594 | BB | BB | BB | BB | BB | BB | 1 | 1 |
| 102 | rs13476229 | 1 | 169381101 | AA | BB | AA | BB | BB | BB | 1 | 1 |
| 103 | rs8245216 | 1 | 171312251 | AA | AA | AA | BB | BB | BB | 1 | 1 |
| 104 | rs13466711 | 1 | 172206556 | BB | BB | BB | AA | AA | AA | 1 | 1 |
| 105 | rs3707910 | 1 | 172614886 | AA | AA | AA | BB | BB | BB | 1 | 1 |
| 106 | rs3669108 | 1 | 174667766 | BB | BB | BB | AA | AA | AA | 1 | 1 |
| 107 | rs3700831 | 1 | 176145762 | BB | BB | BB | AA | AA | AA | 1 | 1 |
| 108 | CEL-1_178482360 | 1 | 178482360 | BB | BB | BB | BB | BB | BB | 1 | 1 |
| 109 | rs13476265 | 1 | 179633768 | AA | BB | BB | BB | BB | BB | 1 | 1 |
| 110 | rs13474399 | 1 | 180675247 | AA | AA | AA | AA | AA | AA | 1 | 1 |
| 111 | rs13476272 | 1 | 181495101 | BB | BB | BB | BB | BB | BB | 1 | 1 |
| 112 | rs13476273 | 1 | 182175880 | BB | BB | BB | BB | BB | BB | 1 | 1 |
| 113 | rs6157620 | 1 | 183197685 | AA | AA | AA | BB | BB | BB | 1 | 1 |
| 114 | mCV22849619 | 1 | 186531848 | BB | BB | BB | AA | AA | AA | 1 | 1 |
| 115 | rs3667164 | 1 | 188355284 | BB | BB | BB | AA | AA | AA | 1 | 1 |
| 116 | rs13476300 | 1 | 190164592 | AA | AA | AA | BB | BB | BB | 1 | 1 |
| 117 | rs13476313 | 1 | 194054190 | BB | BB | AA | BB | BB | BB | 1 | 1 |
| 118 | mCV24145570 | 1 | 195161421 | BB | BB | AA | BB | BB | BB | 1 | 1 |
| 119 | rs3713997 | 2 | 3181746 | AA | BB | BB | BB | BB | BB | 1 | 1 |
| 120 | rs6213083 | 2 | 3972678 | NC | NC | NC | BB | NC | NC | NA | NA |
| 121 | rs4136817 | 2 | 4258057 | AA | BB | BB | BB | BB | BB | 1 | 1 |
| 122 | rs3678168 | 2 | 5606042 | BB | AA | BB | BB | BB | BB | 1 | 1 |
| 123 | rs6359983 | 2 | 6694892 | AA | AA | AA | AA | AA | AA | 1 | 1 |
| 124 | gnf02.006.767 | 2 | 9780767 | BB | BB | BB | BB | BB | BB | 1 | 1 |
| 125 | rs6240512 | 2 | 10929543 | AA | BB | BB | BB | BB | BB | 1 | 1 |
| 126 | rs6172408 | 2 | 12582823 | AA | AA | AA | AA | AA | AA | 1 | 1 |
| 127 | rs6287980 | 2 | 13669366 | BB | BB | BB | BB | BB | BB | 1 | 1 |
| 128 | CZECH-2_15618849 | 2 | 15618849 | BB | BB | BB | BB | BB | BB | 1 | 1 |
| 129 | rs6402127 | 2 | 17856135 | BB | BB | BB | BB | BB | BB | 1 | 1 |
| 130 | rs13476366 | 2 | 19454722 | AA | AA | AA | AA | AA | AA | 1 | 1 |
| 131 | rs3674936 | 2 | 20427488 | BB | AA | BB | AA | AA | AA | 1 | 1 |
| 132 | rs6404309 | 2 | 23451610 | BB | BB | BB | BB | BB | BB | 1 | 1 |
| 133 | rs6286688 | 2 | 24495175 | BB | BB | BB | BB | BB | BB | 1 | 1 |
| 134 | rs13476391 | 2 | 26055543 | AA | AA | AA | AA | AA | AA | 1 | 1 |
| 135 | rs13476399 | 2 | 28249160 | BB | AA | AA | AA | AA | AA | 1 | 1 |
| 136 | rs3154953 | 2 | 30147850 | AA | BB | BB | BB | BB | BB | 1 | 1 |
| 137 | rs6186876 | 2 | 31660228 | BB | BB | BB | BB | BB | BB | 1 | 1 |
| 138 | CEL-2_32981944 | 2 | 32981944 | BB | BB | BB | BB | BB | BB | 1 | 1 |
| 139 | gnf02.035.469 | 2 | 33954610 | AA | AA | AA | AA | AA | AA | 1 | 1 |
| 140 | rs6260403 | 2 | 35804961 | AA | AA | AA | AA | AA | AA | 1 | 1 |
| 141 | rs13476439 | 2 | 38071109 | AA | BB | AA | BB | BB | BB | 1 | 1 |
| 142 | rs13476454 | 2 | 41244144 | BB | AA | BB | AA | AA | AA | 1 | 1 |
| 143 | rs13476467 | 2 | 44361765 | AA | BB | AA | BB | BB | BB | 1 | 1 |
| 144 | rs13476472 | 2 | 45653218 | BB | AA | BB | AA | AA | AA | 1 | 1 |
| 145 | rs6265423 | 2 | 47124603 | AA | AA | BB | AA | AA | AA | 1 | 1 |
| 146 | rs6250599 | 2 | 48633486 | AA | AA | AA | AA | AA | AA | 1 | 1 |
| 147 | CEL-2_50605053 | 2 | 50605053 | AA | BB | AA | BB | BB | BB | 1 | 1 |
| 148 | rs3725341 | 2 | 51425686 | BB | AA | BB | AA | AA | AA | 1 | 1 |
| 149 | rs13476503 | 2 | 53143600 | AA | BB | AA | BB | BB | BB | 1 | 1 |
| 150 | rs3718711 | 2 | 56489184 | BB | AA | BB | AA | AA | AA | 1 | 1 |
| 151 | rs3672719 | 2 | 58142938 | AA | BB | AA | BB | BB | BB | 1 | 1 |
| 152 | rs13476530 | 2 | 59956872 | AA | BB | BB | BB | BB | BB | 1 | 1 |
| 153 | rs4223189 | 2 | 61738719 | BB | AA | AA | AA | AA | AA | 1 | 1 |
| 154 | CEL-2_63143553 | 2 | 63143553 | BB | AA | AA | AA | AA | AA | 1 | 1 |
| 155 | rs6222797 | 2 | 65057687 | BB | AA | AA | AA | AA | AA | 1 | 1 |
| 156 | rs13476553 | 2 | 66906537 | BB | AA | BB | AA | AA | AA | 1 | 1 |
| 157 | rs6381994 | 2 | 68188374 | AA | AA | AA | AA | AA | AA | 1 | 1 |
| 158 | rs4136610 | 2 | 70090167 | BB | AA | AA | BB | BB | BB | 1 | 1 |
| 159 | rs3664661 | 2 | 71492729 | BB | AA | AA | BB | BB | BB | 1 | 1 |
| 160 | CEL-2_73370728 | 2 | 73370728 | BB | AA | BB | AA | AA | AA | 1 | 1 |
| 161 | rs13476580 | 2 | 74776032 | AA | AA | BB | BB | BB | BB | 1 | 1 |
| 162 | gnf02.076.311 | 2 | 77549169 | BB | AA | AA | BB | BB | BB | 1 | 1 |
| 163 | CEL-2_79237503 | 2 | 79237503 | BB | AA | AA | BB | BB | BB | 1 | 1 |
| 164 | rs3722345 | 2 | 80509747 | AA | BB | BB | AA | AA | AA | 1 | 1 |
| 165 | rs3667007 | 2 | 82000176 | BB | AA | AA | BB | BB | BB | 1 | 1 |
| 166 | rs8273639 | 2 | 84666393 | AA | BB | BB | AA | AA | AA | 1 | 1 |
| 167 | rs3689658 | 2 | 85572783 | BB | AA | AA | BB | BB | BB | 1 | 1 |
| 168 | rs13476621 | 2 | 87247149 | AA | BB | BB | AA | AA | AA | 1 | 1 |
| 169 | rs6404809 | 2 | 88899373 | BB | AA | BB | BB | BB | BB | 1 | 1 |
| 170 | rs13476636 | 2 | 91539303 | AA | BB | AA | AA | AA | AA | 1 | 1 |

| | | | | | | | | | | | | | |
|---|---|---|---|---|---|---|---|---|---|---|---|---|---|
| 171 | rs13476639 | 2 | 92720804 | | AA | AA | BB | AA | AA | AA | 1 | 1 |
| 172 | rs13476649 | 2 | 95929798 | | BB | AA | BB | BB | BB | BB | 1 | 1 |
| 173 | rs6316774 | 2 | 96787868 | | AA | BB | AA | BB | BB | BB | 1 | 1 |
| 174 | rs6378047 | 2 | 99378126 | | AA | AA | AA | BB | BB | BB | 1 | 1 |
| 175 | rs6406705 | 2 | 100253963 | | AA | AA | AA | AA | AA | AA | 1 | 1 |
| 176 | rs13476666 | 2 | 101217024 | | BB | BB | BB | AA | AA | AA | 1 | 1 |
| 177 | gnf02.102.146 | 2 | 103792940 | | AA | BB | AA | AA | AA | AA | 1 | 1 |
| 178 | rs13476689 | 2 | 107356662 | | AA | BB | BB | AA | AA | AA | 1 | 1 |
| 179 | rs13476691 | 2 | 108396162 | | AA | BB | AA | AA | AA | AA | 1 | 1 |
| 180 | rs13476698 | 2 | 111095530 | | AA | BB | AA | AA | AA | AA | 1 | 1 |
| 181 | CEL-2_111981058 | 2 | 111981058 | | AA | AA | BB | BB | BB | BB | 1 | 1 |
| 182 | rs4138562 | 2 | 114161459 | | BB | BB | BB | AA | AA | AA | 1 | 1 |
| 183 | rs3699172 | 2 | 115671423 | | BB | BB | AA | AA | AA | AA | 1 | 1 |
| 184 | rs13476723 | 2 | 117074373 | | BB | AA | BB | BB | BB | BB | 1 | 1 |
| 185 | rs8279354 | 2 | 118948317 | | BB | BB | BB | AA | AA | AA | 1 | 1 |
| 186 | rs3658927 | 2 | 120726441 | | BB | BB | BB | AA | AA | AA | 1 | 1 |
| 187 | rs3723643 | 2 | 122067606 | | AA | BB | BB | AA | AA | AA | 1 | 1 |
| 188 | rs6228179 | 2 | 123216313 | | BB | BB | BB | AA | AA | AA | 1 | 1 |
| 189 | rs6401493 | 2 | 125046796 | | BB | BB | BB | AA | AA | AA | 1 | 1 |
| 190 | gnf02.126.027 | 2 | 127549770 | | AA | AA | BB | BB | BB | BB | 1 | 1 |
| 191 | rs3661596 | 2 | 129893838 | | BB | BB | BB | AA | AA | AA | 1 | 1 |
| 192 | rs3665528 | 2 | 130762932 | | BB | BB | AA | BB | BB | BB | 1 | 1 |
| 193 | rs4223511 | 2 | 131742558 | | AA | BB | AA | BB | BB | BB | 1 | 1 |
| 194 | rs13476783 | 2 | 133610154 | | AA | BB | BB | BB | BB | BB | 1 | 1 |
| 195 | CEL-2_135876979 | 2 | 135876979 | | BB | BB | BB | BB | BB | BB | 1 | 1 |
| 196 | rs8246404 | 2 | 136627476 | | AA | BB | BB | BB | BB | BB | 1 | 1 |
| 197 | rs6158085 | 2 | 138928693 | | BB | BB | BB | BB | BB | BB | 1 | 1 |
| 198 | rs13476807 | 2 | 140555557 | | AA | AA | AA | AA | AA | AA | 1 | 1 |
| 199 | rs13476810 | 2 | 142149749 | | BB | BB | BB | BB | BB | BB | 1 | 1 |
| 200 | rs13476817 | 2 | 144125632 | | AA | BB | BB | BB | BB | BB | 1 | 1 |
| 201 | rs6363071 | 2 | 145784318 | | AA | BB | BB | AA | AA | AA | 1 | 1 |
| 202 | rs6209325 | 2 | 147807884 | | AA | BB | BB | AA | AA | AA | 1 | 1 |
| 203 | rs6246342 | 2 | 149614906 | | AA | AA | AA | AA | AA | AA | 1 | 1 |
| 204 | gnf02.149.271 | 2 | 151100533 | | BB | AA | AA | AA | AA | AA | 1 | 1 |
| 205 | rs6247960 | 2 | 152642098 | | BB | AA | AA | BB | BB | BB | 1 | 1 |
| 206 | rs6376291 | 2 | 154204634 | | BB | AA | AA | AA | AA | AA | 1 | 1 |
| 207 | rs13476860 | 2 | 156330826 | | BB | BB | BB | AA | AA | AA | 1 | 1 |
| 208 | rs3695266 | 2 | 158068522 | | BB | BB | BB | AA | AA | AA | 1 | 1 |
| 209 | rs13476874 | 2 | 159733176 | | BB | AA | AA | BB | BB | BB | 1 | 1 |
| 210 | rs3664408 | 2 | 161443571 | | BB | BB | BB | AA | AA | AA | 1 | 1 |
| 211 | rs3671849 | 2 | 163215888 | | BB | AA | AA | BB | BB | BB | 1 | 1 |
| 212 | rs13476889 | 2 | 164370875 | | BB | AA | BB | AA | AA | AA | 1 | 1 |
| 213 | rs13476895 | 2 | 166374505 | | AA | AA | BB | BB | BB | BB | 1 | 1 |
| 214 | CEL-2_168586738 | 2 | 168586738 | | BB | BB | BB | AA | AA | AA | 1 | 1 |
| 215 | rs3726974 | 2 | 169905098 | | AA | AA | AA | BB | BB | BB | 1 | 1 |
| 216 | rs13476917 | 2 | 171452147 | | AA | AA | AA | BB | BB | BB | 1 | 1 |
| 217 | rs13476928 | 2 | 174162530 | | BB | BB | AA | AA | AA | AA | 1 | 1 |
| 218 | rs13476932 | 2 | 174923839 | | BB | BB | AA | AA | AA | AA | 1 | 1 |
| 219 | rs13476934 | 2 | 178315515 | | AA | AA | BB | BB | BB | BB | 1 | 1 |
| 220 | rs6187766 | 2 | 179210967 | | BB | BB | BB | AA | AA | AA | 1 | 1 |
| 221 | rs3679483 | 2 | 179814463 | | BB | BB | BB | AA | AA | AA | 1 | 1 |
| 222 | rs13476950 | 3 | 3793662 | | BB | AA | AA | BB | BB | BB | 1 | 1 |
| 223 | rs13476953 | 3 | 4378945 | | AA | BB | BB | AA | AA | AA | 1 | 1 |
| 224 | rs13476957 | 3 | 5656063 | | AA | BB | BB | AA | AA | AA | 1 | 1 |
| 225 | rs13476963 | 3 | 7703356 | | BB | AA | AA | BB | BB | BB | 1 | 1 |
| 226 | rs13476969 | 3 | 9744167 | | AA | BB | BB | BB | BB | BB | 1 | 1 |
| 227 | rs13476973 | 3 | 11073596 | | AA | BB | BB | BB | BB | BB | 1 | 1 |
| 228 | rs6248752 | 3 | 12161848 | | BB | BB | BB | AA | AA | AA | 1 | 1 |
| 229 | rs13476985 | 3 | 14943619 | | BB | AA | AA | BB | BB | BB | 1 | 1 |
| 230 | rs3659988 | 3 | 16122429 | | AA | BB | BB | AA | AA | AA | 1 | 1 |
| 231 | gnf03.015.035 | 3 | 17691447 | | BB | BB | AA | AA | AA | AA | 1 | 1 |
| 232 | mCV24211562 | 3 | 18932166 | | AA | BB | AA | AA | AA | AA | 1 | 1 |
| 233 | rs6235984 | 3 | 21215374 | | AA | AA | AA | AA | AA | AA | 1 | 1 |
| 234 | rs13477019 | 3 | 23589162 | X | AA | AA | AA | BB | BB | BB | 1 | 1 |
| 235 | rs3715834 | 3 | 26405124 | | BB | AA | BB | AA | AA | AA | 1 | 1 |
| 236 | rs13477030 | 3 | 27365675 | | AA | BB | BB | BB | BB | BB | 1 | 1 |
| 237 | rs3660588 | 3 | 30094761 | | AA | BB | BB | AA | AA | AA | 1 | 1 |
| 238 | rs13477043 | 3 | 31257023 | | BB | BB | AA | BB | BB | BB | 1 | 1 |
| 239 | gnf03.030.222 | 3 | 33096061 | | BB | AA | BB | AA | AA | AA | 1 | 1 |
| 240 | rs4223883 | 3 | 33860283 | | BB | AA | AA | AA | AA | AA | 1 | 1 |
| 241 | rs6246699 | 3 | 36110851 | | BB | AA | BB | AA | AA | AA | 1 | 1 |
| 242 | rs6274061 | 3 | 38689460 | | AA | BB | AA | BB | BB | BB | 1 | 1 |
| 243 | rs6324747 | 3 | 39835273 | | BB | BB | BB | AA | AA | AA | 1 | 1 |
| 244 | rs3661720 | 3 | 41838640 | | BB | BB | AA | AA | AA | AA | 1 | 1 |
| 245 | rs13477083 | 3 | 43361057 | | AA | AA | BB | AA | AA | AA | 1 | 1 |
| 246 | CEL-3_45598106 | 3 | 45598106 | | BB | BB | AA | BB | BB | BB | 1 | 1 |
| 247 | CEL-3_46558020 | 3 | 46558020 | | AA | AA | AA | AA | AA | AA | 1 | 1 |
| 248 | rs13477097 | 3 | 48335184 | | BB | AA | AA | BB | BB | BB | 1 | 1 |
| 249 | rs4139913 | 3 | 50623988 | | BB | AA | BB | BB | BB | BB | 1 | 1 |
| 250 | rs6241331 | 3 | 52675823 | | BB | BB | AA | AA | AA | AA | 1 | 1 |
| 251 | rs6335414 | 3 | 53103565 | | BB | BB | BB | AA | AA | AA | 1 | 1 |
| 252 | rs4223969 | 3 | 55143939 | | AA | BB | BB | AA | AA | AA | 1 | 1 |
| 253 | rs13477126 | 3 | 56753970 | | AA | AA | AA | AA | AA | AA | 1 | 1 |
| 254 | rs6301139 | 3 | 58612475 | | NC | BB | BB | NN | NC | NC | NA | NA |
| 255 | rs13477138 | 3 | 60037290 | | AA | AA | AA | BB | BB | BB | 1 | 1 |
| 256 | rs13477143 | 3 | 61103349 | | BB | BB | BB | AA | AA | AA | 1 | 1 |
| 257 | rs13477154 | 3 | 63787516 | | AA | AA | AA | BB | BB | BB | 1 | 1 |
| 258 | rs6212539 | 3 | 65222079 | | AA | BB | BB | BB | BB | BB | 1 | 1 |
| 259 | gnf03.063.824 | 3 | 66994152 | | BB | AA | BB | BB | BB | BB | 1 | 1 |
| 260 | rs13477178 | 3 | 70089276 | | AA | AA | BB | AA | AA | AA | 1 | 1 |
| 261 | rs6198234 | 3 | 70361430 | | BB | BB | BB | AA | AA | AA | 1 | 1 |
| 262 | rs6264454 | 3 | 71858927 | | AA | AA | BB | BB | BB | BB | 1 | 1 |
| 263 | rs13477201 | 3 | 75852874 | | AA | BB | BB | BB | BB | BB | 1 | 1 |
| 264 | rs13477210 | 3 | 77646357 | | BB | BB | AA | AA | AA | AA | 1 | 1 |

| | | | | | | | | | | | |
|---|---|---|---|---|---|---|---|---|---|---|---|
| 265 | rs13477217 | 3 | 79085242 | AA | AA | BB | AA | AA | AA | 1 | 1 |
| 266 | rs13477218 | 3 | 80321582 | BB | AA | BB | AA | AA | AA | 1 | 1 |
| 267 | rs13477224 | 3 | 81758272 | BB | AA | BB | AA | AA | AA | 1 | 1 |
| 268 | rs13477233 | 3 | 83880528 | AA | AA | AA | BB | BB | BB | 1 | 1 |
| 269 | rs3719390 | 3 | 85880745 | BB | BB | BB | AA | AA | AA | 1 | 1 |
| 270 | rs6376008 | 3 | 87149248 | AA | BB | AA | BB | BB | BB | 1 | 1 |
| 271 | rs13477251 | 3 | 89418525 | BB | AA | AA | BB | BB | BB | 1 | 1 |
| 272 | rs6211610 | 3 | 90650953 | AA | AA | BB | BB | BB | BB | 1 | 1 |
| 273 | rs13477261 | 3 | 92344335 | BB | BB | AA | AA | AA | AA | 1 | 1 |
| 274 | rs13477268 | 3 | 93549679 | AA | AA | AA | AA | AA | AA | 1 | 1 |
| 275 | rs13477272 | 3 | 95678878 | BB | BB | BB | AA | AA | AA | 1 | 1 |
| 276 | rs3022964 | 3 | 97282711 | BB | AA | AA | AA | AA | AA | 1 | 1 |
| 277 | rs3726226 | 3 | 98954988 | BB | BB | BB | AA | AA | AA | 1 | 1 |
| 278 | rs3162061 | 3 | 100657788 | AA | AA | AA | BB | BB | BB | 1 | 1 |
| 279 | rs4138887 | 3 | 102619416 | AA | AA | BB | AA | AA | AA | 1 | 1 |
| 280 | rs3701653 | 3 | 103564280 | BB | BB | AA | AA | AA | AA | 1 | 1 |
| 281 | rs13477309 | 3 | 105788245 | BB | AA | AA | BB | BB | BB | 1 | 1 |
| 282 | rs3702359 | 3 | 107508882 | AA | BB | BB | AA | AA | AA | 1 | 1 |
| 283 | rs13477321 | 3 | 109585764 | AA | BB | AA | BB | BB | BB | 1 | 1 |
| 284 | rs3676545 | 3 | 110649631 | BB | BB | BB | AA | AA | AA | 1 | 1 |
| 285 | rs3698700 | 3 | 112624069 | AA | AA | AA | BB | BB | BB | 1 | 1 |
| 286 | rs3710419 | 3 | 116000138 | AA | BB | BB | BB | BB | BB | 1 | 1 |
| 287 | gnf03.119.970 | 3 | 116888086 | AA | BB | BB | AA | AA | AA | 1 | 1 |
| 288 | rs3708412 | 3 | 118002787 | BB | BB | BB | AA | AA | AA | 1 | 1 |
| 289 | CEL-3_120379605 | 3 | 120379605 | BB | AA | AA | BB | BB | BB | 1 | 1 |
| 290 | rs3659836 | 3 | 122002332 | BB | AA | AA | AA | AA | AA | 1 | 1 |
| 291 | rs13477379 | 3 | 123230785 | AA | BB | BB | BB | BB | BB | 1 | 1 |
| 292 | rs13477385 | 3 | 125504930 | BB | BB | BB | AA | AA | AA | 1 | 1 |
| 293 | rs3671119 | 3 | 126894715 | BB | BB | BB | AA | AA | AA | 1 | 1 |
| 294 | rs3670168 | 3 | 128820535 | AA | AA | AA | BB | BB | BB | 1 | 1 |
| 295 | rs13477404 | 3 | 130952894 | BB | AA | BB | AA | AA | AA | 1 | 1 |
| 296 | rs13477408 | 3 | 132189425 | BB | BB | AA | BB | BB | BB | 1 | 1 |
| 297 | CEL-3_133070717 | 3 | 133070717 | AA | AA | AA | AA | AA | AA | 1 | 1 |
| 298 | rs13477421 | 3 | 134785250 | AA | BB | BB | BB | BB | BB | 1 | 1 |
| 299 | rs3676039 | 3 | 136766271 | BB | AA | AA | BB | BB | BB | 1 | 1 |
| 300 | rs13477439 | 3 | 138624013 | AA | BB | BB | BB | BB | BB | 1 | 1 |
| 301 | rs13477448 | 3 | 140515828 | AA | AA | AA | BB | BB | BB | 1 | 1 |
| 302 | rs3090379 | 3 | 142598970 | BB | BB | BB | BB | BB | BB | 1 | 1 |
| 303 | rs6290401 | 3 | 143193940 | BB | BB | BB | BB | BB | BB | 1 | 1 |
| 304 | rs6407142 | 3 | 143619317 | AA | AA | AA | BB | BB | BB | 1 | 1 |
| 305 | rs3710548 | 3 | 146841800 | BB | BB | BB | AA | AA | AA | 1 | 1 |
| 306 | rs3657112 | 3 | 148942421 | AA | AA | AA | BB | BB | BB | 1 | 1 |
| 307 | rs13477487 | 3 | 150745214 | AA | AA | AA | BB | BB | BB | 1 | 1 |
| 308 | rs13477494 | 3 | 152154652 | BB | AA | AA | BB | BB | BB | 1 | 1 |
| 309 | rs13477506 | 3 | 155444424 | AA | BB | BB | AA | AA | AA | 1 | 1 |
| 310 | gnf03.160.599 | 3 | 157755333 | AA | BB | BB | BB | BB | BB | 1 | 1 |
| 311 | CEL-3_159340478 | 3 | 159340478 | AA | BB | BB | AA | AA | AA | 1 | 1 |
| 312 | rs3695715 | 4 | 3649824 | BB | BB | BB | AA | AA | AA | 1 | 1 |
| 313 | gnf04.002.008 | 4 | 5013576 | AA | AA | BB | AA | AA | AA | 1 | 1 |
| 314 | gnf04.002.599 | 4 | 5606396 | AA | AA | BB | AA | AA | AA | 1 | 1 |
| 315 | rs3660863 | 4 | 7127435 | AA | AA | AA | BB | BB | BB | 1 | 1 |
| 316 | UT_4_10.84692 | 4 | 10825412 | BB | BB | AA | BB | BB | BB | 1 | 1 |
| 317 | rs13477568 | 4 | 13764168 | AA | AA | AA | BB | BB | BB | 1 | 1 |
| 318 | mCV22939387 | 4 | 15321444 | AA | AA | AA | AA | AA | AA | 1 | 1 |
| 319 | rs6287606 | 4 | 18045313 | BB | BB | AA | BB | BB | BB | 1 | 1 |
| 320 | CEL-4_19508304 | 4 | 19508304 | BB | BB | BB | AA | AA | AA | 1 | 1 |
| 321 | rs13477596 | 4 | 20665789 | AA | AA | AA | BB | BB | BB | 1 | 1 |
| 322 | gnf04.019.134 | 4 | 22305486 | BB | BB | BB | AA | AA | AA | 1 | 1 |
| 323 | mCV22919271 | 4 | 24149712 | BB | BB | AA | AA | AA | AA | 1 | 1 |
| 324 | rs13477617 | 4 | 27105003 | BB | BB | AA | AA | AA | AA | 1 | 1 |
| 325 | rs3701432 | 4 | 29487208 | BB | BB | BB | AA | AA | AA | 1 | 1 |
| 326 | CEL-4_30653207 | 4 | 30653207 | BB | BB | AA | AA | AA | AA | 1 | 1 |
| 327 | rs3663744 | 4 | 31215491 | AA | AA | AA | BB | BB | BB | 1 | 1 |
| 328 | rs3674908 | 4 | 32441103 | AA | AA | AA | BB | BB | BB | 1 | 1 |
| 329 | rs13477643 | 4 | 35074381 | BB | BB | AA | BB | BB | BB | 1 | 1 |
| 330 | rs3719299 | 4 | 36221145 | AA | AA | BB | BB | BB | BB | 1 | 1 |
| 331 | rs3684104 | 4 | 38414337 | BB | BB | BB | AA | AA | AA | 1 | 1 |
| 332 | rs13477662 | 4 | 39882315 | BB | BB | BB | AA | AA | AA | 1 | 1 |
| 333 | CEL-4_40541402 | 4 | 40541402 | AA | AA | BB | AA | AA | AA | 1 | 1 |
| 334 | rs3698283 | 4 | 42429891 | BB | AA | AA | BB | BB | BB | 1 | 1 |
| 335 | rs13477676 | 4 | 44111689 | BB | AA | AA | AA | AA | AA | 1 | 1 |
| 336 | rs13477681 | 4 | 45420449 | BB | BB | BB | AA | AA | AA | 1 | 1 |
| 337 | rs3663355 | 4 | 47358427 | BB | AA | AA | AA | AA | AA | 1 | 1 |
| 338 | rs3676423 | 4 | 51035410 | BB | AA | AA | BB | BB | BB | 1 | 1 |
| 339 | rs13477709 | 4 | 52679398 | AA | BB | BB | AA | AA | AA | 1 | 1 |
| 340 | rs3677770 | 4 | 53964528 | AA | AA | AA | BB | BB | BB | 1 | 1 |
| 341 | rs6239799 | 4 | 55765284 | BB | BB | BB | AA | AA | AA | 1 | 1 |
| 342 | rs13477726 | 4 | 57030578 | BB | AA | AA | AA | AA | AA | 1 | 1 |
| 343 | rs3712541 | 4 | 59103430 | AA | AA | AA | BB | BB | BB | 1 | 1 |
| 344 | rs3690581 | 4 | 61034761 | AA | AA | AA | BB | BB | BB | 1 | 1 |
| 345 | rs6254381 | 4 | 62013092 | AA | AA | AA | AA | AA | AA | 1 | 1 |
| 346 | rs13477749 | 4 | 64811196 | AA | BB | AA | AA | AA | AA | 1 | 1 |
| 347 | rs3710245 | 4 | 68727690 | BB | AA | AA | AA | AA | AA | 1 | 1 |
| 348 | rs13477765 | 4 | 69553312 | BB | AA | AA | AA | AA | AA | 1 | 1 |
| 349 | rs6222684 | 4 | 70467819 | BB | AA | AA | AA | AA | AA | 1 | 1 |
| 350 | rs13477774 | 4 | 71868643 | BB | AA | AA | AA | AA | AA | 1 | 1 |
| 351 | rs13477785 | 4 | 74403260 | AA | AA | BB | BB | BB | BB | 1 | 1 |
| 352 | rs3708471 | 4 | 75144974 | BB | BB | AA | AA | AA | AA | 1 | 1 |
| 353 | CEL-4_77952063 | 4 | 77952063 | AA | BB | AA | AA | AA | AA | 1 | 1 |
| 354 | rs4139273 | 4 | 79969982 | AA | AA | BB | BB | BB | BB | 1 | 1 |
| 355 | rs3676928 | 4 | 81040027 | AA | AA | BB | BB | BB | BB | 1 | 1 |
| 356 | rs3699276 | 4 | 81462943 | BB | BB | AA | AA | AA | AA | 1 | 1 |
| 357 | rs3711477 | 4 | 84506191 | BB | BB | BB | AA | AA | AA | 1 | 1 |
| 358 | rs6209043 | 4 | 88269130 | AA | AA | AA | BB | BB | BB | 1 | 1 |

| | | | | | | | | | | | |
|---|---|---|---|---|---|---|---|---|---|---|---|
| 359 | rs13477838 | 4 | 89450763 | BB | AA | AA | BB | BB | BB | 1 | 1 |
| 360 | rs6271003 | 4 | 91308682 | BB | AA | AA | AA | AA | AA | 1 | 1 |
| 361 | rs3659791 | 4 | 94278186 | BB | AA | AA | BB | BB | BB | 1 | 1 |
| 362 | rs13477860 | 4 | 95674511 | BB | AA | AA | AA | AA | AA | 1 | 1 |
| 363 | rs13477866 | 4 | 97650355 | BB | AA | AA | AA | AA | AA | 1 | 1 |
| 364 | rs13477873 | 4 | 99775886 | BB | AA | AA | BB | BB | BB | 1 | 1 |
| 365 | rs6315002 | 4 | 101395000 | BB | AA | AA | BB | BB | BB | 1 | 1 |
| 366 | rs13477883 | 4 | 102307704 | BB | AA | AA | BB | BB | BB | 1 | 1 |
| 367 | rs6324470 | 4 | 104323754 | BB | BB | BB | AA | AA | AA | 1 | 1 |
| 368 | rs6226080 | 4 | 107056497 | AA | AA | AA | BB | BB | BB | 1 | 1 |
| 369 | rs3710617 | 4 | 108380717 | BB | AA | AA | AA | AA | AA | 1 | 1 |
| 370 | rs3709486 | 4 | 109968331 | BB | AA | AA | BB | BB | BB | 1 | 1 |
| 371 | rs6381371 | 4 | 114381685 | BB | AA | AA | BB | BB | BB | 1 | 1 |
| 372 | rs3692563 | 4 | 116737689 | AA | AA | AA | BB | BB | BB | 1 | 1 |
| 373 | rs3675629 | 4 | 119404209 | AA | AA | AA | BB | BB | BB | 1 | 1 |
| 374 | rs13477952 | 4 | 121322200 | AA | BB | BB | AA | AA | AA | 1 | 1 |
| 375 | rs13477959 | 4 | 122566268 | AA | AA | AA | BB | BB | BB | 1 | 1 |
| 376 | rs13477965 | 4 | 125082422 | BB | AA | AA | BB | BB | BB | 1 | 1 |
| 377 | gnf04.123.367 | 4 | 126400415 | BB | AA | AA | BB | BB | BB | 1 | 1 |
| 378 | rs6355837 | 4 | 128083691 | BB | BB | BB | AA | AA | AA | 1 | 1 |
| 379 | UT_4_132.137715 | 4 | 131705391 | BB | BB | BB | AA | AA | AA | 1 | 1 |
| 380 | rs3663950 | 4 | 134187547 | BB | BB | AA | AA | AA | AA | 1 | 1 |
| 381 | rs13478002 | 4 | 135132664 | BB | AA | AA | BB | BB | BB | 1 | 1 |
| 382 | rs4224864 | 4 | 136662000 | BB | AA | AA | BB | BB | BB | 1 | 1 |
| 383 | rs3688566 | 4 | 140026440 | BB | BB | BB | AA | AA | AA | 1 | 1 |
| 384 | rs3719891 | 4 | 140961583 | AA | AA | BB | AA | AA | AA | 1 | 1 |
| 385 | rs3023025 | 4 | 141638718 | BB | AA | AA | AA | AA | AA | 1 | 1 |
| 386 | rs6230717 | 4 | 145785696 | BB | AA | BB | AA | AA | AA | 1 | 1 |
| 387 | rs6268364 | 4 | 149902058 | BB | BB | AA | AA | AA | AA | 1 | 1 |
| 388 | rs13478089 | 4 | 152316000 | AA | AA | AA | BB | BB | BB | 1 | 1 |
| 389 | rs13478068 | 4 | 153104114 | BB | BB | BB | AA | AA | AA | 1 | 1 |
| 390 | rs6279100 | 4 | 154069720 | BB | AA | BB | AA | AA | AA | 1 | 1 |
| 391 | mCV24244050 | 5 | 3061523 | BB | BB | AA | AA | AA | AA | 1 | 1 |
| 392 | rs13478092 | 5 | 3601413 | BB | BB | AA | AA | AA | AA | 1 | 1 |
| 393 | rs13478094 | 5 | 4310159 | BB | BB | AA | BB | BB | BB | 1 | 1 |
| 394 | rs3664617 | 5 | 4474737 | BB | BB | BB | AA | AA | AA | 1 | 1 |
| 395 | rs6402980 | 5 | 5438798 | AA | BB | AA | BB | BB | BB | 1 | 1 |
| 396 | rs6307393 | 5 | 7652759 | BB | AA | AA | AA | AA | AA | 1 | 1 |
| 397 | rs13478110 | 5 | 9748059 | BB | AA | AA | AA | AA | AA | 1 | 1 |
| 398 | rs3714258 | 5 | 11417181 | AA | BB | AA | BB | BB | BB | 1 | 1 |
| 399 | rs3687916 | 5 | 13389454 | AA | BB | AA | BB | BB | BB | 1 | 1 |
| 400 | rs6353097 | 5 | 13875606 | BB | AA | AA | AA | AA | AA | 1 | 1 |
| 401 | rs3692039 | 5 | 16224015 | BB | AA | AA | AA | AA | AA | 1 | 1 |
| 402 | rs6234642 | 5 | 17667733 | BB | AA | AA | AA | AA | AA | 1 | 1 |
| 403 | rs13478133 | 5 | 19993162 | AA | AA | BB | AA | AA | AA | 1 | 1 |
| 404 | rs13478139 | 5 | 21398479 | BB | BB | AA | AA | AA | AA | 1 | 1 |
| 405 | rs6349956 | 5 | 23273638 | AA | AA | BB | AA | AA | AA | 1 | 1 |
| 406 | CEL-5_24211033 | 5 | 24211033 | AA | BB | BB | BB | BB | BB | 1 | 1 |
| 407 | rs13478154 | 5 | 25501830 | BB | BB | BB | AA | AA | AA | 1 | 1 |
| 408 | rs3696671 | 5 | 26095730 | BB | BB | BB | AA | AA | AA | 1 | 1 |
| 409 | rs3680434 | 5 | 27162034 | BB | AA | AA | BB | BB | BB | 1 | 1 |
| 410 | rs13469943 | 5 | 29486094 | BB | BB | BB | AA | AA | AA | 1 | 1 |
| 411 | rs3700706 | 5 | 31071103 | BB | BB | BB | AA | AA | AA | 1 | 1 |
| 412 | rs13459085 | 5 | 33353887 | AA | BB | BB | AA | AA | AA | 1 | 1 |
| 413 | rs3673363 | 5 | 33963604 | AA | BB | BB | AA | AA | AA | 1 | 1 |
| 414 | rs6341620 | 5 | 35567326 | AA | AA | AA | BB | BB | BB | 1 | 1 |
| 415 | rs6256504 | 5 | 38327673 | BB | AA | AA | AA | AA | AA | 1 | 1 |
| 416 | rs13478205 | 5 | 39608047 | BB | BB | AA | AA | AA | AA | 1 | 1 |
| 417 | rs6215373 | 5 | 42914749 | AA | AA | AA | BB | BB | BB | 1 | 1 |
| 418 | rs13478223 | 5 | 43971357 | BB | AA | AA | BB | BB | BB | 1 | 1 |
| 419 | rs3659933 | 5 | 44700900 | NC | NC | NC | BB | NC | NC | NA | NA |
| 420 | CEL-5_45872918 | 5 | 45872918 | BB | AA | AA | BB | BB | BB | 1 | 1 |
| 421 | rs6192958 | 5 | 47975043 | AA | BB | BB | AA | AA | AA | 1 | 1 |
| 422 | rs3714001 | 5 | 49310150 | BB | BB | AA | AA | AA | AA | 1 | 1 |
| 423 | rs3660964 | 5 | 51028268 | AA | AA | BB | BB | BB | BB | 1 | 1 |
| 424 | rs3664008 | 5 | 52283097 | BB | BB | BB | AA | AA | AA | 1 | 1 |
| 425 | mCV23125912 | 5 | 53853311 | AA | BB | AA | BB | BB | BB | 1 | 1 |
| 426 | CEL-5_56167948 | 5 | 56167948 | BB | AA | BB | AA | AA | AA | 1 | 1 |
| 427 | rs3090667 | 5 | 58891807 | AA | AA | AA | BB | BB | BB | 1 | 1 |
| 428 | rs6354160 | 5 | 60155561 | BB | BB | BB | AA | AA | AA | 1 | 1 |
| 429 | rs6187409 | 5 | 61437749 | BB | BB | BB | AA | AA | AA | 1 | 1 |
| 430 | mCV23386455 | 5 | 62818443 | BB | BB | BB | AA | AA | AA | 1 | 1 |
| 431 | rs4225248 | 5 | 65265514 | BB | BB | BB | AA | AA | AA | 1 | 1 |
| 432 | rs13478309 | 5 | 65750331 | BB | AA | AA | BB | BB | BB | 1 | 1 |
| 433 | gnf05.061.650 | 5 | 65952319 | AA | AA | AA | BB | BB | BB | 1 | 1 |
| 434 | rs3695107 | 5 | 69049778 | AA | AA | BB | BB | BB | BB | 1 | 1 |
| 435 | rs6340166 | 5 | 71436027 | BB | BB | AA | BB | BB | BB | 1 | 1 |
| 436 | rs6161105 | 5 | 73093296 | BB | BB | BB | AA | AA | AA | 1 | 1 |
| 437 | mCV22996021 | 5 | 75065363 | BB | BB | AA | BB | BB | BB | 1 | 1 |
| 438 | rs13478337 | 5 | 76181811 | AA | BB | BB | BB | BB | BB | 1 | 1 |
| 439 | rs13478352 | 5 | 79902641 | AA | AA | BB | BB | BB | BB | 1 | 1 |
| 440 | rs3721607 | 5 | 81282125 | BB | BB | BB | AA | AA | AA | 1 | 1 |
| 441 | rs3667334 | 5 | 81819770 | BB | BB | BB | AA | AA | AA | 1 | 1 |
| 442 | rs13459087 | 5 | 85884364 | BB | BB | BB | AA | AA | AA | 1 | 1 |
| 443 | CEL-5_87173557 | 5 | 87173557 | BB | BB | BB | AA | AA | AA | 1 | 1 |
| 444 | gnf05.084.686 | 5 | 88364567 | BB | BB | BB | AA | AA | AA | 1 | 1 |
| 445 | rs3673049 | 5 | 88498569 | AA | AA | AA | BB | BB | BB | 1 | 1 |
| 446 | rs13478388 | 5 | 89674255 | AA | BB | BB | AA | AA | AA | 1 | 1 |
| 447 | rs6232866 | 5 | 90936845 | BB | BB | BB | AA | AA | AA | 1 | 1 |
| 448 | rs13478402 | 5 | 93496397 | AA | AA | AA | BB | BB | BB | 1 | 1 |
| 449 | CEL-5_93945748 | 5 | 93945748 | AA | AA | AA | BB | BB | BB | 1 | 1 |
| 450 | rs3661241 | 5 | 95154383 | AA | AA | AA | BB | BB | BB | 1 | 1 |
| 451 | rs3705458 | 5 | 96618852 | AA | AA | AA | BB | BB | BB | 1 | 1 |
| 452 | rs13478433 | 5 | 101291108 | AA | BB | BB | BB | BB | BB | 1 | 1 |

| | | | | | | | | | | | | |
|---|---|---|---|---|---|---|---|---|---|---|---|---|
| 453 | rs13478451 | 5 | 106102700 | | BB | BB | BB | AA | AA | AA | 1 | 1 |
| 454 | rs13459186 | 5 | 107435156 | | AA | AA | BB | BB | BB | BB | 1 | 1 |
| 455 | UT_5_110.343536 | 5 | 108678291 | | AA | BB | BB | BB | BB | BB | 1 | 1 |
| 456 | gnf05.106.197 | 5 | 109421273 | | BB | BB | BB | AA | AA | AA | 1 | 1 |
| 457 | rs13478473 | 5 | 111603432 | | AA | AA | BB | AA | AA | AA | 1 | 1 |
| 458 | gnf05.110.207 | 5 | 113532900 | | BB | BB | AA | AA | AA | AA | 1 | 1 |
| 459 | rs13478483 | 5 | 115405250 | | AA | AA | AA | BB | BB | BB | 1 | 1 |
| 460 | CEL-5_117374791 | 5 | 117374791 | | AA | AA | AA | BB | BB | BB | 1 | 1 |
| 461 | rs8239888 | 5 | 119078055 | | BB | BB | AA | AA | AA | AA | 1 | 1 |
| 462 | rs13478496 | 5 | 119747337 | | BB | BB | AA | AA | AA | AA | 1 | 1 |
| 463 | rs13478501 | 5 | 121338564 | | AA | AA | BB | BB | BB | BB | 1 | 1 |
| 464 | rs3671202 | 5 | 122343598 | | BB | BB | BB | AA | AA | AA | 1 | 1 |
| 465 | gnf05.120.129 | 5 | 123654667 | | AA | AA | BB | BB | BB | BB | 1 | 1 |
| 466 | rs13478518 | 5 | 125334324 | | BB | AA | BB | AA | AA | AA | 1 | 1 |
| 467 | rs13478527 | 5 | 126818001 | | BB | BB | AA | AA | AA | AA | 1 | 1 |
| 468 | gnf05.124.386 | 5 | 127936509 | | AA | BB | BB | BB | BB | BB | 1 | 1 |
| 469 | rs13478540 | 5 | 131766121 | | AA | AA | AA | AA | AA | AA | 1 | 1 |
| 470 | rs13478546 | 5 | 133978719 | | BB | AA | AA | BB | BB | BB | 1 | 1 |
| 471 | rs4225536 | 5 | 135836567 | | BB | BB | BB | AA | AA | AA | 1 | 1 |
| 472 | rs6298689 | 5 | 137173297 | | AA | BB | AA | AA | AA | AA | 1 | 1 |
| 473 | rs3656197 | 5 | 139206611 | | AA | AA | AA | BB | BB | BB | 1 | 1 |
| 474 | rs13478574 | 5 | 141567331 | | BB | AA | AA | AA | AA | AA | 1 | 1 |
| 475 | rs3718776 | 5 | 147051702 | | AA | AA | AA | BB | BB | BB | 1 | 1 |
| 476 | rs3661828 | 6 | 3167392 | | AA | AA | AA | BB | BB | BB | 1 | 1 |
| 477 | rs13478602 | 6 | 3547547 | | AA | AA | AA | BB | BB | BB | 1 | 1 |
| 478 | rs6172481 | 6 | 4362632 | | BB | BB | BB | AA | AA | AA | 1 | 1 |
| 479 | rs3699833 | 6 | 6161470 | | BB | BB | BB | AA | AA | AA | 1 | 1 |
| 480 | rs13478617 | 6 | 7747436 | | AA | AA | AA | AA | AA | AA | 1 | 1 |
| 481 | rs13478621 | 6 | 8907544 | | BB | AA | AA | AA | AA | AA | 1 | 1 |
| 482 | rs13478626 | 6 | 9890882 | | BB | AA | AA | AA | AA | AA | 1 | 1 |
| 483 | rs13478631 | 6 | 11055603 | | BB | AA | AA | AA | AA | AA | 1 | 1 |
| 484 | rs3678711 | 6 | 14045168 | | AA | BB | BB | AA | AA | AA | 1 | 1 |
| 485 | rs13478641 | 6 | 15816033 | | BB | AA | AA | BB | BB | BB | 1 | 1 |
| 486 | rs3655269 | 6 | 17715100 | | AA | AA | AA | BB | BB | BB | 1 | 1 |
| 487 | rs13478649 | 6 | 18376687 | | BB | AA | AA | AA | AA | AA | 1 | 1 |
| 488 | rs13478656 | 6 | 21755667 | | AA | AA | AA | BB | BB | BB | 1 | 1 |
| 489 | rs3684494 | 6 | 24248321 | | BB | AA | BB | BB | BB | BB | 1 | 1 |
| 490 | rs3671709 | 6 | 25646449 | | BB | BB | AA | BB | BB | BB | 1 | 1 |
| 491 | rs13478677 | 6 | 27804113 | | BB | AA | BB | AA | AA | AA | 1 | 1 |
| 492 | gnf06.026.418 | 6 | 29269458 | | AA | AA | AA | BB | BB | BB | 1 | 1 |
| 493 | rs13478697 | 6 | 32730020 | | BB | BB | BB | AA | AA | AA | 1 | 1 |
| 494 | rs13478705 | 6 | 34409100 | | BB | AA | AA | BB | BB | BB | 1 | 1 |
| 495 | rs3704635 | 6 | 36040358 | | AA | AA | AA | BB | BB | BB | 1 | 1 |
| 496 | rs6330932 | 6 | 37461200 | | AA | AA | AA | AA | AA | AA | 1 | 1 |
| 497 | rs13478719 | 6 | 38473383 | | BB | BB | AA | BB | BB | BB | 1 | 1 |
| 498 | gnf06.037.785 | 6 | 40733942 | | BB | BB | AA | BB | BB | BB | 1 | 1 |
| 499 | rs13478727 | 6 | 43778689 | | BB | BB | BB | AA | AA | AA | 1 | 1 |
| 500 | rs6238771 | 6 | 45234635 | | AA | BB | AA | AA | AA | AA | 1 | 1 |
| 501 | rs13478732 | 6 | 45420260 | | AA | BB | AA | AA | AA | AA | 1 | 1 |
| 502 | rs13478745 | 6 | 48964507 | | BB | AA | AA | BB | BB | BB | 1 | 1 |
| 503 | rs4139698 | 6 | 49813889 | | BB | BB | AA | AA | AA | AA | 1 | 1 |
| 504 | rs13478753 | 6 | 51145321 | | AA | BB | BB | AA | AA | AA | 1 | 1 |
| 505 | rs13478761 | 6 | 53702681 | | AA | BB | AA | BB | BB | BB | 1 | 1 |
| 506 | rs6355719 | 6 | 56316458 | | AA | BB | BB | BB | BB | BB | 1 | 1 |
| 507 | CEL-6_57082524 | 6 | 57082524 | | AA | AA | AA | BB | BB | BB | 1 | 1 |
| 508 | rs13478780 | 6 | 59609561 | | BB | BB | AA | BB | BB | BB | 1 | 1 |
| 509 | rs13478783 | 6 | 60682681 | X | BB | BB | BB | AA | AA | AA | 1 | 1 |
| 510 | rs6378343 | 6 | 63916748 | | AA | AA | BB | AA | AA | AA | 1 | 1 |
| 511 | rs13478801 | 6 | 65211036 | | AA | AA | BB | AA | AA | AA | 1 | 1 |
| 512 | rs6353425 | 6 | 67548202 | | AA | AA | AA | AA | AA | AA | 1 | 1 |
| 513 | rs6195266 | 6 | 69590221 | | BB | BB | BB | BB | BB | BB | 1 | 1 |
| 514 | mhcCD8b4 | 6 | 71532444 | | AA | AA | BB | AA | AA | AA | 1 | 1 |
| 515 | rs13478819 | 6 | 73538842 | | AA | BB | BB | BB | BB | BB | 1 | 1 |
| 516 | rs3672029 | 6 | 75631345 | | AA | BB | AA | BB | BB | BB | 1 | 1 |
| 517 | rs3699367 | 6 | 76679118 | | AA | BB | BB | AA | AA | AA | 1 | 1 |
| 518 | rs13478841 | 6 | 78477103 | | AA | AA | BB | BB | BB | BB | 1 | 1 |
| 519 | rs6377140 | 6 | 80032286 | | BB | BB | AA | AA | AA | AA | 1 | 1 |
| 520 | rs6181382 | 6 | 81674296 | | AA | BB | AA | AA | AA | AA | 1 | 1 |
| 521 | CEL-6_83434907 | 6 | 83434907 | | AA | BB | AA | AA | AA | AA | 1 | 1 |
| 522 | rs13459097 | 6 | 85136988 | | BB | AA | AA | AA | AA | AA | 1 | 1 |
| 523 | CEL-6_86289708 | 6 | 86289708 | | AA | BB | AA | BB | BB | BB | 1 | 1 |
| 524 | rs13478882 | 6 | 90003224 | | BB | AA | BB | AA | AA | AA | 1 | 1 |
| 525 | rs13478891 | 6 | 92361613 | | BB | AA | AA | AA | AA | AA | 1 | 1 |
| 526 | rs6285738 | 6 | 93892091 | | BB | BB | AA | BB | BB | BB | 1 | 1 |
| 527 | rs6239023 | 6 | 94413050 | | AA | AA | BB | BB | BB | BB | 1 | 1 |
| 528 | rs6349084 | 6 | 97121415 | | BB | AA | BB | BB | BB | BB | 1 | 1 |
| 529 | rs13478919 | 6 | 98304818 | | AA | BB | AA | AA | AA | AA | 1 | 1 |
| 530 | rs4138572 | 6 | 98790763 | | AA | BB | BB | AA | AA | AA | 1 | 1 |
| 531 | rs3718735 | 6 | 101508462 | | BB | BB | BB | AA | AA | AA | 1 | 1 |
| 532 | rs13478943 | 6 | 104128964 | | BB | AA | AA | AA | AA | AA | 1 | 1 |
| 533 | rs6208251 | 6 | 105270851 | | BB | AA | AA | BB | BB | BB | 1 | 1 |
| 534 | rs13478952 | 6 | 106695156 | | BB | AA | AA | BB | BB | BB | 1 | 1 |
| 535 | rs3670475 | 6 | 110397055 | | AA | AA | BB | AA | AA | AA | 1 | 1 |
| 536 | rs13478971 | 6 | 111749805 | | BB | AA | AA | BB | BB | BB | 1 | 1 |
| 537 | rs13478977 | 6 | 113036388 | | AA | AA | AA | AA | AA | AA | 1 | 1 |
| 538 | rs6393943 | 6 | 114932370 | | AA | BB | BB | BB | BB | BB | 1 | 1 |
| 539 | rs6401637 | 6 | 116477552 | | BB | AA | BB | AA | AA | AA | 1 | 1 |
| 540 | mCV23042866 | 6 | 117147180 | | BB | AA | BB | AA | AA | AA | 1 | 1 |
| 541 | rs13478997 | 6 | 118461935 | | BB | AA | AA | AA | AA | AA | 1 | 1 |
| 542 | rs3695724 | 6 | 120403722 | | NC | NC | NC | AA | NC | NC | NA | NA |
| 543 | rs13479006 | 6 | 121702158 | | BB | BB | BB | AA | AA | AA | 1 | 1 |
| 544 | gnf06.122.747 | 6 | 124630688 | | BB | AA | AA | BB | BB | BB | 1 | 1 |
| 545 | rs13479014 | 6 | 125666374 | | AA | BB | BB | AA | AA | AA | 1 | 1 |
| 546 | rs6200835 | 6 | 126340874 | | BB | AA | AA | AA | AA | AA | 1 | 1 |

| | | | | | | | | | | | | |
|---|---|---|---|---|---|---|---|---|---|---|---|---|
| 547 | rs6389420 | 6 | 127676012 | | AA | BB | BB | AA | AA | AA | 1 | 1 |
| 548 | rs3681620 | 6 | 128654310 | | BB | BB | BB | AA | AA | AA | 1 | 1 |
| 549 | CEL-6_130920075 | 6 | 130920075 | | BB | BB | BB | AA | AA | AA | 1 | 1 |
| 550 | rs3722480 | 6 | 131616421 | | BB | AA | AA | BB | BB | BB | 1 | 1 |
| 551 | rs6339546 | 6 | 134019679 | | AA | BB | BB | AA | AA | AA | 1 | 1 |
| 552 | rs13479053 | 6 | 134303922 | | AA | BB | BB | AA | AA | AA | 1 | 1 |
| 553 | rs3023102 | 6 | 135439528 | | AA | AA | AA | BB | BB | BB | 1 | 1 |
| 554 | rs13479063 | 6 | 136451163 | | BB | AA | AA | BB | BB | BB | 1 | 1 |
| 555 | rs13479071 | 6 | 138359897 | | AA | BB | BB | BB | BB | BB | 1 | 1 |
| 556 | rs3672808 | 6 | 139965472 | | BB | AA | AA | BB | BB | BB | 1 | 1 |
| 557 | rs6329892 | 6 | 142567031 | | AA | AA | AA | AA | AA | AA | 1 | 1 |
| 558 | rs3658783 | 6 | 144465978 | | BB | BB | BB | AA | AA | AA | 1 | 1 |
| 559 | rs6265387 | 6 | 147380171 | | BB | BB | AA | AA | AA | AA | 1 | 1 |
| 560 | rs3711088 | 6 | 148456534 | | BB | BB | BB | AA | AA | AA | 1 | 1 |
| 561 | gnf06.149.306 | 6 | 149418695 | | BB | BB | BB | AA | AA | AA | 1 | 1 |
| 562 | mCV23738426 | 7 | 4906617 | | AA | AA | BB | BB | BB | BB | 1 | 1 |
| 563 | CEL-7_5627457 | 7 | 5627457 | | BB | AA | BB | BB | BB | BB | 1 | 1 |
| 564 | rs13479139 | 7 | 8241486 | | BB | AA | BB | AA | AA | AA | 1 | 1 |
| 565 | rs6361142 | 7 | 9296425 | | BB | AA | BB | AA | AA | AA | 1 | 1 |
| 566 | rs3689218 | 7 | 10546409 | | BB | AA | BB | BB | BB | BB | 1 | 1 |
| 567 | gnf07.013.809 | 7 | 10926083 | | BB | AA | BB | AA | AA | AA | 1 | 1 |
| 568 | rs13479153 | 7 | 13677268 | | BB | BB | BB | AA | AA | AA | 1 | 1 |
| 569 | CEL-7_17114061 | 7 | 17114061 | | BB | BB | BB | AA | AA | AA | 1 | 1 |
| 570 | rs4226499 | 7 | 17800749 | | BB | BB | AA | BB | BB | BB | 1 | 1 |
| 571 | rs4226520 | 7 | 18758740 | | AA | AA | BB | BB | BB | BB | 1 | 1 |
| 572 | rs3147860 | 7 | 19496283 | | BB | AA | AA | AA | AA | AA | 1 | 1 |
| 573 | rs3719311 | 7 | 22647606 | | BB | AA | BB | BB | BB | BB | 1 | 1 |
| 574 | rs6239372 | 7 | 23113384 | | AA | AA | AA | AA | AA | AA | 1 | 1 |
| 575 | rs13479191 | 7 | 24555108 | | BB | BB | BB | BB | BB | BB | 1 | 1 |
| 576 | gnf07.032.889 | 7 | 28379711 | | AA | BB | AA | AA | AA | AA | 1 | 1 |
| 577 | rs4232449 | 7 | 28755779 | | AA | AA | AA | AA | AA | AA | 1 | 1 |
| 578 | rs3719256 | 7 | 31933809 | | BB | AA | BB | AA | AA | AA | 1 | 1 |
| 579 | rs8255275 | 7 | 33574760 | | AA | AA | AA | BB | BB | BB | 1 | 1 |
| 580 | rs8260975 | 7 | 33835314 | | BB | AA | BB | AA | AA | AA | 1 | 1 |
| 581 | CEL-7_36725559 | 7 | 36725559 | | BB | AA | BB | AA | AA | AA | 1 | 1 |
| 582 | rs3699938 | 7 | 38476481 | | BB | AA | BB | BB | BB | BB | 1 | 1 |
| 583 | rs13479251 | 7 | 39863901 | | AA | AA | AA | BB | BB | BB | 1 | 1 |
| 584 | rs3718641 | 7 | 41170581 | | BB | AA | BB | AA | AA | AA | 1 | 1 |
| 585 | rs3663313 | 7 | 43718739 | | AA | BB | AA | BB | BB | BB | 1 | 1 |
| 586 | mCV23672419 | 7 | 45173762 | | AA | AA | AA | AA | AA | AA | 1 | 1 |
| 587 | rs13479277 | 7 | 46313106 | | BB | BB | BB | AA | AA | AA | 1 | 1 |
| 588 | mCV23423763 | 7 | 47949709 | | BB | BB | BB | AA | AA | AA | 1 | 1 |
| 589 | rs3679779 | 7 | 51392430 | | BB | BB | BB | AA | AA | AA | 1 | 1 |
| 590 | rs3714908 | 7 | 51544526 | | AA | BB | AA | BB | BB | BB | 1 | 1 |
| 591 | rs6160140 | 7 | 53312532 | | AA | BB | AA | BB | BB | BB | 1 | 1 |
| 592 | rs3705155 | 7 | 55557090 | | AA | AA | AA | BB | BB | BB | 1 | 1 |
| 593 | rs13479319 | 7 | 56830620 | | BB | BB | BB | AA | AA | AA | 1 | 1 |
| 594 | rs13479324 | 7 | 57878499 | | BB | BB | BB | AA | AA | AA | 1 | 1 |
| 595 | rs3676254 | 7 | 59722158 | | AA | AA | AA | BB | BB | BB | 1 | 1 |
| 596 | rs13479338 | 7 | 61105319 | | AA | AA | AA | BB | BB | BB | 1 | 1 |
| 597 | rs13479347 | 7 | 63356038 | | AA | AA | AA | BB | BB | BB | 1 | 1 |
| 598 | rs13479355 | 7 | 65348455 | | BB | AA | BB | BB | BB | BB | 1 | 1 |
| 599 | rs13479358 | 7 | 66776784 | | AA | BB | AA | AA | AA | AA | 1 | 1 |
| 600 | rs13479363 | 7 | 68228570 | | BB | BB | BB | AA | AA | AA | 1 | 1 |
| 601 | rs6213614 | 7 | 69422276 | | AA | BB | AA | AA | AA | AA | 1 | 1 |
| 602 | rs13479375 | 7 | 71406934 | | BB | AA | BB | AA | AA | AA | 1 | 1 |
| 603 | rs13479385 | 7 | 74292260 | | AA | BB | AA | AA | AA | AA | 1 | 1 |
| 604 | rs13479395 | 7 | 77234500 | | AA | AA | AA | BB | BB | BB | 1 | 1 |
| 605 | CEL-7_77850273 | 7 | 77850273 | | AA | BB | AA | AA | AA | AA | 1 | 1 |
| 606 | rs4226783 | 7 | 80158909 | | AA | BB | AA | BB | BB | BB | 1 | 1 |
| 607 | rs13479414 | 7 | 82727616 | | BB | AA | AA | BB | BB | BB | 1 | 1 |
| 608 | rs3699086 | 7 | 83322675 | | BB | BB | AA | BB | BB | BB | 1 | 1 |
| 609 | rs3707067 | 7 | 85992410 | | AA | AA | BB | BB | BB | BB | 1 | 1 |
| 610 | rs13479427 | 7 | 87305015 | | AA | AA | BB | BB | BB | BB | 1 | 1 |
| 611 | rs3713052 | 7 | 89115174 | | BB | BB | BB | AA | AA | AA | 1 | 1 |
| 612 | rs6357312 | 7 | 89751283 | | AA | AA | AA | BB | BB | BB | 1 | 1 |
| 613 | rs3673653 | 7 | 94344049 | | BB | BB | BB | AA | AA | AA | 1 | 1 |
| 614 | rs6386601 | 7 | 94870318 | | AA | BB | AA | BB | BB | BB | 1 | 1 |
| 615 | rs13479455 | 7 | 96728523 | | AA | AA | AA | AA | AA | AA | 1 | 1 |
| 616 | rs13479461 | 7 | 99220204 | | AA | AA | AA | BB | BB | BB | 1 | 1 |
| 617 | rs6194926 | 7 | 101647757 | | BB | AA | AA | BB | BB | BB | 1 | 1 |
| 618 | rs13479477 | 7 | 104533846 | | AA | BB | AA | BB | BB | BB | 1 | 1 |
| 619 | rs3023159 | 7 | 106579694 | | AA | BB | BB | AA | AA | AA | 1 | 1 |
| 620 | rs3709679 | 7 | 107424656 | | BB | AA | AA | BB | BB | BB | 1 | 1 |
| 621 | rs6275579 | 7 | 111285662 | | BB | BB | BB | BB | BB | BB | 1 | 1 |
| 622 | rs13479506 | 7 | 112152410 | | AA | AA | BB | BB | BB | BB | 1 | 1 |
| 623 | rs3682038 | 7 | 113814867 | | AA | BB | BB | BB | BB | BB | 1 | 1 |
| 624 | rs13479517 | 7 | 115461663 | | BB | AA | AA | AA | AA | AA | 1 | 1 |
| 625 | CEL-7_115892950 | 7 | 115892950 | | BB | AA | AA | BB | BB | BB | 1 | 1 |
| 626 | rs13479522 | 7 | 116540646 | X | BB | BB | BB | AA | AA | AA | 1 | 1 |
| 627 | rs13479535 | 7 | 119192048 | | AA | BB | BB | BB | BB | BB | 1 | 1 |
| 628 | rs3716088 | 7 | 120621563 | | BB | BB | BB | AA | AA | AA | 1 | 1 |
| 629 | CEL-7_122752866 | 7 | 122752866 | | BB | BB | BB | BB | BB | BB | 1 | 1 |
| 630 | rs13479553 | 7 | 124913079 | | AA | AA | AA | AA | AA | AA | 1 | 1 |
| 631 | rs3663988 | 7 | 126965988 | | AA | AA | AA | BB | BB | BB | 1 | 1 |
| 632 | rs3711570 | 8 | 4193008 | | BB | BB | AA | AA | AA | AA | 1 | 1 |
| 633 | rs6360601 | 8 | 6795642 | | AA | AA | BB | BB | BB | BB | 1 | 1 |
| 634 | rs6153168 | 8 | 8294541 | | BB | AA | AA | AA | AA | AA | 1 | 1 |
| 635 | rs13479608 | 8 | 11675148 | | BB | AA | AA | AA | AA | AA | 1 | 1 |
| 636 | rs6410533 | 8 | 14327885 | | BB | BB | BB | BB | BB | BB | 1 | 1 |
| 637 | rs13479619 | 8 | 15319466 | | BB | AA | AA | BB | BB | BB | 1 | 1 |
| 638 | rs3657963 | 8 | 16576750 | | AA | AA | AA | BB | BB | BB | 1 | 1 |
| 639 | gnf08.014.711 | 8 | 18169937 | | AA | AA | AA | BB | BB | BB | 1 | 1 |
| 640 | rs4140004 | 8 | 21285113 | | AA | AA | AA | BB | BB | BB | 1 | 1 |

| | | | | | | | | | | | | |
|---|---|---|---|---|---|---|---|---|---|---|---|---|
| 641 | rs3661760 | 8 | 22251497 | | AA | AA | AA | BB | BB | BB | 1 | 1 |
| 642 | rs13479656 | 8 | 24309617 | | BB | BB | BB | AA | AA | AA | 1 | 1 |
| 643 | CEL-8_25963079 | 8 | 25963079 | | BB | BB | AA | BB | BB | BB | 1 | 1 |
| 644 | rs13479673 | 8 | 28075869 | | AA | AA | AA | BB | BB | BB | 1 | 1 |
| 645 | rs4227096 | 8 | 30204827 | | BB | BB | BB | AA | AA | AA | 1 | 1 |
| 646 | rs3706948 | 8 | 30816540 | | AA | AA | AA | BB | BB | BB | 1 | 1 |
| 647 | CEL-8_33812776 | 8 | 33812776 | | BB | BB | BB | AA | AA | AA | 1 | 1 |
| 648 | rs3665028 | 8 | 35164032 | | BB | BB | BB | AA | AA | AA | 1 | 1 |
| 649 | rs3667738 | 8 | 37536463 | | AA | AA | AA | BB | BB | BB | 1 | 1 |
| 650 | rs13479716 | 8 | 38775830 | | BB | AA | AA | BB | BB | BB | 1 | 1 |
| 651 | rs3703811 | 8 | 39770568 | | AA | AA | AA | BB | BB | BB | 1 | 1 |
| 652 | rs3666140 | 8 | 42081791 | | BB | BB | AA | AA | AA | AA | 1 | 1 |
| 653 | rs6386110 | 8 | 43934856 | | BB | BB | AA | AA | AA | AA | 1 | 1 |
| 654 | UT_8_46.498556 | 8 | 45775629 | | AA | BB | BB | BB | BB | BB | 1 | 1 |
| 655 | rs3719401 | 8 | 48804736 | | AA | BB | BB | BB | BB | BB | 1 | 1 |
| 656 | rs13479755 | 8 | 50117838 | | BB | AA | AA | AA | AA | AA | 1 | 1 |
| 657 | CEL-8_51607005 | 8 | 51607005 | | AA | BB | BB | BB | BB | BB | 1 | 1 |
| 658 | rs13479768 | 8 | 53532210 | | AA | BB | BB | BB | BB | BB | 1 | 1 |
| 659 | rs13479776 | 8 | 55177326 | | BB | AA | AA | AA | AA | AA | 1 | 1 |
| 660 | rs3725286 | 8 | 56141367 | | AA | BB | BB | BB | BB | BB | 1 | 1 |
| 661 | rs3707439 | 8 | 57724335 | | BB | AA | AA | BB | BB | BB | 1 | 1 |
| 662 | rs3672639 | 8 | 60120308 | | BB | AA | AA | BB | BB | BB | 1 | 1 |
| 663 | rs13479793 | 8 | 60901130 | | AA | BB | BB | AA | AA | AA | 1 | 1 |
| 664 | rs6372901 | 8 | 63043201 | | AA | BB | BB | AA | AA | AA | 1 | 1 |
| 665 | rs13479807 | 8 | 64586401 | | AA | BB | BB | AA | AA | AA | 1 | 1 |
| 666 | rs13479811 | 8 | 66034595 | | AA | AA | BB | AA | AA | AA | 1 | 1 |
| 667 | rs3656875 | 8 | 67222604 | | BB | BB | BB | AA | AA | AA | 1 | 1 |
| 668 | rs3699406 | 8 | 68996069 | | AA | AA | AA | BB | BB | BB | 1 | 1 |
| 669 | rs3667475 | 8 | 70497527 | | AA | AA | AA | BB | BB | BB | 1 | 1 |
| 670 | rs13479830 | 8 | 72013995 | | AA | AA | AA | BB | BB | BB | 1 | 1 |
| 671 | rs4227253 | 8 | 74193741 | | BB | BB | BB | AA | AA | AA | 1 | 1 |
| 672 | rs3696502 | 8 | 74806749 | | AA | AA | BB | BB | BB | BB | 1 | 1 |
| 673 | rs3698093 | 8 | 77144203 | | AA | AA | BB | AA | AA | AA | 1 | 1 |
| 674 | CZECH-8_78291790 | 8 | 78291790 | | BB | BB | BB | BB | BB | BB | 1 | 1 |
| 675 | rs4227276 | 8 | 80165835 | | AA | AA | BB | AA | AA | AA | 1 | 1 |
| 676 | rs13479863 | 8 | 82188194 | | BB | BB | AA | BB | BB | BB | 1 | 1 |
| 677 | rs13479871 | 8 | 84344531 | | BB | BB | AA | BB | BB | BB | 1 | 1 |
| 678 | rs6257357 | 8 | 84826788 | | BB | BB | BB | AA | AA | AA | 1 | 1 |
| 679 | rs13479880 | 8 | 86040626 | | BB | BB | AA | AA | AA | AA | 1 | 1 |
| 680 | rs13479882 | 8 | 86397354 | | BB | BB | AA | BB | BB | BB | 1 | 1 |
| 681 | rs13479884 | 8 | 86954362 | | AA | AA | BB | BB | BB | BB | 1 | 1 |
| 682 | rs6391152 | 8 | 89169668 | | BB | BB | AA | AA | AA | AA | 1 | 1 |
| 683 | rs13479922 | 8 | 91879489 | | AA | AA | BB | BB | BB | BB | 1 | 1 |
| 684 | rs4137596 | 8 | 94037444 | | AA | BB | BB | AA | AA | AA | 1 | 1 |
| 685 | rs6285803 | 8 | 95323284 | | BB | BB | AA | AA | AA | AA | 1 | 1 |
| 686 | rs6287320 | 8 | 96735663 | | BB | BB | BB | AA | AA | AA | 1 | 1 |
| 687 | rs13479947 | 8 | 98654267 | | AA | AA | AA | AA | AA | AA | 1 | 1 |
| 688 | rs3706149 | 8 | 100766333 | | AA | AA | AA | BB | BB | BB | 1 | 1 |
| 689 | rs3669235 | 8 | 101399186 | | AA | AA | BB | AA | AA | AA | 1 | 1 |
| 690 | rs13479956 | 8 | 101681071 | | AA | AA | AA | BB | BB | BB | 1 | 1 |
| 691 | rs3705275 | 8 | 102686478 | | BB | BB | BB | AA | AA | AA | 1 | 1 |
| 692 | gnf08.108.032 | 8 | 106117382 | | BB | BB | BB | AA | AA | AA | 1 | 1 |
| 693 | rs3662808 | 8 | 108727362 | | BB | BB | BB | AA | AA | AA | 1 | 1 |
| 694 | rs6237645 | 8 | 109333466 | | BB | BB | BB | AA | AA | AA | 1 | 1 |
| 695 | rs13479995 | 8 | 113066370 | | BB | BB | BB | AA | AA | AA | 1 | 1 |
| 696 | rs4227398 | 8 | 113744792 | | AA | BB | BB | BB | BB | BB | 1 | 1 |
| 697 | gnf08.118.027 | 8 | 116198601 | | AA | AA | BB | AA | AA | AA | 1 | 1 |
| 698 | rs13480014 | 8 | 118001545 | | BB | AA | AA | BB | BB | BB | 1 | 1 |
| 699 | rs3708073 | 8 | 121235325 | | BB | BB | BB | AA | AA | AA | 1 | 1 |
| 700 | rs6377872 | 8 | 121825605 | | AA | AA | AA | BB | BB | BB | 1 | 1 |
| 701 | rs3705725 | 8 | 123350039 | | BB | BB | BB | AA | AA | AA | 1 | 1 |
| 702 | rs6400423 | 8 | 125966003 | | BB | BB | BB | AA | AA | AA | 1 | 1 |
| 703 | rs3697596 | 8 | 127236890 | | BB | BB | BB | AA | AA | AA | 1 | 1 |
| 704 | mCV23893269 | 9 | 3980881 | | AA | BB | BB | BB | BB | BB | 1 | 1 |
| 705 | mCV23053483 | 9 | 6793269 | | AA | BB | BB | BB | BB | BB | 1 | 1 |
| 706 | rs13480065 | 9 | 9289357 | | AA | BB | BB | BB | BB | BB | 1 | 1 |
| 707 | mCV25073238 | 9 | 10587580 | | AA | BB | BB | AA | AA | AA | 1 | 1 |
| 708 | rs13480071 | 9 | 12387092 | | BB | AA | AA | BB | BB | BB | 1 | 1 |
| 709 | gnf09.012.310 | 9 | 17881329 | | AA | BB | BB | BB | BB | BB | 1 | 1 |
| 710 | rs13480092 | 9 | 18988599 | | BB | AA | AA | AA | AA | AA | 1 | 1 |
| 711 | rs8270115 | 9 | 21900659 | | BB | BB | BB | BB | BB | BB | 1 | 1 |
| 712 | rs13480103 | 9 | 23359729 | | AA | BB | BB | BB | BB | BB | 1 | 1 |
| 713 | rs3088801 | 9 | 24949186 | | AA | AA | AA | AA | AA | AA | 1 | 1 |
| 714 | rs13480112 | 9 | 26555143 | | AA | BB | BB | BB | BB | BB | 1 | 1 |
| 715 | rs6404775 | 9 | 28016429 | | AA | AA | AA | AA | AA | AA | 1 | 1 |
| 716 | rs6385855 | 9 | 29608871 | | AA | AA | AA | AA | AA | AA | 1 | 1 |
| 717 | rs13480122 | 9 | 31136193 | X | BB | BB | BB | AA | AA | AA | 1 | 1 |
| 718 | rs3655898 | 9 | 33657166 | | BB | BB | BB | AA | AA | AA | 1 | 1 |
| 719 | rs3711756 | 9 | 34437206 | | BB | BB | BB | AA | AA | AA | 1 | 1 |
| 720 | UT_9_35.918713 | 9 | 35184595 | | BB | BB | BB | AA | AA | AA | 1 | 1 |
| 721 | rs13480141 | 9 | 36959921 | | BB | BB | BB | AA | AA | AA | 1 | 1 |
| 722 | rs13480150 | 9 | 39740553 | | AA | AA | AA | BB | BB | BB | 1 | 1 |
| 723 | rs3714664 | 9 | 40768895 | | AA | AA | AA | BB | BB | BB | 1 | 1 |
| 724 | rs4135590 | 9 | 43060131 | | BB | BB | BB | AA | AA | AA | 1 | 1 |
| 725 | rs13462199 | 9 | 44740915 | | BB | BB | BB | AA | AA | AA | 1 | 1 |
| 726 | rs13480173 | 9 | 46633516 | | AA | BB | BB | AA | AA | AA | 1 | 1 |
| 727 | rs6395817 | 9 | 47519917 | | AA | BB | BB | AA | AA | AA | 1 | 1 |
| 728 | gnf09.042.496 | 9 | 48315615 | | AA | BB | BB | AA | AA | AA | 1 | 1 |
| 729 | rs13480186 | 9 | 50318725 | | BB | AA | AA | BB | BB | BB | 1 | 1 |
| 730 | rs3723670 | 9 | 52682809 | | BB | BB | BB | AA | AA | AA | 1 | 1 |
| 731 | rs13480208 | 9 | 55395056 | | AA | BB | BB | BB | BB | BB | 1 | 1 |
| 732 | rs3666398 | 9 | 56790950 | | AA | BB | AA | BB | BB | BB | 1 | 1 |
| 733 | rs13480217 | 9 | 58024426 | | BB | BB | AA | BB | BB | BB | 1 | 1 |
| 734 | rs6224703 | 9 | 60196412 | | BB | AA | BB | AA | AA | AA | 1 | 1 |

| | | | | | | | | | | | | |
|---|---|---|---|---|---|---|---|---|---|---|---|---|
| 735 | rs3714012 | 9 | 61377354 | | AA | BB | AA | BB | BB | BB | 1 | 1 |
| 736 | gnf09.057.223 | 9 | 63239299 | | AA | AA | AA | AA | AA | AA | 1 | 1 |
| 737 | rs3655717 | 9 | 65704935 | | BB | AA | BB | AA | AA | AA | 1 | 1 |
| 738 | rs6174757 | 9 | 68381485 | | AA | AA | AA | BB | BB | BB | 1 | 1 |
| 739 | rs6355445 | 9 | 70209362 | | AA | BB | BB | AA | AA | AA | 1 | 1 |
| 740 | rs3721056 | 9 | 71328971 | | AA | AA | AA | BB | BB | BB | 1 | 1 |
| 741 | rs13480271 | 9 | 73145678 | | BB | AA | AA | BB | BB | BB | 1 | 1 |
| 742 | rs3724833 | 9 | 75221496 | | AA | AA | AA | BB | BB | BB | 1 | 1 |
| 743 | rs13480285 | 9 | 76908789 | | BB | AA | AA | BB | BB | BB | 1 | 1 |
| 744 | rs6257131 | 9 | 79059621 | | BB | AA | AA | AA | AA | AA | 1 | 1 |
| 745 | gnf09.074.193 | 9 | 80458981 | | BB | AA | AA | BB | BB | BB | 1 | 1 |
| 746 | rs6223687 | 9 | 82203633 | | BB | BB | BB | BB | BB | BB | 1 | 1 |
| 747 | rs3676124 | 9 | 83548399 | | AA | AA | AA | BB | BB | BB | 1 | 1 |
| 748 | rs3695050 | 9 | 85584599 | | BB | AA | AA | BB | BB | BB | 1 | 1 |
| 749 | rs3700596 | 9 | 86745093 | | BB | BB | BB | AA | AA | AA | 1 | 1 |
| 750 | rs3669564 | 9 | 88325825 | | BB | BB | BB | AA | AA | AA | 1 | 1 |
| 751 | gnf09.087.298 | 9 | 90513305 | | AA | AA | AA | BB | BB | BB | 1 | 1 |
| 752 | rs13480345 | 9 | 92060032 | | AA | BB | BB | AA | AA | AA | 1 | 1 |
| 753 | rs13480351 | 9 | 94137054 | | AA | AA | AA | BB | BB | BB | 1 | 1 |
| 754 | CEL-9_95875215 | 9 | 95875215 | | AA | AA | AA | BB | BB | BB | 1 | 1 |
| 755 | rs3689336 | 9 | 96256381 | | BB | BB | BB | AA | AA | AA | 1 | 1 |
| 756 | rs13480365 | 9 | 98418600 | | BB | AA | AA | BB | BB | BB | 1 | 1 |
| 757 | rs6385971 | 9 | 99710289 | | AA | BB | BB | AA | AA | AA | 1 | 1 |
| 758 | rs3717654 | 9 | 101878542 | | BB | BB | BB | AA | AA | AA | 1 | 1 |
| 759 | rs13480386 | 9 | 103546788 | | AA | BB | BB | AA | AA | AA | 1 | 1 |
| 760 | rs3711089 | 9 | 105418025 | | BB | BB | BB | AA | AA | AA | 1 | 1 |
| 761 | rs13480399 | 9 | 106229354 | | AA | AA | AA | BB | BB | BB | 1 | 1 |
| 762 | rs13480407 | 9 | 108690630 | | AA | BB | BB | AA | AA | AA | 1 | 1 |
| 763 | rs13480413 | 9 | 109861337 | | AA | BB | BB | AA | AA | AA | 1 | 1 |
| 764 | rs13480421 | 9 | 111862825 | | AA | BB | BB | BB | BB | BB | 1 | 1 |
| 765 | gnf09.110.002 | 9 | 113307145 | | BB | AA | AA | BB | BB | BB | 1 | 1 |
| 766 | rs6320810 | 9 | 115090216 | | BB | BB | BB | AA | AA | AA | 1 | 1 |
| 767 | rs3669563 | 9 | 117891342 | | AA | AA | AA | BB | BB | BB | 1 | 1 |
| 768 | rs13459114 | 9 | 121920390 | | AA | BB | BB | AA | AA | AA | 1 | 1 |
| 769 | rs6304156 | 9 | 123162408 | | AA | AA | AA | BB | BB | BB | 1 | 1 |
| 770 | rs3721803 | 10 | 3343120 | | AA | AA | AA | BB | BB | BB | 1 | 1 |
| 771 | CEL-10_3989939 | 10 | 3989939 | | AA | AA | BB | AA | AA | AA | 1 | 1 |
| 772 | rs13480473 | 10 | 4778214 | | BB | BB | AA | AA | AA | AA | 1 | 1 |
| 773 | rs6185923 | 10 | 5384467 | | AA | AA | AA | BB | BB | BB | 1 | 1 |
| 774 | rs3664101 | 10 | 9286770 | | BB | BB | BB | AA | AA | AA | 1 | 1 |
| 775 | rs3685588 | 10 | 10540887 | | BB | BB | BB | AA | AA | AA | 1 | 1 |
| 776 | rs4228112 | 10 | 12719980 | | AA | BB | BB | BB | BB | BB | 1 | 1 |
| 777 | rs3686911 | 10 | 14116427 | | AA | BB | BB | AA | AA | AA | 1 | 1 |
| 778 | rs3699409 | 10 | 15499377 | | AA | AA | AA | BB | BB | BB | 1 | 1 |
| 779 | rs3712394 | 10 | 17639020 | | BB | BB | BB | AA | AA | AA | 1 | 1 |
| 780 | rs13480527 | 10 | 19318252 | | BB | AA | AA | BB | BB | BB | 1 | 1 |
| 781 | rs13459119 | 10 | 20027450 | | BB | BB | BB | AA | AA | AA | 1 | 1 |
| 782 | rs3679120 | 10 | 22685808 | | BB | AA | BB | AA | AA | AA | 1 | 1 |
| 783 | rs13480547 | 10 | 24247475 | | BB | BB | BB | AA | AA | AA | 1 | 1 |
| 784 | rs13480554 | 10 | 25713665 | | AA | AA | AA | BB | BB | BB | 1 | 1 |
| 785 | rs13480563 | 10 | 27924915 | | AA | AA | AA | AA | AA | AA | 1 | 1 |
| 786 | gnf10.026.889 | 10 | 28746498 | | AA | BB | BB | AA | AA | AA | 1 | 1 |
| 787 | rs13480569 | 10 | 30500013 | | BB | AA | BB | BB | BB | BB | 1 | 1 |
| 788 | rs13480570 | 10 | 30794652 | | AA | BB | AA | AA | AA | AA | 1 | 1 |
| 789 | rs13480578 | 10 | 34410603 | | AA | AA | AA | BB | BB | BB | 1 | 1 |
| 790 | rs13480579 | 10 | 36058713 | | BB | BB | BB | AA | AA | AA | 1 | 1 |
| 791 | rs13480581 | 10 | 38833025 | | AA | BB | BB | BB | BB | BB | 1 | 1 |
| 792 | rs3716113 | 10 | 42609040 | | BB | AA | AA | AA | AA | AA | 1 | 1 |
| 793 | rs13480601 | 10 | 44227379 | | AA | AA | AA | BB | BB | BB | 1 | 1 |
| 794 | CEL-10_46671493 | 10 | 46671493 | | AA | BB | BB | AA | AA | AA | 1 | 1 |
| 795 | rs3676667 | 10 | 46923056 | | BB | AA | AA | BB | BB | BB | 1 | 1 |
| 796 | rs6382436 | 10 | 48683209 | | BB | BB | AA | AA | AA | AA | 1 | 1 |
| 797 | gnf10.048.819 | 10 | 50989663 | | AA | AA | AA | AA | AA | AA | 1 | 1 |
| 798 | rs3696307 | 10 | 53783742 | | BB | BB | BB | AA | AA | AA | 1 | 1 |
| 799 | rs6190748 | 10 | 55832573 | | AA | AA | AA | AA | AA | AA | 1 | 1 |
| 800 | rs13480619 | 10 | 57805922 | X | BB | BB | BB | AA | AA | AA | 1 | 1 |
| 801 | CEL-10_58149652 | 10 | 58149652 | X | AA | AA | AA | BB | BB | BB | 1 | 1 |
| 802 | rs6374078 | 10 | 60860895 | | BB | BB | BB | BB | BB | BB | 1 | 1 |
| 803 | rs6359581 | 10 | 64294902 | | AA | AA | AA | AA | AA | AA | 1 | 1 |
| 804 | rs3723140 | 10 | 66179274 | | AA | BB | AA | BB | BB | BB | 1 | 1 |
| 805 | rs13480630 | 10 | 67595648 | | BB | BB | BB | BB | BB | BB | 1 | 1 |
| 806 | rs13480638 | 10 | 69220086 | | BB | AA | BB | AA | AA | AA | 1 | 1 |
| 807 | CEL-10_71736974 | 10 | 71736974 | | AA | AA | AA | BB | BB | BB | 1 | 1 |
| 808 | rs13480652 | 10 | 74437771 | | AA | AA | AA | BB | BB | BB | 1 | 1 |
| 809 | rs13480657 | 10 | 76584143 | | BB | BB | BB | AA | AA | AA | 1 | 1 |
| 810 | rs13480664 | 10 | 80556929 | | BB | AA | BB | BB | BB | BB | 1 | 1 |
| 811 | rs3717445 | 10 | 82649121 | | BB | BB | BB | AA | AA | AA | 1 | 1 |
| 812 | rs13480678 | 10 | 84352470 | | BB | AA | AA | BB | BB | BB | 1 | 1 |
| 813 | rs3679902 | 10 | 85007769 | | BB | AA | AA | BB | BB | BB | 1 | 1 |
| 814 | rs13480684 | 10 | 85606566 | | AA | AA | AA | AA | AA | AA | 1 | 1 |
| 815 | CEL-10_86322095 | 10 | 86322095 | | BB | AA | AA | BB | BB | BB | 1 | 1 |
| 816 | rs3089366 | 10 | 89439033 | | BB | AA | BB | BB | BB | BB | 1 | 1 |
| 817 | rs13480702 | 10 | 90830897 | | BB | AA | AA | BB | BB | BB | 1 | 1 |
| 818 | gnf10.091.965 | 10 | 92745604 | | AA | BB | BB | AA | AA | AA | 1 | 1 |
| 819 | rs13480712 | 10 | 93288075 | | AA | AA | AA | BB | BB | BB | 1 | 1 |
| 820 | rs13480716 | 10 | 94290709 | | BB | BB | BB | AA | AA | AA | 1 | 1 |
| 821 | rs13480722 | 10 | 97430180 | | BB | BB | BB | AA | AA | AA | 1 | 1 |
| 822 | rs6175332 | 10 | 98639384 | | AA | AA | AA | AA | AA | AA | 1 | 1 |
| 823 | rs3683912 | 10 | 99061427 | | BB | BB | AA | BB | BB | BB | 1 | 1 |
| 824 | rs3710293 | 10 | 99892920 | | AA | AA | BB | AA | AA | AA | 1 | 1 |
| 825 | rs13480734 | 10 | 102081906 | | BB | BB | BB | AA | AA | AA | 1 | 1 |
| 826 | rs13480740 | 10 | 103764301 | | BB | AA | BB | BB | BB | BB | 1 | 1 |
| 827 | rs3688351 | 10 | 104194765 | | AA | BB | AA | BB | BB | BB | 1 | 1 |
| 828 | rs13480749 | 10 | 105674831 | | BB | BB | BB | AA | AA | AA | 1 | 1 |

| | | | | | | | | | | | | |
|---|---|---|---|---|---|---|---|---|---|---|---|---|
| 829 | rs6290359 | 10 | 107672808 | | BB | BB | BB | AA | AA | AA | 1 | 1 |
| 830 | rs6243755 | 10 | 108416966 | | BB | BB | BB | AA | AA | AA | 1 | 1 |
| 831 | rs13480759 | 10 | 109059096 | X | AA | AA | AA | BB | BB | BB | 1 | 1 |
| 832 | rs3680872 | 10 | 114181187 | | AA | BB | AA | BB | BB | BB | 1 | 1 |
| 833 | rs13480773 | 10 | 114518973 | | AA | AA | BB | BB | BB | BB | 1 | 1 |
| 834 | rs13480775 | 10 | 115590088 | | AA | BB | AA | AA | AA | AA | 1 | 1 |
| 835 | rs6256918 | 10 | 117348939 | | AA | BB | AA | BB | BB | BB | 1 | 1 |
| 836 | mCV24217147 | 10 | 117613736 | | AA | BB | BB | AA | AA | AA | 1 | 1 |
| 837 | CEL-10_119602638 | 10 | 119602638 | | AA | BB | AA | AA | AA | AA | 1 | 1 |
| 838 | rs13480803 | 10 | 122911418 | | AA | BB | BB | AA | AA | AA | 1 | 1 |
| 839 | mCV22832306 | 10 | 126086653 | | BB | AA | AA | BB | BB | BB | 1 | 1 |
| 840 | rs3697243 | 10 | 126634957 | | BB | AA | BB | AA | AA | AA | 1 | 1 |
| 841 | rs3676330 | 10 | 128337313 | | AA | AA | AA | BB | BB | BB | 1 | 1 |
| 842 | rs13480836 | 11 | 3448985 | | AA | BB | BB | BB | BB | BB | 1 | 1 |
| 843 | rs13480837 | 11 | 3781731 | | BB | BB | AA | AA | AA | AA | 1 | 1 |
| 844 | rs3682937 | 11 | 4575120 | | BB | AA | BB | BB | BB | BB | 1 | 1 |
| 845 | rs6190775 | 11 | 6306994 | | AA | BB | BB | AA | AA | AA | 1 | 1 |
| 846 | rs13480854 | 11 | 7518795 | | BB | BB | AA | AA | AA | AA | 1 | 1 |
| 847 | rs13480863 | 11 | 9188410 | | AA | AA | AA | BB | BB | BB | 1 | 1 |
| 848 | rs3023249 | 11 | 11065936 | | BB | BB | BB | AA | AA | AA | 1 | 1 |
| 849 | rs13480875 | 11 | 12190600 | | BB | AA | AA | AA | AA | AA | 1 | 1 |
| 850 | CEL-11_14992925 | 11 | 14992925 | | AA | BB | AA | AA | AA | AA | 1 | 1 |
| 851 | rs6313050 | 11 | 15647995 | | AA | BB | AA | AA | AA | AA | 1 | 1 |
| 852 | gnf11.017.294 | 11 | 18007841 | | BB | AA | BB | AA | AA | AA | 1 | 1 |
| 853 | rs3723987 | 11 | 19364495 | | BB | BB | BB | AA | AA | AA | 1 | 1 |
| 854 | rs3023251 | 11 | 20848871 | | BB | BB | BB | AA | AA | AA | 1 | 1 |
| 855 | rs13480910 | 11 | 22709634 | | BB | BB | AA | BB | BB | BB | 1 | 1 |
| 856 | rs3723990 | 11 | 26517914 | | BB | BB | AA | AA | AA | AA | 1 | 1 |
| 857 | rs3706694 | 11 | 28310427 | | AA | AA | BB | AA | AA | AA | 1 | 1 |
| 858 | rs3700830 | 11 | 30266839 | | BB | AA | BB | BB | BB | BB | 1 | 1 |
| 859 | rs13459123 | 11 | 30954469 | | AA | AA | AA | AA | AA | AA | 1 | 1 |
| 860 | rs3723833 | 11 | 32946888 | | AA | AA | BB | AA | AA | AA | 1 | 1 |
| 861 | rs6239937 | 11 | 34700816 | | AA | BB | AA | AA | AA | AA | 1 | 1 |
| 862 | rs13480968 | 11 | 36134794 | | AA | BB | BB | AA | AA | AA | 1 | 1 |
| 863 | rs6359329 | 11 | 38177953 | | AA | AA | AA | AA | AA | AA | 1 | 1 |
| 864 | rs6164170 | 11 | 39929979 | | BB | BB | BB | AA | AA | AA | 1 | 1 |
| 865 | rs3701734 | 11 | 40967464 | | BB | BB | BB | AA | AA | AA | 1 | 1 |
| 866 | rs3654344 | 11 | 43847855 | | BB | BB | BB | AA | AA | AA | 1 | 1 |
| 867 | rs13481009 | 11 | 46168151 | | AA | AA | AA | BB | BB | BB | 1 | 1 |
| 868 | rs13481011 | 11 | 46568199 | | AA | AA | AA | BB | BB | BB | 1 | 1 |
| 869 | rs13481014 | 11 | 47757117 | X | BB | BB | BB | AA | AA | AA | 1 | 1 |
| 870 | rs6199956 | 11 | 50385006 | | AA | AA | AA | AA | AA | AA | 1 | 1 |
| 871 | rs13481033 | 11 | 54538623 | | BB | AA | BB | AA | AA | AA | 1 | 1 |
| 872 | rs4228731 | 11 | 55034293 | | BB | AA | BB | AA | AA | AA | 1 | 1 |
| 873 | rs3684076 | 11 | 56050650 | | AA | BB | AA | BB | BB | BB | 1 | 1 |
| 874 | rs3697686 | 11 | 58180077 | | AA | AA | AA | BB | BB | BB | 1 | 1 |
| 875 | rs3711357 | 11 | 61065104 | | BB | AA | AA | AA | AA | AA | 1 | 1 |
| 876 | rs13481061 | 11 | 62605165 | | AA | BB | AA | BB | BB | BB | 1 | 1 |
| 877 | rs13481071 | 11 | 64813366 | | BB | BB | AA | AA | AA | AA | 1 | 1 |
| 878 | rs13481076 | 11 | 66331400 | | BB | BB | AA | AA | AA | AA | 1 | 1 |
| 879 | rs13481084 | 11 | 68383073 | | AA | AA | AA | BB | BB | BB | 1 | 1 |
| 880 | rs6197743 | 11 | 69789936 | | BB | BB | BB | BB | BB | BB | 1 | 1 |
| 881 | mCV24113391 | 11 | 71092401 | | BB | BB | BB | BB | BB | BB | 1 | 1 |
| 882 | rs13481094 | 11 | 72446973 | | AA | BB | BB | BB | BB | BB | 1 | 1 |
| 883 | rs3701609 | 11 | 72876179 | | BB | BB | BB | AA | AA | AA | 1 | 1 |
| 884 | rs13481109 | 11 | 76207708 | | AA | AA | AA | BB | BB | BB | 1 | 1 |
| 885 | rs13481119 | 11 | 79159755 | | AA | BB | AA | BB | BB | BB | 1 | 1 |
| 886 | rs6259742 | 11 | 82221268 | | AA | AA | AA | AA | AA | AA | 1 | 1 |
| 887 | rs13481127 | 11 | 83014191 | | BB | AA | BB | AA | AA | AA | 1 | 1 |
| 888 | rs3661657 | 11 | 84334033 | | BB | AA | BB | AA | AA | AA | 1 | 1 |
| 889 | rs3719581 | 11 | 86560546 | | AA | BB | AA | BB | BB | BB | 1 | 1 |
| 890 | rs13481145 | 11 | 88037356 | | AA | BB | AA | BB | BB | BB | 1 | 1 |
| 891 | rs3688955 | 11 | 90207658 | | BB | AA | BB | AA | AA | AA | 1 | 1 |
| 892 | rs13481161 | 11 | 92132381 | | BB | BB | BB | BB | BB | BB | 1 | 1 |
| 893 | rs3714299 | 11 | 92734680 | | BB | BB | AA | AA | AA | AA | 1 | 1 |
| 894 | rs13481170 | 11 | 95299225 | | AA | BB | BB | AA | AA | AA | 1 | 1 |
| 895 | rs13481173 | 11 | 96275988 | | BB | BB | BB | AA | AA | AA | 1 | 1 |
| 896 | rs3661058 | 11 | 98590564 | | BB | AA | BB | AA | AA | AA | 1 | 1 |
| 897 | rs3090212 | 11 | 99721952 | | AA | BB | AA | AA | AA | AA | 1 | 1 |
| 898 | rs6393948 | 11 | 103272243 | | AA | BB | AA | AA | AA | AA | 1 | 1 |
| 899 | rs3698446 | 11 | 104908478 | | AA | AA | BB | AA | AA | AA | 1 | 1 |
| 900 | rs6386362 | 11 | 106649550 | | BB | BB | BB | AA | AA | AA | 1 | 1 |
| 901 | rs6370458 | 11 | 109065922 | | AA | BB | AA | BB | BB | BB | 1 | 1 |
| 902 | rs13481227 | 11 | 110120256 | | AA | BB | BB | BB | BB | BB | 1 | 1 |
| 903 | rs3672597 | 11 | 111905327 | | BB | AA | BB | AA | AA | AA | 1 | 1 |
| 904 | rs3699056 | 11 | 113674817 | | BB | BB | BB | AA | AA | AA | 1 | 1 |
| 905 | rs13481247 | 11 | 115572156 | | BB | BB | AA | AA | AA | AA | 1 | 1 |
| 906 | rs3712881 | 11 | 120738678 | | BB | AA | BB | BB | BB | BB | 1 | 1 |
| 907 | rs3713137 | 12 | 4720216 | | BB | BB | AA | BB | BB | BB | 1 | 1 |
| 908 | rs3653990 | 12 | 5131626 | | BB | BB | AA | BB | BB | BB | 1 | 1 |
| 909 | rs13481281 | 12 | 5648778 | | AA | BB | AA | AA | AA | AA | 1 | 1 |
| 910 | rs3678128 | 12 | 7371530 | | BB | AA | AA | BB | BB | BB | 1 | 1 |
| 911 | rs6292954 | 12 | 10028881 | | BB | AA | AA | AA | AA | AA | 1 | 1 |
| 912 | rs13481297 | 12 | 10691032 | | AA | NC | NC | AA | AA | AA | 1 | 1 |
| 913 | rs13481303 | 12 | 12036755 | | BB | AA | BB | AA | AA | AA | 1 | 1 |
| 914 | rs3655057 | 12 | 13507742 | | AA | AA | BB | BB | BB | BB | 1 | 1 |
| 915 | rs13481313 | 12 | 14987941 | | BB | AA | BB | BB | BB | BB | 1 | 1 |
| 916 | rs3706330 | 12 | 16713381 | | BB | BB | AA | AA | AA | AA | 1 | 1 |
| 917 | rs13481321 | 12 | 16811399 | | AA | AA | AA | BB | BB | BB | 1 | 1 |
| 918 | rs13481324 | 12 | 17701648 | | AA | BB | BB | BB | BB | BB | 1 | 1 |
| 919 | rs3717860 | 12 | 19689285 | | AA | AA | AA | BB | BB | BB | 1 | 1 |
| 920 | rs6328018 | 12 | 21090189 | | AA | BB | AA | AA | AA | AA | 1 | 1 |
| 921 | rs13481363 | 12 | 22949944 | | AA | BB | AA | BB | BB | BB | 1 | 1 |
| 922 | rs3089800 | 12 | 23976362 | | AA | BB | BB | AA | AA | AA | 1 | 1 |

| | | | | | | | | | | | | |
|---|---|---|---|---|---|---|---|---|---|---|---|---|
| 923 | UT_12_24.561109 | 12 | 24901541 | | AA | AA | AA | BB | BB | BB | 1 | 1 |
| 924 | rs13481371 | 12 | 25180902 | | BB | AA | AA | BB | BB | BB | 1 | 1 |
| 925 | rs6223000 | 12 | 29204179 | | BB | AA | AA | BB | BB | BB | 1 | 1 |
| 926 | rs13481392 | 12 | 30659819 | | AA | BB | BB | BB | BB | BB | 1 | 1 |
| 927 | rs6311081 | 12 | 32032739 | | AA | BB | BB | AA | AA | AA | 1 | 1 |
| 928 | rs3658100 | 12 | 33110635 | | AA | BB | BB | AA | AA | AA | 1 | 1 |
| 929 | rs13481406 | 12 | 34954150 | | AA | AA | AA | AA | AA | AA | 1 | 1 |
| 930 | rs13481408 | 12 | 35475720 | | BB | AA | AA | AA | AA | AA | 1 | 1 |
| 931 | CEL-12_38788391 | 12 | 38788391 | | AA | BB | BB | AA | AA | AA | 1 | 1 |
| 932 | rs3726096 | 12 | 39432172 | | BB | AA | AA | BB | BB | BB | 1 | 1 |
| 933 | CEL-12_40646532 | 12 | 40646532 | | AA | BB | BB | BB | BB | BB | 1 | 1 |
| 934 | gnf12.046.238 | 12 | 43135664 | | BB | AA | AA | BB | BB | BB | 1 | 1 |
| 935 | rs13481445 | 12 | 45537591 | | BB | BB | BB | AA | AA | AA | 1 | 1 |
| 936 | rs13481454 | 12 | 47738222 | | BB | BB | BB | AA | AA | AA | 1 | 1 |
| 937 | rs3670749 | 12 | 48181013 | | AA | AA | AA | BB | BB | BB | 1 | 1 |
| 938 | rs3700857 | 12 | 49142988 | | AA | AA | AA | BB | BB | BB | 1 | 1 |
| 939 | rs13481466 | 12 | 51192106 | | AA | BB | BB | AA | AA | AA | 1 | 1 |
| 940 | rs3706319 | 12 | 53150903 | | AA | AA | AA | BB | BB | BB | 1 | 1 |
| 941 | mCV22351241 | 12 | 54143643 | | AA | BB | BB | BB | BB | BB | 1 | 1 |
| 942 | gnf12.061.363 | 12 | 58421210 | | BB | AA | AA | BB | BB | BB | 1 | 1 |
| 943 | rs3677344 | 12 | 59848542 | | BB | BB | BB | AA | AA | AA | 1 | 1 |
| 944 | rs6344105 | 12 | 63022076 | | AA | AA | AA | AA | AA | AA | 1 | 1 |
| 945 | rs13481514 | 12 | 64869269 | | AA | AA | AA | BB | BB | BB | 1 | 1 |
| 946 | rs13481521 | 12 | 66729742 | | BB | BB | BB | AA | AA | AA | 1 | 1 |
| 947 | rs13481527 | 12 | 68166409 | | AA | AA | AA | BB | BB | BB | 1 | 1 |
| 948 | rs3655558 | 12 | 70010856 | | BB | AA | BB | AA | AA | AA | 1 | 1 |
| 949 | rs13481541 | 12 | 71665916 | | BB | AA | AA | AA | AA | AA | 1 | 1 |
| 950 | gnf12.077.067 | 12 | 73900965 | | AA | AA | BB | BB | BB | BB | 1 | 1 |
| 951 | rs3662628 | 12 | 74558132 | | AA | AA | BB | BB | BB | BB | 1 | 1 |
| 952 | rs13481556 | 12 | 75962840 | | AA | AA | AA | BB | BB | BB | 1 | 1 |
| 953 | rs13481561 | 12 | 77468587 | | AA | AA | BB | AA | AA | AA | 1 | 1 |
| 954 | rs13481565 | 12 | 79092079 | | BB | BB | BB | AA | AA | AA | 1 | 1 |
| 955 | rs3716095 | 12 | 82379744 | | BB | AA | BB | AA | AA | AA | 1 | 1 |
| 956 | CEL-12_84750094 | 12 | 84750094 | | BB | AA | BB | AA | AA | AA | 1 | 1 |
| 957 | rs3670410 | 12 | 85932990 | | BB | AA | BB | AA | AA | AA | 1 | 1 |
| 958 | rs13481588 | 12 | 86574038 | | AA | BB | AA | BB | BB | BB | 1 | 1 |
| 959 | rs6207869 | 12 | 88966851 | | AA | AA | BB | AA | AA | AA | 1 | 1 |
| 960 | rs13481599 | 12 | 90714740 | | AA | AA | BB | AA | AA | AA | 1 | 1 |
| 961 | rs13481604 | 12 | 92693591 | | BB | AA | BB | AA | AA | AA | 1 | 1 |
| 962 | rs3716084 | 12 | 94501426 | | BB | AA | AA | AA | AA | AA | 1 | 1 |
| 963 | rs13481614 | 12 | 95793494 | | AA | AA | BB | BB | BB | BB | 1 | 1 |
| 964 | rs13481618 | 12 | 97207111 | | AA | AA | BB | AA | AA | AA | 1 | 1 |
| 965 | rs8273308 | 12 | 99106508 | | BB | AA | BB | BB | BB | BB | 1 | 1 |
| 966 | rs13481632 | 12 | 101121028 | | AA | BB | AA | AA | AA | AA | 1 | 1 |
| 967 | rs6390948 | 12 | 103432150 | | AA | AA | BB | AA | AA | AA | 1 | 1 |
| 968 | CEL-12_104545022 | 12 | 104545022 | | AA | AA | BB | AA | AA | AA | 1 | 1 |
| 969 | rs13481655 | 12 | 106863515 | | BB | BB | AA | BB | BB | BB | 1 | 1 |
| 970 | CEL-12_108727612 | 12 | 108727612 | | AA | AA | BB | BB | BB | BB | 1 | 1 |
| 971 | rs3023711 | 12 | 111163171 | | AA | AA | AA | BB | BB | BB | 1 | 1 |
| 972 | rs3692361 | 12 | 112704261 | | BB | BB | BB | AA | AA | AA | 1 | 1 |
| 973 | rs6329833 | 12 | 114227574 | | BB | AA | BB | AA | AA | AA | 1 | 1 |
| 974 | rs6215262 | 13 | 3556871 | | AA | AA | BB | BB | BB | BB | 1 | 1 |
| 975 | rs13481668 | 13 | 4242635 | | AA | AA | BB | BB | BB | BB | 1 | 1 |
| 976 | rs13481673 | 13 | 5374001 | | AA | AA | BB | BB | BB | BB | 1 | 1 |
| 977 | rs6301008 | 13 | 7490090 | | BB | BB | BB | BB | BB | BB | 1 | 1 |
| 978 | rs13481683 | 13 | 9267297 | | AA | BB | BB | BB | BB | BB | 1 | 1 |
| 979 | rs13481689 | 13 | 10721776 | | BB | AA | AA | AA | AA | AA | 1 | 1 |
| 980 | rs13481697 | 13 | 12961456 | | AA | BB | BB | BB | BB | BB | 1 | 1 |
| 981 | rs6348604 | 13 | 14769173 | | AA | BB | BB | BB | BB | BB | 1 | 1 |
| 982 | rs13481706 | 13 | 15697964 | | BB | AA | AA | BB | BB | BB | 1 | 1 |
| 983 | rs13481715 | 13 | 18523821 | | BB | BB | AA | AA | AA | AA | 1 | 1 |
| 984 | rs6314295 | 13 | 19481485 | | AA | BB | AA | AA | AA | AA | 1 | 1 |
| 985 | rs3679784 | 13 | 20286264 | | BB | AA | AA | BB | BB | BB | 1 | 1 |
| 986 | rs3663223 | 13 | 22465317 | | BB | BB | BB | AA | AA | AA | 1 | 1 |
| 987 | rs8267104 | 13 | 23085429 | | BB | BB | BB | BB | BB | BB | 1 | 1 |
| 988 | rs6275055 | 13 | 25304682 | | AA | AA | AA | AA | AA | AA | 1 | 1 |
| 989 | rs13481734 | 13 | 26416832 | X | BB | BB | BB | AA | AA | AA | 1 | 1 |
| 990 | CEL-13_27061395 | 13 | 27061395 | | BB | AA | AA | BB | BB | BB | 1 | 1 |
| 991 | rs13481740 | 13 | 30057195 | | BB | AA | AA | BB | BB | BB | 1 | 1 |
| 992 | rs3710348 | 13 | 30653000 | | BB | BB | BB | AA | AA | AA | 1 | 1 |
| 993 | rs3707097 | 13 | 33614779 | | BB | AA | AA | BB | BB | BB | 1 | 1 |
| 994 | rs3725187 | 13 | 34496200 | | BB | AA | AA | BB | BB | BB | 1 | 1 |
| 995 | rs13481764 | 13 | 35994885 | | AA | BB | BB | AA | AA | AA | 1 | 1 |
| 996 | gnf13.035.637 | 13 | 36959616 | | AA | AA | AA | BB | BB | BB | 1 | 1 |
| 997 | gnf13.038.133 | 13 | 39478973 | | AA | BB | BB | BB | BB | BB | 1 | 1 |
| 998 | rs13481783 | 13 | 42287337 | | AA | BB | AA | BB | BB | BB | 1 | 1 |
| 999 | rs3712907 | 13 | 42620079 | | BB | BB | BB | AA | AA | AA | 1 | 1 |
| 1000 | rs3688207 | 13 | 44823434 | | AA | BB | BB | AA | AA | AA | 1 | 1 |
| 1001 | rs6411274 | 13 | 46624183 | | AA | AA | AA | BB | BB | BB | 1 | 1 |
| 1002 | rs6244558 | 13 | 47310947 | | BB | BB | BB | AA | AA | AA | 1 | 1 |
| 1003 | rs13481809 | 13 | 50702277 | | AA | BB | BB | BB | BB | BB | 1 | 1 |
| 1004 | rs3693942 | 13 | 54042656 | | AA | AA | AA | BB | BB | BB | 1 | 1 |
| 1005 | rs3720782 | 13 | 55330594 | | AA | AA | AA | BB | BB | BB | 1 | 1 |
| 1006 | rs3700819 | 13 | 56358945 | | BB | BB | BB | AA | AA | AA | 1 | 1 |
| 1007 | gnf13.056.787 | 13 | 57848844 | | AA | BB | AA | AA | AA | AA | 1 | 1 |
| 1008 | rs3690198 | 13 | 59860578 | | BB | BB | AA | AA | AA | AA | 1 | 1 |
| 1009 | rs4229817 | 13 | 63888326 | | BB | AA | AA | BB | BB | BB | 1 | 1 |
| 1010 | rs3718727 | 13 | 65760534 | | AA | BB | AA | BB | BB | BB | 1 | 1 |
| 1011 | rs13481871 | 13 | 67736821 | | BB | BB | BB | AA | AA | AA | 1 | 1 |
| 1012 | rs13481880 | 13 | 70810674 | | BB | BB | BB | AA | AA | AA | 1 | 1 |
| 1013 | rs13481883 | 13 | 71955117 | | BB | BB | BB | AA | AA | AA | 1 | 1 |
| 1014 | rs13481893 | 13 | 74156236 | | AA | BB | AA | BB | BB | BB | 1 | 1 |
| 1015 | gnf13.079.671 | 13 | 77019901 | | BB | AA | BB | AA | AA | AA | 1 | 1 |
| 1016 | rs13481908 | 13 | 78683446 | | AA | BB | AA | BB | BB | BB | 1 | 1 |

| | | | | | | | | | | | | |
|---|---|---|---|---|---|---|---|---|---|---|---|---|
| 1017 | mCV24625340 | 13 | 81332738 | | BB | AA | BB | BB | BB | BB | 1 | 1 |
| 1018 | rs3686443 | 13 | 83174585 | | AA | AA | AA | BB | BB | BB | 1 | 1 |
| 1019 | gnf13.088.732 | 13 | 84796434 | | BB | AA | AA | BB | BB | BB | 1 | 1 |
| 1020 | rs3655061 | 13 | 86241392 | | AA | AA | BB | BB | BB | BB | 1 | 1 |
| 1021 | rs6288319 | 13 | 87807463 | | AA | AA | BB | AA | AA | AA | 1 | 1 |
| 1022 | rs6316213 | 13 | 88817196 | | AA | BB | BB | BB | BB | BB | 1 | 1 |
| 1023 | gnf13.093.328 | 13 | 89447298 | | AA | AA | AA | BB | BB | BB | 1 | 1 |
| 1024 | rs13481961 | 13 | 94000606 | | AA | BB | AA | BB | BB | BB | 1 | 1 |
| 1025 | rs13481968 | 13 | 95596507 | | BB | AA | AA | BB | BB | BB | 1 | 1 |
| 1026 | rs4230027 | 13 | 97200857 | | BB | AA | AA | AA | AA | AA | 1 | 1 |
| 1027 | rs13481983 | 13 | 100181409 | | BB | BB | BB | AA | AA | AA | 1 | 1 |
| 1028 | rs6389588 | 13 | 100595006 | | BB | BB | BB | BB | BB | BB | 1 | 1 |
| 1029 | rs13481992 | 13 | 102442609 | | AA | AA | AA | AA | AA | AA | 1 | 1 |
| 1030 | rs13481996 | 13 | 103563881 | | AA | AA | AA | BB | BB | BB | 1 | 1 |
| 1031 | rs13482005 | 13 | 105593959 | | BB | AA | AA | BB | BB | BB | 1 | 1 |
| 1032 | rs13482011 | 13 | 107432985 | | BB | AA | AA | AA | AA | AA | 1 | 1 |
| 1033 | rs13482019 | 13 | 109707882 | | BB | BB | BB | AA | AA | AA | 1 | 1 |
| 1034 | gnf13.115.241 | 13 | 110861665 | | AA | AA | AA | AA | AA | AA | 1 | 1 |
| 1035 | rs6247696 | 13 | 112118515 | | AA | AA | AA | AA | AA | AA | 1 | 1 |
| 1036 | rs13482028 | 13 | 113209165 | | BB | BB | BB | AA | AA | AA | 1 | 1 |
| 1037 | rs13482035 | 13 | 115056838 | | BB | AA | BB | BB | BB | BB | 1 | 1 |
| 1038 | rs4230144 | 14 | 3890426 | | AA | AA | BB | AA | AA | AA | 1 | 1 |
| 1039 | rs6322899 | 14 | 5945767 | | BB | AA | BB | AA | AA | AA | 1 | 1 |
| 1040 | rs3150398 | 14 | 7401248 | | AA | BB | AA | BB | BB | BB | 1 | 1 |
| 1041 | rs13482084 | 14 | 8848582 | | AA | BB | AA | BB | BB | BB | 1 | 1 |
| 1042 | rs6290836 | 14 | 9149500 | | BB | BB | BB | AA | AA | AA | 1 | 1 |
| 1043 | rs3719629 | 14 | 12874743 | | AA | AA | AA | BB | BB | BB | 1 | 1 |
| 1044 | rs3696385 | 14 | 14028895 | | BB | AA | BB | AA | AA | AA | 1 | 1 |
| 1045 | rs3687889 | 14 | 15973497 | | BB | AA | AA | AA | AA | AA | 1 | 1 |
| 1046 | rs13482096 | 14 | 19006267 | | AA | BB | AA | BB | BB | BB | 1 | 1 |
| 1047 | rs3692121 | 14 | 20092583 | | BB | AA | AA | AA | AA | AA | 1 | 1 |
| 1048 | rs13482104 | 14 | 22364262 | | BB | BB | BB | AA | AA | AA | 1 | 1 |
| 1049 | rs6396829 | 14 | 24042337 | | BB | AA | AA | BB | BB | BB | 1 | 1 |
| 1050 | rs4230248 | 14 | 27218513 | | BB | AA | AA | AA | AA | AA | 1 | 1 |
| 1051 | rs13482124 | 14 | 27701835 | | BB | AA | AA | AA | AA | AA | 1 | 1 |
| 1052 | rs6313230 | 14 | 28306368 | | BB | AA | AA | AA | AA | AA | 1 | 1 |
| 1053 | rs3695383 | 14 | 29838823 | | AA | BB | BB | BB | BB | BB | 1 | 1 |
| 1054 | rs13482135 | 14 | 31429298 | | BB | AA | AA | AA | AA | AA | 1 | 1 |
| 1055 | rs3701775 | 14 | 33391532 | | AA | BB | BB | BB | BB | BB | 1 | 1 |
| 1056 | rs13482143 | 14 | 35609633 | | BB | BB | BB | BB | BB | BB | 1 | 1 |
| 1057 | rs13482148 | 14 | 37242020 | | BB | BB | BB | BB | BB | BB | 1 | 1 |
| 1058 | rs13482159 | 14 | 38359897 | | AA | AA | AA | BB | BB | BB | 1 | 1 |
| 1059 | rs13482170 | 14 | 41201261 | | BB | BB | BB | AA | AA | AA | 1 | 1 |
| 1060 | mCV24777660 | 14 | 42906842 | | AA | AA | AA | BB | BB | BB | 1 | 1 |
| 1061 | rs3666583 | 14 | 44880408 | | AA | AA | AA | BB | BB | BB | 1 | 1 |
| 1062 | rs13482191 | 14 | 46619173 | | AA | AA | AA | BB | BB | BB | 1 | 1 |
| 1063 | rs13482193 | 14 | 47596815 | | BB | BB | BB | BB | BB | BB | 1 | 1 |
| 1064 | rs13482194 | 14 | 47801247 | | AA | AA | AA | AA | AA | AA | 1 | 1 |
| 1065 | rs3692863 | 14 | 50807707 | | AA | BB | BB | AA | AA | AA | 1 | 1 |
| 1066 | gnf14.055.608 | 14 | 52829293 | | AA | BB | BB | AA | AA | AA | 1 | 1 |
| 1067 | rs13482216 | 14 | 53885592 | | BB | AA | BB | BB | BB | BB | 1 | 1 |
| 1068 | rs3703075 | 14 | 54913181 | | AA | BB | AA | BB | BB | BB | 1 | 1 |
| 1069 | rs13482231 | 14 | 58969551 | | AA | BB | AA | BB | BB | BB | 1 | 1 |
| 1070 | rs3672425 | 14 | 60335045 | | AA | BB | AA | AA | AA | AA | 1 | 1 |
| 1071 | rs13482239 | 14 | 61543475 | | AA | BB | BB | BB | BB | BB | 1 | 1 |
| 1072 | rs13482247 | 14 | 63674408 | | BB | BB | AA | AA | AA | AA | 1 | 1 |
| 1073 | rs6156908 | 14 | 66473686 | | BB | AA | BB | AA | AA | AA | 1 | 1 |
| 1074 | rs13459144 | 14 | 67681669 | | AA | BB | BB | BB | BB | BB | 1 | 1 |
| 1075 | rs13482265 | 14 | 70793464 | | AA | AA | AA | BB | BB | BB | 1 | 1 |
| 1076 | rs3023413 | 14 | 71540901 | | AA | AA | AA | AA | AA | AA | 1 | 1 |
| 1077 | CEL-14_73162771 | 14 | 73162771 | | BB | BB | BB | BB | BB | BB | 1 | 1 |
| 1078 | rs13482272 | 14 | 74092548 | | BB | BB | BB | BB | BB | BB | 1 | 1 |
| 1079 | rs6319148 | 14 | 75261976 | | BB | AA | AA | AA | AA | AA | 1 | 1 |
| 1080 | rs13482284 | 14 | 78061668 | | BB | AA | AA | BB | BB | BB | 1 | 1 |
| 1081 | rs3708535 | 14 | 78686463 | | BB | AA | AA | BB | BB | BB | 1 | 1 |
| 1082 | rs13482296 | 14 | 80784363 | | BB | AA | AA | BB | BB | BB | 1 | 1 |
| 1083 | rs6395984 | 14 | 82944063 | | BB | AA | AA | BB | BB | BB | 1 | 1 |
| 1084 | rs6291434 | 14 | 83887230 | | BB | AA | AA | BB | BB | BB | 1 | 1 |
| 1085 | rs13482311 | 14 | 85287050 | | AA | BB | BB | AA | AA | AA | 1 | 1 |
| 1086 | rs13482327 | 14 | 89372338 | | BB | AA | AA | BB | BB | BB | 1 | 1 |
| 1087 | rs3692362 | 14 | 92002849 | | AA | AA | AA | BB | BB | BB | 1 | 1 |
| 1088 | rs6191117 | 14 | 92434091 | | AA | BB | BB | BB | BB | BB | 1 | 1 |
| 1089 | CEL-14_94845626 | 14 | 94845626 | | BB | BB | BB | AA | AA | AA | 1 | 1 |
| 1090 | rs13482354 | 14 | 98188914 | | BB | AA | AA | AA | AA | AA | 1 | 1 |
| 1091 | rs3654132 | 14 | 98578208 | | AA | BB | BB | AA | AA | AA | 1 | 1 |
| 1092 | rs13482356 | 14 | 99047545 | | AA | AA | AA | BB | BB | BB | 1 | 1 |
| 1093 | gnf14.103.048 | 14 | 99774290 | | AA | BB | BB | BB | BB | BB | 1 | 1 |
| 1094 | rs3708779 | 14 | 103068000 | | BB | AA | AA | AA | AA | AA | 1 | 1 |
| 1095 | rs13482375 | 14 | 103981340 | | BB | AA | AA | AA | AA | AA | 1 | 1 |
| 1096 | rs3726052 | 14 | 104244696 | | AA | AA | BB | BB | BB | BB | 1 | 1 |
| 1097 | rs6256423 | 14 | 106108556 | | BB | BB | BB | BB | BB | BB | 1 | 1 |
| 1098 | rs6169105 | 14 | 109578622 | | BB | BB | BB | AA | AA | AA | 1 | 1 |
| 1099 | rs3665550 | 14 | 111354233 | | BB | BB | BB | AA | AA | AA | 1 | 1 |
| 1100 | rs13482398 | 14 | 112310948 | | BB | AA | AA | BB | BB | BB | 1 | 1 |
| 1101 | rs13482407 | 14 | 114388484 | | BB | BB | AA | AA | AA | AA | 1 | 1 |
| 1102 | CEL-14_116404928 | 14 | 116404928 | X | AA | AA | AA | BB | BB | BB | 1 | 1 |
| 1103 | rs13459176 | 15 | 3104758 | | AA | BB | BB | BB | BB | BB | 1 | 1 |
| 1104 | rs13482418 | 15 | 3498960 | | BB | AA | AA | AA | AA | AA | 1 | 1 |
| 1105 | CEL-15_4222769 | 15 | 4222769 | | AA | BB | BB | BB | BB | BB | 1 | 1 |
| 1106 | rs3665826 | 15 | 5744460 | | BB | BB | AA | BB | BB | BB | 1 | 1 |
| 1107 | CEL-15_8331158 | 15 | 8331158 | | BB | AA | BB | AA | AA | AA | 1 | 1 |
| 1108 | CEL-15_9687257 | 15 | 9687257 | | BB | AA | AA | AA | AA | AA | 1 | 1 |
| 1109 | rs13482431 | 15 | 11218285 | | BB | AA | AA | AA | AA | AA | 1 | 1 |
| 1110 | rs3711814 | 15 | 13122871 | | BB | BB | BB | AA | AA | AA | 1 | 1 |

| | | | | | | | | | | | | |
|---|---|---|---|---|---|---|---|---|---|---|---|---|
| 1111 | CEL-15_14786403 | 15 | 14786403 | | BB | AA | AA | AA | AA | AA | 1 | 1 |
| 1112 | CEL-15_15482356 | 15 | 15482356 | | AA | BB | BB | BB | BB | BB | 1 | 1 |
| 1113 | rs13482455 | 15 | 16643375 | | AA | BB | BB | BB | BB | BB | 1 | 1 |
| 1114 | rs3715857 | 15 | 19261351 | | BB | AA | AA | BB | BB | BB | 1 | 1 |
| 1115 | rs13482469 | 15 | 20978602 | | BB | BB | BB | AA | AA | AA | 1 | 1 |
| 1116 | rs13482477 | 15 | 22545113 | | AA | AA | BB | BB | BB | BB | 1 | 1 |
| 1117 | rs13482482 | 15 | 24640823 | | BB | AA | AA | AA | AA | AA | 1 | 1 |
| 1118 | rs13482485 | 15 | 25491892 | | AA | BB | AA | BB | BB | BB | 1 | 1 |
| 1119 | rs13482497 | 15 | 28363926 | | AA | AA | BB | AA | AA | AA | 1 | 1 |
| 1120 | rs13482501 | 15 | 29311563 | | BB | BB | AA | BB | BB | BB | 1 | 1 |
| 1121 | rs13482504 | 15 | 30361234 | | BB | AA | AA | AA | AA | AA | 1 | 1 |
| 1122 | rs13482509 | 15 | 32096277 | | BB | BB | BB | AA | AA | AA | 1 | 1 |
| 1123 | rs6188239 | 15 | 34383985 | | BB | BB | AA | AA | AA | AA | 1 | 1 |
| 1124 | CEL-15_36490596 | 15 | 36490596 | | BB | BB | BB | BB | BB | BB | 1 | 1 |
| 1125 | rs3695416 | 15 | 38562542 | | BB | AA | BB | AA | AA | AA | 1 | 1 |
| 1126 | rs13482529 | 15 | 39096937 | | BB | BB | BB | BB | BB | BB | 1 | 1 |
| 1127 | rs3683326 | 15 | 41359817 | | BB | BB | AA | BB | BB | BB | 1 | 1 |
| 1128 | CEL-15_43206205 | 15 | 43206205 | | BB | AA | BB | AA | AA | AA | 1 | 1 |
| 1129 | rs13482543 | 15 | 43892080 | | AA | BB | AA | BB | BB | BB | 1 | 1 |
| 1130 | rs13482549 | 15 | 45665306 | | AA | AA | BB | AA | AA | AA | 1 | 1 |
| 1131 | rs13482558 | 15 | 47188758 | | BB | BB | AA | AA | AA | AA | 1 | 1 |
| 1132 | rs13482571 | 15 | 50021404 | | AA | AA | AA | BB | BB | BB | 1 | 1 |
| 1133 | rs3658705 | 15 | 51403508 | | BB | BB | BB | AA | AA | AA | 1 | 1 |
| 1134 | rs3707900 | 15 | 52526197 | | AA | AA | BB | AA | AA | AA | 1 | 1 |
| 1135 | rs13482585 | 15 | 54079758 | | BB | BB | BB | BB | BB | BB | 1 | 1 |
| 1136 | rs6400804 | 15 | 56998500 | | AA | AA | AA | AA | AA | AA | 1 | 1 |
| 1137 | rs13482595 | 15 | 58814425 | | AA | BB | AA | BB | BB | BB | 1 | 1 |
| 1138 | rs3683495 | 15 | 61406689 | | AA | AA | AA | BB | BB | BB | 1 | 1 |
| 1139 | rs13482602 | 15 | 61631955 | | AA | BB | AA | BB | BB | BB | 1 | 1 |
| 1140 | rs3677062 | 15 | 63677792 | | BB | AA | AA | BB | BB | BB | 1 | 1 |
| 1141 | rs6381737 | 15 | 65856370 | | AA | BB | BB | AA | AA | AA | 1 | 1 |
| 1142 | rs13482628 | 15 | 68143270 | | BB | AA | AA | AA | AA | AA | 1 | 1 |
| 1143 | rs13482629 | 15 | 68448503 | | AA | BB | BB | AA | AA | AA | 1 | 1 |
| 1144 | rs13482637 | 15 | 70770335 | | AA | BB | BB | AA | AA | AA | 1 | 1 |
| 1145 | rs13482642 | 15 | 72483350 | | BB | AA | AA | BB | BB | BB | 1 | 1 |
| 1146 | rs8259436 | 15 | 75141907 | | AA | AA | AA | BB | BB | BB | 1 | 1 |
| 1147 | rs3660192 | 15 | 78151819 | | AA | BB | BB | BB | BB | BB | 1 | 1 |
| 1148 | rs13482661 | 15 | 79085767 | | AA | AA | AA | BB | BB | BB | 1 | 1 |
| 1149 | rs3665030 | 15 | 79719777 | | AA | BB | BB | AA | AA | AA | 1 | 1 |
| 1150 | rs6276391 | 15 | 82164497 | | AA | BB | BB | AA | AA | AA | 1 | 1 |
| 1151 | rs13482673 | 15 | 82560799 | | AA | AA | AA | BB | BB | BB | 1 | 1 |
| 1152 | rs3660367 | 15 | 85057715 | | AA | BB | BB | AA | AA | AA | 1 | 1 |
| 1153 | rs13482687 | 15 | 86303733 | | AA | AA | BB | BB | BB | BB | 1 | 1 |
| 1154 | rs13482695 | 15 | 88856958 | | BB | BB | BB | AA | AA | AA | 1 | 1 |
| 1155 | rs13482704 | 15 | 90816455 | | BB | AA | BB | AA | AA | AA | 1 | 1 |
| 1156 | rs13482712 | 15 | 92664963 | | AA | AA | AA | AA | AA | AA | 1 | 1 |
| 1157 | rs3719217 | 15 | 95679367 | | AA | AA | BB | AA | AA | AA | 1 | 1 |
| 1158 | rs6285067 | 15 | 95741617 | | BB | AA | BB | AA | AA | AA | 1 | 1 |
| 1159 | rs13482729 | 15 | 97550224 | | BB | AA | BB | AA | AA | AA | 1 | 1 |
| 1160 | rs13482738 | 15 | 100255519 | | BB | BB | BB | AA | AA | AA | 1 | 1 |
| 1161 | rs13482744 | 15 | 102030597 | | AA | AA | AA | BB | BB | BB | 1 | 1 |
| 1162 | rs13482751 | 15 | 103433393 | | BB | BB | BB | BB | BB | BB | 1 | 1 |
| 1163 | rs4152638 | 16 | 4009670 | | BB | BB | BB | BB | BB | BB | 1 | 1 |
| 1164 | rs4152790 | 16 | 4532147 | | BB | BB | BB | BB | BB | BB | 1 | 1 |
| 1165 | rs4231060 | 16 | 5907681 | | BB | BB | BB | AA | AA | AA | 1 | 1 |
| 1166 | rs4158907 | 16 | 7650712 | | AA | AA | AA | BB | BB | BB | 1 | 1 |
| 1167 | rs4160288 | 16 | 9258154 | | AA | BB | BB | BB | BB | BB | 1 | 1 |
| 1168 | rs4162800 | 16 | 12215630 | | AA | BB | AA | BB | BB | BB | 1 | 1 |
| 1169 | rs4163196 | 16 | 13143895 | | AA | AA | BB | AA | AA | AA | 1 | 1 |
| 1170 | rs4165065 | 16 | 17188907 | X | BB | BB | BB | AA | AA | AA | 1 | 1 |
| 1171 | rs4165081 | 16 | 19654956 | | BB | AA | BB | AA | AA | AA | 1 | 1 |
| 1172 | rs4165279 | 16 | 21155526 | | BB | AA | BB | AA | AA | AA | 1 | 1 |
| 1173 | rs4165440 | 16 | 24022362 | | BB | BB | AA | BB | BB | BB | 1 | 1 |
| 1174 | rs4165467 | 16 | 25257147 | | BB | BB | BB | BB | BB | BB | 1 | 1 |
| 1175 | rs4165602 | 16 | 27277369 | | BB | BB | AA | BB | BB | BB | 1 | 1 |
| 1176 | rs4167031 | 16 | 28698520 | | AA | AA | BB | BB | BB | BB | 1 | 1 |
| 1177 | rs4168640 | 16 | 30855920 | | AA | AA | BB | BB | BB | BB | 1 | 1 |
| 1178 | rs4170308 | 16 | 32338346 | | AA | BB | BB | AA | AA | AA | 1 | 1 |
| 1179 | rs4171932 | 16 | 34183107 | | BB | AA | BB | AA | AA | AA | 1 | 1 |
| 1180 | rs4172915 | 16 | 35504262 | | AA | AA | BB | AA | AA | AA | 1 | 1 |
| 1181 | rs4173902 | 16 | 37207323 | | BB | AA | AA | BB | BB | BB | 1 | 1 |
| 1182 | rs4175608 | 16 | 39046740 | | BB | AA | AA | BB | BB | BB | 1 | 1 |
| 1183 | rs4177651 | 16 | 40548715 | | AA | BB | AA | BB | BB | BB | 1 | 1 |
| 1184 | rs4179075 | 16 | 42205435 | | BB | AA | BB | BB | BB | BB | 1 | 1 |
| 1185 | rs4182243 | 16 | 46008686 | | AA | BB | AA | BB | BB | BB | 1 | 1 |
| 1186 | rs4183448 | 16 | 47148630 | | BB | AA | BB | AA | AA | AA | 1 | 1 |
| 1187 | rs4185639 | 16 | 50209266 | | BB | AA | AA | AA | AA | AA | 1 | 1 |
| 1188 | rs4186744 | 16 | 51371684 | | AA | BB | BB | AA | AA | AA | 1 | 1 |
| 1189 | rs3696661 | 16 | 51606253 | | AA | AA | BB | AA | AA | AA | 1 | 1 |
| 1190 | rs6163640 | 16 | 53434895 | | BB | BB | AA | BB | BB | BB | 1 | 1 |
| 1191 | CZECH-16_55104521 | 16 | 55104521 | | AA | AA | AA | AA | AA | AA | 1 | 1 |
| 1192 | rs4189277 | 16 | 57472587 | | BB | AA | BB | AA | AA | AA | 1 | 1 |
| 1193 | rs4191367 | 16 | 59391239 | | AA | AA | BB | BB | BB | BB | 1 | 1 |
| 1194 | rs4193069 | 16 | 61234639 | | BB | AA | BB | BB | BB | BB | 1 | 1 |
| 1195 | rs4194417 | 16 | 63055086 | | BB | BB | BB | AA | AA | AA | 1 | 1 |
| 1196 | rs4197150 | 16 | 66573423 | | BB | BB | BB | AA | AA | AA | 1 | 1 |
| 1197 | rs4197715 | 16 | 67541594 | | AA | BB | BB | AA | AA | AA | 1 | 1 |
| 1198 | rs4198737 | 16 | 69301525 | | AA | BB | BB | AA | AA | AA | 1 | 1 |
| 1199 | rs4200124 | 16 | 71033149 | | AA | AA | AA | BB | BB | BB | 1 | 1 |
| 1200 | rs4201998 | 16 | 72860280 | | BB | BB | BB | AA | AA | AA | 1 | 1 |
| 1201 | rs4204106 | 16 | 74547672 | | BB | BB | BB | BB | BB | BB | 1 | 1 |
| 1202 | rs3718160 | 16 | 77227010 | | AA | BB | BB | BB | BB | BB | 1 | 1 |
| 1203 | rs6317052 | 16 | 79873189 | | AA | AA | AA | AA | AA | AA | 1 | 1 |
| 1204 | rs4211364 | 16 | 81210555 | | BB | AA | AA | AA | AA | AA | 1 | 1 |

| | | | | | | | | | | | | |
|---|---|---|---|---|---|---|---|---|---|---|---|---|
| 1205 | rs4211664 | 16 | 83161949 | | AA | AA | AA | BB | BB | BB | 1 | 1 |
| 1206 | rs3680665 | 16 | 84938923 | | AA | AA | AA | BB | BB | BB | 1 | 1 |
| 1207 | rs4212102 | 16 | 85479261 | | AA | BB | BB | AA | AA | AA | 1 | 1 |
| 1208 | rs4213268 | 16 | 86836511 | | AA | BB | BB | AA | AA | AA | 1 | 1 |
| 1209 | rs4214396 | 16 | 87920304 | | AA | AA | BB | AA | AA | AA | 1 | 1 |
| 1210 | petM-01322-2 | 16 | 88587815 | | AA | AA | BB | BB | BB | BB | 1 | 1 |
| 1211 | rs4219905 | 16 | 93471889 | | BB | BB | BB | AA | AA | AA | 1 | 1 |
| 1212 | rs3712360 | 16 | 94018736 | | AA | AA | AA | BB | BB | BB | 1 | 1 |
| 1213 | rs3696981 | 16 | 98191753 | | BB | BB | BB | AA | AA | AA | 1 | 1 |
| 1214 | rs4136382 | 17 | 3388654 | | AA | AA | AA | BB | BB | BB | 1 | 1 |
| 1215 | rs13482843 | 17 | 4044700 | | AA | AA | AA | BB | BB | BB | 1 | 1 |
| 1216 | rs13482845 | 17 | 4592511 | | AA | BB | BB | AA | AA | AA | 1 | 1 |
| 1217 | UT_17_3.221024 | 17 | 5989632 | | BB | AA | AA | BB | BB | BB | 1 | 1 |
| 1218 | rs6196216 | 17 | 8381669 | | BB | AA | AA | AA | AA | AA | 1 | 1 |
| 1219 | rs3662575 | 17 | 9388595 | | AA | BB | BB | AA | AA | AA | 1 | 1 |
| 1220 | rs3662820 | 17 | 11723443 | | BB | BB | AA | BB | BB | BB | 1 | 1 |
| 1221 | rs3672065 | 17 | 13064499 | | AA | AA | BB | BB | BB | BB | 1 | 1 |
| 1222 | rs3726555 | 17 | 15215815 | | BB | BB | BB | AA | AA | AA | 1 | 1 |
| 1223 | rs13482899 | 17 | 16276466 | | AA | AA | AA | BB | BB | BB | 1 | 1 |
| 1224 | rs13482914 | 17 | 19510335 | | AA | AA | AA | BB | BB | BB | 1 | 1 |
| 1225 | rs3696835 | 17 | 21394398 | | BB | BB | BB | AA | AA | AA | 1 | 1 |
| 1226 | rs3719497 | 17 | 24100880 | | AA | AA | AA | BB | BB | BB | 1 | 1 |
| 1227 | rs6397584 | 17 | 26039914 | | AA | AA | AA | BB | BB | BB | 1 | 1 |
| 1228 | rs3693494 | 17 | 28381655 | | AA | AA | AA | BB | BB | BB | 1 | 1 |
| 1229 | rs3672987 | 17 | 31726297 | | AA | AA | AA | BB | BB | BB | 1 | 1 |
| 1230 | rs3682923 | 17 | 34343989 | | AA | BB | AA | BB | BB | BB | 1 | 1 |
| 1231 | rs6298471 | 17 | 35059374 | | AA | AA | BB | AA | AA | AA | 1 | 1 |
| 1232 | rs6390174 | 17 | 37542832 | | AA | BB | BB | AA | AA | AA | 1 | 1 |
| 1233 | rs3702604 | 17 | 39103029 | | BB | AA | BB | AA | AA | AA | 1 | 1 |
| 1234 | CEL-17_39772541 | 17 | 39772541 | | AA | AA | BB | BB | BB | BB | 1 | 1 |
| 1235 | rs13482997 | 17 | 41975280 | | BB | AA | AA | BB | BB | BB | 1 | 1 |
| 1236 | rs13483002 | 17 | 43897393 | | BB | BB | BB | BB | BB | BB | 1 | 1 |
| 1237 | rs6409750 | 17 | 45506664 | | AA | AA | BB | BB | BB | BB | 1 | 1 |
| 1238 | rs13483016 | 17 | 47737011 | | AA | BB | BB | AA | AA | AA | 1 | 1 |
| 1239 | rs3700227 | 17 | 50793087 | | BB | BB | BB | AA | AA | AA | 1 | 1 |
| 1240 | rs6272475 | 17 | 51663908 | | AA | AA | AA | BB | BB | BB | 1 | 1 |
| 1241 | rs3714226 | 17 | 53552802 | | BB | BB | BB | AA | AA | AA | 1 | 1 |
| 1242 | rs3715723 | 17 | 56999568 | | AA | BB | BB | BB | BB | BB | 1 | 1 |
| 1243 | rs13483055 | 17 | 58655424 | X | BB | BB | BB | AA | AA | AA | 1 | 1 |
| 1244 | gnf17.064.100 | 17 | 61107080 | | AA | BB | AA | BB | BB | BB | 1 | 1 |
| 1245 | rs6402097 | 17 | 62066360 | | AA | AA | AA | AA | AA | AA | 1 | 1 |
| 1246 | rs3727008 | 17 | 66156395 | | AA | AA | AA | BB | BB | BB | 1 | 1 |
| 1247 | rs13483085 | 17 | 66984514 | | BB | AA | BB | BB | BB | BB | 1 | 1 |
| 1248 | rs3660112 | 17 | 69021924 | | AA | AA | AA | BB | BB | BB | 1 | 1 |
| 1249 | rs3675634 | 17 | 69670995 | | AA | AA | AA | BB | BB | BB | 1 | 1 |
| 1250 | rs3691628 | 17 | 70833240 | | AA | AA | AA | BB | BB | BB | 1 | 1 |
| 1251 | rs13483103 | 17 | 72668814 | | BB | AA | AA | BB | BB | BB | 1 | 1 |
| 1252 | rs6229946 | 17 | 73658199 | | AA | BB | AA | BB | BB | BB | 1 | 1 |
| 1253 | rs3663088 | 17 | 75526825 | | BB | BB | BB | AA | AA | AA | 1 | 1 |
| 1254 | rs13483117 | 17 | 77391928 | | BB | BB | AA | AA | AA | AA | 1 | 1 |
| 1255 | gnf17.082.284 | 17 | 79515223 | | AA | BB | AA | BB | BB | BB | 1 | 1 |
| 1256 | gnf17.083.842 | 17 | 81077502 | | AA | BB | AA | BB | BB | BB | 1 | 1 |
| 1257 | rs13483135 | 17 | 82051202 | | AA | BB | AA | BB | BB | BB | 1 | 1 |
| 1258 | rs13483144 | 17 | 84456436 | | BB | AA | AA | BB | BB | BB | 1 | 1 |
| 1259 | rs4231720 | 17 | 85385338 | | BB | BB | BB | AA | AA | AA | 1 | 1 |
| 1260 | rs13483157 | 17 | 87503632 | | AA | BB | BB | AA | AA | AA | 1 | 1 |
| 1261 | rs6288047 | 17 | 90215134 | | BB | BB | BB | AA | AA | AA | 1 | 1 |
| 1262 | rs6397044 | 17 | 91938734 | | BB | AA | BB | AA | AA | AA | 1 | 1 |
| 1263 | rs3706382 | 17 | 92912930 | | AA | AA | BB | AA | AA | AA | 1 | 1 |
| 1264 | rs13483183 | 18 | 3687056 | | AA | AA | AA | AA | AA | AA | 1 | 1 |
| 1265 | rs13483184 | 18 | 3967037 | | BB | BB | BB | BB | BB | BB | 1 | 1 |
| 1266 | gnf18.001.688 | 18 | 4813500 | | BB | BB | BB | BB | BB | BB | 1 | 1 |
| 1267 | CEL-18_5565618 | 18 | 5565618 | | BB | BB | BB | BB | BB | BB | 1 | 1 |
| 1268 | rs3689558 | 18 | 8254573 | | BB | AA | AA | BB | BB | BB | 1 | 1 |
| 1269 | rs3660245 | 18 | 9491813 | | BB | BB | BB | AA | AA | AA | 1 | 1 |
| 1270 | rs4231742 | 18 | 11306822 | | AA | BB | BB | AA | AA | AA | 1 | 1 |
| 1271 | rs13483212 | 18 | 12477417 | | AA | AA | AA | BB | BB | BB | 1 | 1 |
| 1272 | mCV23617245 | 18 | 14895705 | | BB | BB | BB | AA | AA | AA | 1 | 1 |
| 1273 | rs6361186 | 18 | 15373312 | | BB | BB | BB | AA | AA | AA | 1 | 1 |
| 1274 | rs6358426 | 18 | 16784949 | | BB | AA | AA | AA | AA | AA | 1 | 1 |
| 1275 | rs13483244 | 18 | 21226461 | | BB | AA | AA | AA | AA | AA | 1 | 1 |
| 1276 | rs4138020 | 18 | 23001325 | | AA | AA | BB | BB | BB | BB | 1 | 1 |
| 1277 | gnf18.021.931 | 18 | 24860622 | | BB | BB | AA | BB | BB | BB | 1 | 1 |
| 1278 | gnf18.022.796 | 18 | 25729264 | | AA | AA | BB | AA | AA | AA | 1 | 1 |
| 1279 | rs13483263 | 18 | 26881733 | | AA | BB | AA | BB | BB | BB | 1 | 1 |
| 1280 | rs13483271 | 18 | 29410281 | | AA | BB | BB | AA | AA | AA | 1 | 1 |
| 1281 | rs3722973 | 18 | 31395543 | | AA | AA | AA | BB | BB | BB | 1 | 1 |
| 1282 | rs3718586 | 18 | 33572164 | | BB | AA | AA | BB | BB | BB | 1 | 1 |
| 1283 | rs3725637 | 18 | 34867922 | | BB | BB | BB | AA | AA | AA | 1 | 1 |
| 1284 | rs13483299 | 18 | 36563136 | | BB | AA | AA | BB | BB | BB | 1 | 1 |
| 1285 | rs3664831 | 18 | 37737388 | | BB | BB | BB | AA | AA | AA | 1 | 1 |
| 1286 | rs3699816 | 18 | 39756682 | | BB | BB | BB | AA | AA | AA | 1 | 1 |
| 1287 | rs13483319 | 18 | 41351739 | | BB | BB | AA | AA | AA | AA | 1 | 1 |
| 1288 | rs3676196 | 18 | 43364740 | | AA | AA | AA | BB | BB | BB | 1 | 1 |
| 1289 | rs4231834 | 18 | 44463060 | | AA | BB | BB | BB | BB | BB | 1 | 1 |
| 1290 | CEL-18_46082735 | 18 | 46082735 | | AA | BB | BB | BB | BB | BB | 1 | 1 |
| 1291 | rs6184541 | 18 | 47884501 | | AA | BB | BB | AA | AA | AA | 1 | 1 |
| 1292 | mCV24106092 | 18 | 49464960 | | BB | BB | BB | AA | AA | AA | 1 | 1 |
| 1293 | rs3674314 | 18 | 51674308 | | AA | BB | BB | BB | BB | BB | 1 | 1 |
| 1294 | gnf18.051.412 | 18 | 53592447 | | BB | BB | BB | BB | BB | BB | 1 | 1 |
| 1295 | rs13483368 | 18 | 54949689 | | BB | BB | BB | AA | AA | AA | 1 | 1 |
| 1296 | rs3683378 | 18 | 56183873 | | AA | BB | BB | AA | AA | AA | 1 | 1 |
| 1297 | rs6328845 | 18 | 58310005 | | AA | AA | AA | BB | BB | BB | 1 | 1 |
| 1298 | CEL-18_60214752 | 18 | 60214752 | | AA | AA | BB | BB | BB | BB | 1 | 1 |

| | | | | | | | | | | | |
|---|---|---|---|---|---|---|---|---|---|---|---|
| 1299 | rs8237402 | 18 | 62695790 | AA | AA | BB | BB | BB | BB | 1 | 1 |
| 1300 | rs3720827 | 18 | 63808511 | AA | AA | AA | BB | BB | BB | 1 | 1 |
| 1301 | rs3688789 | 18 | 65035105 | BB | AA | AA | AA | AA | AA | 1 | 1 |
| 1302 | rs3691542 | 18 | 67000836 | BB | AA | BB | AA | AA | AA | 1 | 1 |
| 1303 | rs3658163 | 18 | 69187029 | BB | AA | AA | BB | BB | BB | 1 | 1 |
| 1304 | rs13483426 | 18 | 70651591 | AA | AA | AA | BB | BB | BB | 1 | 1 |
| 1305 | rs6161154 | 18 | 71978261 | AA | AA | BB | AA | AA | AA | 1 | 1 |
| 1306 | rs13483436 | 18 | 73957870 | BB | AA | AA | BB | BB | BB | 1 | 1 |
| 1307 | rs13459193 | 18 | 75265583 | BB | AA | BB | AA | AA | AA | 1 | 1 |
| 1308 | rs13483446 | 18 | 77080840 | AA | AA | BB | AA | AA | AA | 1 | 1 |
| 1309 | rs3706601 | 18 | 77890660 | BB | BB | BB | AA | AA | AA | 1 | 1 |
| 1310 | rs3720876 | 18 | 80361633 | BB | BB | AA | AA | AA | AA | 1 | 1 |
| 1311 | rs13483462 | 18 | 81619936 | AA | AA | BB | BB | BB | BB | 1 | 1 |
| 1312 | rs13483466 | 18 | 82712912 | BB | AA | AA | BB | BB | BB | 1 | 1 |
| 1313 | mCV24836796 | 18 | 86034550 | AA | BB | BB | AA | AA | AA | 1 | 1 |
| 1314 | rs13483482 | 18 | 86617418 | BB | AA | AA | BB | BB | BB | 1 | 1 |
| 1315 | rs4137441 | 18 | 89120861 | BB | AA | AA | AA | AA | AA | 1 | 1 |
| 1316 | rs3671671 | 19 | 4208173 | BB | AA | AA | BB | BB | BB | 1 | 1 |
| 1317 | rs3713033 | 19 | 4818261 | BB | AA | AA | BB | BB | BB | 1 | 1 |
| 1318 | CEL-19_5283144 | 19 | 5283144 | AA | BB | BB | AA | AA | AA | 1 | 1 |
| 1319 | rs6236348 | 19 | 6000186 | AA | BB | BB | AA | AA | AA | 1 | 1 |
| 1320 | rs13483525 | 19 | 9543124 | BB | AA | AA | BB | BB | BB | 1 | 1 |
| 1321 | UT_19_10.709331 | 19 | 9813271 | AA | AA | BB | AA | AA | AA | 1 | 1 |
| 1322 | rs6316813 | 19 | 10572580 | BB | AA | BB | BB | BB | BB | 1 | 1 |
| 1323 | CEL-19_12595293 | 19 | 12595293 | AA | AA | BB | AA | AA | AA | 1 | 1 |
| 1324 | rs13483540 | 19 | 14743248 | BB | AA | AA | BB | BB | BB | 1 | 1 |
| 1325 | rs3686467 | 19 | 16159229 | BB | AA | AA | AA | AA | AA | 1 | 1 |
| 1326 | rs6223359 | 19 | 17804343 | AA | AA | AA | BB | BB | BB | 1 | 1 |
| 1327 | gnf19.017.711 | 19 | 19283950 | AA | BB | AA | AA | AA | AA | 1 | 1 |
| 1328 | rs6372656 | 19 | 21112530 | BB | AA | BB | AA | AA | AA | 1 | 1 |
| 1329 | rs6309315 | 19 | 22859563 | AA | AA | AA | BB | BB | BB | 1 | 1 |
| 1330 | rs3720897 | 19 | 24396755 | AA | BB | AA | AA | AA | AA | 1 | 1 |
| 1331 | rs6293693 | 19 | 25362165 | BB | BB | AA | BB | BB | BB | 1 | 1 |
| 1332 | rs3090325 | 19 | 26007713 | BB | AA | AA | AA | AA | AA | 1 | 1 |
| 1333 | UT_19_29.979736 | 19 | 29540192 | AA | BB | AA | BB | BB | BB | 1 | 1 |
| 1334 | rs13459194 | 19 | 31358105 | BB | AA | AA | BB | BB | BB | 1 | 1 |
| 1335 | rs6237466 | 19 | 31672951 | AA | AA | AA | BB | BB | BB | 1 | 1 |
| 1336 | CEL-19_34542259 | 19 | 34542259 | BB | AA | BB | BB | BB | BB | 1 | 1 |
| 1337 | gnf19.035.019 | 19 | 36467112 | AA | AA | BB | BB | BB | BB | 1 | 1 |
| 1338 | rs3710829 | 19 | 37393165 | AA | AA | AA | BB | BB | BB | 1 | 1 |
| 1339 | rs3655407 | 19 | 39594395 | BB | BB | AA | AA | AA | AA | 1 | 1 |
| 1340 | rs3656289 | 19 | 41749395 | AA | AA | AA | BB | BB | BB | 1 | 1 |
| 1341 | rs3687275 | 19 | 42406846 | AA | AA | BB | BB | BB | BB | 1 | 1 |
| 1342 | rs13483643 | 19 | 44651448 | AA | AA | BB | BB | BB | BB | 1 | 1 |
| 1343 | mCV23390953 | 19 | 45356002 | AA | BB | AA | AA | AA | AA | 1 | 1 |
| 1344 | rs3023496 | 19 | 47482330 | AA | AA | AA | BB | BB | BB | 1 | 1 |
| 1345 | rs6194426 | 19 | 49475053 | AA | BB | BB | BB | BB | BB | 1 | 1 |
| 1346 | mCV23069572 | 19 | 52162185 | AA | AA | AA | BB | BB | BB | 1 | 1 |
| 1347 | rs6304326 | 19 | 52797648 | BB | BB | BB | AA | AA | AA | 1 | 1 |
| 1348 | rs13483682 | 19 | 54535312 | BB | BB | BB | AA | AA | AA | 1 | 1 |
| 1349 | rs6211533 | 19 | 56380821 | AA | AA | BB | AA | AA | AA | 1 | 1 |
| 1350 | rs6191324 | 19 | 58720409 | AA | AA | BB | AA | AA | AA | 1 | 1 |
| 1351 | UT_4_59.889271 | 19 | 59475231 | BB | BB | BB | AA | AA | AA | 1 | 1 |
| 1352 | rs6413270 | 3_randc | 804035 | BB | BB | BB | BB | BB | BB | 1 | 1 |
| 1353 | rs3714915 | _randor | 12206182 | BB | BB | BB | AA | AA | AA | 1 | 1 |
| 1354 | rs6384973 | _randor | 12916620 | BB | BB | BB | AA | AA | AA | 1 | 1 |
| 1355 | rs3659551 | _randor | 25331885 | AA | AA | BB | BB | BB | BB | 1 | 1 |
| 1356 | rs3658362 | randor | 37176366 | BB | BB | BB | AA | AA | AA | 1 | 1 |
| 1357 | rs3700068 | _randor | 38982522 | BB | BB | BB | AA | AA | AA | 1 | 1 |
| 1358 | mCV24845756 | 1 randc | 24466918 | BB | BB | BB | AA | AA | AA | 1 | 1 |
| 1359 | rs4217260 | 1 randc | 82875108 | BB | BB | BB | BB | BB | BB | 1 | 1 |
| 1360 | rs13483712 | X | 7885141 | BB | AA | BB | AA | AA | AA | 1 | 1 |
| 1361 | CEL-X_8334947 | X | 8334947 | BB | AA | BB | AA | AA | AA | 1 | 1 |
| 1362 | CEL-X_9031623 | X | 9031623 | BB | BB | AA | BB | BB | BB | 1 | 1 |
| 1363 | rs13483724 | X | 28552142 | AA | AA | AA | BB | BB | BB | 1 | 1 |
| 1364 | gnfX.023.543 | X | 31247994 | BB | BB | BB | AA | AA | AA | 1 | 1 |
| 1365 | gnfX.026.801 | X | 34572975 | BB | BB | BB | AA | AA | AA | 1 | 1 |
| 1366 | rs13483731 | X | 34801132 | AA | BB | BB | AA | AA | AA | 1 | 1 |
| 1367 | CEL-X_39961894 | X | 39961894 | AA | AA | BB | BB | BB | BB | 1 | 1 |
| 1368 | rs13483738 | X | 40510546 | BB | BB | AA | AA | AA | AA | 1 | 1 |
| 1369 | rs13483746 | X | 42770100 | BB | BB | BB | AA | AA | AA | 1 | 1 |
| 1370 | gnfX.035.350 | X | 43278349 | BB | BB | BB | AA | AA | AA | 1 | 1 |
| 1371 | rs13483750 | X | 43720683 | AA | AA | AA | BB | BB | BB | 1 | 1 |
| 1372 | CEL-X_44311522 | X | 44311522 | BB | AA | AA | BB | BB | BB | 1 | 1 |
| 1373 | rs13483756 | X | 45475262 | BB | AA | AA | BB | BB | BB | 1 | 1 |
| 1374 | rs13483761 | X | 47895370 | AA | BB | BB | AA | AA | AA | 1 | 1 |
| 1375 | rs13483765 | X | 49186978 | AA | BB | BB | BB | BB | BB | 1 | 1 |
| 1376 | gnfX.044.260 | X | 52389338 | AA | AA | AA | BB | BB | BB | 1 | 1 |
| 1377 | rs13483777 | X | 52741694 | BB | AA | AA | BB | BB | BB | 1 | 1 |
| 1378 | rs13483781 | X | 53942181 | AA | BB | BB | AA | AA | AA | 1 | 1 |
| 1379 | rs13483783 | X | 55210782 | AA | BB | BB | AA | AA | AA | 1 | 1 |
| 1380 | rs13483786 | X | 56181989 | AA | BB | BB | AA | AA | AA | 1 | 1 |
| 1381 | CEL-X_59515625 | X | 59515625 | AA | BB | BB | AA | AA | AA | 1 | 1 |
| 1382 | CEL-X_60181392 | X | 60181392 | AA | AA | AA | BB | BB | BB | 1 | 1 |
| 1383 | petM-05810-1 | X | 61228987 | BB | AA | AA | AA | AA | AA | 1 | 1 |
| 1384 | rs3157124 | X | 63007260 | BB | BB | BB | AA | AA | AA | 1 | 1 |
| 1385 | rs13483825 | X | 65765926 | BB | AA | AA | BB | BB | BB | 1 | 1 |
| 1386 | CEL-X_66015326 | X | 66015326 | NC | BB | BB | AA | AA | AA | 1 | 1 |
| 1387 | rs13483831 | X | 67285372 | BB | AA | AA | AA | AA | AA | 1 | 1 |
| 1388 | CEL-X_68179178 | X | 68179178 | AA | BB | BB | AA | AA | AA | 1 | 1 |
| 1389 | CEL-X_72627341 | X | 72627341 | BB | AA | AA | BB | BB | BB | 1 | 1 |
| 1390 | CEL-X_72875547 | X | 72875547 | AA | BB | BB | AA | AA | AA | 1 | 1 |
| 1391 | rs13483858 | X | 73756646 | AA | BB | BB | AA | AA | AA | 1 | 1 |
| 1392 | rs13483862 | X | 74580193 | BB | AA | AA | BB | BB | BB | 1 | 1 |

| | | | | | | | | | | | |
|---|---|---|---|---|---|---|---|---|---|---|---|
| 1393 | CEL-X_75125049 | X | 75125049 | BB | AA | AA | BB | BB | BB | 1 | 1 |
| 1394 | rs13483868 | X | 76146750 | BB | AA | AA | BB | BB | BB | 1 | 1 |
| 1395 | rs3725966 | X | 77048128 | BB | BB | BB | AA | AA | AA | 1 | 1 |
| 1396 | CEL-X_77780392 | X | 77780392 | BB | BB | BB | AA | AA | AA | 1 | 1 |
| 1397 | rs13483877 | X | 78499387 | BB | BB | BB | AA | AA | AA | 1 | 1 |
| 1398 | rs13483805 | X | 81745577 | AA | AA | AA | AA | AA | AA | 1 | 1 |
| 1399 | gnfX.076.619 | X | 84227028 | BB | AA | AA | AA | AA | AA | 1 | 1 |
| 1400 | rs13483884 | X | 85456399 | AA | BB | BB | AA | AA | AA | 1 | 1 |
| 1401 | rs13459181 | X | 86087663 | BB | AA | AA | BB | BB | BB | 1 | 1 |
| 1402 | gnfX.080.189 | X | 87586756 | BB | AA | AA | BB | BB | BB | 1 | 1 |
| 1403 | rs13483894 | X | 87902633 | AA | BB | BB | AA | AA | AA | 1 | 1 |
| 1404 | rs6182892 | X | 88379974 | BB | AA | AA | BB | BB | BB | 1 | 1 |
| 1405 | CEL-X_89752158 | X | 89752158 | BB | AA | AA | BB | BB | BB | 1 | 1 |
| 1406 | CEL-X_91222960 | X | 91222960 | BB | AA | AA | BB | BB | BB | 1 | 1 |
| 1407 | gnfX.084.751 | X | 92235622 | BB | AA | AA | BB | BB | BB | 1 | 1 |
| 1408 | gnfX.086.039 | X | 93530235 | AA | AA | AA | AA | AA | AA | 1 | 1 |
| 1409 | rs13483921 | X | 95063466 | AA | AA | AA | BB | BB | BB | 1 | 1 |
| 1410 | rs13483926 | X | 97492766 | BB | BB | BB | AA | AA | AA | 1 | 1 |
| 1411 | rs13483929 | X | 98226460 | AA | BB | BB | BB | BB | BB | 1 | 1 |
| 1412 | CEL-X_100299803 | X | 100299803 | BB | AA | AA | BB | BB | BB | 1 | 1 |
| 1413 | rs13483937 | X | 102010268 | BB | AA | AA | BB | BB | BB | 1 | 1 |
| 1414 | rs13483941 | X | 102845364 | BB | AA | AA | BB | BB | BB | 1 | 1 |
| 1415 | rs6342003 | X | 103875234 | BB | AA | AA | BB | BB | BB | 1 | 1 |
| 1416 | CEL-X_106858553 | X | 106858553 | AA | BB | BB | BB | BB | BB | 1 | 1 |
| 1417 | rs6363550 | X | 109582439 | AA | BB | BB | AA | AA | AA | 1 | 1 |
| 1418 | rs13483971 | X | 111135758 | AA | BB | BB | AA | AA | AA | 1 | 1 |
| 1419 | CEL-X_112457192 | X | 112457192 | AA | BB | BB | AA | AA | AA | 1 | 1 |
| 1420 | CEL-X_112904656 | X | 112904656 | AA | BB | BB | AA | AA | AA | 1 | 1 |
| 1421 | CZECH-X_116527625 | X | 116527625 | BB | AA | AA | BB | BB | BB | 1 | 1 |
| 1422 | CEL-X_117683749 | X | 117683749 | BB | AA | AA | BB | BB | BB | 1 | 1 |
| 1423 | rs6205221 | X | 120300412 | BB | BB | BB | AA | AA | AA | 1 | 1 |
| 1424 | rs6221690 | X | 121042456 | BB | AA | AA | AA | AA | AA | 1 | 1 |
| 1425 | rs13483997 | X | 122120659 | AA | AA | AA | BB | BB | BB | 1 | 1 |
| 1426 | rs13484004 | X | 123782683 | BB | BB | BB | AA | AA | AA | 1 | 1 |
| 1427 | rs3702256 | X | 124956381 | BB | BB | BB | AA | AA | AA | 1 | 1 |
| 1428 | CEL-X_125736335 | X | 125736335 | AA | AA | AA | BB | BB | BB | 1 | 1 |
| 1429 | rs3697198 | X | 126223821 | AA | BB | AA | BB | BB | BB | 1 | 1 |
| 1430 | rs13484024 | X | 128014181 | BB | BB | AA | BB | BB | BB | 1 | 1 |
| 1431 | rs13484031 | X | 129847872 | BB | BB | AA | AA | AA | AA | 1 | 1 |
| 1432 | rs13484034 | X | 130685594 | AA | AA | BB | BB | BB | BB | 1 | 1 |
| 1433 | rs13484042 | X | 132280571 | BB | BB | AA | AA | AA | AA | 1 | 1 |
| 1434 | rs13484043 | X | 132699243 | BB | BB | AA | AA | AA | AA | 1 | 1 |
| 1435 | CEL-X_133525088 | X | 133525088 | BB | AA | BB | BB | BB | BB | 1 | 1 |
| 1436 | rs13484050 | X | 134426687 | BB | AA | BB | BB | BB | BB | 1 | 1 |
| 1437 | rs13484060 | X | 136857358 | BB | AA | BB | AA | AA | AA | 1 | 1 |
| 1438 | rs13484070 | X | 140595720 | AA | BB | AA | AA | AA | AA | 1 | 1 |
| 1439 | CEL-X_142652525 | X | 142652525 | AA | AA | BB | BB | BB | BB | 1 | 1 |
| 1440 | CEL-X_143595976 | X | 143595976 | BB | AA | BB | AA | AA | AA | 1 | 1 |
| 1441 | rs13484087 | X | 145863727 | BB | AA | BB | BB | BB | BB | 1 | 1 |
| 1442 | rs13484094 | X | 147274623 | AA | BB | AA | AA | AA | AA | 1 | 1 |
| 1443 | rs6365259 | X | 150148872 | AA | BB | AA | AA | AA | AA | 1 | 1 |
| 1444 | gnfX.141.820 | X | 151555476 | AA | AA | BB | AA | AA | AA | 1 | 1 |
| 1445 | CEL-X_154048891 | X | 154048891 | BB | BB | BB | AA | AA | AA | 1 | 1 |
| 1446 | CEL-X_155542834 | X | 155542834 | BB | BB | BB | AA | AA | AA | 1 | 1 |
| 1447 | gnfX.146.867 | X | 156799296 | BB | BB | BB | AA | AA | AA | 1 | 1 |
| 1448 | gnfX.148.995 | X | 158940488 | AA | BB | BB | BB | BB | BB | 1 | 1 |
| 1449 | rs13483844 | _rando | 10762134 | AA | BB | BB | AA | AA | AA | 1 | 1 |

| | | |
|---|---|---|
| **SNP's** | 1445 | 1445 |
| **Total SNPs** | 1445 | 1445 |
| **% C57BL/6J** | 100 | 100 |